

# **Synthesis and Characterization of Molecularly Imprinted Polymer Particles (MIPs) for Biomedical Applications**

**Ana Filipa Fernandes Lobo de Freitas**

Final Report of the Work Project presented to the

**Escola Superior de Tecnologia e Gestão**

**Instituto Politécnico de Bragança**

To obtain the Master Degree in

**Biomedical Technology**

October 2015



# **Synthesis and Characterization of Molecularly Imprinted Polymer Particles (MIPs) for Biomedical Applications**

Ana Filipa Fernandes Lobo de Freitas

Final Report of the Work Project presented to the

**Escola Superior de Tecnologia e Gestão**

**Instituto Politécnico de Bragança**

To obtain the Master Degree in

**Biomedical Technology**

Supervisor: Prof. Dr. Rolando Carlos Pereira Simões Dias

October 2015



*“Never be sure of anything,  
because wisdom begins with doubt.”*

*Freud*



## Acknowledgements

I would like to start by thanking my supervisor Professor Rolando Dias for providing me with the opportunity to work in this research and for his encouragement, support, and supervision at all levels. I am grateful to Dr. Porkodi Kadhivel for all her help and guidance in the laboratory.

I want to express my appreciation to the chemistry technicians Maria João Afonso and Paula Matos for the assistance provided. To the laboratory, LSRE, for all the materials waived for the preparation of this work. To the company, Qlabo<sup>®</sup> - Equipamentos de Laboratório Serviços, Lda., for the synthesis equipment Discovery<sup>®</sup>SP and to the technician Francisco Carvalho for the help in the procedure.

This work would not have been possible without the financial support given by FCT and FEDER, particularly under programs COMPETE (Project PEst-C/eqb/LA0020/2013), QREN/ON2/Project NORTE-07-0162-FEDER-000050 and QREN/ON2/Project NORTE-07-0124-FEDER-0000014 - Polymer Reaction Engineering.

I want to thank to all my friends and to all colleagues of the laboratory for their help, support and patience during this time.

Finally, a special thanks to my parents and to my brothers for the encouragement, love, patience and for always being there, no matter what.

THANK YOU ALL!





## Abstract

In this work the synthesis of Molecularly Imprinted Polymers (MIPs) was made using different techniques of polymerization, such as, in solution (micro-reactor and batch reactor) and inverse suspension, aiming the study of the effect of synthesis conditions on the properties and performance of materials obtained.

The mechanisms used in the reactions were: free radical polymerization (FRP) and chain transfer polymerization by reversible addition-fragmentation (RAFT). For the production of the MIPs were used as base monomers the acrylic acid (AA), methacrylic acid (MAA) and N-isopropylacrylamide (NIPA) and as target molecules the 5-fluorouracil (5FU, used in the treatment of cancer) and caffeine (CAF, stimulant of the central nervous system).

The characterization of the MIPs was made by two quantitative methods, solid phase extraction (SPE) with subsequent analysis through ultraviolet (UV) spectroscopy, and frontal analysis using a gel permeation chromatography (GPC) system, in order to evaluate the adsorption (saturation) and desorption (release) of molecules considered. The obtained particles were also analyzed by scanning electron microscopy (SEM).

It was concluded that the combination of different synthesis tools (molecular imprinting/controlled radical polymerization) can be used to produce polymer particles with applications in molecular recognition and controlled drug delivery.

**Keywords:** *5-Fluorouracil; Caffeine; Molecularly Imprinted Polymers; Molecular Recognition.*



## Resumo

Neste trabalho foi realizada a síntese de Polímeros Impressos Molecularmente (MIPs) por diferentes técnicas de polimerização, em solução (micro reator e reator “batch”) e por suspensão inversa, com o objetivo de estudar o efeito das condições de síntese sobre as propriedades e desempenho dos materiais obtidos.

Os mecanismos usados nas reações foram: polimerização radicalar clássica (FRP) e polimerização por transferência de cadeia reversível por adição-fragmentação (RAFT). Para a produção dos MIPs foram usados como monómeros base o ácido acrílico (AA), ácido Metacrílico (MAA) e N-isopropilacrilamida (NIPA) e como moléculas alvo o 5-fluorouracilo (5FU, usado no tratamento do cancro) e a cafeína (CAF, estimulante do sistema nervoso central).

Procedeu-se à caracterização dos MIPs através de dois métodos quantitativos, extração em fase sólida (SPE) com posterior análise por espectroscopia ultravioleta (UV), e análise frontal através de um sistema de cromatografia de permeação em gel (GPC), na determinação da adsorção (saturação) e dessorção (libertação) dos princípios ativos considerados. As partículas obtidas foram ainda analisadas por microscopia eletrónica de varrimento (SEM).

Mostra-se que a combinação de diferentes ferramentas de síntese (Impressão Molecular/Polimerização Radicalar Controlada) pode ser usada na produção de partículas de polímeros com aplicações no reconhecimento molecular e na libertação controlada de fármacos.

**Palavras-chave:** *5-Fluorouracilo; Cafeína; Polímeros Impressos Molecularmente; Reconhecimento Molecular.*



# Contents

Acknowledgements .....	v
Abstract .....	vii
Resumo .....	ix
List of Abbreviations and Symbols .....	xv
List of Figures .....	xix
List of Tables.....	xxiii
List of Annexes .....	xxv
Chapter 1. Introduction .....	1
1.1. Objectives.....	1
1.2. Organization of the Chapters.....	2
Chapter 2. Bibliographic Review.....	3
2.1. A brief history of molecular imprinting .....	3
2.2. Molecularly imprinted Polymers.....	4
2.2.1. Components of MIPs.....	5
2.2.1.1. Template.....	5
2.2.1.2. Functional monomers .....	5
2.2.1.3. Cross-linkers.....	6
2.2.1.4. Solvent (Porogen).....	6
2.2.1.5. Initiator .....	6
2.2.2. MIP preparative approaches .....	7
2.2.2.1. Covalent approach.....	7
2.2.2.2. Non-covalent approach.....	7
2.2.2.3. Semi-covalent approach .....	7
2.3. Polymerization Mechanisms .....	8
2.3.1. Free radical polymerization.....	8
2.3.1.1. Initiation .....	9

2.3.1.2.	Propagation.....	9
2.3.1.3.	Termination .....	10
2.3.2.	Controlled Radical Polymerization (CRP) using Reversible addition-fragmentation chain transfer (RAFT) agent .....	10
2.4.	Formats of MIPs.....	11
2.4.1.	Bulk by Solution and Bulk Polymerization.....	12
2.4.1.1.	Solution Polymerization .....	12
2.4.1.2.	Bulk Polymerization.....	12
2.4.2.	Spherical by Emulsion, Suspension and Inverse Suspension Polymerization ....	12
2.4.2.1.	Emulsion Polymerization .....	12
2.4.2.2.	Suspension Polymerization .....	13
2.4.2.3.	Inverse Suspension Polymerization.....	13
2.5.	Drugs .....	13
2.5.1.	5-Fluorouracil.....	13
2.5.2.	Caffeine .....	14
2.6.	Biomedical Applications of MIPs .....	14
2.6.1.	Artificial Antibody .....	15
2.6.2.	Biosensors .....	15
2.6.3.	Drug Delivery.....	15
2.6.4.	Tissue Engineering.....	16
Chapter 3.	Materials and Equipments .....	17
3.1.	Materials (Reagents) .....	17
3.2.	Equipments.....	20
Chapter 4.	Synthesis of Molecularly Imprinted Polymers .....	21
4.1.	Synthesis of MIPs using Controlled Radicalar Polymerization .....	21
4.1.1.	Micro-reactor.....	21
4.1.1.1.	Experimental procedure .....	22
4.1.1.1.1.	Preparation of the monomer solution .....	22
4.1.1.1.2.	Preparation of the system and polymerization .....	23
4.2.	Synthesis of MIPs using Free Radical Polymerization .....	23
4.2.1.	Experimental Procedure .....	24
4.2.1.1.	Batch reactor .....	24
4.2.1.2.	Inverse Suspension.....	25

---

4.3.	Template Removal .....	27
4.3.1.1.	Experimental procedure .....	27
4.4.	Analysis by Scanning Electron Microscopy (SEM).....	28
Chapter 5.	Characterization of Molecularly Imprinted Polymers .....	33
5.1.	Solid Phase Extraction .....	33
5.1.1.	Experimental Procedure .....	35
5.1.2.	Results and Discussion.....	37
5.2.	Frontal Analysis .....	39
5.2.1.	Measurement of Drug Adsorption and Release.....	39
5.2.1.1.	Tests with an Anionic Polymer based in Methacrylic Acid .....	40
5.2.1.1.1.	Injection of aqueous solutions containing drugs .....	40
5.2.1.1.2.	General Aspects about Experimental Procedure for Saturation and Release of Drugs in Continuous Mode Operation .....	42
5.2.1.1.2.1.	Saturation process .....	42
5.2.1.1.2.2.	Release process .....	42
5.2.2.	Theoretical Foundations of Frontal Analysis .....	44
5.2.3.	Experimental Procedure .....	48
5.2.3.1.	Packing the columns.....	48
5.2.3.2.	Injection of drug .....	49
5.2.3.3.	Saturation with the drug .....	50
5.2.3.4.	Release of the drug.....	50
5.2.4.	Results and discussion.....	51
5.3.	Fourier transform infrared spectroscopy (FTIR).....	63
Chapter 6.	Conclusion.....	69
6.1.	Future Work .....	71
Chapter 7.	References .....	73
Annexes	.....	I



## List of Abbreviations and Symbols

<i>5FU</i>	5-Fluorouracil
<i>AA</i>	Acrylic acid
<i>AIBN</i>	2,2'-Azobis(2-methylpropionitrile)
<i>AU</i>	Arbitrary units
<i>bp</i>	Boiling point
<i>CAF</i>	Caffeine
<i>CL</i>	Cross-linker
<i>CPA</i>	4-Cyano-4-(phenylcarbonothioylthio)pentanoic acid
<i>CRP</i>	Controlled radical polymerization
<i>D</i>	Drug
<i>DMF</i>	Dimethylformamide
<i>EGDMA</i>	Ethylene glycol dimethacrylate
<i>GPC</i>	Gel permeation chromatography
<i>FA</i>	Frontal analysis
<i>FRP</i>	Free radical polymerization
<i>FTIR</i>	Fourier transform infrared spectroscopy
<i>I</i>	Initiator
<i>IBU</i>	Ibuprofen
<i>ID</i>	Internal diameter
<i>IF</i>	Imprinting factor
<i>IL</i>	Internal length
<i>IR</i>	Refractive index
<i>IV-DP</i>	Intrinsic viscosity
<i>LS</i>	Light scattering

<i>M</i>	Functional monomer
<i>MAA</i>	Methacrylic acid
<i>MBAm</i>	<i>N,N'</i> -Methylenebis(acrylamide)
<i>MIP / MIPs</i>	Molecularly imprinted polymer/s
<i>m<sub>p</sub></i>	The mass of polymer (expressed in mg) used in the adsorption process.
<i>mp</i>	Melting point
<i>M<sub>w</sub></i>	The molar mass of the drug expressed in mg/mmol=g/mol
<i>MW</i>	Molecular weight
<i>NIPA</i>	<i>N</i> -isopropylacrylamide
<i>NIP / NIPs</i>	Non-imprinted polymer/s
<i>N/A</i>	Not available
<i>PTFE</i>	Polytetrafluoroethylene
<i>q*</i>	Amount of drug adsorbed
<i>Q</i>	Flow rate
<i>RAFT</i>	Reversible addition-fragmentation chain transfer
<i>RAFTag</i>	RAFT agent
<i>Ref.</i>	Reference
<i>r<sub>F</sub></i>	Retention factor
<i>S</i>	Solvent
<i>SEM</i>	Scanning electron microscopy
<i>SF</i>	Selectivity factor
<i>Span80</i>	Sorbitan monooleate
<i>SPE</i>	Solid phase extraction
<i>SR</i>	Swelling ratio
<i>SUR</i>	Surfactant
<i>t<sub>0</sub></i>	Retention time of a void marker
<i>T</i>	Template
<i>T °C</i>	Temperature in celsius
<i>THY</i>	Thymine

<i>TMPTA</i>	Trimethylolpropane triacrylate
$t_R$	Retention time of the molecule under study in the packed column
<i>U</i>	Uracil
<i>UV</i>	Ultraviolet
<i>V</i>	Volume
$V_0$	Void volume
$V_{50}$	2,2'-Azobis (2-methylpropionamidine) dihydrochloride
$V_a$	Volume of stationary phase
$V_{eq}$	Equivalent volume
$V_G$	Geometric volume of the column
$W_{DI}$	Deionized water
$W_F$	Filtered water
$Y_C$	Solvent mole ratio
$Y_{CL}$	Cross-linker mole fraction
$Y_{CL/T}$	Cross-linker/Template mole ratio
$Y_I$	Initiator mole fraction
$Y_m$	Weight fraction of monomer
$Y_{M/T}$	Functional monomer/Template mole ratio
$Y_{RAFTag/I}$	RAFT agent mole ratio
$Y_{SUR}$	Surfactant mole fraction



## List of Figures

Figure 2.1 - Representation of the number of publications about molecular imprinting per year, between 1930 and 2014. In 2015, and at the time of writing, 791 reports were already published (source: MIP Database [46]).	4
Figure 2.2 - Illustration of molecular imprinting process (Adapted from [56]).	5
Figure 2.3 - Schematic representation of the molecular imprinting process: The formation of reversible interactions between the template and polymerizable functionality may involve one or more of the previous interactions (Figure as presented in [63]).	8
Figure 2.4 - Schematic representation of initiator decomposition step (e.g. AIBN) (Figure as presented in [67]).	9
Figure 2.5 - Schematic representation of the monomer initiation step (e.g. AA) (Figure as presented in [67]).	9
Figure 2.6 - Schematic representation of the monomer propagation step (e.g. AA) (Figure as presented in [67]).	9
Figure 2.7 - Schematic representation of termination step by combinations (Figure as presented in [67]).	10
Figure 2.8 - Schematic representation of termination step by disproportionation (Figure as presented in [67]).	10
Figure 2.9 - Schematic representation of the mechanism of activation/deactivation by RAFT polymerization (Figure as presented in [67]).	11
Figure 2.10 - Schematic illustration of the biomedical applications of MIPs.	14
Figure 4.1 - Schematic illustration of droplet-based micro-reactor device build up in LSRE (Adapted from [56]).	22
Figure 4.2 - Microscopic image of NIP <sub>01</sub> obtained in continuous flow micro-reactor (Figure as presented in [56]).	23
Figure 4.3 - Schematic illustration of different techniques of free radical polymerization used in this work.	24
Figure 4.4 - Scheme of the polymerization in batch reactor.	24
Figure 4.5 - A scheme of inverse suspension polymerization.	25
Figure 4.6 - Discovery <sup>®</sup> SP equipment with a microwave synthesis system.	25
Figure 4.7 - Scheme of the Soxhlet used in this work.	27
Figure 4.8 - SEM micrographs of MIPs and NIPs produced. a) and b) MIP <sub>06</sub> synthesized by batch reactor with 5FU.	28
Figure 4.9 - SEM micrographs of MIPs and NIPs produced. a) and b) NIP <sub>06</sub> synthesized by batch reactor.; c) and d) MIP <sub>07</sub> synthesized by inverse suspension with 5FU; e) and f) NIP <sub>07</sub> synthesized by inverse suspension.	29
Figure 4.10 - SEM micrographs of MIPs and NIPs produced a) and b. MIP <sub>08</sub> synthesized by inverse suspension with 5FU; c) and d) NIP <sub>08</sub> synthesized by inverse suspension, e) and f) MIP <sub>09</sub> synthesized by inverse suspension with CAF.	30

Figure 5.1 - Scheme of SPE steps, 1. Conditioning, 2. Loading, 3. Washing, 4. Eluting. ....	34
Figure 5.2 - SPE system connected to a vacuum pump. ....	37
Figure 5.3 - UV Spectrophotometer system installed in the laboratory (LPQ). ....	37
Figure 5.4 - Comparison of the amount of drug adsorbed and released in the different MIPs and NIPs. ....	38
Figure 5.5 - Comparison of the amount of 5FU and CAF retained in MIPs and NIPs. ....	38
Figure 5.6 - Packing columns used in experimental studies of the saturation and release of drugs in polymers considering continuous operation mode. ....	39
Figure 5.7 - Simplified schematic representation of the GPC system used in this work to study experimentally the saturation and release of drugs in polymers considering continuous operation mode. ....	40
Figure 5.8 - Signal recorded on UV absorption detector as a result of injection into the GPC system an aqueous solution of the 5-Fluorouracil with 0.1 mM concentration. Here is presented normalized UV signal which is obtained by dividing the actual value by the maximum signal observed. This test was performed assuming a flow rate of eluent of 0.1 mL/min monitoring with UV absorbance at 265 nm. Comparison of the peaks observed in the presence and absence of polymer column allows to conclude that there is an effective affinity between the drug and the polymer network determined (note the high retention of the drug in the system when the polymer column is used). ....	41
Figure 5.9 - Schematic representation of the experimental procedure associated with the saturation of a material with a drug considering continuous operation mode. With this purpose, the GPC system with the material column is supplied with pure water (concentration of drug $C = 0$ ) for a sufficiently long period of time until a stable behavior of the detectors (null drug concentration). At a given instant ( $t = 0$ ) the system is feed with an aqueous solution containing the selected drug (drug concentration $C = C_0$ ), thereby causing a step change of the drug concentration at the entrance of the column. After some time of operation is detected (e.g. using UV) the presence of the drug in the output stream of the column. If this process is carried out for a sufficiently long period of time, this material will reach saturation of the drug (i.e. becomes incapable of adsorbing additional amounts of this molecule), and the concentration at the column outlet becomes constant (Adapted from [107]). ....	43
Figure 5.10 - Schematic representation of the experimental procedure associated with the release of a drug from a material considering continuous operation mode. Starting with the material in a state of saturation (see Figure 5.9), at a given instant, the feed containing the drug ( $C = C_0$ ) is replaced with the feed containing pure water ( $C = 0$ ). In this way it causes a negative step change on the drug concentration at the column inlet. The percolate of pure water in the hydrogel causes desorption (release) of the drug and after a sufficiently long operating time it should release the drug entirely. After the end of drug release, the detectors measured the presence of pure water (Adapted from [107]). ....	43
Figure 5.11 - Schematic representation of different liquid/solid adsorption phases in a column operating in a continuous process. In Phase I, the column has not been fully covered by the solute. There are adsorption sites occupied and other ones free with zero solute concentration at the column outlet. In Phase II, the column has been completely percolated by the solute but there are still free adsorption sites. At the outlet of the column is observed a value lower than the input concentration. In Phase III, all the adsorption places were occupied with a	

concentration observed in the outlet of the column equal to the initial concentration (saturation) (Adapted from [107]).	44
Figure 5.12 - Schematic representation of the ideal "breakthrough" curve (without output of the solute before the saturation) and a real "breakthrough" curve (including Phases I, II and III with exit of solute from the column before adsorbent saturation) (Adapted from [107]).	45
Figure 5.13 - Schematic representation of the adsorption process between the beginning of the "breakthrough" curve (elution volume = $V_{BR0}$ ) and the saturation (elution volume= $V_f$ ). This period corresponds to Phase II. At this time, the total amount of solute introduced into the system is $C_0 \times (V_f - V_{BR0})$ corresponding to the area $B_1 + B_2$ . The area $B_1$ represents the observed amount of solute in the mobile phase and, by difference, $B_2$ is the amount of solute that was adsorbed in the solid during this period (Adapted from [107]).	45
Figure 5.14 - Schematic representation of the calculation of equivalent volume ( $V_{eq}$ ) to quantify the amount of solute adsorbed. The objective is to calculate the area $B_2$ shown in Figure 5.13. In fact, comparing Figures 5.13 and 5.14, the area $B_2$ may be substituted for the rectangle area $C_0 \times (V_{eq}-V_{BR0})$ since it is ensured that the areas $C_1$ and $C_2$ are equal. Calculation of the equivalent volume ( $V_{eq}$ ) is therefore to find elution volume in which $C_1 = C_2$ (Adapted from [107]).	46
Figure 5.15 - General representation of the quantification of the adsorption process running in column operating in a continuous mode including the void volume (quantifies the entrapped solute in the mobile phase inside the column or in the capillary transport), the adsorbed solute in Phase I, which matches the area of the rectangle $C_0 \times (V_0-V_{BR0})$ and also the amount of solute adsorbed in Phase II, which corresponds to the area of the rectangle $C_0 \times (V_{eq}-V_{BR0})$ . The total amount of solute adsorbed onto the stationary phase is thus: $C_0 \times (V_{BR0}-V_0) + C_0 \times (V_{eq}-V_{BR0}) = C_0 \times (V_{eq}-V_0)$ (Adapted from [107]).	46
Figure 5.16 - Representation of the retention time of a void marker $t_0$ and the retention time of the molecule under study in the packed column ( $t_R$ ).	47
Figure 5.17 - Illustration of a column packing, a- elements of the column and polymer, b- column before packing, c- column after packing.	48
Figure 5.18 - GPC system installed in the laboratory (LSRE).	49
Figure 5.19 - Illustration of the integration of the column into the system, a. checking the flow, b. column packing (swelling).	49
Figure 5.20 - Illustration of a purge process.	50
<b>Figure 5.21</b> - Profile observed for the injection of 5FU in a column packed with a MIP <sub>07</sub> .	51
<b>Figure 5.22</b> - Profile observed for the saturation with 5FU in a column packed with a MIP <sub>07</sub> .	51
<b>Figure 5.23</b> - Profile observed for the release of 5FU in a column packed with a MIP <sub>07</sub> .	51
<b>Figure 5.24</b> - Profiles observed for the saturation and release of 5FU in a column packed with a MIP <sub>07</sub> .	51
Figure 5.25 - Profile observed for the injection, saturation and release of 5FU in a column packed with a MIP <sub>07</sub> .	52
Figure 5.26 - Profiles observed for the saturation of 5FU, 5FU pH 2 and 5FU pH 8 in a column packed with a MIP <sub>07</sub> .	52
Figure 5.27 - Profiles observed for the release of 5FU, 5FU pH 2 and 5FU pH 8 in a column packed with a MIP <sub>07</sub> .	53
<b>Figure 5.28</b> - Profile observed for the injection of 5FU in a column packed with a NIP <sub>07</sub> .	53
<b>Figure 5.29</b> - Profile observed for the saturation with 5FU in a column packed with a NIP <sub>07</sub> .	53
Figure 5.30 - Profile observed for the release of 5FU in a column packed with a NIP <sub>07</sub> .	54

Figure 5.31 - Profiles observed for the saturation and release of 5FU in a column packed with a NIP <sub>07</sub> .....	54
Figure 5.32 - Profile observed for the injection, saturation and release of 5FU in a column packed with a NIP <sub>07</sub> .....	54
Figure 5.33 - Profiles observed for the saturation with 5FU, 5FU pH 2 and 5FU pH 8 in a column packed with a NIP <sub>07</sub> .....	54
Figure 5.34 - Profiles observed for the release of 5FU, 5FU pH 2 and 5FU pH 8 in a column packed with a NIP <sub>07</sub> .....	55
Figure 5.35 - Profile observed for the injection of 5FU in a column packed with a MIP <sub>08</sub> . ....	55
Figure 5.36 - Profile observed for the saturation with 5FU in a column packed with a MIP <sub>08</sub> ...	55
Figure 5.37 - Profile observed for the release of 5FU in a column packed with a MIP <sub>08</sub> . ....	56
Figure 5.38 - Profiles observed for the saturation and release of 5FU in a column packed with a MIP <sub>08</sub> . ....	56
Figure 5.39 - Profiles observed for the injection, saturation and release of 5FU in a column packed with a MIP <sub>08</sub> .....	56
Figure 5.40 - Profiles observed for the saturation with 5FU and CAF in a column packed with a MIP <sub>08</sub> . ....	57
Figure 5.41 - Profiles observed for the release of 5FU and CAF in a column packed with a MIP <sub>08</sub> . ....	57
Figure 5.42 - Profile observed for the injection of 5FU in a column packed with a NIP <sub>08</sub> . ....	57
Figure 5.43 - Profile observed for the saturation with 5FU in a column packed with a NIP <sub>08</sub> ....	57
Figure 5.44 - Profile observed for the release of 5FU in a column packed with a NIP <sub>08</sub> . ....	58
Figure 5.45 - Profiles observed for the saturation and release of 5FU in a column packed with a NIP <sub>08</sub> .....	58
Figure 5.46 - Profiles observed for the injection, saturation and release of 5FU in a column packed with a NIP <sub>08</sub> .....	58
Figure 5.47 - Profiles observed for the saturation with 5FU and CAF in a column packed with a NIP <sub>08</sub> .....	59
Figure 5.48 - Profiles observed for the release of 5FU and CAF in a column packed with a NIP <sub>08</sub> .....	59
Figure 5.49 - Profile observed for the injection of 5FU in a column packed with a MIP <sub>09</sub> . ....	59
Figure 5.50 - Profile observed for the saturation with 5FU in a column packed with a MIP <sub>09</sub> ...	59
Figure 5.51 - Profile observed for the release of 5FU in a column packed with a NIP <sub>08</sub> . ....	60
Figure 5.52 - Profiles observed for the saturation and release of 5FU in a column packed with a NIP <sub>08</sub> .....	60
Figure 5.53 - Profiles observed for the injection, saturation and release of 5FU in a column packed with a MIP <sub>09</sub> . ....	60
Figure 5.54 - Profiles observed for the saturation with 5FU and CAF in a column packed with a MIP <sub>09</sub> . ....	61
Figure 5.55 - Profiles observed for the release of 5FU and CAF in a column packed with a MIP <sub>09</sub> . ....	61
Figure 5.56 - FTIR spectra of non-imprinted and imprinted dried polymers produced through FRP and RAFT polymerization.....	63
Figure 5.57 - FTIR spectra of non-imprinted and imprinted dried polymers produced through FRP and RAFT polymerization.....	64

## List of Tables

Table 3.1 - Chemical structures and properties of the reagents used in the synthesis process....	17
Table 3.2 - Chemical structures and properties of the reagents used in the synthesis process (continuation of Table 3.1).....	18
Table 3.3 - Chemical structures and properties of the reagents used in the synthesis process (continuation of Table 3.2).....	19
Table 3.4 - Chemical structures and properties of the reagents used in the synthesis process (continuation of Table 3.3).....	20
Table 3.5 - Equipment used in the experimental procedure performed in this work. ....	20
Table 4.1 - Experimental conditions used in Micro-reactor synthesis of NIPs. ....	31
Table 4.2 - Experimental conditions used in Batch Reactor synthesis of MIPs and NIPs. ....	31
Table 4.3 - Experimental conditions used in Inverse Suspension synthesis of MIPs and NIPs..	32
Table 4.4 - Experimental conditions used in CEM <sup>®</sup> Discovery synthesis of MIPs and NIPs.....	32
Table 5.1 - Amount of polymer and solvents used in SPE tests.....	36
Table 5.2 - Dimensions of columns used in experimental studies. ....	39
Table 5.3 - Results of imprinting factor obtained by frontal analysis. ....	62
Table 5.4 - Summary of results obtained by frontal analysis of MIPs and NIPs with different drugs (tests for adsorption).....	65
Table 5.5 - Summary of results obtained by frontal analysis of MIPs and NIPs with different drugs (tests for adsorption) (Continuation of Table 5.4).....	66
Table 5.6 - Summary of results obtained by frontal analysis of MIPs and NIPs with different drugs (tests for desorption).....	67
Table 5.7 - Summary of results obtained by frontal analysis of MIPs and NIPs with different drugs (tests for desorption) (Continuation of Table 5.6).....	68



## List of Annexes

Annex 1 - Report of synthesis performed in the microwave system in a Discovery®SP equipment.....	III
Annex 2 - SEM micrographs of MIPs and NIPs produced. a), b), c), d) MIP <sub>06</sub> synthesized by batch reactor with 5FU; e), f), g), h) NIP <sub>06</sub> synthesized by batch reactor.....	IV
Annex 3 - SEM micrographs of MIPs and NIPs produced. a), b), c), d) MIP <sub>07</sub> synthesized by inverse suspension with 5FU; e), f), g) NIP <sub>07</sub> synthesized by inverse suspension. ....	V
Annex 4 - SEM micrographs of MIPs and NIPs produced. a), b), c) MIP <sub>08</sub> synthesized by inverse suspension with 5FU; d), e), f) NIP <sub>08</sub> synthesized by inverse suspension. ....	VI
Annex 5 - SEM micrographs of MIPs produced. a), b), c), d) MIP <sub>08</sub> synthesized by inverse suspension with CAF. ....	VII
Annex 6 - Study of adsorption and desorption of 5FU in the MIP <sub>03</sub> /NIP <sub>03</sub> (see Table 4.2). Characterization of the MIP by SPE (Loading, Washing and Eluting step). ....	VIII
Annex 7 - Study of adsorption and desorption of 5FU in the MIP <sub>06</sub> /NIP <sub>06</sub> (see Table 4.2). Characterization of the MIP by SPE (Loading, Washing and Eluting step). ....	IX
Annex 8 - Study of adsorption and desorption of CAF in the MIP <sub>06</sub> /NIP <sub>06</sub> (see Table 4.2). Characterization of the MIP by SPE (Loading, Washing and Eluting step). ....	X
Annex 9 - Study of adsorption and desorption of 5FU in the MIP <sub>07</sub> /NIP <sub>07</sub> (see Table 4.3). Characterization of the MIP by SPE (Loading, Washing and Eluting step). ....	XI
Annex 10 - Study of adsorption and desorption of 5FU pH2 in the MIP <sub>07</sub> /NIP <sub>07</sub> (see Table 4.3). Characterization of the MIP by SPE (Loading, Washing and Eluting step). ....	XII
Annex 11 - Study of adsorption and desorption of 5FU pH8 in the MIP <sub>07</sub> /NIP <sub>07</sub> (see Table 4.3). Characterization of the MIP by SPE (Loading, Washing and Eluting step). ....	XIII
Annex 12 - Study of adsorption and desorption of CAF in the MIP <sub>07</sub> /NIP <sub>07</sub> (see Table 4.3). Characterization of the MIP by SPE (Loading, Washing and Eluting step). ....	XIV
Annex 13 - Study of adsorption and desorption of U in the MIP <sub>07</sub> /NIP <sub>07</sub> (see Table 4.3). Characterization of the MIP by SPE (Loading, Washing and Eluting step). ....	XV
Annex 14 - Study of adsorption and desorption of 5FU in the MIP <sub>08</sub> /NIP <sub>08</sub> (see Table 4.3). Characterization of the MIP by SPE (Loading, Washing and Eluting step). ....	XVI
Annex 15 - Study of adsorption and desorption of CAF in the MIP <sub>08</sub> /NIP <sub>08</sub> (see Table 4.3). Characterization of the MIP by SPE (Loading, Washing and Eluting step). ....	XVII
Annex 16 - Study of adsorption and desorption of 5FU in the MIP <sub>09</sub> /NIP <sub>07</sub> (see Table 4.3). Characterization of the MIP by SPE (Loading, Washing and Eluting step). ....	XVIII
Annex 17 - Study of adsorption and desorption of CAF in the MIP <sub>09</sub> /NIP <sub>07</sub> (see Table 4.3). Characterization of the MIP by SPE (Loading, Washing and Eluting step). ....	XIX
Annex 18 - Study of injection, adsorption and desorption of 5FU in the MIP <sub>03</sub> (see Table 4.2). Characterization of the MIP frontal analysis by filling a column operating in continuous mode. ....	XX

Annex 19 - Study of injection, adsorption and desorption of CAF in the MIP<sub>03</sub> (see Table 4.1).  
Characterization of the MIP frontal analysis by filling a column operating in continuous mode.  
..... XXI

Annex 20 - Study of injection, adsorption and desorption of IBU in the MIP<sub>03</sub> (see Table 4.2).  
Characterization of the MIP frontal analysis by filling a column operating in continuous mode.  
..... XXII

Annex 21 - Study of injection, adsorption and desorption of U in the MIP<sub>03</sub> (see Table 4.2).  
Characterization of the MIP frontal analysis by filling a column operating in continuous mode.  
..... XXIII

Annex 22 - Study of injection, adsorption and desorption of 5FU in the MIP<sub>05</sub> (see Table 4.2).  
Characterization of the MIP frontal analysis by filling a column operating in continuous mode.  
..... XXIV

Annex 23 - Study of injection, adsorption and desorption of 5FU in the MIP<sub>05</sub> (see Table 4.2).  
Characterization of the MIP frontal analysis by filling a column operating in continuous mode.  
..... XXV

Annex 24 - Study of injection, adsorption and desorption of THY in the MIP<sub>05</sub> (see Table 4.2).  
Characterization of the MIP frontal analysis by filling a column operating in continuous mode.  
..... XXVI

Annex 25 - Study of injection, adsorption and desorption of U in the MIP<sub>05</sub> (see Table 4.2).  
Characterization of the MIP frontal analysis by filling a column operating in continuous mode.  
..... XXVII

Annex 26 - Study of injection, adsorption and desorption of 5FU in the MIP<sub>05</sub> (see Table 4.2).  
Characterization of the MIP frontal analysis by filling a column operating in continuous mode.  
..... XXVIII

Annex 27 - Study of injection, adsorption and desorption of 5FU in the MIP<sub>05</sub> (see Table 4.2).  
Characterization of the MIP frontal analysis by filling a column operating in continuous mode.  
..... XXIX

Annex 28 - Study of injection, adsorption and desorption of U in the MIP<sub>05</sub> (see Table 4.2).  
Characterization of the MIP frontal analysis by filling a column operating in continuous mode.  
..... XXX

Annex 29 - Study of injection, adsorption and desorption of 5FU in the NIP<sub>05</sub> (see Table 4.2).  
Characterization of the NIP frontal analysis by filling a column operating in continuous mode.  
..... XXXI

Annex 30 - Study of injection, adsorption and desorption of 5FU in the NIP<sub>05</sub> (see Table 4.2).  
Characterization of the NIP frontal analysis by filling a column operating in continuous mode.  
..... XXXII

Annex 31 - Study of injection, adsorption and desorption of THY in the NIP<sub>05</sub> (see Table 4.2).  
Characterization of the NIP frontal analysis by filling a column operating in continuous mode.  
..... XXXIII

Annex 32 - Study of injection, adsorption and desorption of U in the NIP<sub>05</sub> (see Table 4.2).  
Characterization of the NIP frontal analysis by filling a column operating in continuous mode.  
..... XXXIV

Annex 33 - Study of injection, adsorption and desorption of U in the NIP<sub>05</sub> (see Table 4.2).  
Characterization of the NIP frontal analysis by filling a column operating in continuous mode.  
..... XXXV

Annex 34 - Study of injection, adsorption and desorption of 5FU in the MIP<sub>06</sub> (see Table 4.2). Characterization of the MIP frontal analysis by filling a column operating in continuous mode. .... XXXVI

Annex 35 - Study of injection, adsorption and desorption of 5FU pH2 in the MIP<sub>06</sub> (see Table 4.2). Characterization of the MIP frontal analysis by filling a column operating in continuous mode. .... XXXVII

Annex 36 - Study of injection, adsorption and desorption of 5FU pH8 in the MIP<sub>06</sub> (see Table 4.2). Characterization of the MIP frontal analysis by filling a column operating in continuous mode. .... XXXVIII

Annex 37 - Study of injection, adsorption and desorption of CAF in the MIP<sub>06</sub> (see Table 4.2). Characterization of the MIP frontal analysis by filling a column operating in continuous mode. .... XXXIX

Annex 38 - Study of injection, adsorption and desorption of U in the MIP<sub>06</sub> (see Table 4.2). Characterization of the MIP frontal analysis by filling a column operating in continuous mode. .... XL

Annex 39 - Study of injection, adsorption and desorption of 5FU in the NIP<sub>06</sub> (see Table 4.2). Characterization of the NIP frontal analysis by filling a column operating in continuous mode. .... XLI

Annex 40 - Study of injection, adsorption and desorption of 5FU pH2 in the NIP<sub>06</sub> (see Table 4.2). Characterization of the NIP frontal analysis by filling a column operating in continuous mode. .... XLII

Annex 41 - Study of injection, adsorption and desorption of 5FU pH8 in the NIP<sub>06</sub> (see Table 4.2). Characterization of the NIP frontal analysis by filling a column operating in continuous mode. .... XLIII

Annex 42 - Study of injection, adsorption and desorption of 5FU in the MIP<sub>07</sub> (see Table 4.3). Characterization of the MIP frontal analysis by filling a column operating in continuous mode. .... XLIV

Annex 43 - Study of injection, adsorption and desorption of 5FU pH2 in the MIP<sub>07</sub> (see Table 4.3). Characterization of the MIP frontal analysis by filling a column operating in continuous mode. .... XLV

Annex 44 - Study of injection, adsorption and desorption of 5FU pH8 in the MIP<sub>07</sub> (see Table 4.3). Characterization of the MIP frontal analysis by filling a column operating in continuous mode. .... XLVI

Annex 45 - Study of injection, adsorption and desorption of 5FU in the NIP<sub>07</sub> (see Table 4.3). Characterization of the NIP frontal analysis by filling a column operating in continuous mode. .... XLVII

Annex 46 - Study of injection, adsorption and desorption of 5FU pH2 in the NIP<sub>07</sub> (see Table 4.3). Characterization of the NIP frontal analysis by filling a column operating in continuous mode. .... XLVIII

Annex 47 - Study of injection, adsorption and desorption of 5FU pH8 in the NIP<sub>07</sub> (see Table 4.3). Characterization of the NIP frontal analysis by filling a column operating in continuous mode. .... XLIX

Annex 48 - Study of injection, adsorption and desorption of 5FU in the MIP<sub>08</sub> (see Table 4.3). Characterization of the MIP frontal analysis by filling a column operating in continuous mode. L

Annex 49 - Study of injection, adsorption and desorption of CAF in the MIP<sub>08</sub> (see Table 4.3).  
Characterization of the MIP frontal analysis by filling a column operating in continuous mode.  
..... LI

Annex 50 - Study of injection, adsorption and desorption of 5FU in the NIP<sub>08</sub> (see Table 4.3).  
Characterization of the NIP frontal analysis by filling a column operating in continuous mode.  
..... LII

Annex 51 - Study of injection, adsorption and desorption of CAF in the NIP<sub>08</sub> (see Table 4.3).  
Characterization of the NIP frontal analysis by filling a column operating in continuous mode.  
..... LIII

Annex 52 - Study of injection, adsorption and desorption of 5FU in the MIP<sub>09</sub> (see Table 4.3).  
Characterization of the MIP frontal analysis by filling a column operating in continuous mode.  
..... LIV

Annex 53 - Study of injection, adsorption and desorption of CAF in the MIP<sub>09</sub> (see Table 4.3).  
Characterization of the MIP frontal analysis by filling a column operating in continuous mode.  
..... LV

# Chapter 1. Introduction

In the last decades, there has been increased interest in the rational design of polymer networks for the recognition of molecules. The preparation of synthetic molecular networks with designed artificial recognitive domains exhibiting tailored recognition and release properties is beginning to attract interest of the drug delivery researchers. Imprinting technology has direct impact in enhanced drug loading of controlled-release carriers for the sustained release of therapeutic agents as well as robust biosensors for novel therapeutic and diagnostic devices[1]. Moreover, the MIPs stability, low cost of preparation and the potential application to a wide range of target molecules have attracted much attention [2, 3].

Recently, a number of significant advances have been made in the development of new technologies for optimizing drug delivery [4]. To maximize the efficacy and safety of medicines, drug delivery systems must be capable of regulating the rate of release (delayed- or extended-release systems) and/or targeting the drug to a specific site [5].

Can be found in the references some research works that show the interest in molecular imprinting of drugs for biomedical applications [6-34].

## 1.1. Objectives

The two main objectives of this project is to synthesize and characterize particles of molecularly imprinted polymers. It is intended to synthesize MIPs through different techniques, such as polymerization in solution and inverse suspension, in order to verify the effect of the conditions of synthesis on the properties and performance of the materials obtained. In the characterization can be checked if there is molecular recognition through the affinity between the template and the material.

## **1.2. Organization of the Chapters**

This work is organized into seven chapters, this is the first one: the introduction and objectives of this project. In Chapter 2 are described some theoretical concepts important for this work, such as the molecularly imprinted polymers (MIPs), the different techniques of polymerization and applications. In Chapter 3 is presented the description of materials and instruments used during the development of the work. In Chapter 4 are described all the experimental procedures involved in synthesis processes. In Chapter 5 are presented the results of quantification for SPE adsorption of drugs and the results of quantification by frontal analysis of adsorption and drug release. The Chapter 6 contains the main conclusions derived from the present work and suggestions for future work and in Chapter 7 are presented the references.

In the end, there are a set of Annexes that support the accomplished work. In this section it can also be found the remaining results of the developed work that supports the conclusions. Three papers published in conferences selected for oral presentations and one article published in *Journal of Chemical Technology and Biotechnology* were also included.

## Chapter 2. Bibliographic Review

### 2.1. A brief history of molecular imprinting

The origin of molecular imprinting goes back to 1931 when M.V. Polyakov synthesized silica particles and observed that when prepared in the presence of a specific solvent (e.g. benzene, toluene or xylene) the resulting silica demonstrated preferential binding capacity for that solvent [35, 36]. At the same time that Polyakov published the first article, the origin of the selectivity of antibodies in immunological systems was in great debate. The possible formation of antibodies in living organism was presented by Breinell and Haurowitz [37] than by Mudd [38]. Later, in 1942 Pauling and Campbell published the preparation of antibodies using molecules as templates [39, 40]. In 1949, Frank Dickey (a senior student of Linus Pauling), published the results of experiments performed with silica gels obtained in the presence of dyes [41]. Dickey observed that silica prepared in the presence of one of several dyes showed higher selectivity with this dye even in the presence of other dyes [36].

Several studies were published since the first discoveries made by Polyakov. After two decades of intensive research in the area, there was a decrease in the studies involving the molecular imprinting of silica simultaneously with the introduction of the first works of molecularly imprinting organic polymer. In 1972, Takagishi and Klotz reported that the introduction of cross-linker restricted mobility of the polymer chain, lead to the improvement in adsorption capacity [40, 42]. After, Wulff used what is now termed a “covalent approach” to prepare an organic molecularly imprinted polymer capable of discriminating between the enantiomers of glyceric acid [43]. Subsequently, throughout the 1970s and 1980s, Wulff’s group published extensively using this approach. The second major breakthrough in organic polymer imprinting occurred in 1981 when Mosbach and Arshady reported that they had prepared an organic MIP using non-covalent interactions only [36, 44]. This approach was designated the “non-covalent

approach”, as opposed to the covalent approach used by Wulff. This approach, implying a simple methodology, remarkably increased the studies in this area that occurred during the 90s. In 1995 Whitcombe et al. reported an intermediate approach that appeared to combine the advantages of both approaches [45]. This approach consist on covalent interaction during the polymerization stage but non-covalent interactions during rebinding. In order to improve subsequent non-covalent binding geometry, Whitcombe’s approach incorporated a sacrificial spacer group that was designed to be lost during template removal. The non-covalent approach is the most used approach in MIP synthesis [36].

Nowadays, molecular imprinting has been widely recognized as the most promising methodology and has convinced many researchers in different aspects of the scientific field to explore its wonders. In Figure 2.1 is illustrated the remarkable growth in the papers published since 1930 until now.

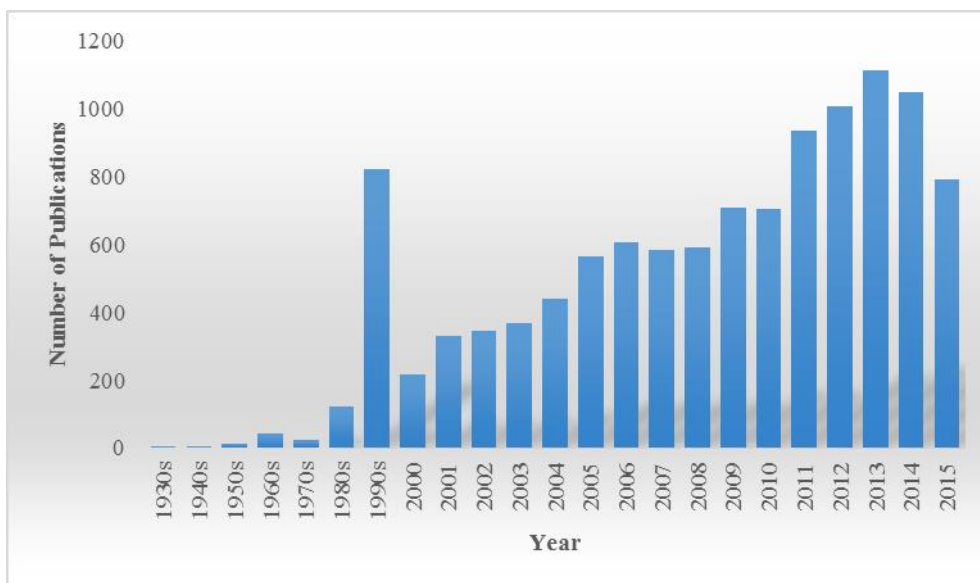


**Figure 2.1** - Representation of the number of publications about molecular imprinting per year, between 1930 and 2014. In 2015, and at the time of writing, 791 reports were already published (source: MIP Database [46]).

## 2.2. Molecularly imprinted Polymers

Molecularly imprinted polymers (MIPs) are polymers prepared in presence of a template (see Figure 2.2) [47-49] that serves as a mold for the formation of template

complementary binding sites. The MIPs can recognize a large variety of target structures with antibody-like affinities and selectivity. These properties, in addition to the robustness, resistance to high temperatures and pressures, and ease of preparation of these artificial receptors, have made them extremely attractive for problem solving in the areas of preparative chemical separations [50], solid phase extraction [51, 52], catalysis [53], sensing [54], and drug development and screening [55].

The selectivity of MIPs is directly related to the recognition of a molecule of interest, which was previously used as a template in the synthesis process. The design and synthesis of MIPs is a complex process which complexity becomes even more accentuated in the number of experimental variables involved, e.g. the nature and levels of template, functional monomer(s), cross-linker(s), solvent(s) and initiator, the method of initiation and the duration of polymerization.

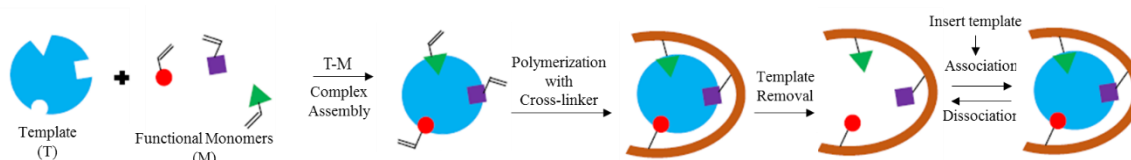


Figure 2.2 - Illustration of molecular imprinting process (Adapted from [56]).

## 2.2.1. Components of MIPs

### 2.2.1.1. Template

In all molecular imprinting processes the template plays a fundamental role, the molecular structure determines the type of functional monomer to be used in the synthesis, since the chemical bonds between both substantiates the molecular recognition. The template should ideally be chemically inert under the polymerization conditions and stable under the synthesis conditions (e.g. temperature) [57].

### 2.2.1.2. Functional monomers

Functional monomers are substances responsible for binding sites on the imprinted polymer resulting from their interaction with the template [58]. Generally, the type and concen-

tration of the functional monomers used in non-covalent imprinting are chosen from experience or from published reviews. The choice of functional monomers will determine the structure of the recognition site [59] and the concentration will influence the number of binding sites [60].

### **2.2.1.3. Cross-linkers**

According to Cormack and Elorza [57] the cross-linker used to obtain a MIP has three main roles: (i) the cross-linker is important in controlling the morphology of the polymer matrix (gel-type, macroporous or a microgel), (ii) it serves to stabilize the imprinted binding site and (iii) it imparts mechanical stability to the polymer matrix.

Generally high cross-link ratios are preferable from polymerization perspective, in order to access permanently porous (macroporous) materials and to be able to generate materials with adequate mechanical stability.

### **2.2.1.4. Solvent (Porogen)**

The solvent is part of the medium where the polymerization is carried out. It serves to drive the formation of monomers and template complexes forward or in reverse depending on the strength and the form of interactions. Because of the creation of pores in macroporous polymers, it is common to refer to the solvent as the “porogen” [57].

### **2.2.1.5. Initiator**

Initiators have been extensively used in conventional free radical polymerization. The initiator generates the first radical through its decomposition by thermolysis or photolysis, and initiates the first molecule polymerization of cross-linking agent to the last molecule, getting the chain lock with all monomers and forming a polymer. Initiator such as 2,2'-Azobis(2-methylpropionitrile) (AIBN) can be decomposed by both temperature and by photolysis [48].

## **2.2.2. MIP preparative approaches**

MIPs can be synthesized by three distinct approaches, such as, covalent, non-covalent and semi-covalent. In Figure 2.3 is presented a schematic representation of the above approaches.

### **2.2.2.1. Covalent approach**

In covalent approach, the complex is formed by covalent-linkage of a functional monomer and template prior to polymerization. After the removal of the template by chemical reaction, the MIPs obtained rebind template molecules via the same covalent interactions. The advantages of this approach are that the monomer/template complexes are stable and stoichiometric, and a wide variety of polymerization conditions can be employed [48, 61].

### **2.2.2.2. Non-covalent approach**

As already mentioned the non-covalent approach is the most used technique for preparing MIPs. This approach relies on multiple non-covalent interactions between the print molecules and the monomers. The monomers are chosen to allow hydrogen bonds, ionic interactions,  $\pi$ - $\pi$  interactions, hydrophobic interactions and Van der Waals forces. Furthermore, the rebinding of template molecules with MIPs is also carried out by the same non-covalent interactions. The association/dissociation kinetics of non-covalent MIPs is in general faster than that observed on polymers prepared by the covalent approach [48]. The advantages of this approach is the easy preparation of the template/monomer complex, easy removal of the templates from the polymers, fast binding of templates to MIPs, and its potential application to a wide range of target molecules [62].

### **2.2.2.3. Semi-covalent approach**

Another approach for preparing MIPs is the semi-covalent, which can be looked upon as a hybrid approach relying on covalent bonds to first form the template/monomer

complex with subsequent rebinding to the polymer occurring via non-covalent interactions [45, 62]. Therefore, semi-covalent imprinting combines the advantages of the above two approaches, the stable and stoichiometric complex in covalent imprinting and the fast guest binding in non-covalent imprinting.

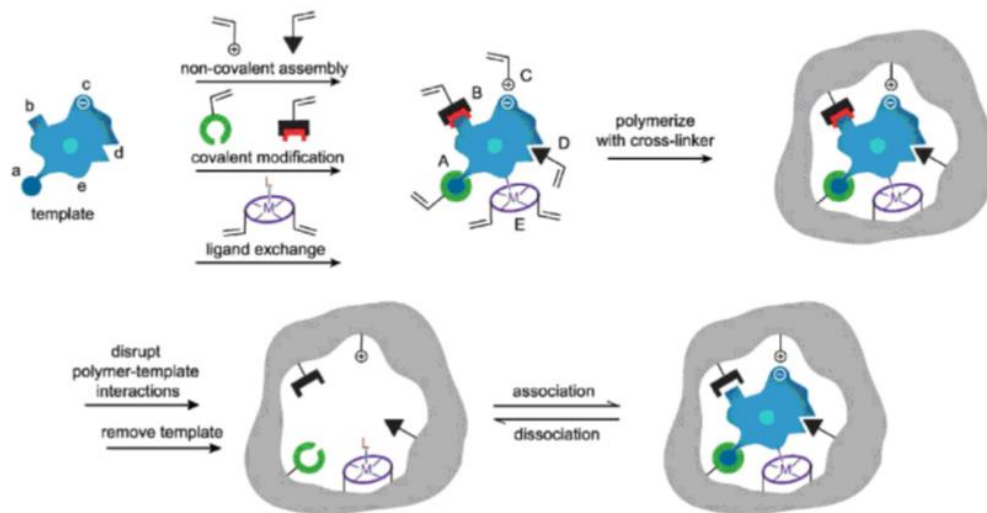


**Figure 2.3** - Schematic representation of the molecular imprinting process: The formation of reversible interactions between the template and polymerizable functionality may involve one or more of the previous interactions (Figure as presented in [63]).

## 2.3. Polymerization Mechanisms

### 2.3.1. Free radical polymerization

Free radical polymerizations (FRP) can be performed under mild reaction conditions (e.g. ambient temperatures and atmospheric pressures) in bulk or in solution, and is very tolerant to functional groups in the monomers and impurities in the system (e.g. water) [57]. For these reasons, as well as the fact that many vinyl monomers are available commercially at low cost, that free radical polymerization is, in general, the method selected for preparing MIPs [48, 64, 65].

The mechanism of free radical polymerization is characterized by three well define stages: initiation, propagation, and termination [66]. Note that the number and type of kinetic mechanisms involved in radical polymerization can be substantially larger, being here just a simple illustration of these processes of reaction [67].

### 2.3.1.1. Initiation

This stage involves creation of the free-radical active center and usually takes place in two steps. The first is the formation of free radicals from a decomposition of the initiator (see Figure 2.4) and the second is the addition of one of these free radicals to a molecule of monomer. (Figure 2.5) [65].

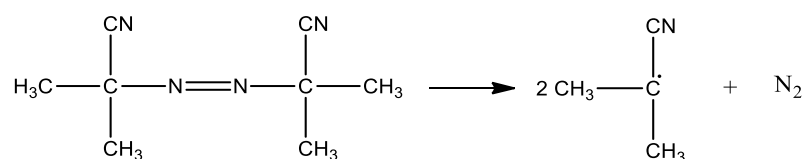


Figure 2.4 - Schematic representation of initiator decomposition step (e.g. AIBN) (Figure as presented in [67]).

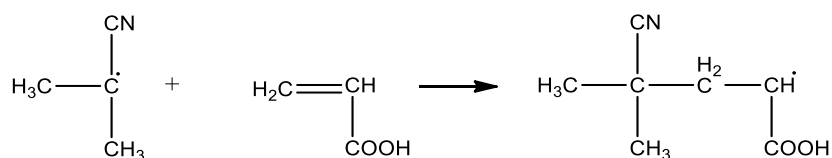


Figure 2.5 - Schematic representation of the monomer initiation step (e.g. AA) (Figure as presented in [67]).

### 2.3.1.2. Propagation

The second stage, involves growth of polymer chain by rapidly sequential addition of monomer to the active center (Figure 2.6). The time required for each monomer addition typically is a millisecond and so several thousand additions can take place within a few seconds [65].

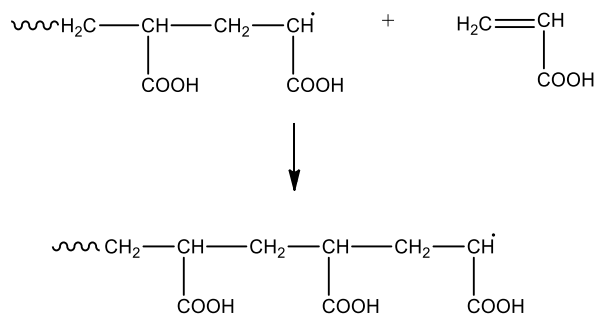
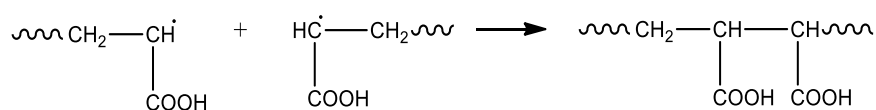


Figure 2.6 - Schematic representation of the monomer propagation step (e.g. AA) (Figure as presented in [67]).

### 2.3.1.3. Termination

In this stage, the active center is destroyed irreversibly and propagation ceases. The two most common mechanisms of termination in radical polymerizations are combination and disproportionation. Combination involve the coupling together of two growing chains to form a single polymer molecule (Figure 2.7). Disproportionation involves a transfer of one hydrogen atom from one growing polymer chain to another, forming different end groups without an inter-linking chain (Figure 2.8) [65].



**Figure 2.7** - Schematic representation of termination step by combinations (Figure as presented in [67]).

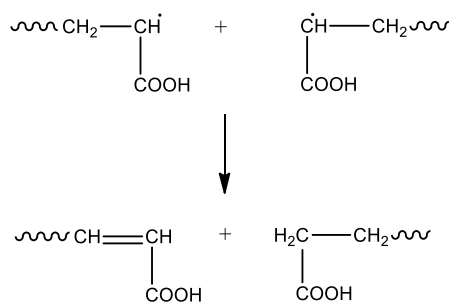


**Figure 2.8** - Schematic representation of termination step by disproportionation (Figure as presented in [67]).

### 2.3.2. Controlled Radical Polymerization (CRP) using Reversible addition-fragmentation chain transfer (RAFT) agent

In the last years, reversible addition-fragmentation chain transfer (RAFT) polymerization has been considered one of most versatile synthesis techniques to improve the molecular architectures of the polymers [68-70]. Because of the versatility of the RAFT polymerization involving the use of RAFT agents carrying many useful reactive end groups and the capability to polymerize many monomers that are inherently troublesome for other polymerization techniques [64].

The minimization of the termination and transfer reactions is critical in this context. This effect can be achieved if induced reversible kinetic mechanisms of activation/deactivation of radicals, as illustrated in the Figure 2.9. Such as in FRP the basic mechanisms are present in RAFT polymerization, namely initiation and propagation. In practice, the main difference between the FRP and CRP/RAFT is the addition of RAFT agent (e.g. CPA) in the initial reaction mixture. The inclusion of RAFT agent ensures the reversible steps for activation/deactivation of the radical [67].

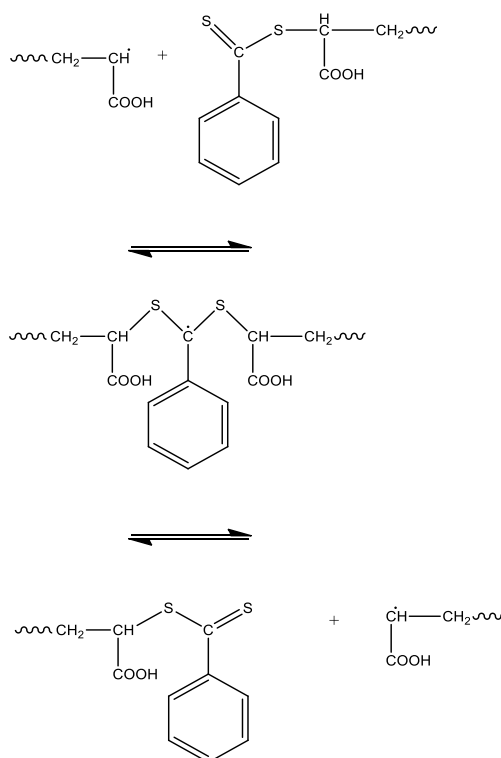


**Figure 2.9** - Schematic representation of the mechanism of activation/deactivation by RAFT polymerization (Figure as presented in [67]).

## 2.4. Formats of MIPs

MIPs can be prepared in a variety of physical forms, using different techniques depending on their final application. The format of the MIPs can influence on its capacity and accessibility of the binding sites by the template. Therefore, it is understandable that the format and size of the materials also influences their time of response when the materials are assessed as molecular recognition elements [71].

## **2.4.1. Bulk by Solution and Bulk Polymerization**

### **2.4.1.1. Solution Polymerization**

In solution polymerization, the monomer, initiator, and resulting polymer are all soluble in the solvent. This polymerization can involve a simple process in which a monomer, catalyst, and solvent are stirred together to form a solution that reacts without the need for heating or cooling or any special handling [72]. In most cases the macroporous imprinted polymers are prepared in bulk and are then crushed and sieved [48].

### **2.4.1.2. Bulk Polymerization**

Bulk polymerization occurs within the monomer itself. The reaction is catalyzed by additives such as initiator and transfer agents under the influence of heat or light. Since this polymerization process is highly exothermic, it is difficult to control and hence the polymer obtained is generally of non-uniform molecular mass distribution. However, molecular-weight distribution can be easily changed by the use of chain transfer agent. The temperature and pressure can also be varied to control the properties of the final polymer [73].

## **2.4.2. Spherical by Emulsion, Suspension and Inverse Suspension Polymerization**

### **2.4.2.1. Emulsion Polymerization**

It is a type of radical polymerization in which the liquid monomer is dispersed in an insoluble liquid leading to an emulsion. The most common type of emulsion polymerization is an oil-in-water emulsion, wherein droplets of monomer (the oil) are emulsified (with surfactants) in a continuous phase of water. These techniques were used to manufacture several commercially important polymers [73].

#### **2.4.2.2. Suspension Polymerization**

In the suspension polymerization, the monomer containing initiator, modifier, etc., is dispersed in a solvent (generally water) [74] by vigorous stirring. The stirring action helps to keep the monomer droplets separated and creates a uniform suspension, which leads to a more narrow size distribution of the final polymer beads [73].

This polymerization is one of the simplest and most common approaches for the production of MIP beads. In this suspension technique instead of water it can be used perfluorocarbon as solvent [75] but this method is somewhat expensive.

#### **2.4.2.3. Inverse Suspension Polymerization**

Inverse-suspension polymerization is defined as a dispersion of water-soluble monomer in a continuous organic matrix [76]. The original size of the droplets is reflected in the size of the corresponding polymer beads or pearls. The size of the droplets depends on stirring speed, volume ratio of water to monomer, concentration, and type of the stabilizer and the viscosities of both phases [77]. Span 80, has been reported as a suitable surfactant for polymerization in inverse suspension polymerization [78].

## **2.5. Drugs**

### **2.5.1. 5-Fluorouracil**

5-Fluorouracil (5FU) is an anticancer agent widely used in the clinical treatment of several solid cancers such as breast, colorectal, liver and brain cancer. This drug is rapidly metabolized in the body, thus the maintenance of high serum concentrations of this drug is needed to improve its therapeutic activity. For the maintenance of high serum concentrations continuous administrations are necessary. On the other hand 5FU shows severe toxic effects, and, of course, reaching and/or exceeding the toxic concentration must be avoided [79]. The association of anticancer drugs to delivery systems has been an interesting approach to selectively delivering these active agents and, at the same

time, reduce their toxicity [31]. In Table 3.4 (Chapter 3) are presented the chemical structure and properties of 5-Fluorouracil.

### 2.5.2. Caffeine

Caffeine may be considered as the most widely used behavioral active drug in the world [80, 81]. Every day caffeine is consumed in coffee, cocoa, tea, chocolate, some energy or soft drinks, chocolate milk, as well as in many painkillers and anti-migraine drugs. Caffeine is a mild diuretic as well as a metabolic stimulant which reacts on the central nervous system [80]. It is very frequently used as an ingredient of analgesics, appetite inhibition drugs or additive of stimulating preparations [81]. In Table 3.4 (Chapter 3) are presented the chemical structure and properties of caffeine.

## 2.6. Biomedical Applications of MIPs

Molecularly imprinted polymers are easy to synthesize, cheap and robust moreover they offer a great potential in specific recognition capacities for template molecules[48]. Recently, the number of publications of MIPs has been increasing, as well as their applications. In Figure 2.10 is present a schematic illustration of the biomedical applications.

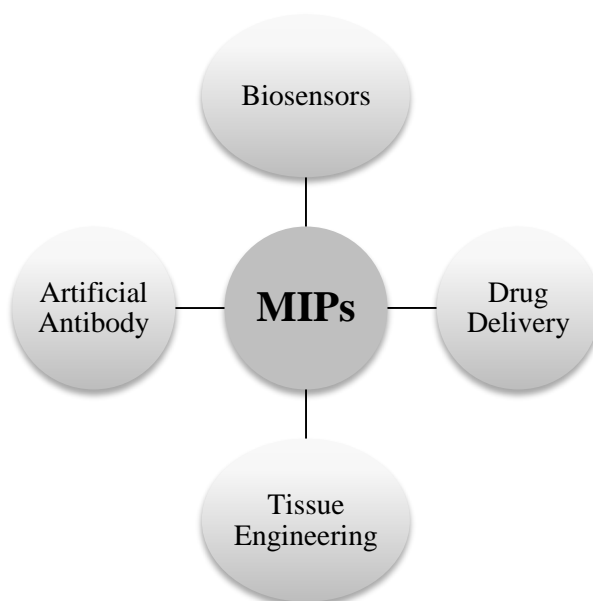


**Figure 2.10** - Schematic illustration of the biomedical applications of MIPs.

### **2.6.1. Artificial Antibody**

MIPs have a common feature with antibodies in that they both bind target molecules selectively and reversibly. This could potentially be used for immunoassay type binding analysis replacing antibodies. The Mosbach group [82] has designed a molecular imprint sorbent assay for the detection of theophylline and tranquilizer diazepam in organic solvent as conventional immunoassays that can only be used in aqueous solutions. Other compounds assayed are drugs, herbicide and corticosteroids [58].

### **2.6.2. Biosensors**

MIPs can be used to produce biosensors. Their selectivity, robustness and low costs of production make these materials an ideal choice for the development of sensing devices. The area involves drug agent detection, environment monitoring, food analysis, medical diagnostics, drug screening with more potential applications continue to emerge [83-85].

### **2.6.3. Drug Delivery**

In the last few years, a number of significant advances have been made in the development of new technologies for optimizing drug delivery [5].

Drug delivery systems are required whenever an administered therapeutic agent needs to be protected against metabolic attack, or when there are absorption barriers or dosage limitations. The ideal delivery vehicle will ensure that the drug is released at the right site, in the right dose and for the required time. It will also be biocompatible or biodegradable in such way that the delivery system is transformed into non-toxic fragments that are eliminated harmlessly from the body. The importance of this field of research is growing as even more complex drugs and biopharmaceuticals are being developed, many of which cannot be administered without a controlled dosage system [86]. The application of MIPs in different drug delivery systems has dramatically expanded in the past decade [29, 33, 87-92].

#### **2.6.4. Tissue Engineering**

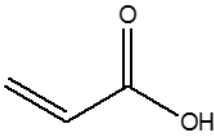
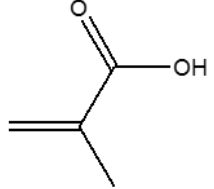
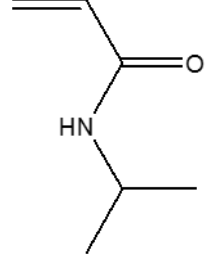
Molecular imprinting hydrogels in tissue engineering have attracted significant interest because of the ability to control release of the active biomolecules in a localized area [93]. Heparin-functionalized hydrogels including an imprinted scaffold to control porosity, have been used to enhance cell-adhesion and tissue in-growth [94]. Molecular recognition materials can potentially be applied on a biomaterial surface to specifically recognize template from the biological fluid.

## Chapter 3. Materials and Equipments

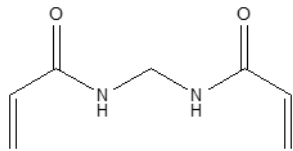
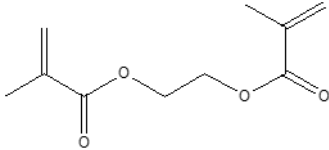
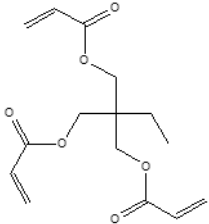
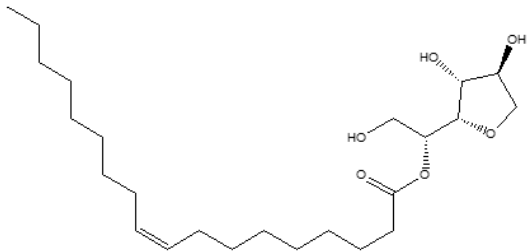
### 3.1. Materials (Reagents)

The chemical structures and properties of different reagents (monomers, cross-linkers, initiator, solvent, RAFT agent, surfactant, drugs) used in synthesis are detailed in Tables 3.1 to 3.4. The reagents were used as received in order to try to reproduce the industrial practice in the synthesis of polymers. They were acquired at Sigma Aldrich<sup>®</sup>[95], Acros Organics<sup>®</sup> [96], Fisher Scientific [97], Panreac [98] and ESA [99].

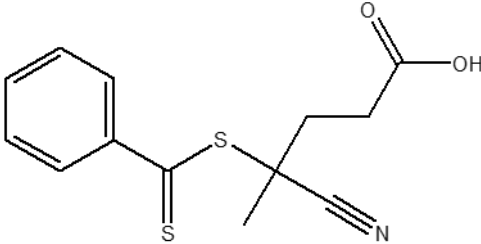
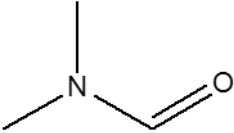
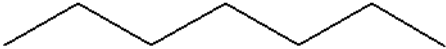
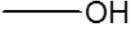
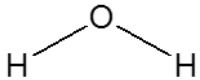
**Table 3.1** - Chemical structures and properties of the reagents used in the synthesis process.

Monomer	Chemical Formula	Chemical Structure	bp (°C)	mp (°C)	MW (g/mol)	Density (g/mL) (at 25 °C)	Ref.
AA	C <sub>3</sub> H <sub>4</sub> O <sub>2</sub>		139	13	72.06	1.05	[95]
MAA	C <sub>4</sub> H <sub>6</sub> O <sub>2</sub>		163	12 - 16	86.09	1.02	[95]
NIPA	C <sub>6</sub> H <sub>11</sub> NO		89 - 92	60 - 63	113.16	-	[95]

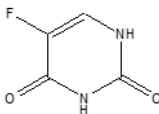
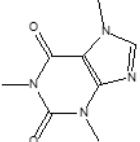
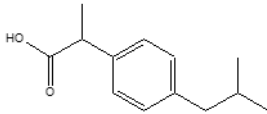
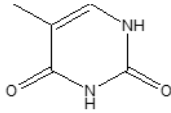
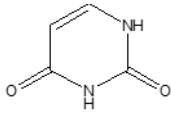
**Table 3.2** - Chemical structures and properties of the reagents used in the synthesis process (continuation of Table 3.1).

Cross-inker	Chemical Formula	Chemical Structure	bp (°C)	mp (°C)	MW (g/mol)	Density (g/mL) (at 25 °C)	Ref.
MBAm	C <sub>7</sub> H <sub>10</sub> N <sub>2</sub> O <sub>2</sub>		-	>300	154.17	-	[95]
EGDMA	C <sub>10</sub> H <sub>14</sub> O <sub>4</sub>		98 -100	-	198.22	1.05	[95]
TMPTA	(H <sub>2</sub> C=CHCO <sub>2</sub> CH <sub>2</sub> ) <sub>3</sub> CC <sub>2</sub> H <sub>5</sub>		-	-	296.32	1.1	[95]
<b>Surfactant</b>							
Span80	C <sub>24</sub> H <sub>44</sub> O <sub>6</sub>		>100	149	428.68	-	[98]

**Table 3.3** - Chemical structures and properties of the reagents used in the synthesis process (continuation of Table 3.2).

RAFT agent	Chemical Formula	Chemical Structure	bp (°C)	mp (°C)	MW (g/mol)	Density (g/mL) (at 25 °C)	Ref.
CPA	$C_{13}H_{13}NO_2S_2$		-	94 - 98	279.38	-	[95]
<b>Solvent</b>							
DMF	$C_3H_7NO$		153	-61	73.09	0.94 - 0.95	[97]
Heptane	$C_7H_{16}$		98	-91	100.20	0.68	[95]
Methanol	$CH_3OH$		64.7	-98	32.04	0.79	[95]
$W_{DI} / W_F$	$H_2O$		100	-	18.02	1	[99]

**Table 3.4** - Chemical structures and properties of the reagents used in the synthesis process (continuation of Table 3.3).

Drug	Chemical Formula	Chemical Structure	bp (°C)	mp (°C)	MW (g/mol)	Density (g/mL) (at 25 °C)	Ref.
5FU	C <sub>4</sub> H <sub>3</sub> FN <sub>2</sub> O <sub>2</sub>		190 - 200	278 - 282	130.08	-	[96]
CAF	C <sub>8</sub> H <sub>10</sub> N <sub>4</sub> O <sub>2</sub>		-	234 - 239	194.19	1.23	[96]
IBU	C <sub>13</sub> H <sub>18</sub> O <sub>2</sub>		157	75 - 78	206.28	-	[96]
THY	C <sub>5</sub> H <sub>6</sub> N <sub>2</sub> O <sub>2</sub>		-	~320	126.11	-	[95]
U	C <sub>4</sub> H <sub>4</sub> N <sub>2</sub> O <sub>2</sub>		-	>300	112.09	-	[95]

## 3.2. Equipments

In Table 3.5 is presented the equipment used in the experimental procedure performed in this work.

**Table 3.5** - Equipment used in the experimental procedure performed in this work.

Equipment	Model	Company	Software
Analytical Balance	AS 220/C/2	RADWAG®	-
Heater	VMS-C7	VWR®	-
GPC	GPCmax VE 2001 TDA 305	VISCOTEK®	OmniSEC 4.7.0
	UV detector 2520	Knauer®	
Soxhlet	HM01 series	Labbox®	-
FTIR	MB154s	BOMEM	Grams/32
UV Spectrophotometer	V-530	JASCO®	VWS-580 Secptra Manager
Pump	Azura P 4. 1S	Knauer – Azura®	-
Vacuum pump	RE3022C	Stuart®	-

## **Chapter 4. Synthesis of Molecularly Imprinted Polymers**

In this chapter is presented the experimental work for all the synthesis of molecularly imprinted polymers particles (MIPs) and non-imprinted polymers particles (NIPs). Two different mechanisms were used, namely Controlled Radical Polymerization (CRP) by RAFT and free radical polymerization (FRP). The synthesis by CRP was performed in a micro-reactor while for FRP was made by two methods, batch reactor and inverse suspension. To perform the syntheses presented in this section was used chemical compounds described in Table 3.1 to 3.4. The whole experimental procedure is described in the following section.

### **4.1. Synthesis of MIPs using Controlled Radical Polymerization**

Controlled Radical Polymerization (CRP) by RAFT agent has been considered in several research lines to improve the molecular architectures of vinyl polymers (e.g. aiming at low chain heterogeneity, controlled topologies, etc.) [49, 56, 69, 70].

#### **4.1.1. Micro-reactor**

In the last years, micro-reactors have been an alternative approach to produce spherical particles continuously by using a microfluidic droplet based technique. These droplets are generated at T-junctions mixing points. Is used an immiscible and chemically inert oil as a carrier fluid between droplets. This way, a sequence of droplets flows continuously within tubes [100]. This kind of polymerizations offer the possibility to increase the throughput at low operating costs, and the polymer product is obtained with constant quality.

#### 4.1.1.1. Experimental procedure

The synthesis using CRP was performed in a micro-reactor that was built up using two pumps, with maximum delivery pressure of 40 MPa and flow rate in the range 0.001 to 10 mL/min. Each pump is connected to a container, one container has the aqueous phase (monomer solution) and the other one has the oil phase (paraffin). Valco tee devices were used to connect the two lines coming from the pumps with generation of the feed to the micro-reactor. Different T connectors with internal diameters 0.25, 0.5, 0.75, and 1.0 mm were considered. PTFE tubings with different internal diameters (0.2, 0.5, 0.8, 1.0 and 1.5 mm) were used as continuous flow micro-reactors. The maximum length of all micro-reactors used is 20 m. The micro-reactor tubing was rolled up on a metallic cylinder and immersed in a paraffin bath with controlled temperature. A container was connected to the end of the reactor in order to collect the carrier fluid (often liquid paraffin) and the aqueous-phase polymer particles. In this container, a polymer precipitating solvent (e.g. methanol or acetone) was also often included and mixing by a magnetic stirrer was also promoted [56]. A scheme of the micro-reactor is shown in Figure 4.1.

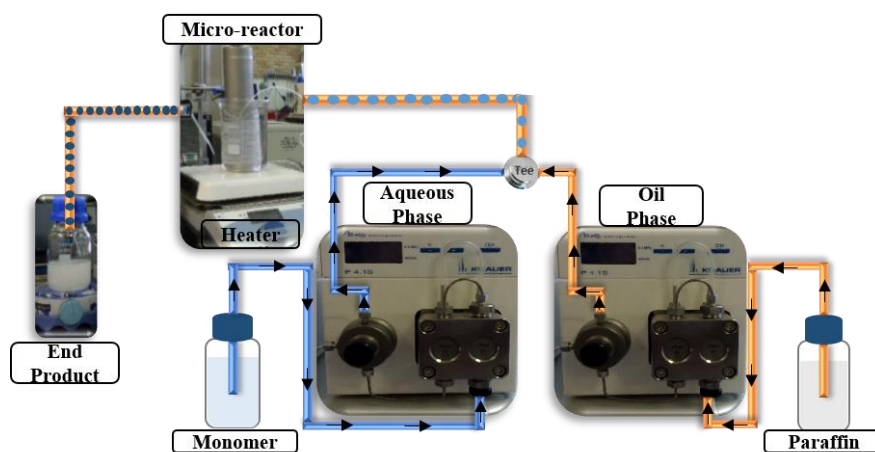


Figure 4.1 - Schematic illustration of droplet-based micro-reactor device build up in LSRE (Adapted from [56]).

##### 4.1.1.1.1. Preparation of the monomer solution

To obtain a monomer solution it was necessary to weigh the amounts of monomer, cross-linker, initiator, solvent (Table 4.1). Next, the monomer with the cross-linker, half the amount of the solvent, were mixed in a flask. In another flask the initiator with the

remaining solvent and RAFT agent were mixed. The flasks were placed on ultrasound to ensure that all the elements were dissolved. After the dissolution of the elements, the flask containing the monomer was degassed. Finally, the elements of both flasks were mixed. To produce Non Imprinted Polymers (NIPs) the procedure was the same, excluding the presence of drugs.

#### 4.1.1.1.2. Preparation of the system and polymerization

To ensure that the synthesis would happen it was necessary to verify if the residence time in the micro-reactor was superior to the polymerization time. So, it was needed to put a colored solution connected with aqueous phase pump, turn on the system and with a chronometer the residence time was checked. For the polymerization time it was necessary to put a flask with a small amount of monomer solution in paraffin bath and with a chronometer the time was verified. Thereafter, the system was cleaned with  $W_{DI}$  and then began the process of synthesis with the monomer solution. This process took approximately six hours. In Figure 4.2 is presented a microscopic image of NIP<sub>01</sub>.

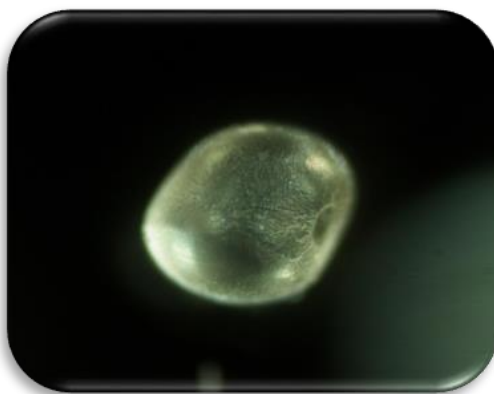


Figure 4.2 - Microscopic image of NIP<sub>01</sub> obtained in continuous flow micro-reactor (Figure as presented in [56]).

## 4.2. Synthesis of MIPs using Free Radical Polymerization

Free radical polymerization (FRP) is the most important synthetic method for the conversion of monomer into polymer [57]. This synthesis was applied by two different techniques (Figure 4.3), namely batch reactor and inverse suspension.

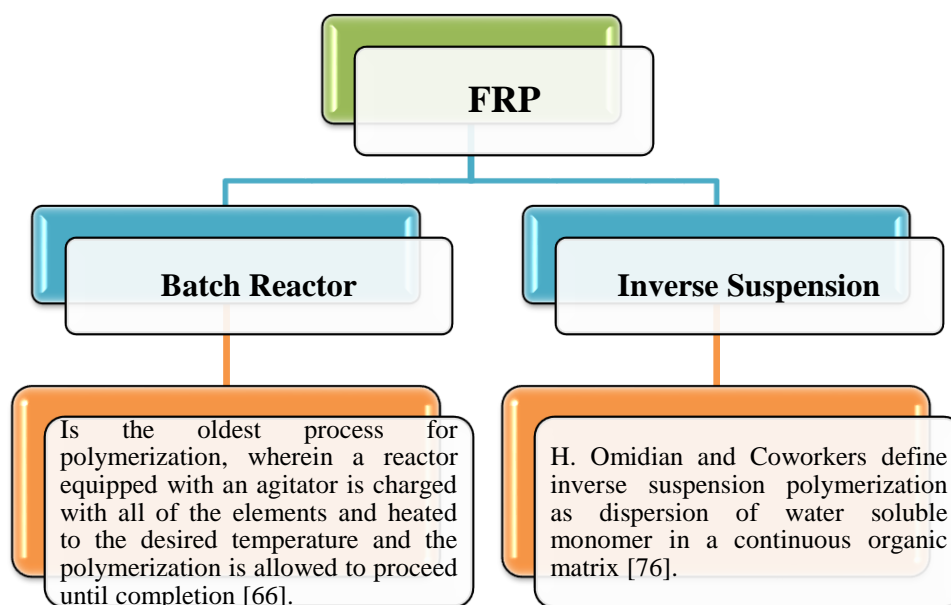


Figure 4.3 - Schematic illustration of different techniques of free radical polymerization used in this work.

## 4.2.1. Experimental Procedure

In FRP the procedure to obtain a monomer solution was the same used in CRP (section 4.1.1.1.1) but without the RAFT agent. In the following sections the procedure used in the two methods is described in detail.

### 4.2.1.1. Batch reactor

To produce MIPs is necessary add a template in the monomer solution, the templates used in this study were the selected drugs. After mixing all the elements in the flask and with an agitator, these were placed in paraffin bath, previously prepared on a heating plate at temperature mentioned in Table 4.2, and remained there during 24 hours. A scheme of the batch reactor is presented in Figure 4.4.

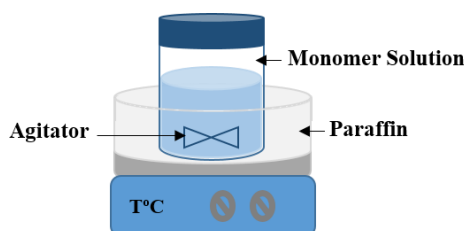


Figure 4.4 - Scheme of the polymerization in batch reactor.

#### 4.2.1.2. Inverse Suspension

In inverse suspension not only was it necessary to prepare the monomer solution but also an oil solution. The surfactant and the solvent were weighed (see Table 4.3). The elements were mixed in a flask and placed in a preheated paraffin bath, with vigorous stirring. After stabilizing the temperature, the monomer solution was added to oil solution, as shown Figure 4.5.

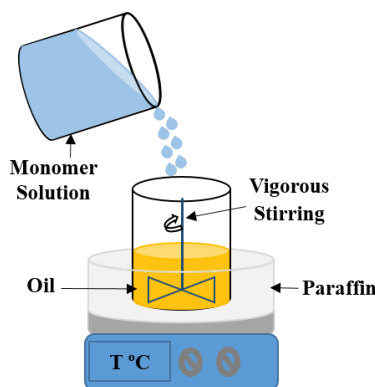


Figure 4.5 - A scheme of inverse suspension polymerization.

The synthesis can also be performed through the microwave synthesis system in a Discovery<sup>®</sup>SP equipment (see Figure 4.6). This equipment has the advantages of synthesize more quickly than conventional system, with the camera, that can be integrated into the system, it checks the different phases that occur during the synthesis and by Synergy<sup>™</sup> software a detailed report of temperature, pressure and time required in the synthesis reaction can be obtained. In Table 4.4 are presented the materials and amounts used in the synthesis, and in Annex 1 is present the detailed report of the synthesis.



Figure 4.6 - Discovery<sup>®</sup>SP equipment with a microwave synthesis system.

The equations 4.1 to 4.8 are presented to describe some of the parameters in Tables 4.1 to 4.4.

Weight fraction of monomer:

$$Y_m = \frac{\text{mass of functional monomer} + \text{mass of crosslinker}}{\text{mass of functional monomer} + \text{mass of crosslinker} + \text{mass of solvent}} \times 100 \quad (4.1)$$

Initiator mole fraction:

$$Y_I = \frac{\text{mol of initiator}}{\text{mol of functional monomer} + \text{mol of initiator}} \times 100 \quad (4.2)$$

Cross-linker mole fraction:

$$Y_{CL} = \frac{\text{mol of crosslinker}}{\text{mol of functional monomer} + \text{mol of crosslinker}} \times 100 \quad (4.3)$$

Cross-linker/Template mole ratio:

$$Y_{CL/T} = \frac{\text{mol of crosslinker}}{\text{mol of template}} \quad (4.4)$$

Functional monomer/Template mole ratio:

$$Y_{M/T} = \frac{\text{mol of functional monomer}}{\text{mol of template}} \quad (4.5)$$

RAFT agent mole ratio:

$$Y_{RAFTag/I} = \frac{\text{mol of RAFT agent}}{\text{mol of initiator}} \quad (4.6)$$

Solvent mole ratio:

$$Y_C = \frac{\text{mass of oil solvent}}{\text{mass of functional monomer} + \text{mass of crosslinker} + \text{mass of initiator} + \text{mass of solvent}} \quad (4.7)$$

Surfactant mole fraction:

$$Y_{SUR} = \frac{\text{mass of surfactant}}{\text{mol of oil solvent}} \times 100 \quad (4.8)$$

### 4.3. Template Removal

After synthesis, the template removal is a crucial step for a correct characterization of the MIP. For this purpose, an Soxhlet extractor was used, this technique was developed by Franz von Soxhlet in 1879 [101]. It has been a standard technique for more than a century, it serves, not only to remove and separate compounds of interest, but also other compounds that could interfere with subsequent steps of the analytical process [102].

#### 4.3.1.1. Experimental procedure

This equipment as shown in Figure 4.7 consists in four connected components, such as a condenser, an extraction chamber, a boiling flask and a heating mantle. The sample was placed in the extraction chamber, in this case the MIP (within a cartridge and covered with filter paper in order not to lose the sample). The solvent used for the extraction of the template was a solution of methanol and  $W_{DI}$  (50/50) that was poured into the boiling flask and afterwards in the heating mantle. The condenser is connected to two tubes, one connected to a water tap, and the other to a drainpipe, in order to ensure the permanent passage of water.

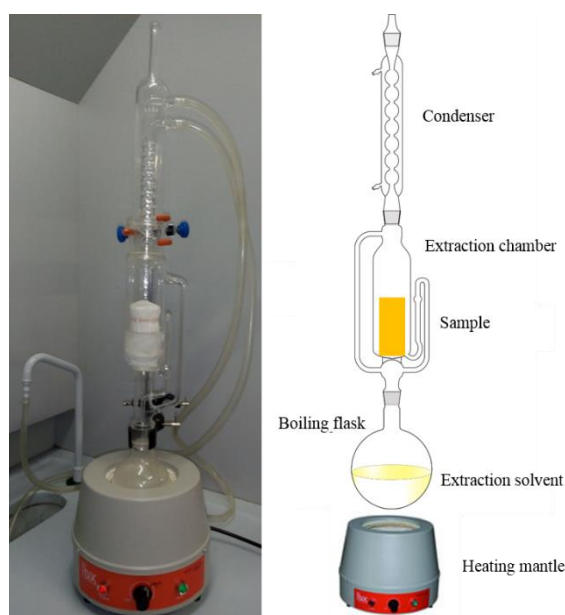
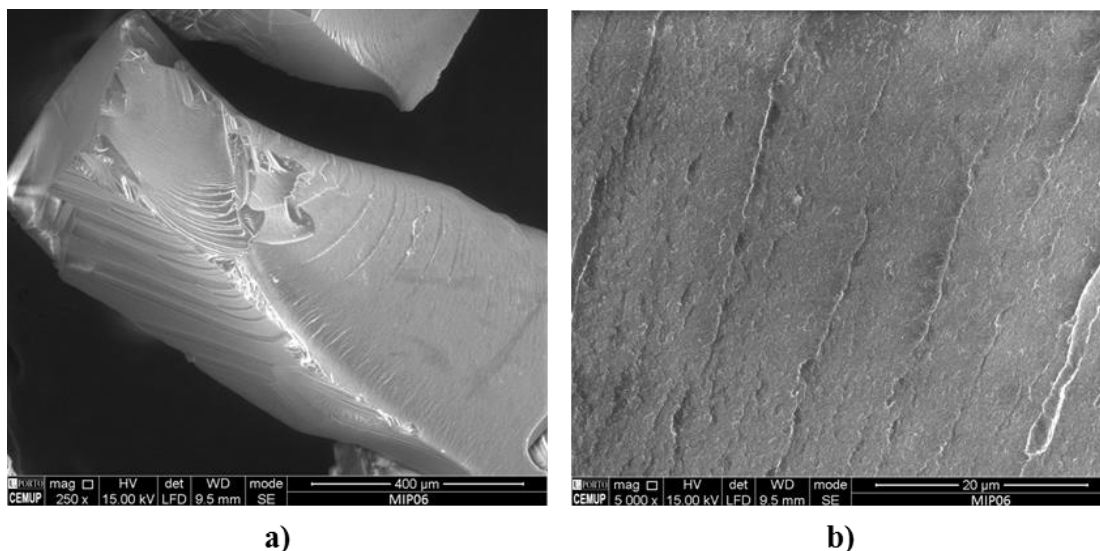


Figure 4.7 - Scheme of the Soxhlet used in this work.

After connecting the components of the equipment, the cleaning process will start as soon as the solvent reaches the boiling point. When this happens, the steam will go through the system to the condenser, where it will cool and fall into the chamber in drop form. Once the chamber is full, the solvent will go back into the boiling flask and starts a new cycle. As this is a slow process, it may take several days until the template is completely removed. To check if the MIP was cleaned, a sample was withdrawn of the solvent and it was analyzed in the UV Spectrophotometer. If the MIP was not clean, the process would be repeated for some time until it was cleaned.

#### 4.4. Analysis by Scanning Electron Microscopy (SEM)

In Figure 4.8 to 4.10 are present some examples of SEM micrographs related to MIPs and NIPs, synthesized by batch and inverse suspension. Small particles were obtained (some with less than 1  $\mu\text{m}$ ) when synthesized by inverse suspension and monoliths synthesized by batch. The analysis by scanning electron microscopy shown in Figure 4.8 to 4.10 were held in the Microscopy Center of Porto University (CEMUP).



**Figure 4.8** - SEM micrographs of MIPs and NIPs produced. a) and b) MIP<sub>06</sub> synthesized by batch reactor with 5FU.

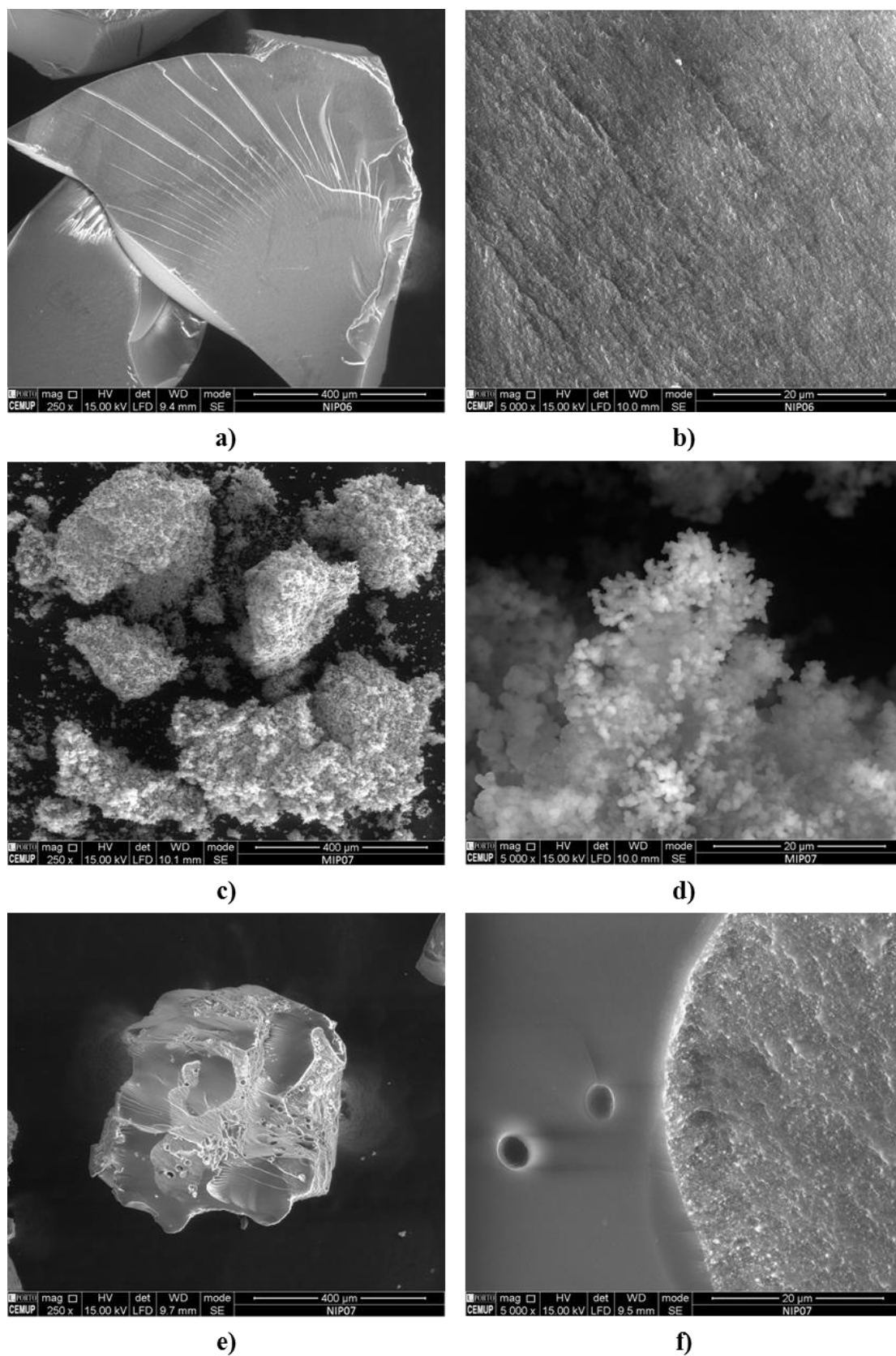


**Figure 4.9** - SEM micrographs of MIPs and NIPs produced. a) and b) NIP<sub>06</sub> synthesized by batch reactor.; c) and d) MIP<sub>07</sub> synthesized by inverse suspension with 5FU; e) and f) NIP<sub>07</sub> synthesized by inverse suspension.

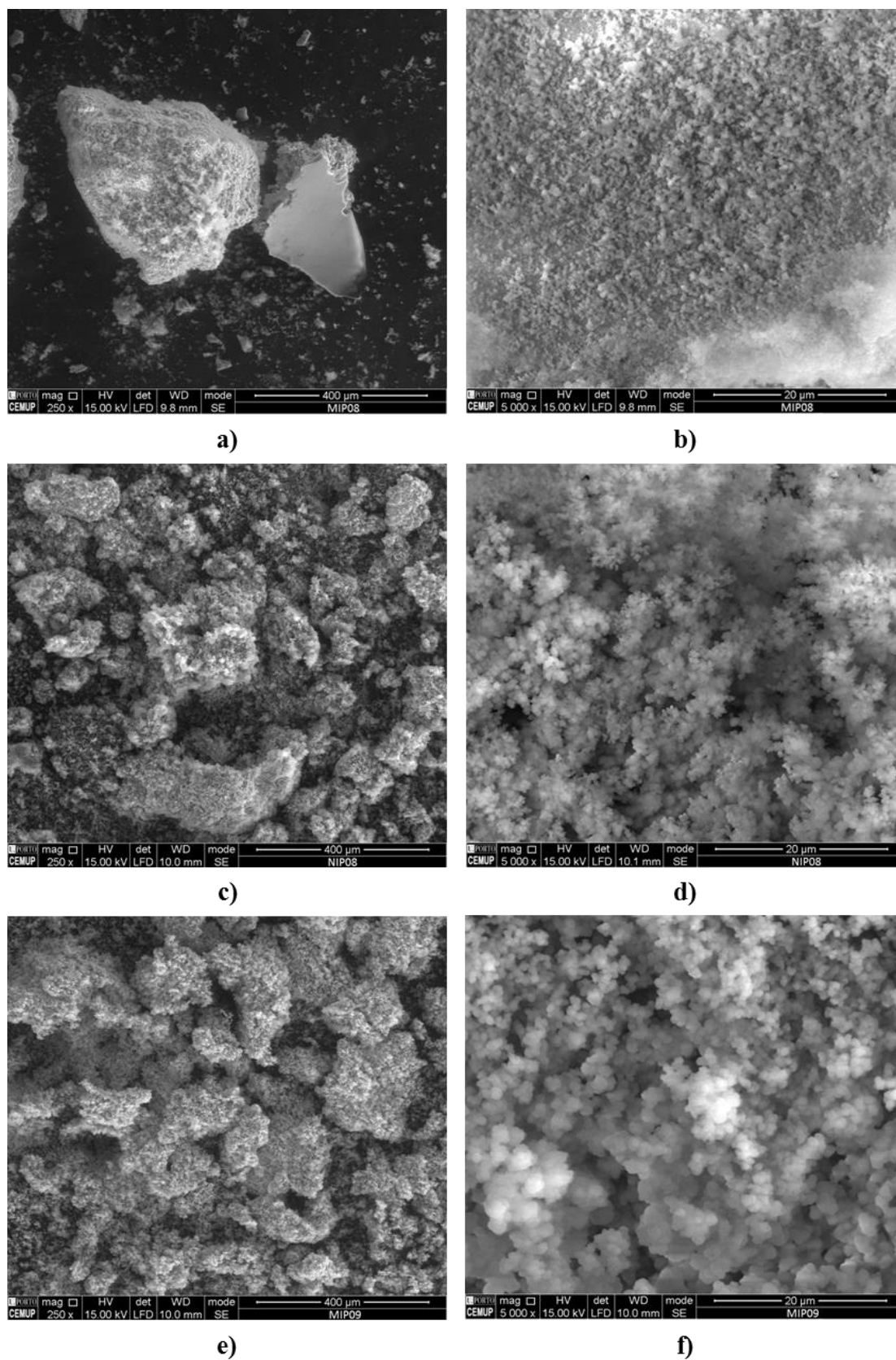


**Figure 4.10** - SEM micrographs of MIPs and NIPs produced a) and b) MIP<sub>08</sub> synthesized by inverse suspension with 5FU; c) and d) NIP<sub>08</sub> synthesized by inverse suspension, e) and f) MIP<sub>09</sub> synthesized by inverse suspension with CAF.

**Table 4.1** - Experimental conditions used in Micro-reactor synthesis of NIPs.

Material	Monomer (M)	Cross-linker (CL)	Template (T)	Initiator (I)	Solvent (S)	RAFTag	Y <sub>m</sub>	Y <sub>I</sub>	Y <sub>CL</sub>	Y <sub>CL/T</sub>	Y <sub>M/T</sub>	Y <sub>RAFTag/I</sub>	T (°C)
NIP <sub>01</sub>	AA	MBAm	-	AIBN	DMF	CPA	41.13	1.04	2.12	-	-	0.10	70 (± 2)
NIP <sub>02</sub>	AA	MBAm	-	V50	W <sub>DI</sub>	CPA	40.00	1.00	2.00	-	-	0.10	70 (± 2)

**Table 4.2** - Experimental conditions used in Batch Reactor synthesis of MIPs and NIPs.

Material	Monomer (M)	Cross-linker (CL)	Template (T)	Initiator (I)	Solvent (S)	Y <sub>m</sub>	Y <sub>I</sub>	Y <sub>CL</sub>	Y <sub>CL/T</sub>	Y <sub>M/T</sub>	T (°C)
MIP <sub>03</sub>	MAA	MBAm	5FU	V50	W <sub>DI</sub>	40.54	1.04	2.07	1.00	47.15	50 (± 2)
NIP <sub>03</sub>	MAA	MBAm	-	V50	W <sub>DI</sub>	40.54	1.04	2.07	-	-	50 (± 2)
MIP <sub>04</sub>	NIPA	MBAm	5FU	V50	W <sub>DI</sub>	9.33	0.997	2.03	0.99	48.00	50 (± 2)
NIP <sub>04</sub>	NIPA	MBAm	-	V50	W <sub>DI</sub>	9.33	1.00	2.04	-	-	50 (± 2)
MIP <sub>05</sub>	MAA	EGDMA	5FU	AIBN	DMF	30.77	3.42	4.77	0.44	8.71	70 (± 2)
NIP <sub>05</sub>	MAA	EGDMA	-	AIBN	DMF	30.77	3.44	4.77	-	-	70 (± 2)
MIP <sub>06</sub>	MAA	EGDMA	5FU	AIBN	DMF	58.39	1.79	55.46	9.98	8.01	70 (± 2)
NIP <sub>06</sub>	MAA	EGDMA	-	AIBN	DMF	58.61	1.76	55.28	-	-	70 (± 2)

**Table 4.3** - Experimental conditions used in Inverse Suspension synthesis of MIPs and NIPs.

Material	Monomer (M)	Cross-linker (CL)	Template (T)	Initiator (I)	Solvent (S)	SUR	Y <sub>m</sub>	Y <sub>I</sub>	Y <sub>CL</sub>	Y <sub>CL/T</sub>	Y <sub>MT</sub>	Y <sub>C</sub>	Y <sub>SUR</sub>	T (°C)
MIP <sub>07</sub>	MAA	EGDMA	5FU	AIBN	DMF /Heptane	Span80	58.47	1.74	55.54	10.00	8.00	1.48	0.99	70 (± 2)
NIP <sub>07</sub>	MAA	EGDMA	-	AIBN	DMF /Heptane	Span80	58.46	1.79	55.42	-	-	1.48	0.99	70 (± 2)
MIP <sub>08</sub>	MAA	TMPTA	5FU	AIBN	DMF /Heptane	Span80	65.87	1.74	55.61	10.03	8.00	1.22	0.99	70 (± 2)
NIP <sub>08</sub>	MAA	TMPTA	-	AIBN	DMF /Heptane	Span80	65.87	1.74	55.61	-	-	1.22	0.99	70 (± 2)
MIP <sub>09</sub>	MAA	EGDMA	CAF	AIBN	DMF /Heptane	Span80	58.48	1.74	55.56	10.01	8.01	1.48	0.99	70 (± 2)

**Table 4.4** - Experimental conditions used in CEM<sup>®</sup> Discovery synthesis of MIPs and NIPs

Material	Monomer (M)	Cross-linker (CL)	Template (T)	Initiator (I)	Solvent (S)	Surfactant (SUR)	Y <sub>m</sub>	Y <sub>I</sub>	Y <sub>CL</sub>	Y <sub>CL/T</sub>	Y <sub>MT</sub>	Y <sub>C</sub>	Y <sub>SUR</sub>	T (°C)
MIP <sub>10</sub>	MAA	TMPTA	CAF	AIBN	DMF /Heptane	Span80	65.87	1.75	55.61	10.00	7.98	1.22	1.02	80

## **Chapter 5. Characterization of Molecularly Imprinted Polymers**

This chapter presents theoretical and experimental concepts about the techniques used in the characterization of imprinted and non-imprinted polymers, such as solid phase extraction and frontal analysis. The adsorption and desorption of the drugs was tested in the MIPs/NIPs.

To perform the characterization tasks presented in this section were used the equipments described in Table 3.5.

### **5.1. Solid Phase Extraction**

Solid phase extraction (SPE) is an extraction technique based on the selective partitioning of one or more components (analyte) between two phases, one of which is a solid phase (sorbent) and the second phase typically is a liquid [103], but it may also be a gas or a fluid [104]. According to Sellergen [48] SPE has become a widely used technique for sample pretreatment as it is easily automated, flexible and environmental friendly. This method can be performed off-line, the sample preparation being separated from the subsequent chromatographic analysis, or on-line by direct connection to the chromatographic system [48, 105].

MIPs can be applied to the clean-up and pre-concentration of analyte of environmental and pharmaceutical interest [48], as the selective sorbent of SPE [106]. The off-line mode it has been mainly used in the MIPs before using some detection technique [48].

The SPE process usually includes four steps as shown in Figure 5.1:

### 1. Conditioning

The conditioning step, it is important to create equilibrium between the aqueous solution and the sorbent. The solvent A is used to remove impurities that may be present in the material.

### 2. Loading

In this step the load solvent passes through the column using a vacuum pump. The flow rate is made more slowly as possible, to promote efficient mass transfer of the solutes to the sorbent.

### 3. Washing

The washing step uses the solvent B to remove some impurities in the load solvent without eluting the solutes.

### 4. Eluting

Eluting is the last step, where the analyte of interest is eluted from the sorbent with a solvent C, this solvent needs to be appropriated to break the analyte-sorbent interaction and should be compatible with the final analysis.

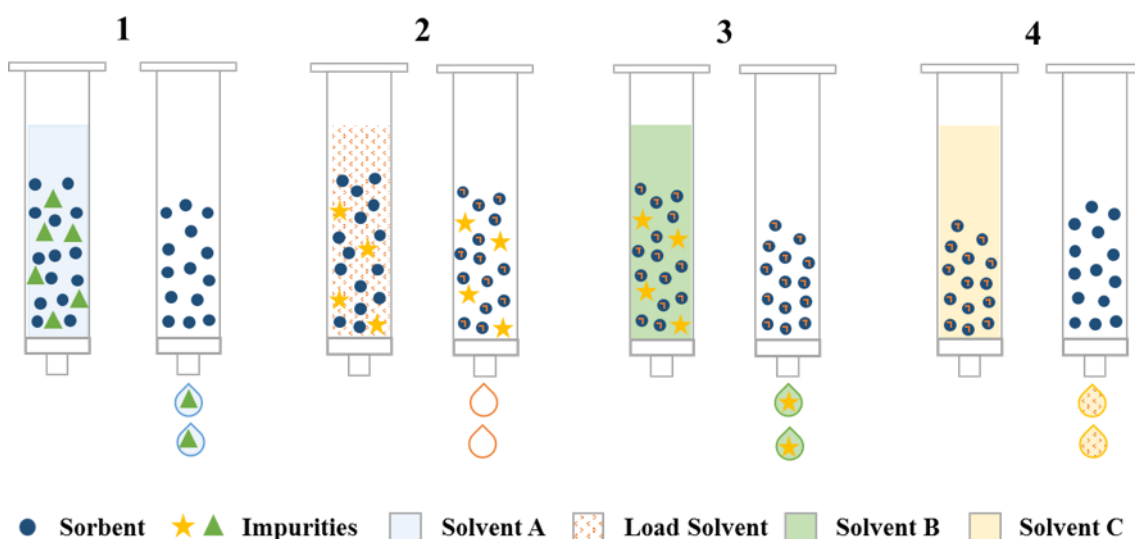


Figure 5.1 - Scheme of SPE steps, 1. Conditioning, 2. Loading, 3. Washing, 4. Eluting.

The SPE is a method of preparing samples that is widely used because it is quite simple, fast, easy to perform and inexpensive to verify the affinity the material with the molecule.

### 5.1.1. Experimental Procedure

The SPE tests were performed in four steps as described in section 5.1 the materials and the solvents that were used are described in Table 5.1. The first step was the conditioning of the material with deionized water ( $W_{DI}$ ) during 24 hours, and then the solvent was removed with the vacuum pump connected in SPE system (see Figure 5.2). Thereafter in the loading step 5 mL of solutions with different drugs at a concentration of 0.1 mM were used. In order to have a reference, a small amount of the mother solution of each drug was measured by UV before being placed with the material. After that, the solution was placed in the column, and was removed drop by drop into a flask for analysis in the UV spectrophotometer, where was measured the absorbance of each solution collected, to calculate the fraction of drug which was retained in the polymer. The adsorbed fraction was obtained by the equation 5.1.

$$R = \frac{A_0 - A_1}{A_0} \quad (5.1)$$

Where:

$R$  – Fraction of drug that is retained in the polymer;

$A_0$  – The UV absorption (in UV units) of the mother solution;

$A_1$  – The UV absorption (in UV units) of the aqueous solution after the adsorption process.

In the third step, washing, 5 mL of WDI was placed in the column. When removed and analyzed in UV it was verified if there was drug release. The elution step has the objective to release the remaining drug in the polymer. For that, 5 mL of a solution of methanol and deionized water (50/50) was placed in the column, and afterwards removed and analyzed in UV. The released fraction is obtained by the equation 5.2.

$$R_1 = \frac{A_2}{A_0 - A_1} \quad (5.2)$$

Where:

$R_1$  – Amount of drug released;

$A_0$  – The UV absorption (in UV units) of the mother solution;

$A_1$  – The UV absorption (in UV units) of the aqueous solution after the adsorption process;

$A_2$  – The UV absorption (in UV units) of the aqueous solution after passing  $W_{DI}$  or MeOH/ $W_{DI}$

After, the materials were cleaned with 10 mL MeOH solution and  $W_{DI}$ . The material was conditioned for 1 hour with  $W_{DI}$ , then steps Loading, washing and Eluting were repeated. At the end this procedure was repeated once again.

**Table 5.1** - Amount of polymer and solvents used in SPE tests.

Material	Mass (mg)	Load Solvent 0.1 mM	V (mL)	Solvent A / Solvent B	V (mL)	Solvent C	V (mL)
MIP <sub>03</sub>	160.0		5		≈3 / 5		5
NIP <sub>03</sub>	160.1		5		≈3 / 5		5
MIP <sub>04</sub>	160.8	5FU	5		≈3 / 5		5
NIP <sub>04</sub>	159.5		5		≈3 / 5		5
MIP <sub>06</sub>	159.9		5		≈3 / 5		5
NIP <sub>06</sub>	159.8	5FU, CAF	5		≈3 / 5	MeOH/ $W_{DI}$	5
MIP <sub>07</sub>	160.0		5	$W_{DI}$	≈3 / 5	(50 / 50)	5
NIP <sub>07</sub>	160.6	5FU <sup>pH 2</sup> , 5FU <sup>pH 8</sup> , CAF, U	5		≈3 / 5		5
MIP <sub>08</sub>	160.8		5		≈3 / 5		5
NIP <sub>08</sub>	160.5		5		≈3 / 5		5
MIP <sub>09</sub>	160.2	5FU, CAF	5		≈3 / 5		5
NIP <sub>07</sub>	160.4		5		≈3 / 5		5

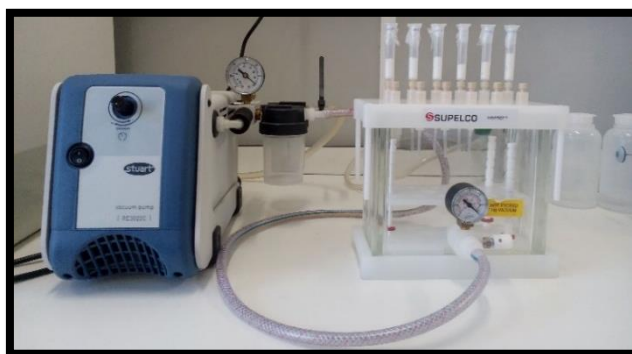


Figure 5.2 - SPE system connected to a vacuum pump.



Figure 5.3 - UV Spectrophotometer system installed in the laboratory (LPQ).

### 5.1.2. Results and Discussion

All the materials in Table 5.1 have been tested with a solution of 5FU, in Figure 5.4 are present the results obtained. It wasn't possible to obtain results of MIP<sub>04</sub> and NIP<sub>04</sub>, because they blocked the outlet of the column, blocking the passage of the solutions for analysis. The NIP<sub>08</sub> had better results than MIP<sub>08</sub>, this can be explained by the possible exchange of materials in the synthesis process, which was confirmed by subsequent studies. In the others materials, as expected the MIPs have a higher affinity for the molecule than the NIPs, i.e. retained more drug. The rate of adsorption of the materials synthesized by inverse suspension (MIP<sub>07</sub>, NIP<sub>07</sub>, MIP<sub>09</sub>) is higher ( $\approx 148\%$ ) than the rate of the materials synthesized in batch (MIP<sub>03</sub>, NIP<sub>03</sub>, MIP<sub>06</sub>, NIP<sub>06</sub>). Observing the same figure it can be seen that the highest release rate occurs in the washing step.

It was studied the adsorption of CAF in some materials, in order to compare with the adsorption of 5FU, because they have a very different molecular structure. In Figure 5.5 are presented the comparison of the amounts of drugs retained and it is clear that the MIP<sub>06</sub> and MIP<sub>07</sub> adsorb more CAF than 5FU. It can be explained by the fact that ionic interactions overlap the molecular imprinting.

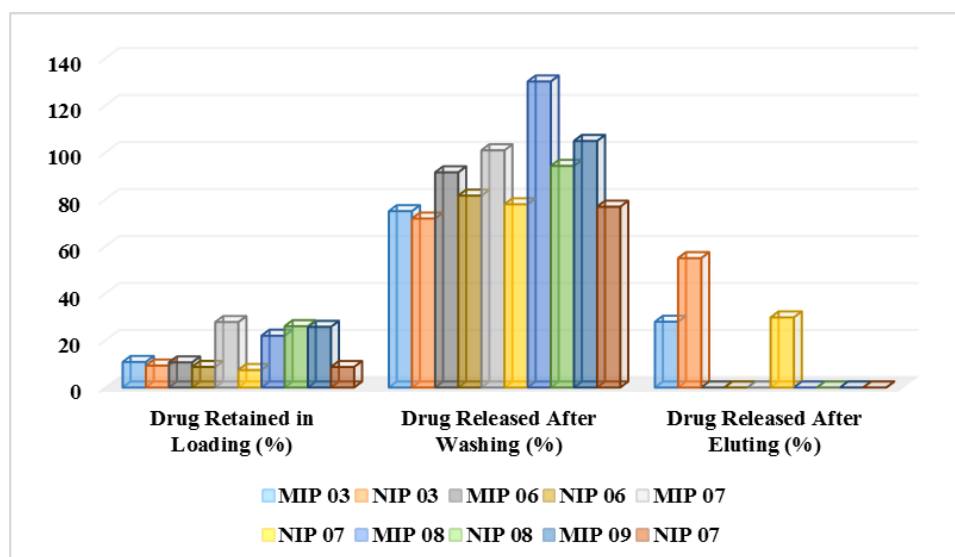


Figure 5.4 - Comparison of the amount of drug adsorbed and released in the different MIPs and NIPs.

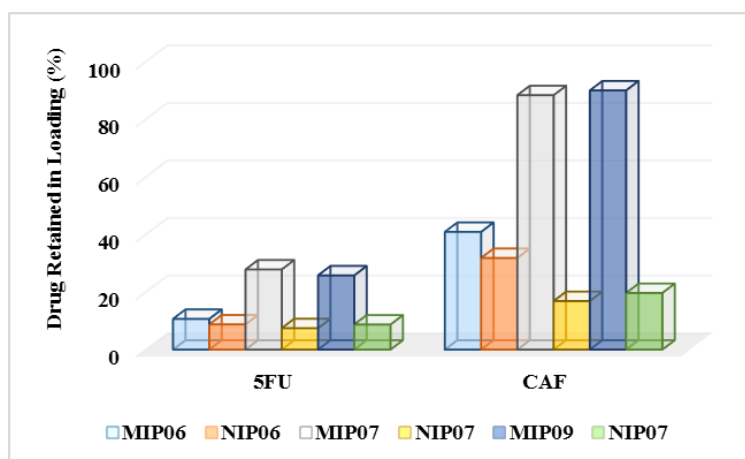


Figure 5.5 - Comparison of the amount of 5FU and CAF retained in MIPs and NIPs.

It was also tested for MIP<sub>07</sub> and NIP<sub>07</sub> the adsorption of uracil (UR) and the variation of pH of the 5FU solution (pH 2 and pH 8). The results of the adsorption of pH<sub>2</sub>, pH<sub>8</sub> and U were similar to results of 5FU as can be seen in Annex 10, 11 and 13, respectively. These results are a consequence of the similar structure of the 5FU and U molecules.

## 5.2. Frontal Analysis



### 5.2.1. Measurement of Drug Adsorption and Release

With the objective to evaluate the adsorption and release of different drugs in different types of polymers, the experimental study of these processes in packed columns operating in continuous way was accomplished. For that purpose, a predefined dry mass of polymer was placed in one of the columns showed in Figure 5.6 (the dimensions of the columns are detailed in Table 5.2), and then made the packaging (swelling) of the polymer by pumping water through the column to obtain stable pressure conditions in the system (e.g. 2.5 MPa considering a pumping rate of 0,33 mL/min).



**Figure 5.6** - Packing columns used in experimental studies of the saturation and release of drugs in polymers considering continuous operation mode.

**Table 5.2** - Dimensions of columns used in experimental studies.

Column	Internal Length (mm) 	Internal Diameter (mm) 	V (mL)
1	10.00	4.60	0.17
2	33.00	4.60	0.55
3	50.00	4.60	0.83
4	33.00	8.00	1.66
5	33.00	8.00	1.66

To accomplish these studies a system of Gel Permeation Chromatography (GPC) or Size Exclusion Chromatography was used (SEC), including a pumping module for solvent and sample injection that is also equipped with four detection signals, namely

refractive index (IR), light scattering (LS), Intrinsic viscosity (IV-DP) and ultraviolet (UV). UV detection is especially useful in the context of the tests conducted here as will be detailed below. In Figure 5.7 it is presented a simplified schematic representation of the GPC system used in this work.

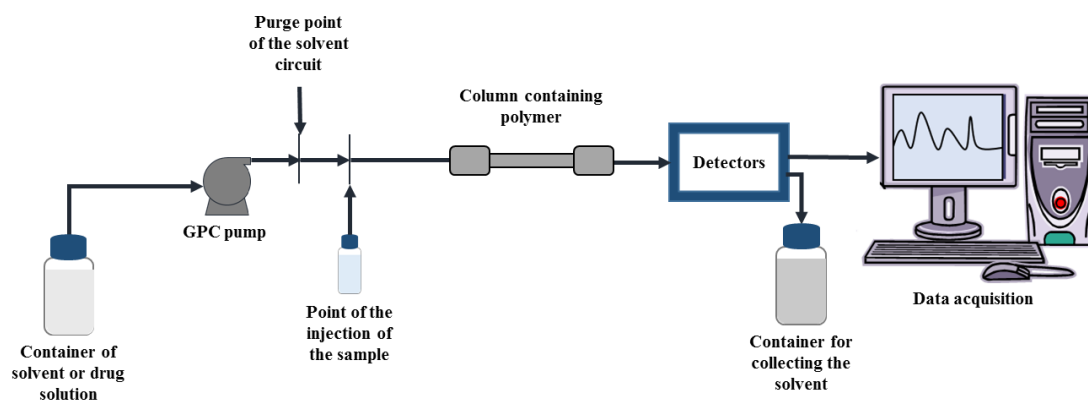


**Figure 5.7** - Simplified schematic representation of the GPC system used in this work to study experimentally the saturation and release of drugs in polymers considering continuous operation mode.

### 5.2.1.1. Tests with an Anionic Polymer based in Methacrylic Acid

In order to evaluate the affinity between some drugs considered in this work and anionic polymers structure, tests were conducted using the network MIP<sub>06</sub> polymer (polymer of methacrylic acid with synthesis by FRP) as filler for the column. For this purpose 15 mg of dry polymer were placed in the packed column that was subsequently integrated in the GPC system. During 24 hours water was pumped into the GPC system at a flow rate of 0.1 mL/min in order to pack the polymer inside the column since it is known that it will swell in the presence of this solvent. Note that the amount of dried polymer that was packed in the column was estimated based on the swelling ratio of the polymer (over 100 times) and the internal volume of the column (0.17 mL) [107].

#### 5.2.1.1.1. Injection of aqueous solutions containing drugs

In these tests, the injection (impulse concentration) of aqueous solutions of different drugs on the GPC system has been performed. For this purpose, it was considered the mechanism of the automatic injection on the GPC device (the volume of the injected solution is 100  $\mu$ L). In order to evaluate the effect of the polymer in the retention of different types of molecules, in each case, the injection was performed in the presence

and absence of the column containing the polymer. These tests were performed considering the GPC system operating at 25 °C and 30 °C. Given the high UV absorption of the drugs considered in this work, the signal from the detector was used to monitor the concentration at the column outlet of the molecules considered [107].

Figure 5.8 shows the signal recorded on UV absorption detector as a result of injection into the GPC system of an aqueous solution of the 5-Fluorouracil with 0.1 mM concentration. Here is presented normalized UV signal which is obtained by dividing the actual value by the maximum signal observed. This test was performed assuming a flow rate of eluent of 0.1 mL/min monitoring with UV absorbance at 265 nm. Comparison of the peaks observed in the presence and absence of polymer column allows concluding that there is an effective affinity between the drug and the material under consideration (note the high retention of the drug in the system when the polymer column is used).

It should also be noted that the retention time (or elution) of drug molecules in the system ( $t_e$ ) and the corresponding retention volume (or elution) ( $V_e$ ) are related by the flow considered in the operation of the system ( $Q$ ):

$$V_e = Q \times t_e \quad (5.3)$$

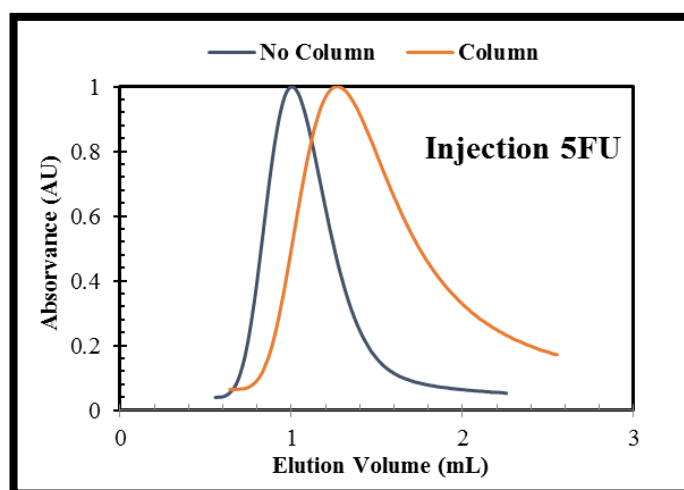


**Figure 5.8** - Signal recorded on UV absorption detector as a result of injection into the GPC system an aqueous solution of the 5-Fluorouracil with 0.1 mM concentration. Here is presented normalized UV signal which is obtained by dividing the actual value by the maximum signal observed. This test was performed assuming a flow rate of eluent of 0.1 mL/min monitoring with UV absorbance at 265 nm. Comparison of the peaks observed in the presence and absence of polymer column allows to conclude that there is an effective affinity between the drug and the polymer network determined (note the high retention of the drug in the system when the polymer column is used).

### **5.2.1.1.2. General Aspects about Experimental Procedure for Saturation and Release of Drugs in Continuous Mode Operation**

In Figure 5.9 and 5.10 it is showed the schematic representation of the ideal saturation (adsorption) and release (desorption) process of drugs in polymers placed in columns operating in continuous mode.

#### **5.2.1.1.2.1. Saturation process**

To accomplish the saturation process, the GPC system with the polymer column is initially supplied with pure water (drug concentration  $C = 0$ ) during approximately 4 hours to stabilize the detectors (null concentration of drug). After that, the system will be supplied with an aqueous solution containing the selected drug (drug concentration  $C=C_0$ ), thus causing a variation in the drug concentration in the entry of the column. After some time of operation is detected (in these tests UV monitoring was used) the presence of drug in the output current of the column. If this process is carried out during a sufficiently long period of time, the polymer presented in the column will reach saturation of the drug (i.e. becomes unable to adsorb additional amounts of the molecule) and the concentration at the column outlet becomes constant [107].

#### **5.2.1.1.2.2. Release process**

To perform the study of the release (desorption) of the drug, the saturated polymer (as describe in 5.2.1.1.2.1) is used, and at a given time, the feed containing the drug ( $C = C_0$ ) is replaced by the feed of pure water ( $C = 0$ ). This causes a negative step change on the drug concentration at the entry of the column. The passage of pure water in the polymer causes the release (desorption) of the drug which at the end of a long time of operation should be totally released. After the end of drug release, the detectors measured the presence of pure water [107].

The procedures described in 5.2.1.1.2.1 and 5.2.1.1.2.2 and outlined in Figures 5.9 and 5.10 respectively, are in ideal operating conditions. However, in practice, some experimental problems cause variations from this ideal behavior. One of the aspects to be

taken into special consideration when carrying out these tests relates to the initiation of the processes of drug supply or water in steps of saturation and release, respectively. In fact, when the change of feed reservoir is made (see Figure 5.7), it is necessary to conveniently purge the tubing located between the reservoir and the entry of the column (see Figure 5.7) to ensure that it does not supply a mixing of the two solutions. It should be noted that the volume of fluid present in these feed pipes is large enough to cause mixing of the two solutions (containing/not containing drug) therefore causing deviations to the feed steps represented in Figures 5.9 and 5.10. This difficulty is enhanced by the fact that in these tests relatively low feed rates are being used (to ensure acceptable pressures in the columns) which worsens the effects of possible mixing of these solutions [107].

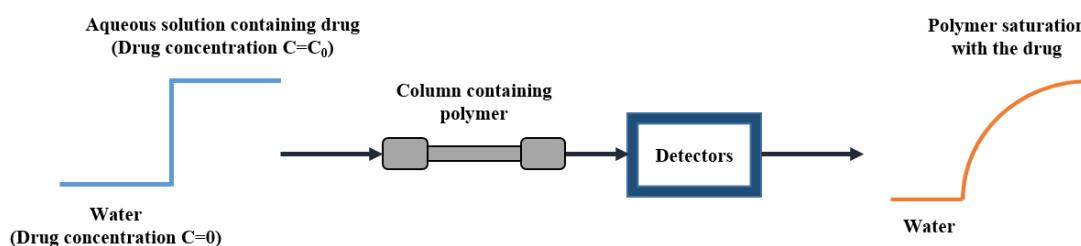


**Figure 5.9** - Schematic representation of the experimental procedure associated with the saturation of a material with a drug considering continuous operation mode. With this purpose, the GPC system with the material column is supplied with pure water (concentration of drug  $C = 0$ ) for a sufficiently long period of time until a stable behavior of the detectors (null drug concentration). At a given instant ( $t = 0$ ) the system is feed with an aqueous solution containing the selected drug (drug concentration  $C = C_0$ ), thereby causing a step change of the drug concentration at the entrance of the column. After some time of operation is detected (e.g. using UV) the presence of the drug in the output stream of the column. If this process is carried out for a sufficiently long period of time, this material will reach saturation of the drug (i.e. becomes incapable of adsorbing additional amounts of this molecule), and the concentration at the column outlet becomes constant (Adapted from [107]).

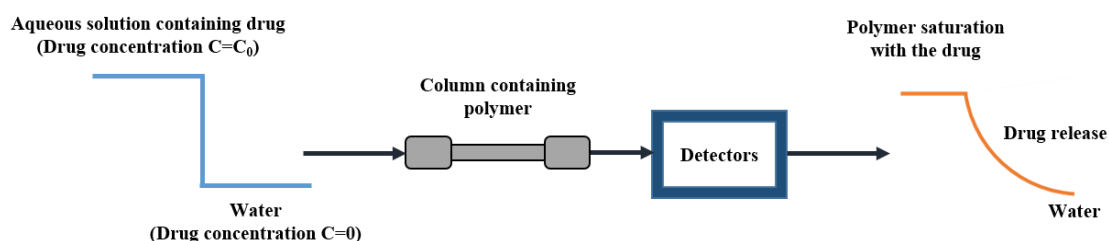


**Figure 5.10** - Schematic representation of the experimental procedure associated with the release of a drug from a material considering continuous operation mode. Starting with the material in a state of saturation (see Figure 5.9), at a given instant, the feed containing the drug ( $C = C_0$ ) is replaced with the feed containing pure water ( $C = 0$ ). In this way it causes a negative step change on the drug concentration at the column inlet. The percolate of pure water in the hydrogel causes desorption (release) of the drug and after a sufficiently long operating time it should release the drug entirely. After the end of drug release, the detectors measured the presence of pure water (Adapted from [107]).

### 5.2.2. Theoretical Foundations of Frontal Analysis

Frontal analysis is considered the most accurate chromatographic technique for determination of adsorption isotherms of a component on the stationary phase (e.g. in a liquid / solid process). As described above, this method consists in replacing the current of the mobile phase (e.g. water) to a solution containing the studied component (e.g. a drug) with a known concentration. The "breakthrough" curve (elution curve) of the solute is registered on the outlet of the column (e.g. using a UV detector). A material balance of the solute (mass conservation) between the moment when the solution begins to flow through the column, and the instant it reaches saturation (concentration step) allows to calculate the amount adsorbed on the stationary phase ( $q^*$ ) that is in equilibrium with the mobile phase (where the solute concentration is  $C_0$ ) [107].

In Figure 5.11 are schematically represented the different stages in an adsorption process for a column operating in continuous mode.

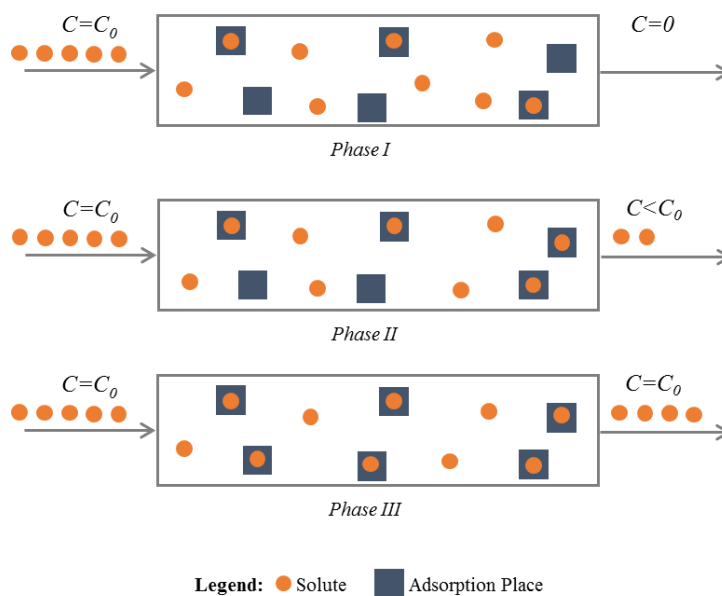


**Figure 5.11** - Schematic representation of different liquid/solid adsorption phases in a column operating in a continuous process. In Phase I, the column has not been fully covered by the solute. There are adsorption sites occupied and other ones free with zero solute concentration at the column outlet. In Phase II, the column has been completely percolated by the solute but there are still free adsorption sites. At the outlet of the column is observed a value lower than the input concentration. In Phase III, all the adsorption places were occupied with a concentration observed in the outlet of the column equal to the initial concentration (saturation) (Adapted from [107]).

In Figure 5.12 to Figure 5.15 are given the details relating to the calculation method of the quantities of solute (e.g. drug) adsorbed onto the stationary phase (adsorbent) in a packed column operating continuously.

Amount of solute adsorbed per unit of volume of stationary phase, ( $V_a$ ):

$$q^* = \frac{C_0(V_{eq} - V_0)}{V_a} \quad (5.4)$$

Amount of solute adsorbed per unit of dry mass of the stationary phase, ( $m_s$ ):

$$q^* = \frac{C_0(V_{eq} - V_0)}{m_s} \quad (5.5)$$

The values of  $m_s$  and  $V_a$  are known by weighing the amount of dry material that is packed in the column and estimate of the volume that the material is going to occupy after the swelling process. One possibility is to consider that the materials can fill all of the geometrical volume of the column ( $VG$ ) once they have a high swelling capacity.

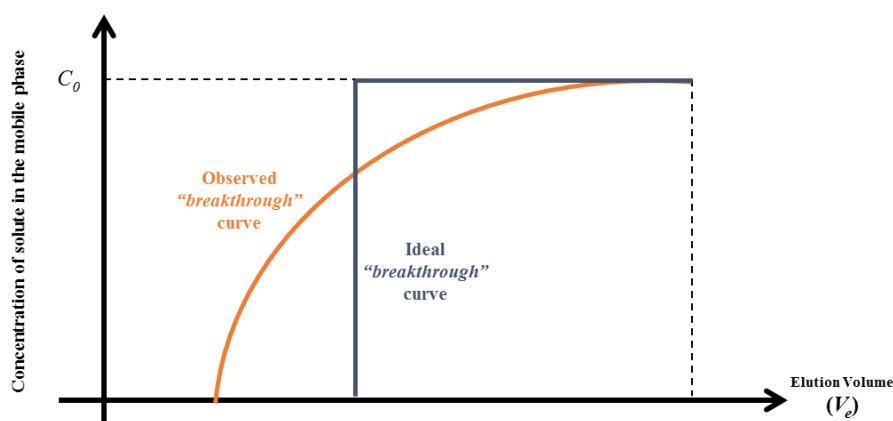


**Figure 5.12** - Schematic representation of the ideal "breakthrough" curve (without output of the solute before the saturation) and a real "breakthrough" curve (including Phases I, II and III with exit of solute from the column before adsorbent saturation) (Adapted from [107]).

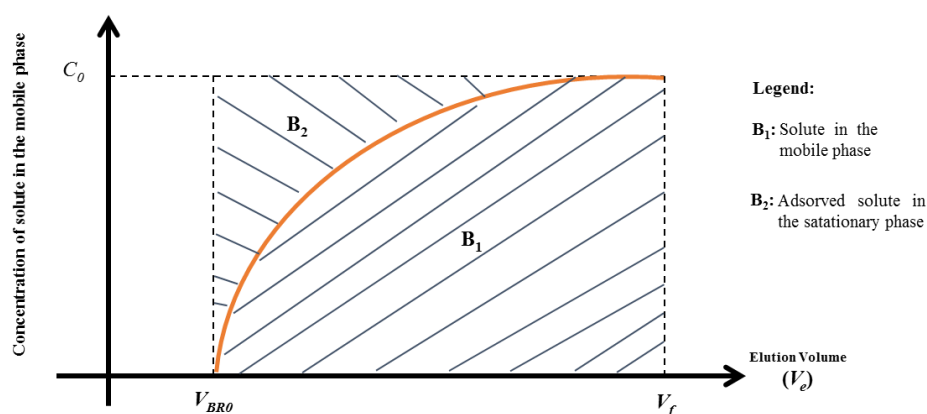


**Figure 5.13** - Schematic representation of the adsorption process between the beginning of the "breakthrough" curve (elution volume =  $V_{BRO}$ ) and the saturation (elution volume =  $V_f$ ). This period corresponds to Phase II. At this time, the total amount of solute introduced into the system is  $C_0 \times (V_f - V_{BRO})$  corresponding to the area  $B_1 + B_2$ . The area  $B_1$  represents the observed amount of solute in the mobile phase and, by difference,  $B_2$  is the amount of solute that was adsorbed in the solid during this period (Adapted from [107]).

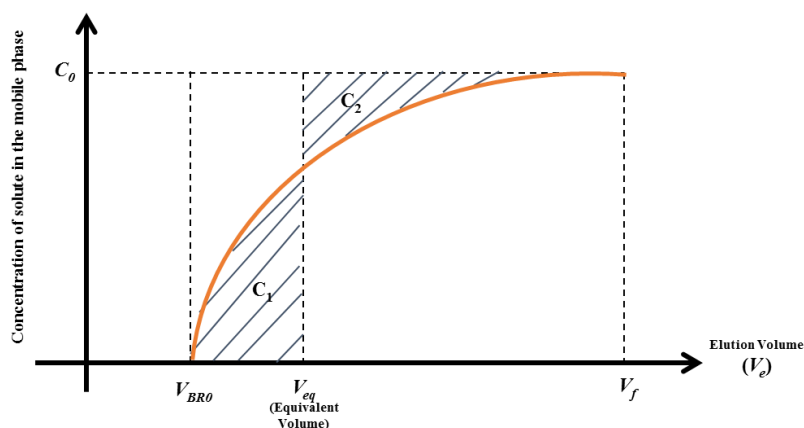


**Figure 5.14** - Schematic representation of the calculation of equivalent volume ( $V_{eq}$ ) to quantify the amount of solute adsorbed. The objective is to calculate the area  $B_2$  shown in Figure 5.13. In fact, comparing Figures 5.13 and 5.14, the area  $B_2$  may be substituted for the rectangle area  $C_0 \times (V_{eq} - V_{BR0})$  since it is ensured that the areas  $C_1$  and  $C_2$  are equal. Calculation of the equivalent volume ( $V_{eq}$ ) is therefore to find elution volume in which  $C_1 = C_2$  (Adapted from [107]).

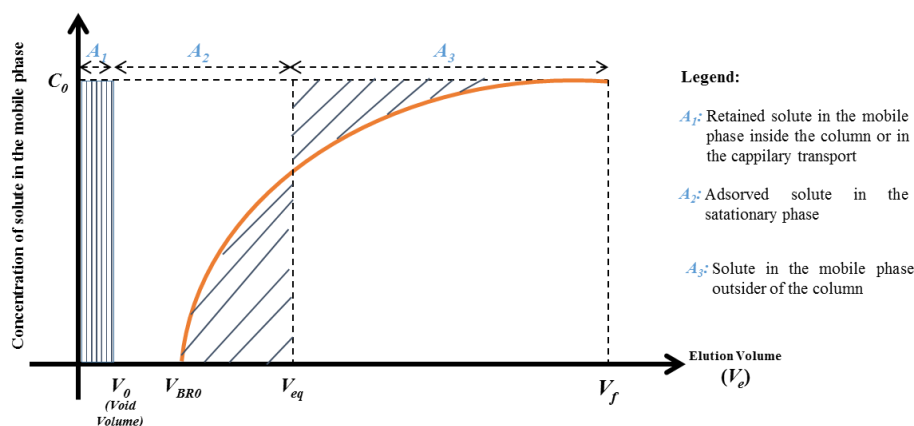


**Figure 5.15** - General representation of the quantification of the adsorption process running in column operating in a continuous mode including the void volume (quantifies the entrapped solute in the mobile phase inside the column or in the capillary transport), the adsorbed solute in Phase I, which matches the area of the rectangle  $C_0 \times (V_0 - V_{BR0})$  and also the amount of solute adsorbed in Phase II, which corresponds to the area of the rectangle  $C_0 \times (V_{eq} - V_{BR0})$ . The total amount of solute adsorbed onto the stationary phase is thus:  $C_0 \times (V_{BR0} - V_0) + C_0 \times (V_{eq} - V_{BR0}) = C_0 \times (V_{eq} - V_0)$  (Adapted from [107]).

Besides Frontal Analysis (FA), other simpler and faster chromatographic methods can be used to perform the evaluation of the performance of MIPs.

A simple test can be performed by packing MIP and NIP materials in chromatographic columns and try to obtain the recognition capabilities of MIPs through the comparison of the retention time of specific molecules (e.g. template) in the MIP and NIP stationary phases.

The retention factor  $r_F$  is a measure of the capability of the material that is used as stationary phase (MIP or NIP) to retain a specific molecule and is quantified through the equation 5.6:

$$r_F = \frac{t_R - t_0}{t_0} \quad (5.6)$$

With  $t_R$  representing the retention time of the molecule under study in the packed column and  $t_0$  representing the retention time of a void marker (e.g. acetone or methanol) in the same column (see Figure 5.16).

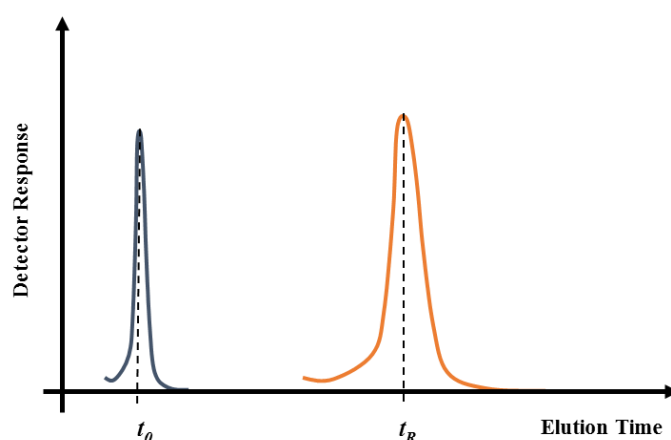


**Figure 5.16** - Representation of the retention time of a void marker  $t_0$  and the retention time of the molecule under study in the packed column ( $t_R$ ).

Through the comparison of the retention factors measured for the MIP and NIP materials, it is calculated the imprinting factor ( $IF$ ), defined by the equation 5.7:

$$IF = \frac{r_{F/MIP}}{r_{F/NIP}} \quad (5.7)$$

If high imprinting factors are observed (e.g.  $IF > 3$ ), the MIP material is effective in the retention of the target molecule comparatively to the NIP analogue material. Values of imprinting factors close to one indicate that the MIP material presents retention capabilities similar to the NIP adsorbent. Better adsorption performance of NIP comparatively to MIP is observed when imprinting factor is lower than the one measured.

The selectivity factor ( $SF$ ) allows evaluating the ability of the stationary phase (MIP or NIP adsorbent) to distinguish different molecules. This parameter is quantified through the ratio between the retention factor measured for the target molecule and the

retention factor measured for another non-target molecule, using the same adsorbent material:

$$SF = \frac{r_{Target}}{r_{Non-Target}} \quad (5.8)$$

High selectivity factors indicate the presence of specific (imprinted) sites in the material for retention of the target molecule preferentially to the non-target molecule.

### 5.2.3. Experimental Procedure

To perform the tests of FA were used three columns, number 2, 3 and 4 as shown in Figure 5.6, being that the most used was the column 2.

#### 5.2.3.1. Packing the columns

The first step is packing the column, for that, it was necessary the selected amount of MIP/NIP, as shown in Figure 5.17a. In this figure it can also be seen the elements of the column. On each end of the column there is a filter and two frits, these elements prevent the passage of the polymer or any impurities contained in solvents when the system is triggered. The Figures 5.17b and 5.17c, show the column before and after packaging the polymer, respectively.



**Figure 5.17** - Illustration of a column packing, a- elements of the column and polymer, b- column before packing, c- column after packing.

After packed, the column was integrated into a part of the GPC system (see Figure 5.18), where a test was made to check the flow (see Figure 5.19a), and then integrated throughout the system (see Figure 5.19b). This system must be previously cleaned, first

with a solution of filtered water ( $W_F$ ) and azide, and then only with  $W_F$ , to eliminate any bacteria or other impurities in the system.

When the column has been integrated in the system, the polymer packaging through the passage of  $W_F$  with a flow rate of 0.1 mL/min during 24 hours begins.

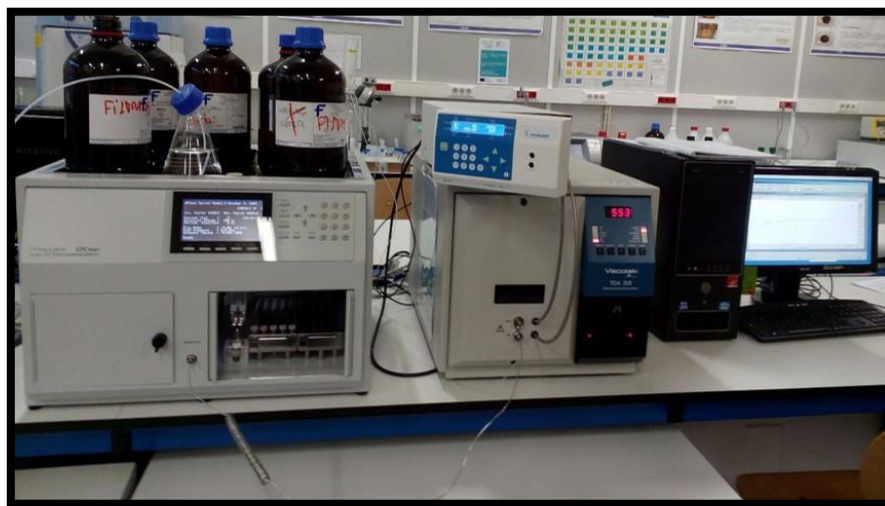


Figure 5.18 - GPC system installed in the laboratory (LSRE).

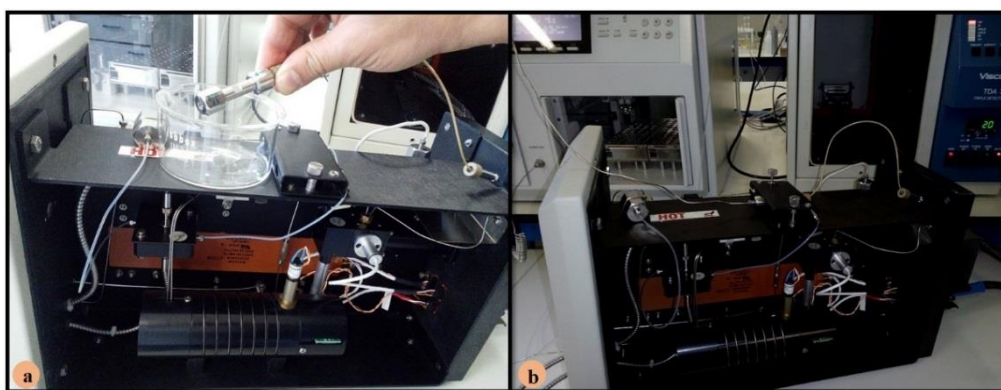


Figure 5.19 - Illustration of the integration of the column into the system, a. checking the flow, b. column packing (swelling).

### 5.2.3.2. Injection of drug

The injection was made through the automatic mechanism of GPC. It was injected 100  $\mu$ L of aqueous solutions of different drugs, in order to evaluate the recognition capabilities of the MIPs of the different types of drugs. The first tests were performed with the GPC system operating at 30  $^{\circ}$ C (particularly, MIP<sub>03</sub>, MIP<sub>05</sub> and NIP<sub>05</sub>) in the others tests the system was operating at 25  $^{\circ}$ C.

### 5.2.3.3. Saturation with the drug

The analysis of the drug adsorption capability of the polymer was evaluated by saturation tests. Before starting the saturation test, it was necessary to do a purge (see Figure 5.20), i.e. withdraw the dead volume between the solution container and the column inlet by pumping the solution for a container, in order to eliminate  $\approx 50$  mL of dead volume. This step is performed to ensure that the two solutions don't mix in the system. After that, the column was plugged to the pumping system and the saturation procedure was started at flow-rate of 0.5 mL/min or 1 mL/min. The retention of the drug in the polymer present in the column is measured by the UV detector and recorded in the GPC data acquisition system. The saturation test was performed until the polymer is unable to adsorb more drug, i.e., the concentration at the column exit becomes constant.

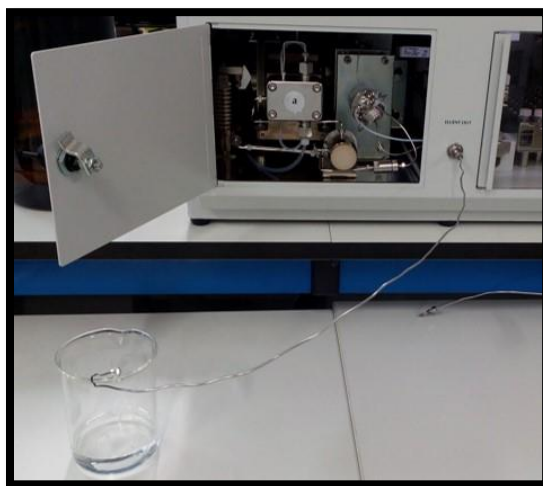


Figure 5.20 - Illustration of a purge process.

### 5.2.3.4. Release of the drug

The release of the drug from the saturated polymer was performed in the reverse way: the pumping system was turned off, feeding container was changed to WF, column was disconnected from the pumping system and the dead volume was purged again by removing  $\approx 50$  mL of solution. Then, the column was plugged (Figure 5.20) again in the system and the pumping was started at the same flow rate used in the saturation procedure. This process was also recorded in the GPC data acquisition system and was finished when the concentration at the column exit became constant.

## 5.2.4. Results and discussion

In Figure 5.21 to Figure 5.25 are presented the results of the adsorption (saturation) and desorption (release) tests with a solution of 5FU (0.1 mM) in a molecularly imprinted polymer (MIP<sub>07</sub>) synthesized by inverse suspension with 5FU as template. It can be seen that the MIP recognized the imprinted molecule. The point observed in Figure 5.22 and Figure 5.23 determines the equivalent volume, i.e. determines the exact amount of drug adsorbed and released. The equivalent volume is obtained through the equality of areas (where the area behind and above the curve has the same value). All the results of MIP<sub>07</sub> can be found in the annexes of this work (see Annexes 42 to 44).

In Table 5.3 to 5.6 are presented all tests of adsorption and desorption performed with the different drugs in different MIPs and NIPs, showing also the amount of adsorption and desorption of drugs calculated through the equivalent volume.

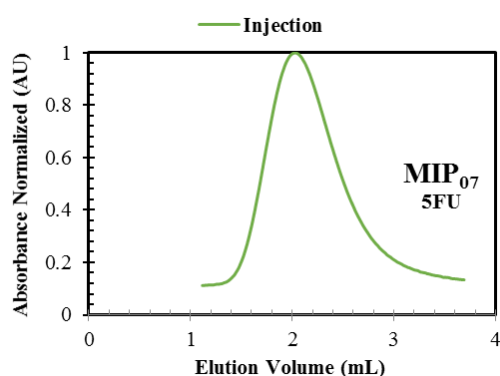


**Figure 5.21** - Profile observed for the injection of 5FU in a column packed with a MIP<sub>07</sub>.

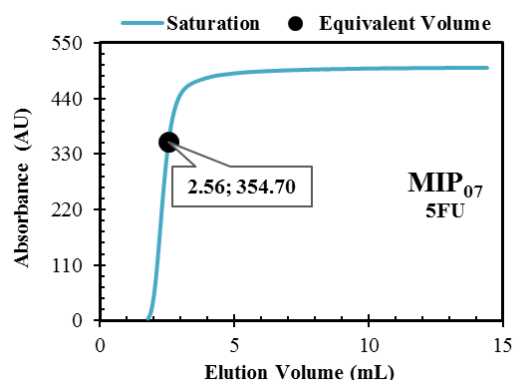


**Figure 5.22** - Profile observed for the saturation with 5FU in a column packed with a MIP<sub>07</sub>.

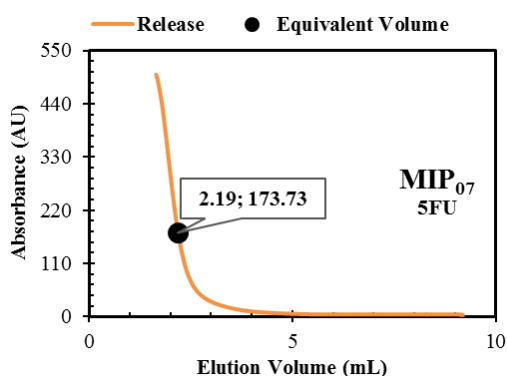


**Figure 5.23** - Profile observed for the release of 5FU in a column packed with a MIP<sub>07</sub>.

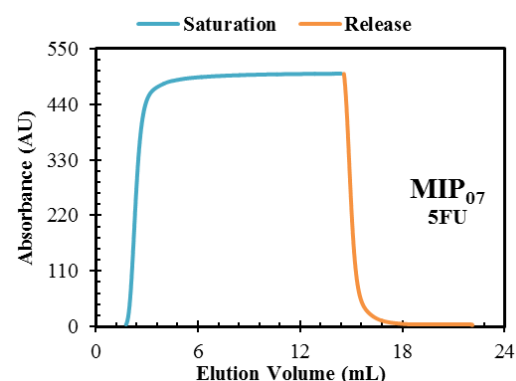


**Figure 5.24** - Profiles observed for the saturation and release of 5FU in a column packed with a MIP<sub>07</sub>.

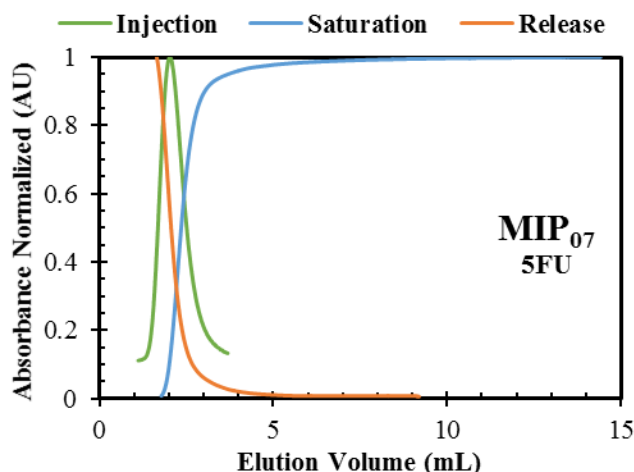


Figure 5.25 - Profile observed for the injection, saturation and release of 5FU in a column packed with a MIP<sub>07</sub>.

For the MIP<sub>07</sub> was also tested the influence of the variation of pH, an acid solution (pH 2) and an alkaline solution was used (pH 8) of 5FU (0.1 mM). In Figure 5.26 is presented the comparison of the adsorption results of the different solutions tested in the MIP<sub>07</sub> and in Figure 5.27 is presented the comparison of the release results.

The variation of the pH does not influence the adsorption, because of the high amount of cross-linker present in the MIP which leads to the loss of sensitivity to pH. While with release, only slight differences are observed, as can be seen in Table 5.4.

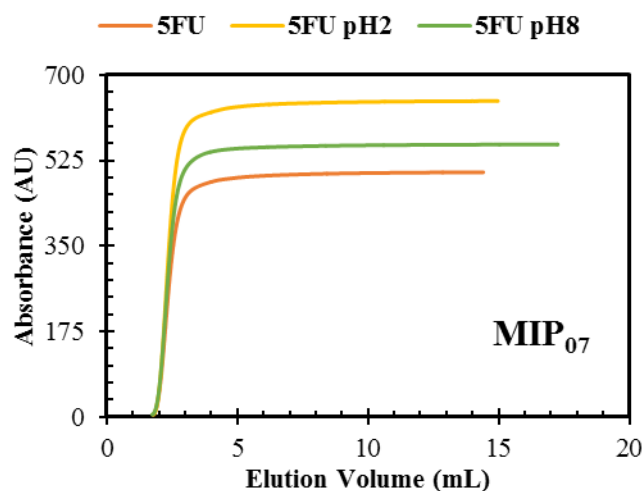
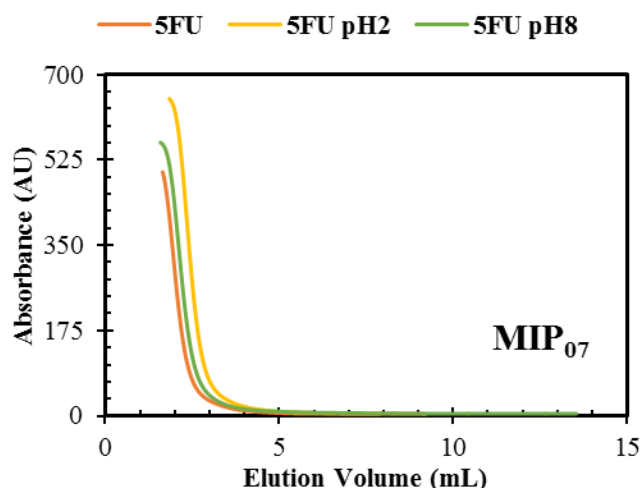


Figure 5.26 - Profiles observed for the saturation of 5FU, 5FU pH 2 and 5FU pH 8 in a column packed with a MIP<sub>07</sub>.



**Figure 5.27** - Profiles observed for the release of 5FU, 5FU pH 2 and 5FU pH 8 in a column packed with a MIP<sub>07</sub>.

In Figure 5.28 to Figure 5.32 are presented the results for the adsorption (saturation) and desorption (release) tests with a solution of 5FU (0.1 mM) in a non-imprinted polymer (NIP<sub>07</sub>) synthesized by inverse suspension. Comparing with the results of the MIP<sub>07</sub> is visible that this material has less affinity with the drug as expected. All the results of NIP<sub>07</sub> can be found in the annexes of this work (see Annexes 45 to 47).

For the NIP<sub>07</sub> was also tested the influence of the variation of pH, it was used an acid solution (pH 2) and an alkaline solution (pH 8) of 5FU (0.1 mM). In Figure 5.33 is presented the comparison of the adsorption results of the different solutions tested in the NIP<sub>07</sub> and in Figure 5.34 is presented the comparison of the release results. As for the MIP it was not verified the influence of pH variation.

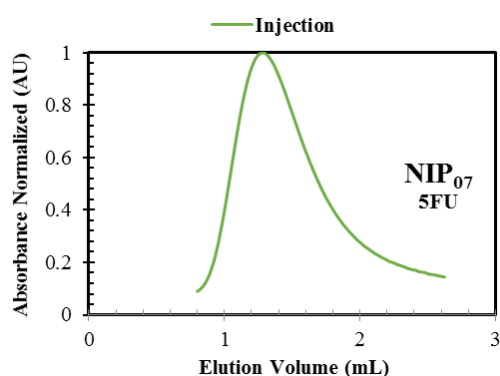


**Figure 5.28** - Profile observed for the injection of 5FU in a column packed with a NIP<sub>07</sub>.

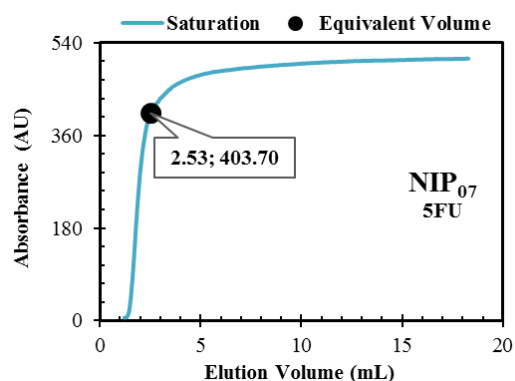


**Figure 5.29** - Profile observed for the saturation with 5FU in a column packed with a NIP<sub>07</sub>.

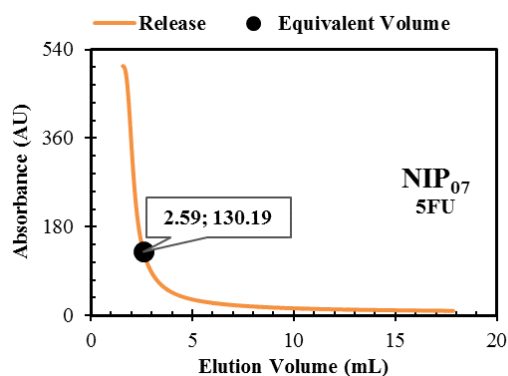


Figure 5.30 - Profile observed for the release of 5FU in a column packed with a NIP<sub>07</sub>.

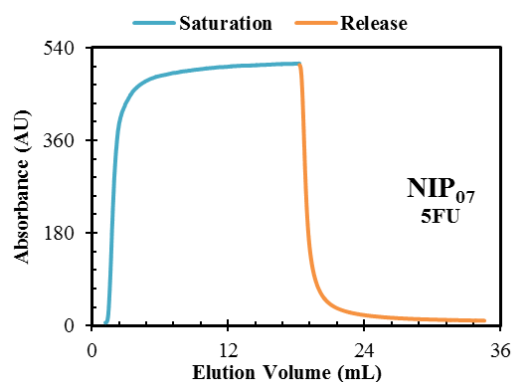


Figure 5.31 - Profiles observed for the saturation and release of 5FU in a column packed with a NIP<sub>07</sub>.

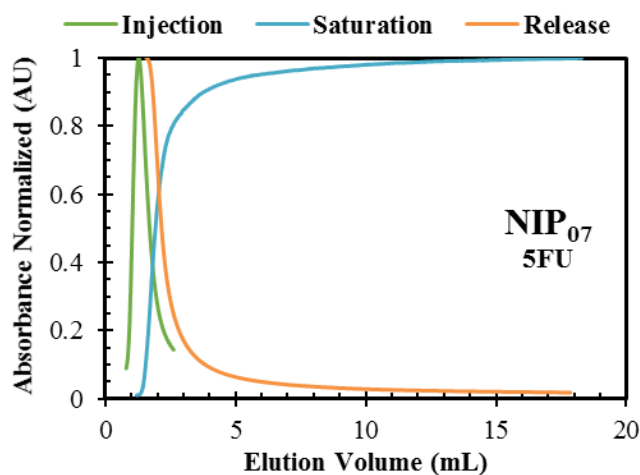


Figure 5.32 - Profile observed for the injection, saturation and release of 5FU in a column packed with a NIP<sub>07</sub>.

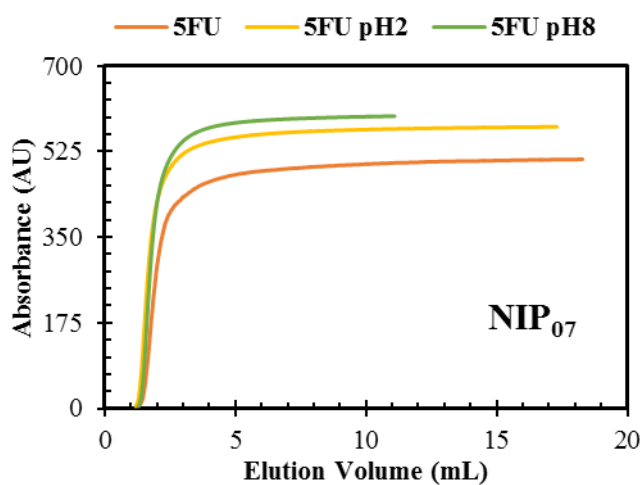
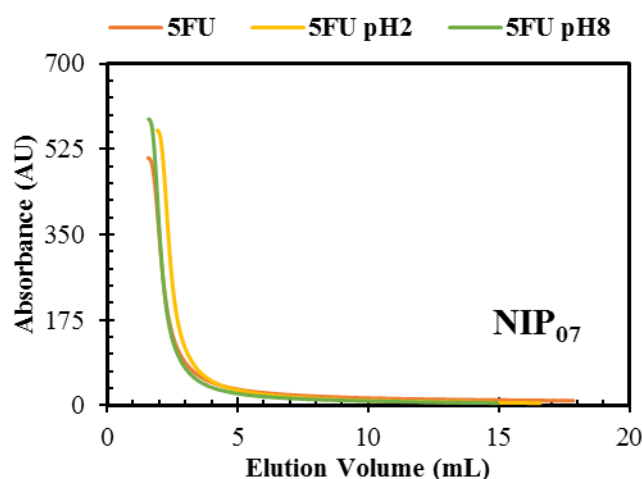
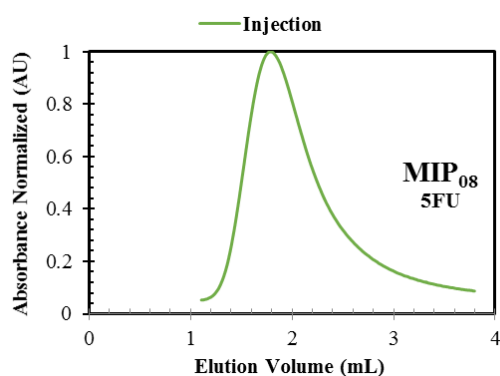


Figure 5.33 - Profiles observed for the saturation with 5FU, 5FU pH 2 and 5FU pH 8 in a column packed with a NIP<sub>07</sub>.



**Figure 5.34** - Profiles observed for the release of 5FU, 5FU pH 2 and 5FU pH 8 in a column packed with a NIP<sub>07</sub>.

In Figure 5.35 to Figure 5.39 are presented the results for the adsorption (saturation) and desorption (release) tests with a solution of 5FU (0.1 mM) in a molecularly imprinted polymer (MIP<sub>08</sub>) synthesized by inverse suspension with 5FU as template and three-functional cross-linker. The plateau of adsorption (Figure 5.36) and desorption (Figure 5.37) is well-defined approaching to the ideality. The results presented in Table 5.4 and compared with the MIP<sub>07</sub> (synthesized with a bi-functional cross-linker), do not show improvements in the adsorption and in the release of the drug. All the results of MIP<sub>08</sub> can be found in the annexes of this work (see Annexes 48 and 49).



**Figure 5.35** - Profile observed for the injection of 5FU in a column packed with a MIP<sub>08</sub>.

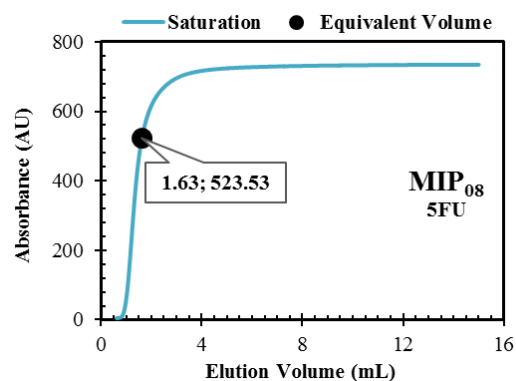


**Figure 5.36** - Profile observed for the saturation with 5FU in a column packed with a MIP<sub>08</sub>.

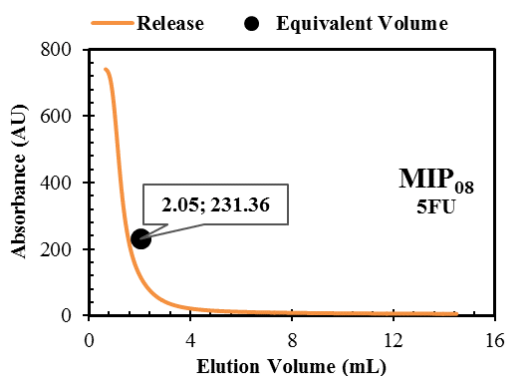


Figure 5.37 - Profile observed for the release of 5FU in a column packed with a MIP<sub>08</sub>.

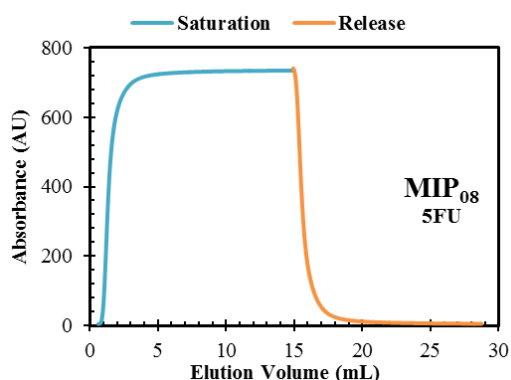


Figure 5.38 - Profiles observed for the saturation and release of 5FU in a column packed with a MIP<sub>08</sub>.

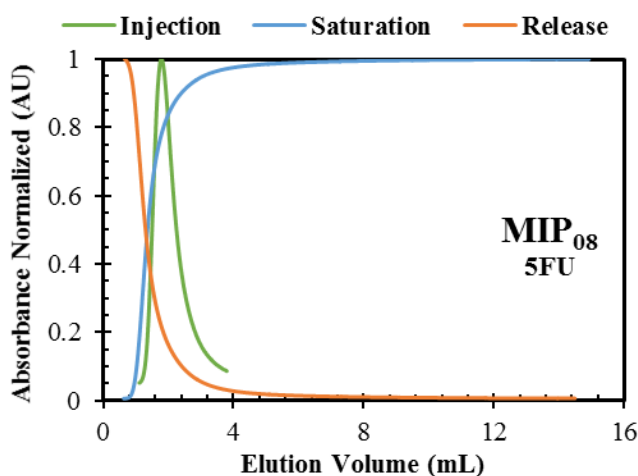


Figure 5.39 - Profiles observed for the injection, saturation and release of 5FU in a column packed with a MIP<sub>08</sub>.

It was tested to the adsorption of CAF in the MIP<sub>08</sub>, in order to compare with the adsorption of 5FU, because they have a different molecular structure. For that it was used a solution of CAF with a concentration of 0.1mM. The comparison of adsorption is presented in Figure 5.40 and in Figure 5.41 is presented the comparison of the release process. It is visible that the caffeine has higher affinity with the MIP than the 5-fluorouracil.

In Figure 5.42 to Figure 5.46 are presented the results of the adsorption (saturation) and desorption (release) tests with a solution of 5FU (0.1 mM) in a non-imprinted polymer (NIP<sub>08</sub>) synthesized by inverse suspension. All the results of NIP<sub>08</sub> can be found in the annexes of this work (see Annexes 50 and 51).

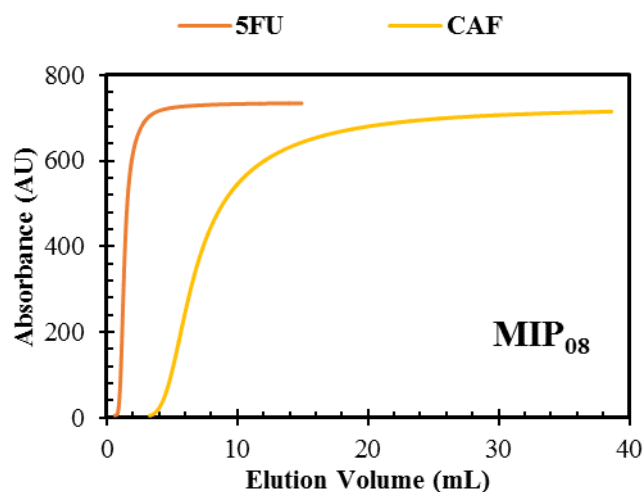


Figure 5.40 - Profiles observed for the saturation with 5FU and CAF in a column packed with a MIP<sub>08</sub>.

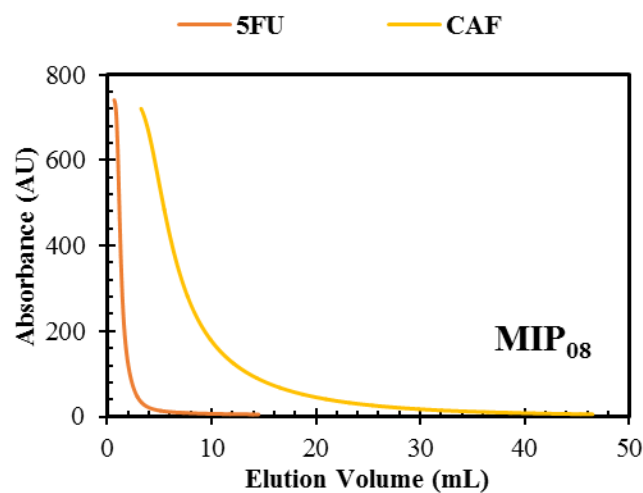


Figure 5.41 - Profiles observed for the release of 5FU and CAF in a column packed with a MIP<sub>08</sub>.

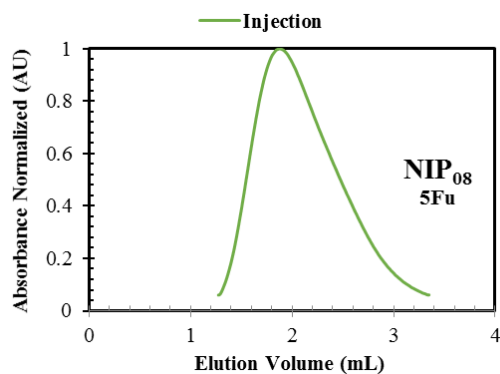


Figure 5.42 - Profile observed for the injection of 5FU in a column packed with a NIP<sub>08</sub>.

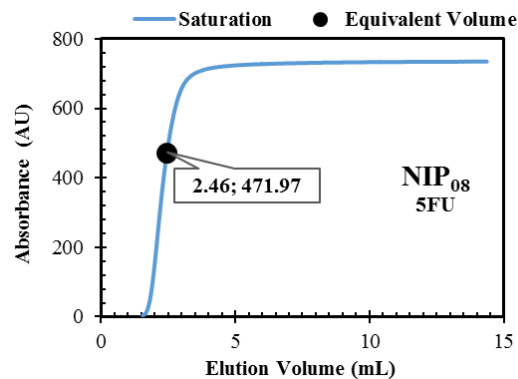


Figure 5.43 - Profile observed for the saturation with 5FU in a column packed with a NIP<sub>08</sub>.

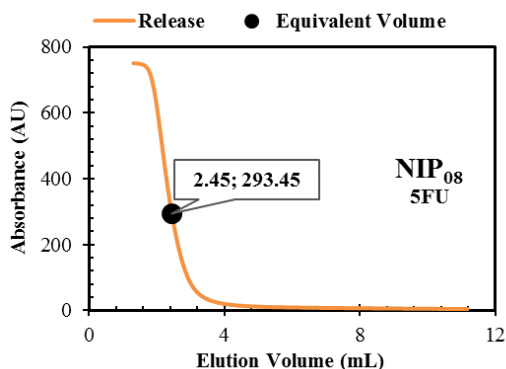


Figure 5.44 - Profile observed for the release of 5FU in a column packed with a NIP<sub>08</sub>.

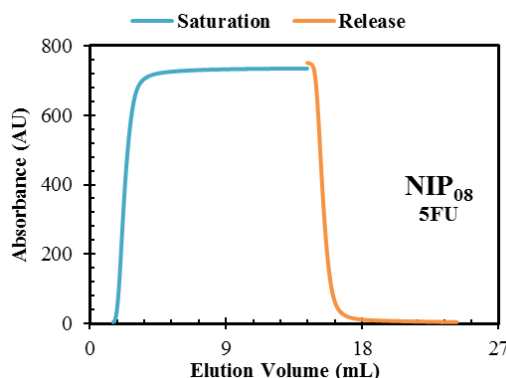


Figure 5.45 - Profiles observed for the saturation and release of 5FU in a column packed with a NIP<sub>08</sub>.

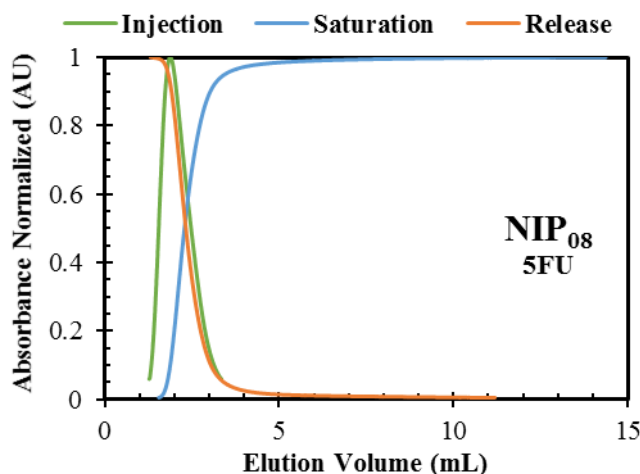


Figure 5.46 - Profiles observed for the injection, saturation and release of 5FU in a column packed with a NIP<sub>08</sub>.

For the NIP<sub>08</sub> was also tested a solution of CAF (0.1 mM). In Figure 5.47 is presented the comparison of the adsorption results of the two solutions tested in the NIP<sub>08</sub> and in Figure 5.48 is presented the comparison of the release.

After the good results of the test with CAF in MIPs synthesized with 5FU, the MIP<sub>09</sub> was synthesized with CAF and tested with 5FU in order to verify that improves absorption.

In Figure 5.49 to Figure 5.53 are presented the results for the adsorption (saturation) and desorption (release) tests with a solution of 5FU (0.1 mM) in a molecularly imprinted polymer (MIP<sub>09</sub>) synthesized by inverse suspension. The results are similar to the ones synthesized with 5FU as it can be seen in Table 5.4. All the results of MIP<sub>09</sub> can be found in the annexes of this work (see Annexes 52 and 53).

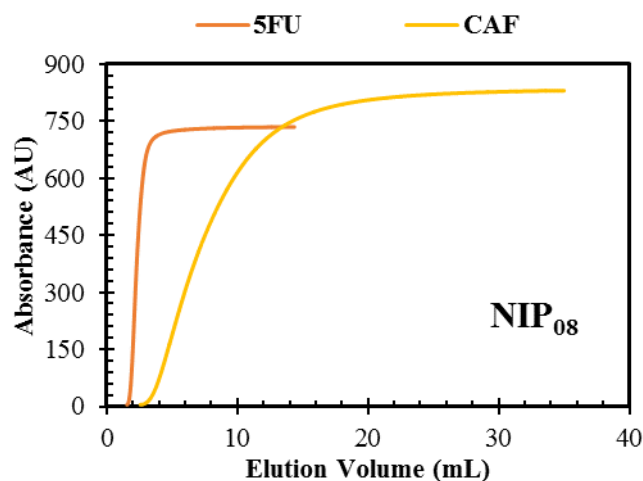


Figure 5.47 - Profiles observed for the saturation with 5FU and CAF in a column packed with a NIP<sub>08</sub>.

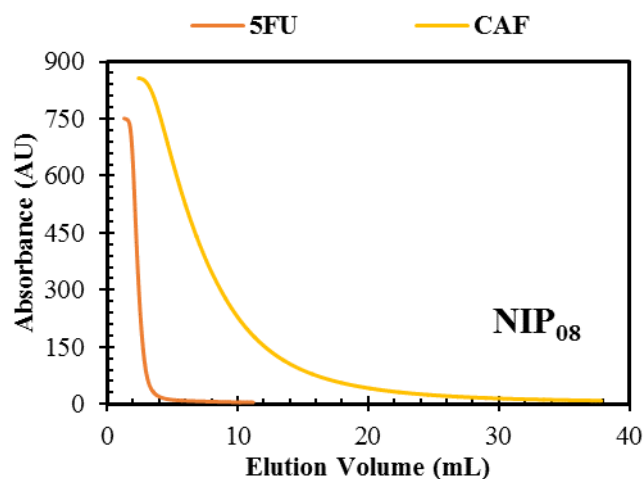


Figure 5.48 - Profiles observed for the release of 5FU and CAF in a column packed with a NIP<sub>08</sub>.

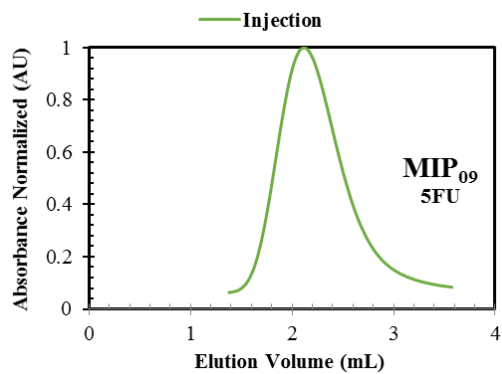


Figure 5.49 - Profile observed for the injection of 5FU in a column packed with a MIP<sub>09</sub>.

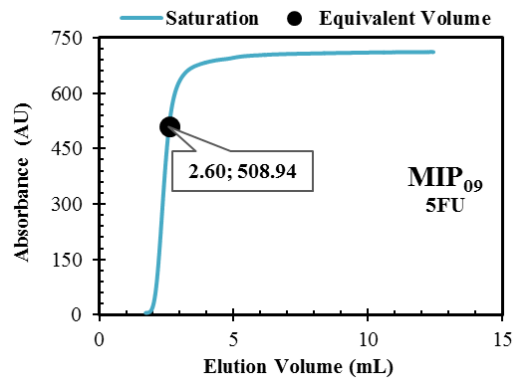


Figure 5.50 - Profile observed for the saturation with 5FU in a column packed with a MIP<sub>09</sub>.

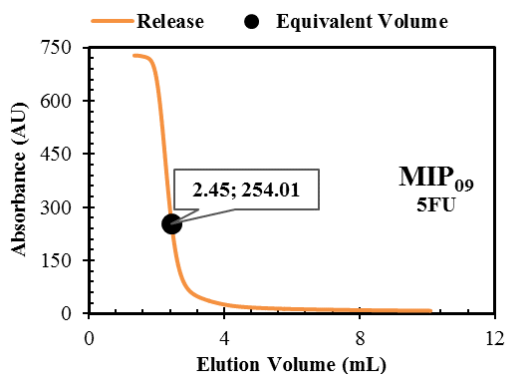


Figure 5.51 - Profile observed for the release of 5FU in a column packed with a NIP<sub>08</sub>.

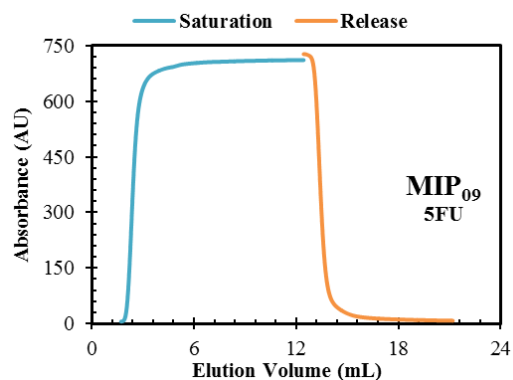


Figure 5.52 - Profiles observed for the saturation and release of 5FU in a column packed with a NIP<sub>08</sub>.

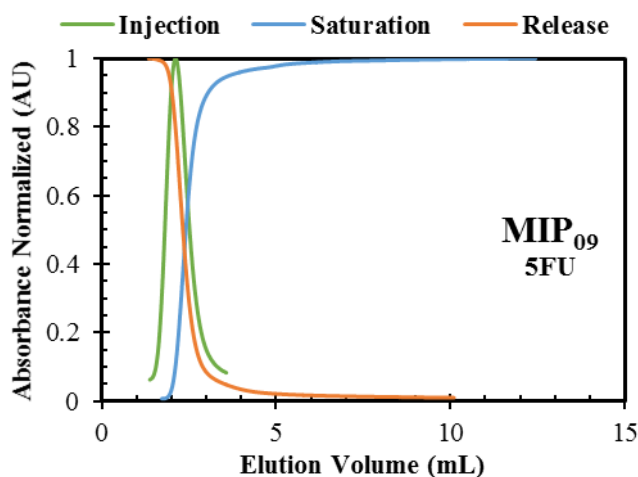


Figure 5.53 - Profiles observed for the injection, saturation and release of 5FU in a column packed with a MIP<sub>09</sub>.

For the MIP<sub>09</sub> was also tested a solution of CAF (0.1 mM). In Figure 5.54 is presented the comparison of the adsorption results of the different solutions tested in the MIP<sub>09</sub> and in Figure 5.55 is presented the comparison of the release results. Comparing the results is visible that the MIP adsorb more CAF than 5FU, showing higher affinity. The release of CAF shows that there is also higher affinity with the MIP than 5FU

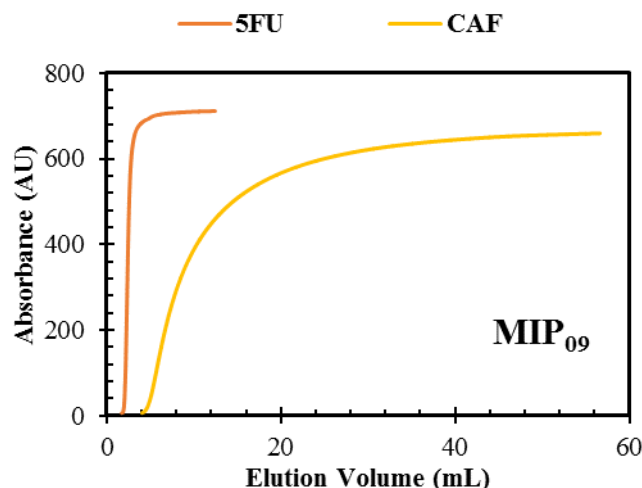


Figure 5.54 - Profiles observed for the saturation with 5FU and CAF in a column packed with a MIP<sub>09</sub>.

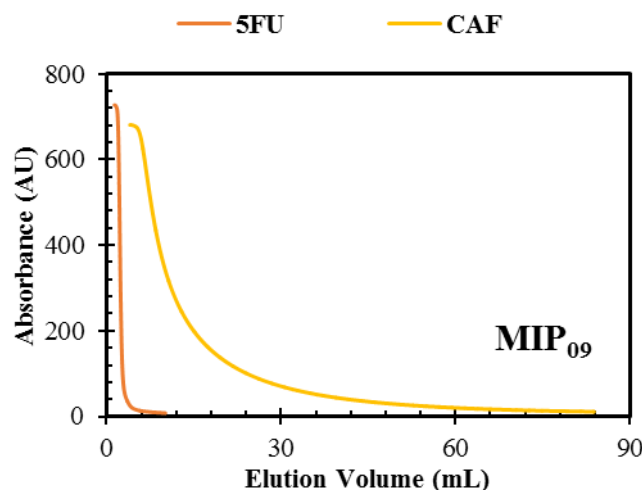


Figure 5.55 - Profiles observed for the release of 5FU and CAF in a column packed with a MIP<sub>09</sub>.

For MIP<sub>03</sub> different solutions were tested, such as 5FU, CAF, IBU and UR. Having CAF presented more affinity as demonstrated in Table 5.3.

In the case of MIP<sub>05</sub> which has been tested with 5FU, THY and UR, the results presented in Table 5.3 shows that the MIP absorb more 5FU. Comparing with the non-imprinted (NIP<sub>05</sub>), this one shows higher affinity.

The MIP<sub>06</sub> was tested with different solutions, such as 5FU at different pH (neutral, pH 2 and pH 8), CAF and UR. The variation of pH shows slight improvement in adsorption of 5FU, but again caffeine provides the best results of adsorption. The variation of pH in the 5FU adsorption also occurs in NIP<sub>06</sub>.

The results of MIP<sub>03</sub>, MIP<sub>05</sub>, NIP<sub>05</sub>, MIP<sub>06</sub> and NIP<sub>06</sub> can be found in the annexes of this work (see Annexes 18 to 41).

Based on the results of Table 5.3 is confirmed that the MIP<sub>09</sub>, imprinted with CAF is the most efficient, with  $IF > 3$ . For the MIPs imprinted with 5FU, the one that has better efficiency is the MIP<sub>07</sub>.

**Table 5.3** - Results of imprinting factor obtained by frontal analysis.

Material	D	$t_0$	$tr$	$rF$	$SF$	$IF$
MIP <sub>06</sub>	5FU	1.07	1.50	0.40	1.00	1.44
NIP <sub>06</sub>		1.07	1.45	0.34	1.00	
MIP <sub>06</sub>	U	1.08	1.50	0.40	1.00	-
NIP <sub>06</sub>		1.08	1.45	0.34	0.80	
MIP <sub>06</sub>	CAF	1.08	1.73	0.60	0.66	-
NIP <sub>06</sub>		1.08	1.53	0.41	0.67	
MIP <sub>07</sub>	5FU	1.07	2.16	1.01	1.00	2.98
NIP <sub>07</sub>		1.07	1.44	0.34	1.00	
MIP <sub>07</sub>	U	1.08	1.95	0.81	1.24	-
NIP <sub>07</sub>		1.08	1.46	0.35	0.96	
MIP <sub>07</sub>	CAF	1.08	7.23	5.69	0.18	-
NIP <sub>07</sub>		1.08	1.56	0.45	0.76	
MIP <sub>08</sub>	5FU	1.07	1.98	0.84	1.00	0.93
NIP <sub>08</sub>		1.07	2.04	0.90	1.00	
MIP <sub>08</sub>	U	1.08	1.91	0.78	1.08	-
NIP <sub>08</sub>		1.08	1.93	0.79	1.14	
MIP <sub>08</sub>	CAF	1.08	2.04	0.90	1.00	-
NIP <sub>08</sub>		1.08	7.51	5.95	0.15	
MIP <sub>09</sub>	5FU	1.07	2.14	1.00	1.00	-
NIP <sub>07</sub>		1.07	1.44	0.34	1.00	
MIP <sub>09</sub>	U	1.08	2.00	0.86	1.16	-
NIP <sub>07</sub>		1.08	1.46	0.35	0.96	
MIP <sub>09</sub>	CAF	1.08	8.82	7.17	0.14	16.05
NIP <sub>07</sub>		1.08	1.56	0.45	0.76	

### 5.3. Fourier transform infrared spectroscopy (FTIR)

FTIR spectroscopy is useful for monitoring changes in chemical environment resulting from the addition or removal of functional groups in the imprinted polymer [57]. FTIR procedures involve incorporating polymer into a KBr disc. For that, was used 2-4 mg of polymer and 175-225 mg of KBr. The analysis was performed in a range of frequencies between 600 and 4000  $\text{cm}^{-1}$ . In Figure 5.56 and 5.57 are presented the FTIR spectra of the NIP<sub>01</sub>, NIP<sub>02</sub>, MIP<sub>07</sub> and MIP<sub>09</sub>. For comparison, the FTIR spectrum of a similar MIP and NIPs was also included. Through the spectra were observed simple structural features of the synthesized networks, such as, C=O vibration in the 1750  $\text{cm}^{-1}$  region, different CH<sub>2</sub> vibrations in the regions 1150, 1250  $\text{cm}^{-1}$ , and CH<sub>2</sub>/C-O-H vibrations in the 1400  $\text{cm}^{-1}$  region.

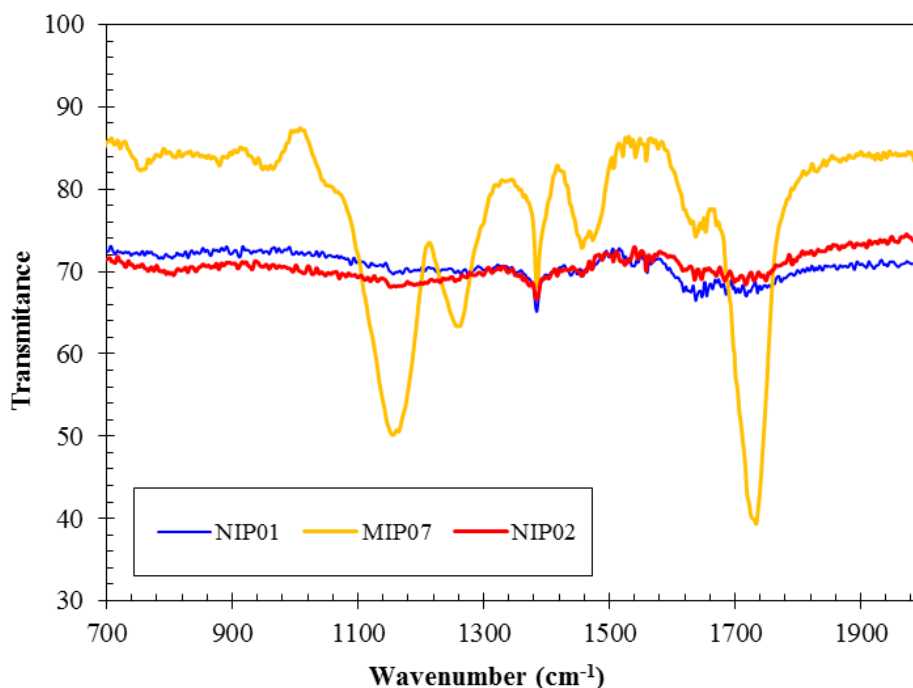


**Figure 5.56** - FTIR spectra of non-imprinted and imprinted dried polymers produced through FRP and RAFT polymerization.

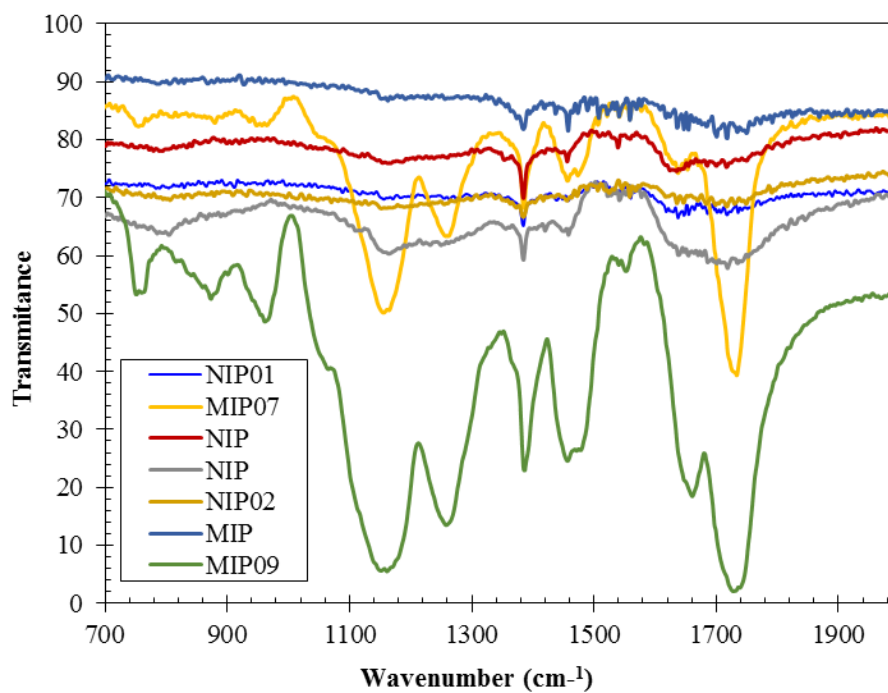


**Figure 5.57** - FTIR spectra of non-imprinted and imprinted dried polymers produced through FRP and RAFT polymerization.

**Table 5.4** - Summary of results obtained by frontal analysis of MIPs and NIPs with different drugs (tests for adsorption).

Material	Packed dried mass (mg)	Drug	C <sub>0</sub> (mM)	Q (mL/min)	V <sub>G</sub> (mL)	V <sub>0</sub> (mL)	V <sub>a</sub> (mL)	V <sub>eq</sub> (mL)	q* (mmol/mL stationary phase)	q* (mmol/Kg dried stationary phase)
MIP <sub>03</sub>	580.00	5FU	0.10	1.00	1.66	0	1.66	2.42	0.15	0.42
		CAF	0.10	1.00	1.66	0	1.66	4.69	0.28	0.81
		IBU	0.10	1.00	1.66	0	1.66	2.48	0.15	0.43
		U	0.10	1.00	1.66	0	1.66	2.90	0.17	0.50
MIP <sub>05</sub>	206.20	5FU	0.10	0.50	0.55	0	0.55	1.62	0.29	0.79
		5FU	0.10	1.00	0.55	0	0.55	3.69	0.67	1.79
		THY	0.10	1.00	0.55	0	0.55	2.14	0.39	1.04
		U	0.10	1.00	0.55	0	0.55	3.14	0.57	1.52
MIP <sub>05</sub>	319.80	5FU	0.10	1.00	0.83	0	0.83	2.39	0.29	0.75
		5FU rep.	0.10	1.00	0.83	0	0.83	2.31	0.28	0.72
		U	0.10	1.00	0.83	0	0.83	2.45	0.30	0.77
NIP <sub>05</sub>	204.30	5FU	0.10	1.00	0.55	0	0.55	2.28	0.42	1.12
		THY	0.10	1.00	0.55	0	0.55	2.11	0.39	1.03
		U	0.10	1.00	0.55	0	0.55	6.58	1.20	3.22
MIP <sub>06</sub>	300.20	5FU	0.10	1.00	0.55	0	0.55	2.40	0.44	0.80
		5FU pH2	0.10	1.00	0.55	0	0.55	2.73	0.50	0.91
		5FU pH8	0.10	1.00	0.55	0	0.55	2.62	0.48	0.87
		CAF	0.10	1.00	0.55	0	0.55	9.00	1.64	3.00
		U	0.10	1.00	0.55	0	0.55	2.25	0.41	0.75

**Table 5.5** - Summary of results obtained by frontal analysis of MIPs and NIPs with different drugs (tests for adsorption) (Continuation of Table 5.4).

Material	Packed dried mass (mg)	Drug	C <sub>0</sub> (mM)	Q (mL/min)	V <sub>G</sub> (mL)	V <sub>0</sub> (mL)	V <sub>a</sub> (mL)	V <sub>eq</sub> (mL)	q* (mmol/mL stationary phase)	q* (mmol/Kg dried stationary phase)
NIP <sub>06</sub>	300.20	5FU	0.10	1.00	0.55	0	0.55	2.36	0.43	0.79
		5FU pH2	0.10	1.00	0.55	0	0.55	2.51	0.46	0.84
		5FU pH8	0.10	1.00	0.55	0	0.55	2.40	0.44	0.80
MIP <sub>07</sub>	162.90	5FU	0.10	1.00	0.55	0	0.55	2.56	0.47	1.57
		5FU pH2	0.10	1.00	0.55	0	0.55	2.53	0.46	1.55
		5FU pH8	0.10	1.00	0.55	0	0.55	2.51	0.46	1.54
NIP <sub>07</sub>	300.20	5FU	0.10	1.00	0.55	0	0.55	2.53	0.46	0.84
		5FU pH2	0.10	1.00	0.55	0	0.55	2.10	0.38	0.70
		5FU pH8	0.10	1.00	0.55	0	0.55	2.06	0.38	0.69
MIP <sub>08</sub>	162.90	5FU	0.10	1.00	0.55	0	0.55	1.63	0.30	1.00
		CAF	0.10	1.00	0.55	0	0.55	8.73	1.59	5.36
NIP <sub>08</sub>	162.90	5FU	0.10	1.00	0.55	0	0.55	2.46	0.45	1.51
		CAF	0.10	1.00	0.55	0	0.55	8.39	1.53	5.15
MIP <sub>09</sub>	162.90	5FU	0.10	1.00	0.55	0	0.55	2.60	0.47	1.59
		CAF	0.10	1.00	0.55	0	0.55	12.13	2.21	7.45

**Table 5.6** - Summary of results obtained by frontal analysis of MIPs and NIPs with different drugs (tests for desorption).

Material	Packed dried mass (mg)	Drug	C <sub>0</sub> (mM)	Q (mL/min)	V <sub>G</sub> (mL)	V <sub>0</sub> (mL)	V <sub>a</sub> (mL)	V <sub>eq</sub> (mL)	q* (mmol/mL stationary phase)	q* (mmol/Kg dried stationary phase)
MIP <sub>03</sub>	580.00	5FU	0.10	1.00	1.66	0	1.66	2.48	0.15	0.43
		CAF	0.10	1.00	1.66	0	1.66	5.13	0.31	0.88
		IBU	0.10	1.00	1.66	0	1.66	2.75	0.17	0.47
		U	0.10	1.00	1.66	0	1.66	2.75	0.17	0.47
MIP <sub>05</sub>	206.20	5FU	0.10	0.50	0.55	0	0.55	3.66	0.67	1.78
		5FU	0.10	1.00	0.55	0	0.55	1.97	0.36	0.96
		THY	0.10	1.00	0.55	0	0.55	2.19	0.40	1.06
		U	0.10	1.00	0.55	0	0.55	1.98	0.36	0.96
MIP <sub>05</sub>	319.80	5FU	0.10	1.00	0.83	0	0.83	2.38	0.29	0.74
		5FU rep.	0.10	1.00	0.83	0	0.83	2.27	0.27	0.71
		U	0.10	1.00	0.83	0	0.83	2.46	0.30	0.77
NIP <sub>05</sub>	204.30	5FU	0.10	1.00	0.55	0	0.55	2.76	0.50	1.35
		THY	0.10	1.00	0.55	0	0.55	2.35	0.43	1.15
		U	0.10	1.00	0.55	0	0.55	2.48	0.45	1.21
MIP <sub>06</sub>	300.20	5FU	0.10	1.00	0.55	0	0.55	2.43	0.44	0.81
		5FU pH2	0.10	1.00	0.55	0	0.55	2.41	0.44	0.80
		5FU pH8	0.10	1.00	0.55	0	0.55	2.29	0.42	0.76
		CAF	0.10	1.00	0.55	0	0.55	9.57	1.75	3.19
		U	0.10	1.00	0.55	0	0.55	2.73	0.50	0.91

**Table 5.7** - Summary of results obtained by frontal analysis of MIPs and NIPs with different drugs (tests for desorption) (Continuation of Table 5.6).

Material	Packed dried mass (mg)	Drug	C <sub>0</sub> (mM)	Q (mL/min)	V <sub>G</sub> (mL)	V <sub>0</sub> (mL)	V <sub>a</sub> (mL)	V <sub>eq</sub> (mL)	q* (mmol/mL stationary phase)	q* (mmol/Kg dried stationary phase)
NIP <sub>06</sub>	300.20	5FU	0.10	1.00	0.55	0	0.55	2.67	0.49	1.08
		5FU pH2	0.10	1.00	0.55	0	0.55	3.23	0.59	0.81
		5FU pH8	0.10	1.00	0.55	0	0.55	2.82	0.51	0.94
MIP <sub>07</sub>	162.90	5FU	0.10	1.00	0.55	0	0.55	2.19	0.40	1.34
		5FU pH2	0.10	1.00	0.55	0	0.55	2.54	0.46	1.56
		5FU pH8	0.10	1.00	0.55	0	0.55	2.31	0.42	1.42
NIP <sub>07</sub>	300.20	5FU	0.10	1.00	0.55	0	0.55	2.59	0.47	0.86
		5FU pH2	0.10	1.00	0.55	0	0.55	2.84	0.52	0.95
		5FU pH8	0.10	1.00	0.55	0	0.55	2.44	0.45	0.81
MIP <sub>08</sub>	162.90	5FU	0.10	1.00	0.55	0	0.55	2.05	0.37	1.26
		CAF	0.10	1.00	0.55	0	0.55	8.61	1.57	5.29
NIP <sub>08</sub>	162.90	5FU	0.10	1.00	0.55	0	0.55	2.45	0.45	1.50
		CAF	0.10	1.00	0.55	0	0.55	8.41	1.53	5.16
MIP <sub>09</sub>	162.90	5FU	0.10	1.00	0.55	0	0.55	2.45	0.45	1.50
		CAF	0.10	1.00	0.55	0	0.55	14.40	2.63	8.84

## Chapter 6. Conclusion

This research was devoted to the synthesis and characterization of molecularly imprinted particles (MIPs) for biomedical applications. 5-fluorouracil (5FU), a drug used in cancer treatment, was considered as the main target molecule, methacrylic acid (MAA) as functional monomer and ethylene glycol dimethacrylate (EGDMA) as crosslinker. For comparison purposes and assessment of the efficiency of the produced materials, other drugs such as uracil (UR), thymine (THY), ibuprofen (IBU) and caffeine (CAF) were also included in the developed studies. Moreover, acrylic acid (AA) and isopropyl acrylamide (NIPA) were also considered as alternative functional monomers and trimethylolpropane triacrylate (TMPTA) or methylenebis(acrylamide) (MBAm) as crosslinkers. These changes in the initial composition of the polymerization system were performed in order to study the effect of the synthesis conditions on the performance of the obtained MIPs.

Different production strategies were used in order to obtain MIP materials with distinct morphologies, namely the solution polymerization leading to monoliths, the inverse-suspension polymerization with MIP microparticles formation and the operation in continuous-flow micro-reactor allowing also the synthesis of spherical/oval polymer particles with controllable size (using classical free radical polymerization or controlled radical polymerization, namely RAFT). Analysis by SEM of the produced materials show that inverse-suspension polymerization can be used to produce MIP microparticles, with size in the range of 1  $\mu\text{m}$ , and presenting higher performance than the monoliths in the drug adsorption/desorption processes, possibly due to the enhancement of mass transfer. The research here performed is also a contribution to show the feasibility of the production of polymer particles in continuous-flow micro-reactor [56]. Nevertheless, only polymerization compositions with low crosslinker content (e.g. 1 to 2%), leading to hydrogels, were explored until now when operating with continuous-flow micro-reactor. Materials thus obtained present high swelling ratio (and viscoelasticity)

but the molecular imprinting process is hampered due to the low stability of the stereospecific cavities generated in the networks. Additional studies in this research line should be performed increasing the crosslinker content (eventually approaching the 50 to 80% used in classical MIPs) in order to optimize the network stimulation (e.g. due to changes in pH and/or temperature) simultaneously with their molecular recognition capabilities. Microwave assisted synthesis of MIPs was also here explored in order to test the fast and facile synthesis of these kind of materials (a CEM technology equipment was used). Preliminary results obtained are encouraging in view of the application of this technique for polymer particles production.

The performance of the produced MIPs for drug adsorption/desorption was characterized using different techniques, namely Solid Phase Extraction (SPE) and Frontal Analysis (FA). This latter technique involved the packing of the MIP particles in small columns and their integration in a GPC system with UV signal detection. Some information about the chemical composition of the formed polymer networks was obtained by FTIR. Comparison of the tests performed with the different materials synthesized show that the best performance for 5FU molecular recognition was attained with the MIP micro-particles obtained by inverse-suspension with MAA/EGDMA as functional monomer/crosslinker (c.a. 55% crosslinker and MAA/5FU=8). In fact, an imprinting factor  $IF=2.98$  was measured for the pair MIP<sub>07</sub>/NIP<sub>07</sub> (e.g. see SPE results presented in Annexes 6 through 17) and a retention capability for 5FU of 1.57 mmol/kg was measured by FA for MIP<sub>07</sub> using an 0.1 mM aqueous solution of the drug (see Tables 5.4 and 5.5). Nevertheless, a low selectivity of 5FU MIPs was measured considering the comparison with the structural analogues uracil and thymine (e.g. with MIP<sub>07</sub>,  $SF=1.2$  was measured for the pair 5FU/uracil, as can be conclude from the results presented in Annexes 9 and 13). Moreover, high retention capabilities of caffeine were measured for materials imprinted with 5FU. For instance, MIP<sub>08</sub> is able to retain 5.36 mmol/kg of caffeine and only 1.00 mmol/kg of 5FU (0.1 mM aqueous solutions of the drugs were used in both FA measurements). Using SPE, was showed that MIP<sub>07</sub> is able to retain 88.40% of caffeine and only 27.84% of 5FU (see Annexes 9 and 12). These results should be a consequence of the high affinity between caffeine and the MAA based polymer network due to ionic/hydrogen bonding interactions. These non-specific effects

are dominant comparatively to the 5FU molecular imprinting process (only hydrogen bonding interactions are expected between 5FU and MAA). On other hand, a low ability to stimulate the 5FU MIPs by changing the environmental conditions, namely the pH of the aqueous solutions, was found. Very similar retention capabilities were measured for 5FU considering aqueous solutions of this drug with deionized water, solutions at pH=2 (trying to resemble acidic conditions in the stomach) and solutions at pH=8 (trying to resemble alkaline conditions in the intestine), as presented in tables 5.4 and 5.5 (see e.g. results thus obtained with MIP<sub>06</sub> and MIP<sub>07</sub>). This behavior should be a consequence of the high amount of crosslinker classically used in the synthesis of MIPs (around 55% in MIP<sub>06</sub> and MIP<sub>07</sub>) which prevents the possibility to trigger the stimulation of the materials by changing the external conditions (e.g. pH). Materials thus produced are very stiff, in opposite to hydrogels that exhibit high viscoelasticity (allowing huge changes in their swelling ratio).

## 6.1. Future Work

It is proposed the exploitation of the following research lines in order to improve the performance of molecularly imprinted materials, namely 5FU MIPs, and to address the main difficulties identified in this research, as above described:

- Extension of the work concerning the production of polymer particles in continuous-flow micro-reactor [56], considering different levels/types of crosslinking agents, in order to try de production of MIP particles with controlled size/format and eventually combining molecular recognition capabilities (stability of the imprinted cavities) and ability to be stimulated by changes in the environmental conditions (stimuli responsive due to some degree of viscoelasticity). Use of RAFT polymerization should benefit the outcomes of these new studies.
- Consideration of different functional monomers (e.g. 2,6-bis(acrylamide)pyridine) in order to increase the specific interactions with 5FU, aiming the production of 5FU MIPs with improved retention capabilities and also higher selectivity (e.g. comparatively to the structural analogues uracil and thymine).

- Use of new polymerization techniques to obtain advanced MIP functional particles showing stimuli responsive behavior. In the last few years [108] were developed polymerization techniques that include a first step for creation of a molecular imprinted core and a second step for grafting functionalized polymer chains in the surface of the previously synthesized particle. Controlled radical polymerization (e.g. RAFT) play a central role in this strategy because allows the implementation of this two-step synthesis technique. In principle, is thus possible to combine in the final product the molecular recognition capabilities associated with classical MIPs (the imprinted core is produced with a high cross-linker content) and the stimuli responsive features incorporated in the grafted brushes (e.g. linear chains with sensitivity to pH/temperature changes).

## Chapter 7. References

1. Hilt, J.Z. and Byrne, M.E., *Configurational biomimesis in drug delivery: molecular imprinting of biologically significant molecules*. *Advanced Drug Delivery Reviews*, 2004. 56(11): p. 1599-1620.
2. He, C.Y., Liu, F., Li, K.A. and Liu, H.W., *Molecularly imprinted polymer film grafted from porous silica for selective recognition of testosterone*. *Analytical Letters*, 2006. 39(2): p. 275-286 DOI: 10.1080/00032710500476946.
3. Yang, H.H., Zhang, S.Q., Tan, F., Zhuang, Z.X. and Wang, X.R., *Surface molecularly imprinted nanowires for biorecognition*. *Journal of the American Chemical Society*, 2005. 127(5): p. 1378-1379 DOI: 10.1021/ja0467622.
4. Dias, M.M.R., Raghavan, S.L., Pellett, M.A. and Hadgraft, J., *The effect of beta-cyclodextrins on the permeation of diclofenac from supersaturated solutions*. *International Journal of Pharmaceutics*, 2003. 263(1-2): p. 173-181 DOI: 10.1016/s0378-5173(03)00366-1.
5. Alvarez-Lorenzo, C. and Concheiro, A., *Molecularly imprinted polymers for drug delivery*. *Journal of Chromatography B-Analytical Technologies in the Biomedical and Life Sciences*, 2004. 804(1): p. 231-245 DOI: 10.1016/j.jchromb.2003.12.032.
6. Turkmen, D., Bereli, N., Corman, M.E., Shaikh, H., Akgol, S. and Denizli, A., *Molecular imprinted magnetic nanoparticles for controlled delivery of mitomycin C*. *Artificial Cells Nanomedicine and Biotechnology*, 2014. 42(5): p. 316-322 DOI: 10.3109/21691401.2013.823094.
7. Whitcombe, M.J., Kirsch, N. and Nicholls, I.A., *Molecular imprinting science and technology: a survey of the literature for the years 2004-2011*. *Journal of Molecular Recognition*, 2014. 27(6): p. 297-401 DOI: 10.1002/jmr.2347.
8. Schirhagl, R., *Bioapplications for Molecularly Imprinted Polymers*. *Analytical Chemistry*, 2014. 86(1): p. 250-261 DOI: 10.1021/ac401251j.
9. Kan, W.T. and Li, X., *Mathematical modeling and sustained release property of a 5-fluorouracil imprinted vehicle*. *European Polymer Journal*, 2013. 49(12): p. 4167-4175 DOI: 10.1016/j.eurpolymj.2013.09.024.
10. Shen, X.T., Xu, C.G. and Ye, L., *Molecularly Imprinted Polymers for Clean Water: Analysis and Purification*. *Industrial & Engineering Chemistry Research*, 2013. 52(39): p. 13890-13899 DOI: 10.1021/ie302623s.
11. Barde, L.N., Ghule, M.M., Roy, A.A., Mathur, V.B. and Shivhare, U.D., *Development of molecularly imprinted polymer as sustain release drug carrier for propranolol HCL*. *Drug Development and Industrial Pharmacy*, 2013. 39(8): p. 1247-1253 DOI: 10.3109/03639045.2012.710236.
12. Lulinski, P., *Molecularly imprinted polymers as the future drug delivery devices*. *Acta Poloniae Pharmaceutica*, 2013. 70(4): p. 601-609.
13. Tian, S., Guo, Z.F., Zhang, X.X. and Wu, X.Y., *Synthesis of molecularly imprinted copolymers for recognition of ephedrine*. *Analytical Methods*, 2013. 5(19): p. 5179-5187 DOI: 10.1039/c3ay41202d.
14. Piacham, T., Nantasenamat, C., Isarankura-Na-Ayudhya, C. and Prachayasittikul, V., *Synthesis and computational investigation of molecularly imprinted nanospheres for selective recognition of alpha-tocopherol succinate*. *Excli Journal*, 2013. 12: p. 701-718.

15. Krishnaiah, Y.S.R. and Khan, M.A., *Strategies of targeting oral drug delivery systems to the colon and their potential use for the treatment of colorectal cancer*. Pharmaceutical Development and Technology, 2012. 17(5): p. 521-540 DOI: 10.3109/10837450.2012.696268.
16. Prasad, B.B., Kumar, D., Madhuri, R. and Tiwari, M.P., *Nonhydrolytic sol-gel derived imprinted polymer-multiwalled carbon nanotubes composite fiber sensors for electrochemical sensing of uracil and 5-fluorouracil*. Electrochimica Acta, 2012. 71: p. 106-115 DOI: 10.1016/j.electacta.2012.03.110.
17. Singh, B., Chauhan, N. and Sharma, V., *Design of Molecular Imprinted Hydrogels for Controlled Release of Cisplatin: Evaluation of Network Density of Hydrogels*. Industrial & Engineering Chemistry Research, 2011. 50(24): p. 13742-13751 DOI: 10.1021/ie200758b.
18. Sun, Q., Yao, Q.Q., Sun, Z.L., Zhou, T.S., Nie, D.X., Shi, G.Y. and Jin, L.T., *Determination of Parathion-methyl in Vegetables by Fluorescent-Labeled Molecular Imprinted Polymer*. Chinese Journal of Chemistry, 2011. 29(10): p. 2134-2140 DOI: 10.1002/cjoc.201180370.
19. Puoci, F., Cirillo, G., Curcio, M., Parisi, O.I., Iemma, F. and Picci, N., *Molecularly imprinted polymers in drug delivery: state of art and future perspectives*. Expert Opinion on Drug Delivery, 2011. 8(10): p. 1379-1393 DOI: 10.1517/17425247.2011.609166.
20. Lopez, C., Claude, B., Morin, P., Pelissou, M., Pena, R., Max, J.P. and Ribet, J.P., *Synthesis and study of a molecularly imprinted polymer for specific solid-phase extraction of vinflunine and its metabolite from biological fluids*. Journal of Separation Science, 2011. 34(15): p. 1902-1909 DOI: 10.1002/jssc.201100015.
21. Lulinski, P., *Molecularly imprinted polymers in pharmaceutical sciences. Part I. The principles of molecular imprinting applications in drug synthesis and drug delivery systems*. Polimery, 2010. 55(11-12): p. 799-805.
22. Wang, C.Y., Javadi, A., Ghaffari, M. and Gong, S.Q., *A pH-sensitive molecularly imprinted nanospheres/hydrogel composite as a coating for implantable biosensors*. Biomaterials, 2010. 31(18): p. 4944-4951 DOI: 10.1016/j.biomaterials.2010.02.073.
23. Curcio, M., Parisi, O.I., Cirillo, G., Spizzirri, U.G., Puoci, F., Iemma, F. and Picci, N., *Selective recognition of methotrexate by molecularly imprinted polymers*. E-Polymers, 2009.
24. Kryscio, D.R. and Peppas, N.A., *Mimicking Biological Delivery Through Feed back-Controlled Drug Release Systems Based on Molecular Imprinting*. Aiche Journal, 2009. 55(6): p. 1311-1324 DOI: 10.1002/aic.11779.
25. Puoci, F., Iemma, F., Cirillo, G., Curcio, M., Parisi, O.I., Spizzirri, U.G. and Picci, N., *New restricted access materials combined to molecularly imprinted polymers for selective recognition/release in water media*. European Polymer Journal, 2009. 45(6): p. 1634-1640 DOI: 10.1016/j.eurpolymj.2009.01.021.
26. Lulinski, P. and Maciejewska, D., *Examination of Imprinting Process with Molsidomine as a Template*. Molecules, 2009. 14(6): p. 2212-2225 DOI: 10.3390/molecules14062212.
27. Prasad, B.B., Tiwari, K., Singh, M., Sharma, P.S., Patel, A.K. and Srivastava, S., *Ultratrace analysis of uracil and 5-fluorouracil by molecularly imprinted polymer brushes grafted to silylated solid-phase microextraction fiber in combination with complementary molecularly imprinted polymer-based sensor*. Biomedical Chromatography, 2009. 23(5): p. 499-509 DOI: 10.1002/bmc.1145.
28. Chouhan, R. and Bajpai, A.K., *An in vitro release study of 5-fluoro-uracil (5-FU) from swellable poly-(2-hydroxyethyl methacrylate) (PHEMA) nanoparticles*. Journal of Materials Science-Materials in Medicine, 2009. 20(5): p. 1103-1114 DOI: 10.1007/s10856-008-3677-x.

29. Cirillo, G., Iemma, F., Puoci, F., Parisi, O.I., Curcio, M., Spizzirri, U.G. and Picci, N., *Imprinted hydrophilic nanospheres as drug delivery systems for 5-fluorouracil sustained release*. Journal of Drug Targeting, 2009. 17(1): p. 72-77 DOI: 10.1080/10611860802455813.
30. Prasad, B.B., Srivastava, S., Tiwari, K. and Sharma, P.S., *Development of Uracil and 5-Fluorouracil Sensors Based on Molecularly Imprinted Polymer-Modified Hanging Mercury Drop Electrode*. Sensors and Materials, 2009. 21(6): p. 291-306.
31. Arias, J.L., *Novel Strategies to Improve the Anticancer Action of 5-Fluorouracil by Using Drug Delivery Systems*. Molecules, 2008. 13(10): p. 2340-2369 DOI: 10.3390/molecules13102340.
32. Figueiredo, E.C., Dias, A.C.B. and Arruda, M.A.Z., *Molecular Imprinting: a promising strategy in matrices elaboration for drug delivery systems*. Revista Brasileira De Ciencias Farmaceuticas, 2008. 44(3): p. 361-375.
33. Puoci, F., Cirillo, G., Curcio, M., Iemma, F., Parisi, O.I., Castiglione, M. and Picci, N., *Molecularly imprinted polymers for alpha-tocopherol delivery*. Drug Delivery, 2008. 15(4): p. 253-258 DOI: 10.1080/10717540802006724.
34. BelBruno, J.J., Richter, A. and Gibson, U.J., *Amazing pores: Processing, morphology and functional states of molecularly imprinted polymers as sensor materials*. Molecular Crystals and Liquid Crystals, 2008. 483: p. 179-190 DOI: 10.1080/15421400801905135.
35. Polyakov, M.V., *Adsorption properties and structure of silica gel*. Zhurnal Fizieskoj Khimii, 1931. 2: p. 799-805.
36. Sousa, M.D. and Barbosa, C.M., *Molecularly imprinted polymers for controlling drug release. Part 1: Synthesis and characterization*. Quimica Nova, 2009. 32(6): p. 1609-1619.
37. Haurowitz, F. and Breinl, F., *A quantitative investigation into the distribution of an arsenical antigen in an organism*. Hoppe-Seylers Zeitschrift Fur Physiologische Chemie, 1932. 205: p. 259-270 DOI: 10.1515/bchm2.1932.205.5-6.259.
38. Mudd, S., *A hypothetical mechanism of antibody formation*. Journal of Immunology, 1932. 23(6): p. 423-427.
39. Pauling, L. and Campbell, D.H., *The manufacture of antibodies in vitro*. Journal of Experimental Medicine, 1942. 76: p. 211-220.
40. Grassi, V., *Polímeros molecularmente impressos (MIPs) como extratores em fase sólida em sistemas de análises em fluxo.*, in *Centro de energia nuclear na agricultura*. 2008, Universidade de São Paulo.
41. Dickey, F.H., *The preparation of specific adsorbents*. Proceedings of the National Academy of Sciences of the United States of America, 1949. 35((5)): p. 227-229.
42. Takagishi, T. and Klotz, I.M., *Macromolecule-small molecule interactions; introduction of additional binding sites in polyethyleneimine by disulfide cross-linkages*. Biopolymers, 1972. 11((2)): p. 483-491.
43. Wulff, G. and Sarhan, A., *The use of polymers with enzyme-analogous structures for the resolution of racemates*. Angewandte Chemie-International Edition In English, 1972. 11((4)): p. 341.
44. Arshady, R. and Mosbach, K., *Synthesis of substrate-selective polymers by host-guest polymerization*. Macromolecular Chemistry And Physics, 1981. 182((2)): p. 687-692.
45. Whitcombe, M.J., Rodriguez, M.E., Villar, P. and Vulfson, E.N., *A new method for the introduction of recognition site functionality into polymers prepared by molecular imprinting - synthesis and characterization of polymeric receptors for cholesterol*. Journal of the American Chemical Society, 1995. 117((27)): p. 7105-7111.
46. Imprinting, T.S.f.M. [cited 2015 August]; Available from: <http://mipdatabase.com/>.

47. Sellergren, B., *Imprinted polymers with memory for small molecules, proteins, or crystals*. *Angewandte Chemie-International Edition*, 2000. 39(6): p. 1031 DOI: 10.1002/(sici)1521-3773(20000317)39:6<1031::aid-anie1031>3.0.co;2-f.
48. Sellergren, B., *Molecularly Imprinted Polymers: Man-Made Mimics of Antibodies and their Application in Analytical Chemistry*. Vol. 23. 2001, Amsterdam: Elsevier Science.
49. Freitas, A. and Dias, R.C.S. *Síntese e Caracterização de Partículas de Polímeros Impressos Molecularmente (MIPs) para Aplicações Biomédicas*. in *II Encontro de Jovens Investigadores*. 2014. Bragança, Portugal.
50. B, S., *Enantiomer separations using designed imprinted chiral phases.*, in *Chiral Separation Techniques: A Practical Approach*, S. G, Editor. 2001, Wiley-VCH Verlag GmbH: Weinheim. p. 153-184.
51. Lanza, F. and Sellergren, B., *Molecularly imprinted extraction materials for highly selective sample cleanup and analyte enrichment.*, in *Advances in Chromatography*, G.E. Brown PR, Editor. 2001, Marcel Dekker. p. 137-173.
52. Andersson, L.I. and Schweitz, L., *Solid-phase extraction on molecularly imprinted polymers.*, in *Bioanalytical Separations*, W. I, Editor. 2003, Elsevier: Amsterdam. p. 45-71.
53. Wulff, G., *Enzyme-like catalysis by molecularly imprinted polymers*. *Chemical Reviews*, 2002. 102(1): p. 1-27 DOI: 10.1021/cr980039a.
54. Haupt, K. and Mosbach, K., *Molecularly imprinted polymers and their use in biomimetic sensors*. *Chemical Reviews*, 2000. 100(7): p. 2495-2504 DOI: 10.1021/cr990099w.
55. Ye, L. and Mosbach, K., *Polymers recognizing biomolecules based on a combination of molecular imprinting and proximity scintillation: A new sensor concept*. *Journal of the American Chemical Society*, 2001. 123(12): p. 2901-2902 DOI: 10.1021/ja005896m.
56. Kadhivel, P., Machado, C., Freitas, A., Oliveira, T., Dias, R.C.S. and Costa, M.R.P.F.N., *Molecular imprinting in hydrogels using reversible addition-fragmentation chain transfer polymerization and continuous flow micro-reactor*. *Journal of Chemical Technology and Biotechnology*, 2015 DOI: 10.1002/jctb.4681.
57. Cormack, P.A.G. and Elorza, A.Z., *Molecularly imprinted polymers: synthesis and characterisation*. *Journal of Chromatography B-Analytical Technologies in the Biomedical and Life Sciences*, 2004. 804(1): p. 173-182 DOI: 10.1016/j.jchromb.2004.02.013.
58. Haupt, K., *Molecularly imprinted polymers in analytical chemistry*. *Analyst*, 2001. 126(6): p. 747-756 DOI: 10.1039/b102799a.
59. Haginaka, J., Tabo, H. and Kagawa, C., *Uniformly sized molecularly imprinted polymers for d-chlorpheniramine: Influence of a porogen on their morphology and enantioselectivity*. *Journal of Pharmaceutical and Biomedical Analysis*, 2008. 46(5): p. 877-881 DOI: 10.1016/j.jpba.2007.05.030.
60. He, J.F., Zhu, Q.H. and Deng, Q.Y., *Investigation of imprinting parameters and their recognition nature for quinine-molecularly imprinted polymers*. *Spectrochimica Acta Part a-Molecular and Biomolecular Spectroscopy*, 2007. 67(5): p. 1297-1305 DOI: 10.1016/j.saa.2006.09.040.
61. Yan, M., *Molecularly Imprinted Materials: Science and Technology*. 2004: CRC Press.
62. Lisichkin, G.V. and Krutyakov, Y.A., *Molecularly imprinted materials: Synthesis, properties, applications*. *Uspekhi Khimii*, 2006. 75(10): p. 998-1017.
63. Kadhivel, P., *Molecular imprints for pharmaceutical drugs of different classes: comparison of sol-gel and acrylic approaches in different formats*, in *Química e Bioquímica*. 2013, Universidade do Porto: Porto (Portugal).
64. Chanda, M., *Introduction to Polymer Science and Chemistry: A Problem-Solving Approach, Second Edition*. 2013: Taylor & Francis.

65. Young, R.J. and Lovell, P.A., *Introduction to Polymers, Third Edition*. 2011: CRC Press.
66. Saldivar-Guerra, E. and Vivaldo-Lima, E., *Handbook of Polymer Synthesis, Characterization, and Processing*. 2013: Wiley.
67. Costa, R.A.S., *Síntese e Teste de Hidrogéis Inteligentes para a Libertação Controlada de Fármacos*, in *Tecnologia Biomédica*. 2013, Instituto Politécnico de Bragança: Bragança (Portugal).
68. Atanase, L.I., Winninger, J., Delaite, C. and Riess, G., *Reversible addition-fragmentation chain transfer synthesis and micellar characteristics of biocompatible amphiphilic poly(vinyl acetate)-graft-poly(N-vinyl-2-pyrrolidone) copolymers*. *European Polymer Journal*, 2014. 53: p. 109-117 DOI: 10.1016/j.eurpolymj.2014.01.029.
69. Freitas, A., Machado, C., Kadhivel, P., Dias, R.C.S. and Costa, M.R.P.F.N. *Production of RAFT Imprinted Smart Hydrogel Particles in a Continuous Flow Micro-reactor*. in *12th International Chemical and Biological Engineering Conference*. 2014. Porto (Portugal).
70. Freitas, A., Machado, C., Oliveira, T., Reitor, P., Kadhivel, P., Dias, R.C.S. and Costa, M.R.P.F.N. *Development of Tailored Hydrogels using RAFT Polymerization in Continuous Flow Microreactor*. in *8th ECNP International Conference on Nanostructured Polymers and Nanocomposites*. 2014. Dresden, Germany.
71. Ornelas, M., *Development and evaluation of general emulsion methods for the preparation of molecularly imprinted silicas in spherical format*, in *Departamento de Química e Bioquímica*. 2014, Universidade do Porto: Porto (Portugal).
72. Ebewele, R.O., *Polymer Science and Technology*. 2000: Taylor & Francis.
73. Kumbar, S., Laurencin, C. and Deng, M., *Natural and Synthetic Biomedical Polymers*. 2014: Elsevier Science.
74. He, C.Y., Long, Y.Y., Pan, J.L., Li, K. and Liu, F., *Application of molecularly imprinted polymers to solid-phase extraction of analytes from real samples*. *Journal of Biochemical and Biophysical Methods*, 2007. 70(2): p. 133-150 DOI: 10.1016/j.jbbm.2006.07.005.
75. Mayes, A.G. and Mosbach, K., *Molecularly imprinted polymer beads: Suspension polymerization using a liquid perfluorocarbon as the dispersing phase*. *Analytical Chemistry*, 1996. 68(21): p. 3769-3774 DOI: 10.1021/ac960363a.
76. Omidian, H., Zohuriaan-Mehr, M.J. and Bouhendi, H., *Polymerization of sodium acrylate in inverse-suspension stabilized by sorbitan fatty esters*. *European Polymer Journal*, 2003. 39(5): p. 1013-1018 DOI: 10.1016/s0014-3057(02)00352-x.
77. Matyjaszewski, K. and Davis, T.P., *Handbook of Radical Polymerization*. 2003: Wiley.
78. Texter, J., *Reactions And Synthesis In Surfactant Systems*. 2001: Taylor & Francis.
79. Puoci, F., Iemma, F., Cirillo, G., Picci, N., Matricardi, P. and Alhaique, F., *Molecularly imprinted polymers for 5-fluorouracil release in biological fluids*. *Molecules*, 2007. 12(4): p. 805-814 DOI: 10.3390/12040805.
80. Zhu, Q.F., Ma, C., Chen, H.X., Wu, Y.Q. and Huang, J.L., *A molecular imprint-coated stirrer bar for selective extraction of caffeine, theobromine and theophylline*. *Microchimica Acta*, 2014. 181(3-4): p. 303-311 DOI: 10.1007/s00604-013-1117-1.
81. Poleszak, E., Szopa, A., Wyska, E., Wośko, S., Serefko, A., Wlaź, A., Pieróg, M., Wróbel, A. and Wlaź, P., *The influence of caffeine on the activity of moclobemide, venlafaxine, bupropion and milnacipran in the forced swim test in mice*. *Life Sciences*, 2015. 136: p. 13-18.
82. Vlatakis, G., Andersson, L.I., Muller, R. and Mosbach, K., *Drug assay using antibody mimics made by molecular imprinting*. *Nature*, 1993. 361(6413): p. 645-647 DOI: 10.1038/361645a0.

83. Huang, H.C., Lin, C.I., Joseph, A.K. and Lee, Y.D., *Photo-lithographically impregnated and molecularly imprinted polymer thin film for biosensor applications*. Journal of Chromatography A, 2004. 1027(1-2): p. 263-268 DOI: 10.1016/j.chroma.2003.08.106.
84. Yano, K. and Karube, I., *Molecularly imprinted polymers for biosensor applications*. Trac-Trends in Analytical Chemistry, 1999. 18(3): p. 199-204 DOI: 10.1016/s0165-9936(98)00119-8.
85. Barrios, C.A., Carrasco, S., Francesca, M., Yurrita, P., Navarro-Villoslada, F. and Moreno-Bondi, M.C., *Molecularly imprinted polymer for label-free integrated optical waveguide bio(mimetic)sensors*. Sensors and Actuators B-Chemical, 2012. 161(1): p. 607-614 DOI: 10.1016/j.snb.2011.11.008.
86. Cunliffe, D., Kirby, A. and Alexander, C., *Molecularly imprinted drug delivery systems*. Advanced Drug Delivery Reviews, 2005. 57(12): p. 1836-1853.
87. Piletsky, S.A., Turner, N.W. and Laitenberger, P., *Molecularly imprinted polymers in clinical diagnostics - Future potential and existing problems*. Medical Engineering & Physics, 2006. 28(10): p. 971-977 DOI: 10.1016/j.medengphy.2006.05.004.
88. Cirillo, G., Parisi, O.I., Curcio, M., Puoci, F., Iemma, F., Spizzirri, U.G. and Picci, N., *Molecularly imprinted polymers as drug delivery systems for the sustained release of glycyrrhizic acid*. Journal of Pharmacy and Pharmacology, 2010. 62(5): p. 577-582 DOI: 10.1211/jpp.62.05.0003.
89. Zhao, W.F., Fang, B.H., Li, N., Nie, S.Q., Wei, Q. and Zhao, C.S., *Fabrication of pH-Responsive Molecularly Imprinted Polyethersulfone Particles for Bisphenol-A Uptake*. Journal of Applied Polymer Science, 2009. 113(2): p. 916-921 DOI: 10.1002/app.30014.
90. Singh, B. and Chauhan, N., *Preliminary evaluation of molecular imprinting of 5-fluorouracil within hydrogels for use as drug delivery systems*. Acta Biomaterialia, 2008. 4(5): p. 1244-1254 DOI: 10.1016/j.actbio.2008.03.017.
91. Ruela, A.L.M., Figueiredo, E.C. and Pereira, G.R., *Molecularly imprinted polymers as nicotine transdermal delivery systems*. Chemical Engineering Journal, 2014. 248: p. 1-8 DOI: 10.1016/j.cej.2013.12.106.
92. Mirzaei, M., Najafabadi, S.A.H., Abdouss, M., Azodi-Deilami, S., Asadi, E., Hosseini, M.R.M. and Piramoon, M., *Preparation and utilization of microporous molecularly imprinted polymer for sustained release of tetracycline*. Journal of Applied Polymer Science, 2013. 128(3): p. 1557-1562 DOI: 10.1002/app.38311.
93. Byrne, M.E. and Salian, V., *Molecular imprinting within hydrogels II: Progress and analysis of the field*. International Journal of Pharmaceutics, 2008. 364(2): p. 188-212 DOI: 10.1016/j.ijpharm.2008.09.002.
94. Nie, T., Baldwin, A., Yamaguchi, N. and Kiick, K.L., *Production of heparin-functionalized hydrogels for the development of responsive and controlled growth factor delivery systems*. Journal of Controlled Release, 2007. 122(3): p. 287-296 DOI: 10.1016/j.jconrel.2007.04.019.
95. Sigma-Aldrich. Available from: <http://www.sigmaaldrich.com/portugal.html>.
96. Organics, A. 08/10/2014]; Available from: <http://www.acros.com/Welcome.aspx>.
97. Scientific, F. 08/10/2014]; Available from: <http://www.fishersci.com/us/en/home.html>.
98. Panreac. Span 80. 09/10/2014]; Available from: <http://pub.panreac.com/ds/156094IN.HTM>.
99. Bragança, E.S.A.-I.P.d., *WDI*. 2014.
100. Lorber, N., Pavageau, B. and Mignard, E., *Investigating Acrylic Acid Polymerization by Using a Droplet-Based Microfluidics Approach*, in *Modern Trends in Polymer Science-Epf 09*, F. Stelzer and E. Wiesbrock, Editors. 2010, Wiley-V C H Verlag GmbH: Weinheim. p. 203-209.

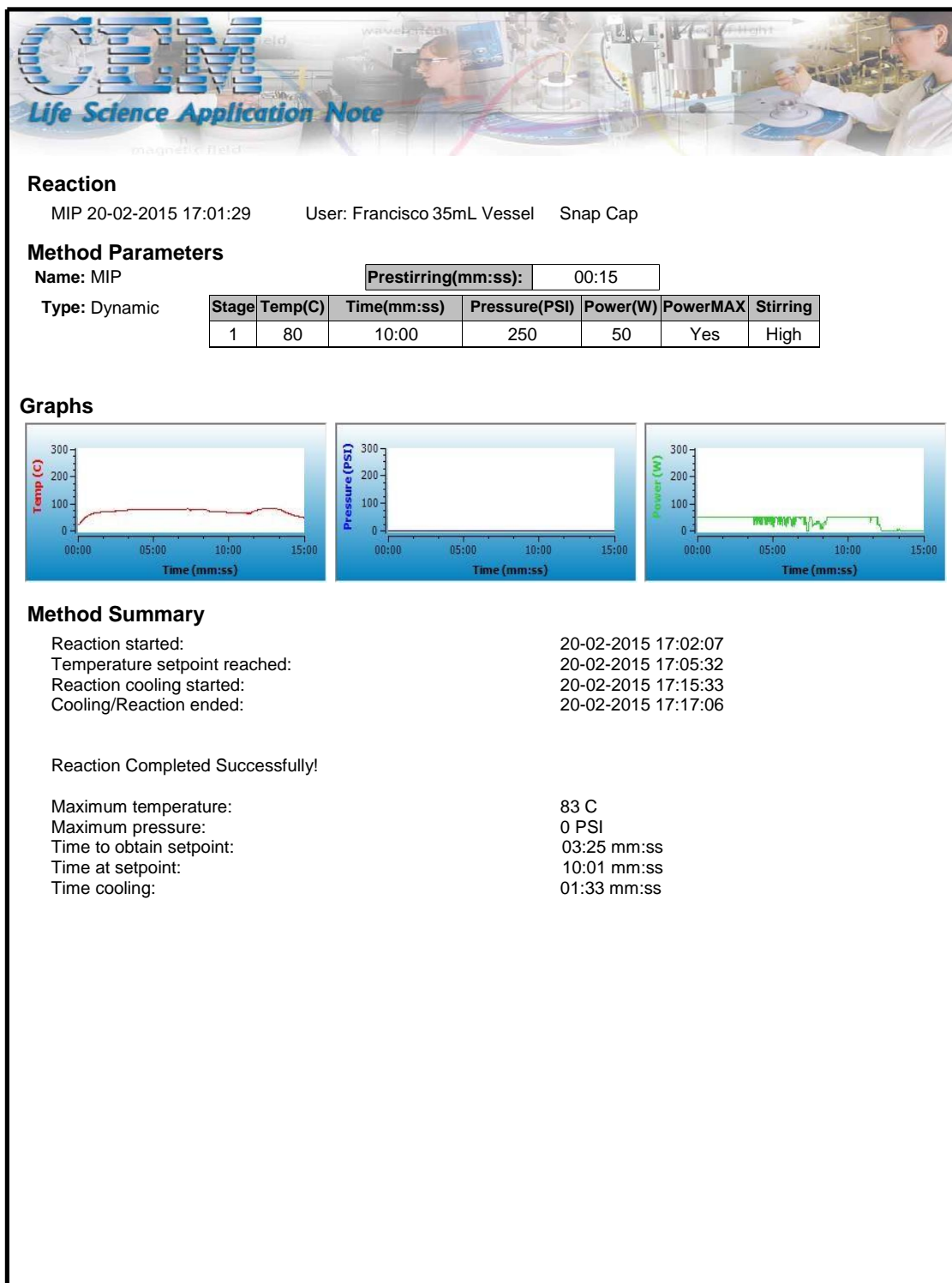
101. Cruz, R.M.S., Khmelinskii, I. and Vieira, M., *Methods in Food Analysis*. 2014: Taylor & Francis.
102. Luque de Castro, M.D. and Priego-Capote, F., *Soxhlet extraction: Past and present panacea*. *Journal of Chromatography A*, 2010. 1217(16): p. 2383-2389.
103. Poole, C.F., *New trends in solid-phase extraction*. *Trac-Trends in Analytical Chemistry*, 2003. 22(6): p. 362-373 DOI: 10.1016/s0165-9936(03)00605-8.
104. Zwir-Ferenc, A. and Biziuk, M., *Solid phase extraction technique - Trends, opportunities and applications*. *Polish Journal of Environmental Studies*, 2006. 15(5): p. 677-690.
105. Hennion, M.C., *Solid-phase extraction: method development, sorbents, and coupling with liquid chromatography*. *Journal of Chromatography A*, 1999. 856(1-2): p. 3-54 DOI: 10.1016/s0021-9673(99)00832-8.
106. Yi, L.X., Fang, R. and Chen, G.H., *Molecularly Imprinted Solid-Phase Extraction in the Analysis of Agrochemicals*. *Journal of Chromatographic Science*, 2013. 51(7): p. 608-618 DOI: 10.1093/chromsci/bmt024.
107. Dias, R.C.S., *Principios Básicos de Análise Frontal*. 2014: Instituto Politécnico de Bragança.
108. Zhang, H.Q., *Controlled/"living" radical precipitation polymerization: A versatile polymerization technique for advanced functional polymers*. *European Polymer Journal*, 2013. 49(3): p. 579-600 DOI: 10.1016/j.eurpolymj.2012.12.016.



# **Annexes**



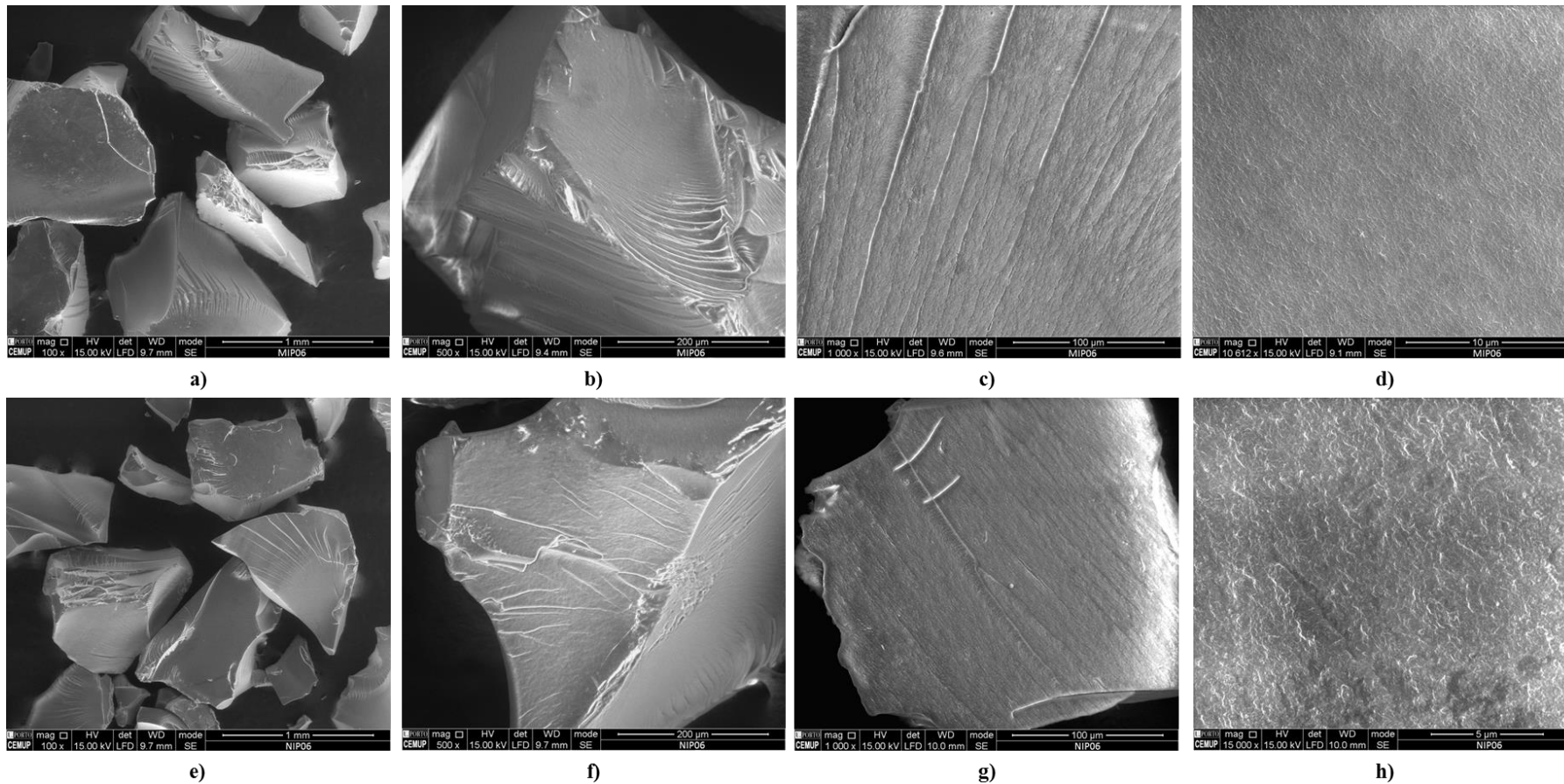
**Annex 1** - Report of synthesis performed in the microwave system in a Discovery®SP equipment.



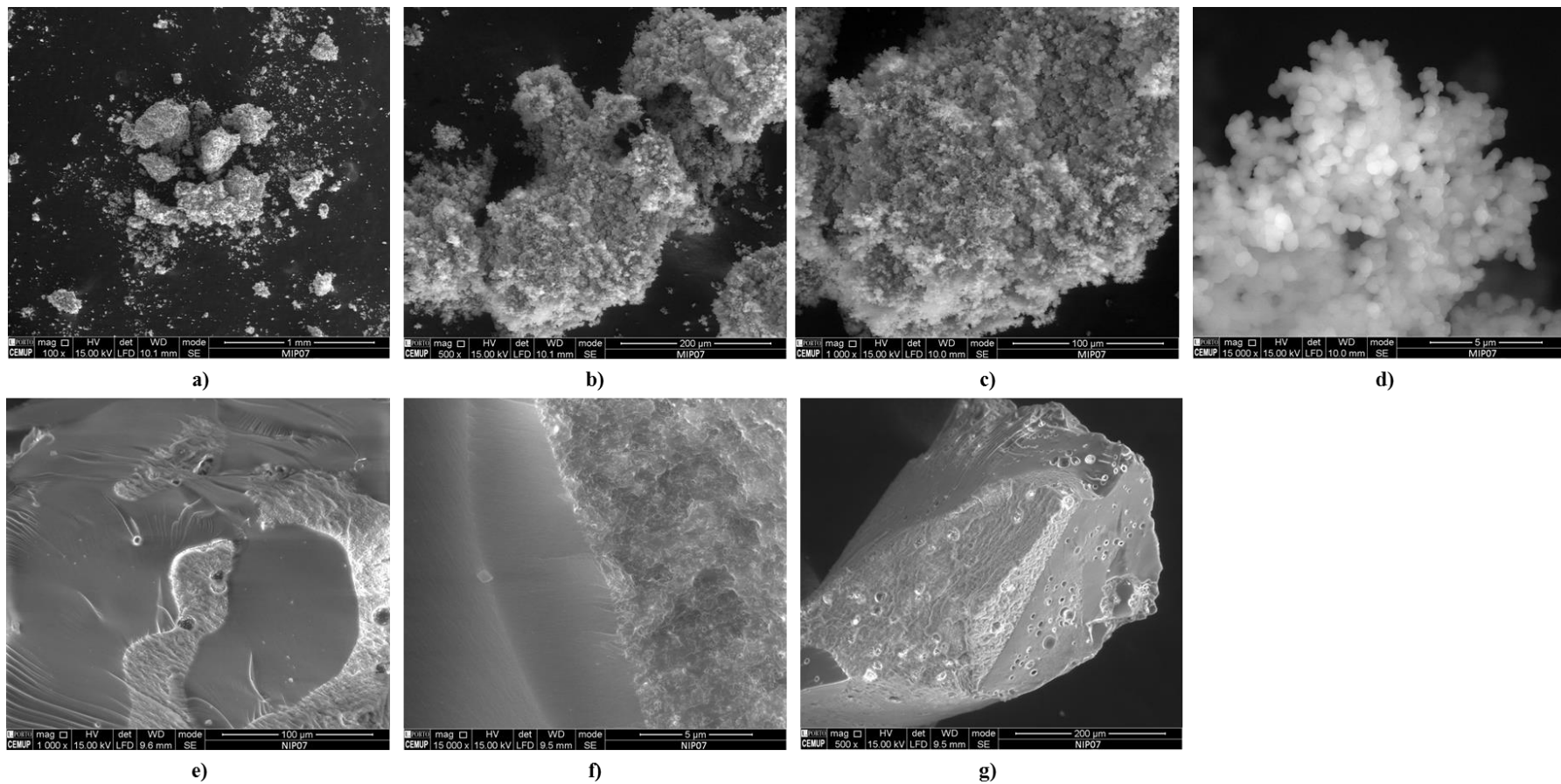
Accelerating the transformation of concept to cure

P.O. Box 200 Matthews, NC 28106 • 800.726.3331 • www.cemsynthesis.com

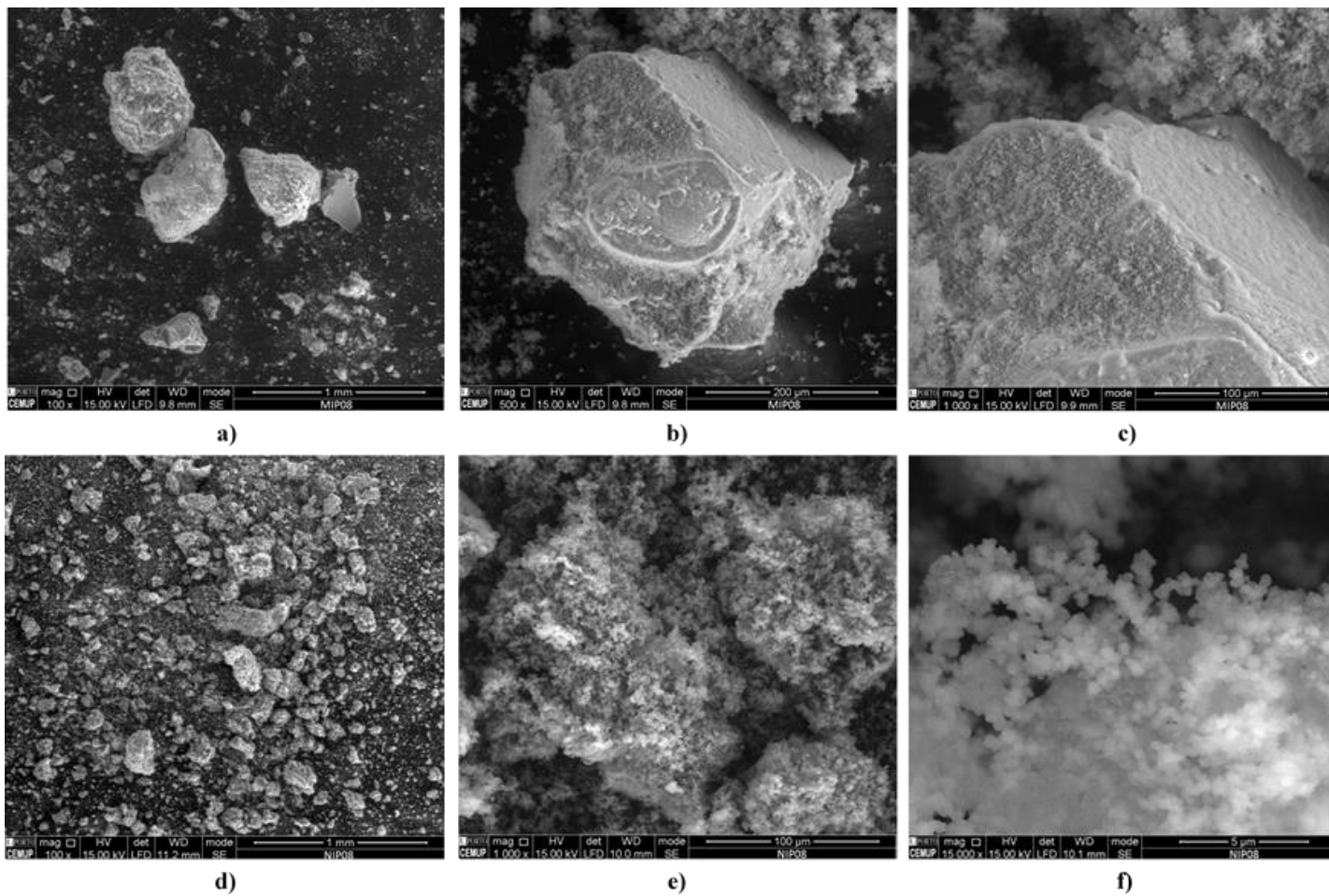
Annex 2 - SEM micrographs of MIPs and NIPs produced. a), b), c), d) MIP<sub>06</sub> synthesized by batch reactor with 5FU; e), f), g), h) NIP<sub>06</sub> synthesized by batch reactor.



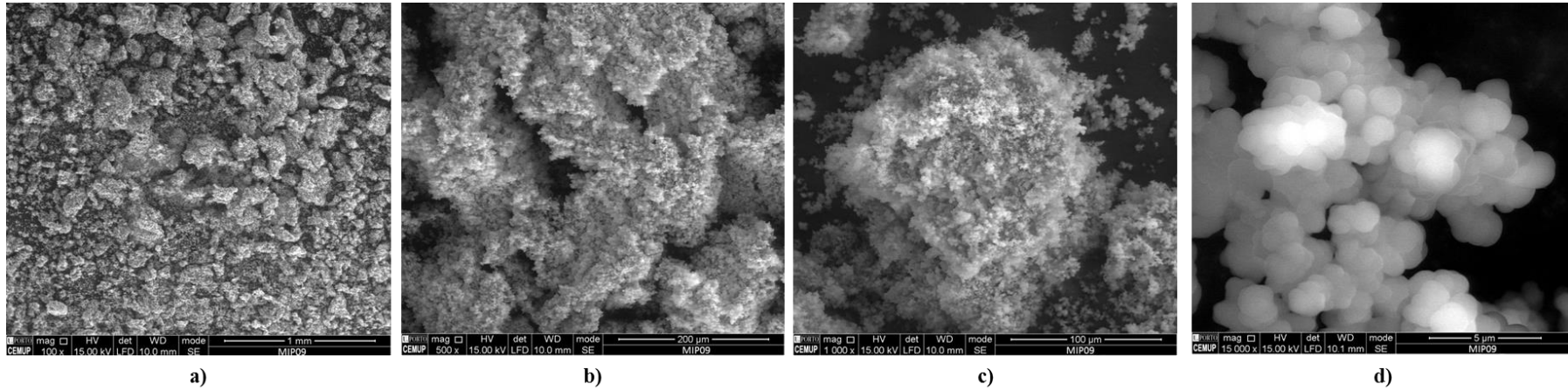
Annex 3 - SEM micrographs of MIPs and NIPs produced. a), b), c), d) MIP<sub>07</sub> synthesized by inverse suspension with 5FU; e), f), g) NIP<sub>07</sub> synthesized by inverse suspension.



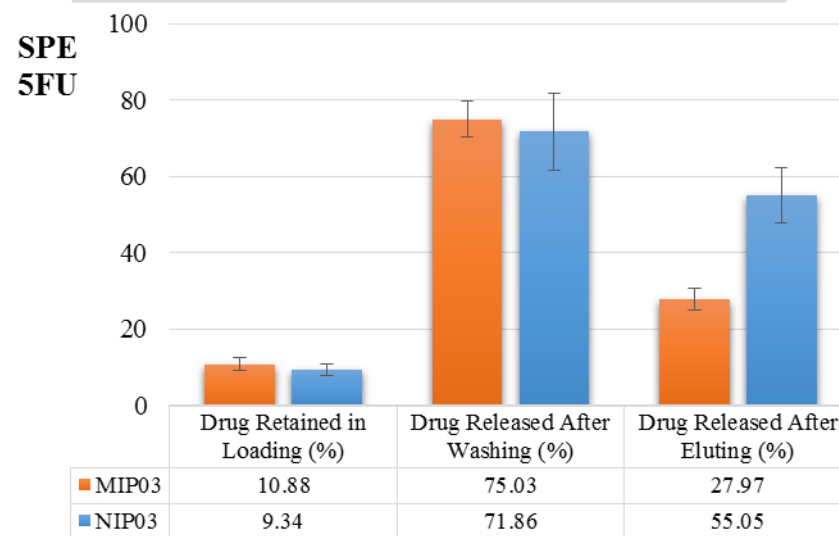
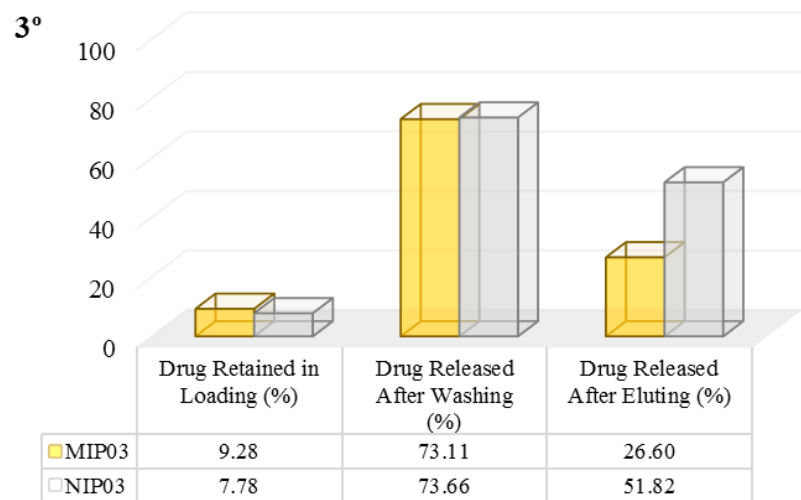
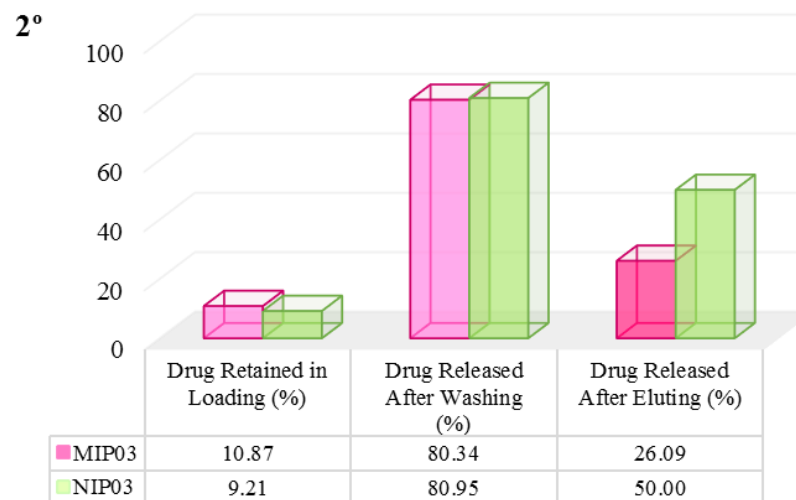
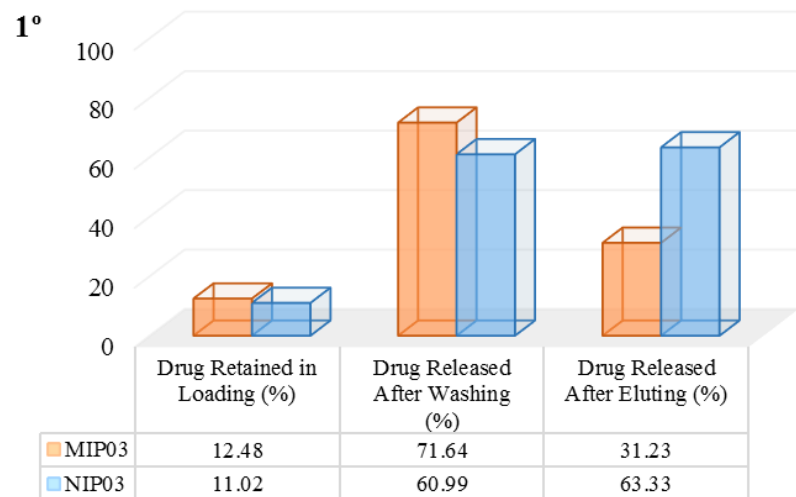
**Annex 4** - SEM micrographs of MIPs and NIPs produced. a), b), c) MIP<sub>08</sub> synthesized by inverse suspension with 5FU; d), e), f) NIP<sub>08</sub> synthesized by inverse suspension.



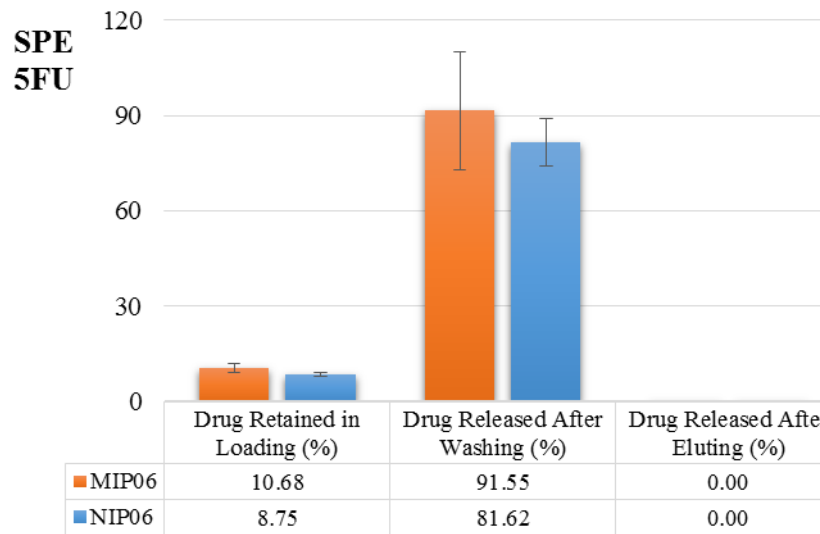
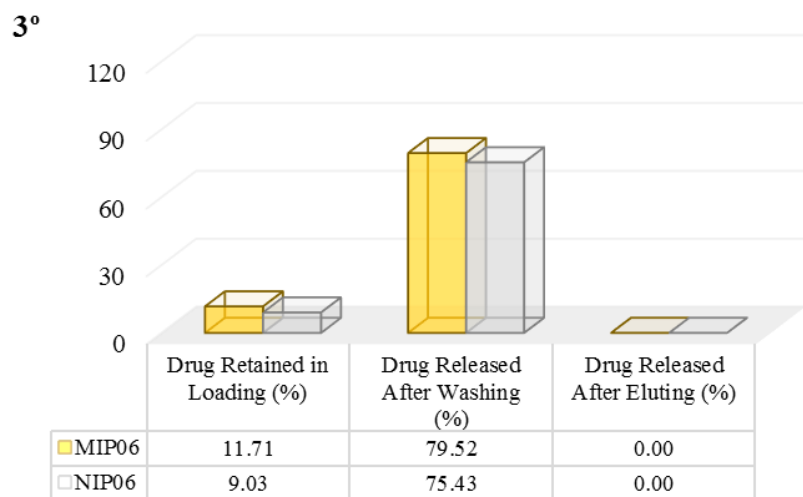
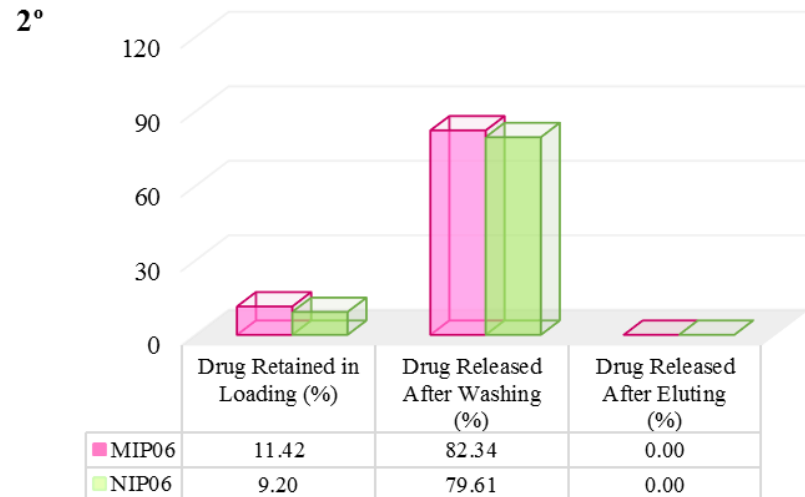
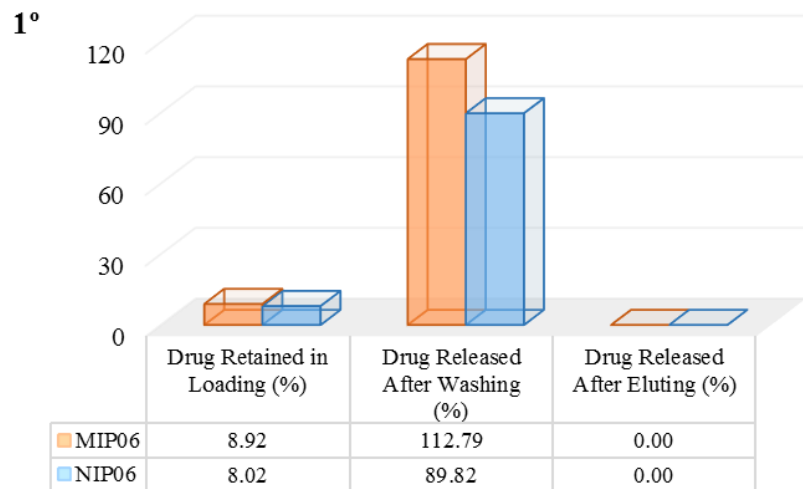
**Annex 5** - SEM micrographs of MIPs produced. a), b), c), d) MIP<sub>08</sub> synthesized by inverse suspension with CAF.



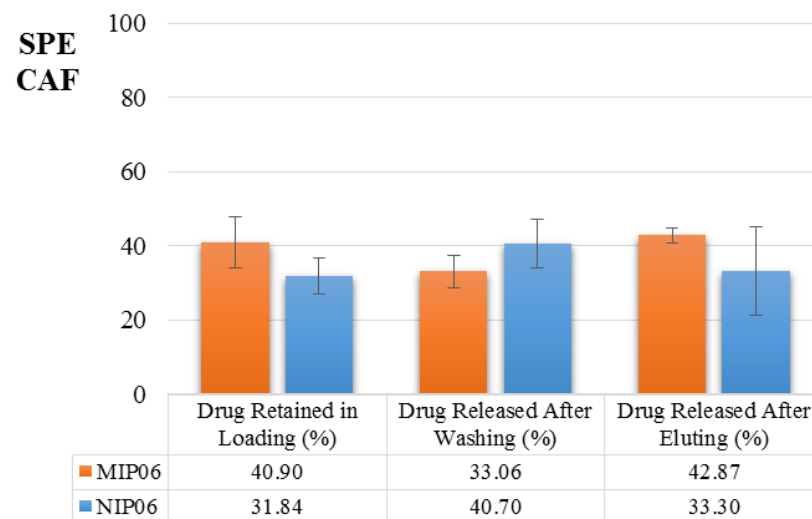
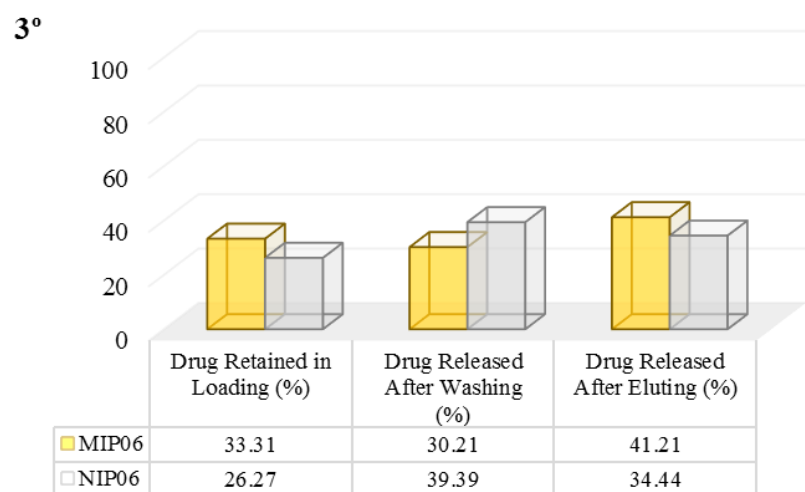
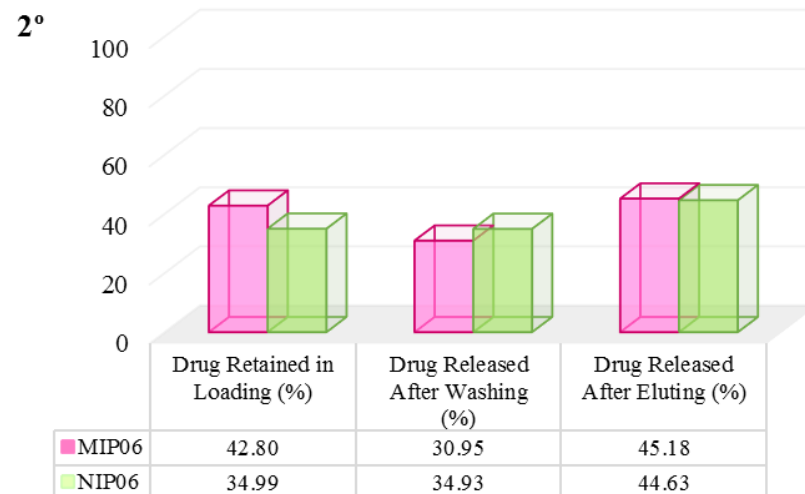
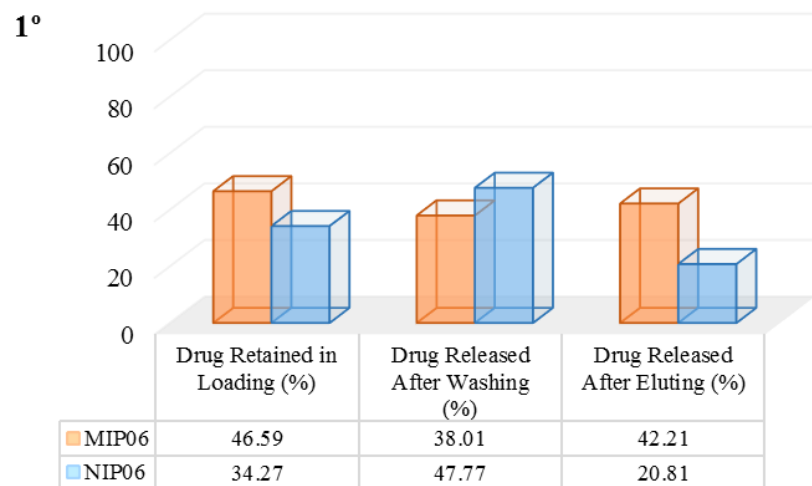
**Annex 6** - Study of adsorption and desorption of 5FU in the MIP<sub>03</sub>/NIP<sub>03</sub> (see Table 4.2). Characterization of the MIP by SPE (Loading, Washing and Eluting step).



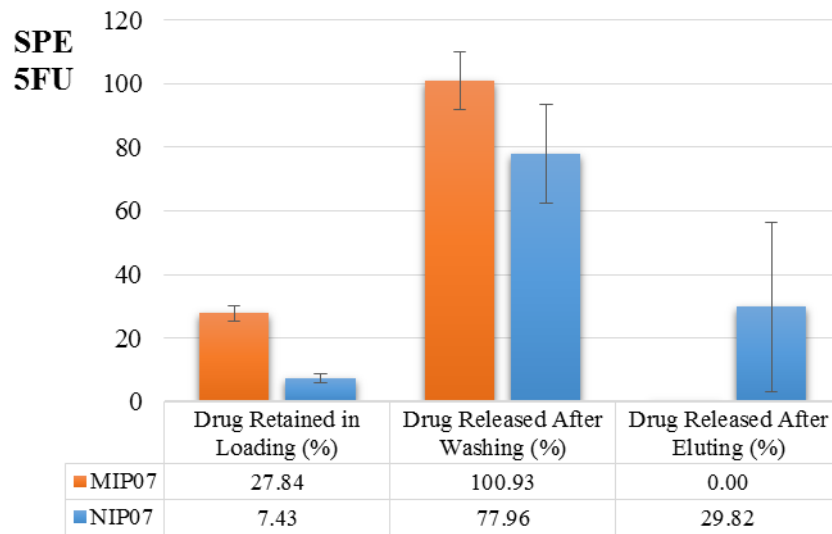
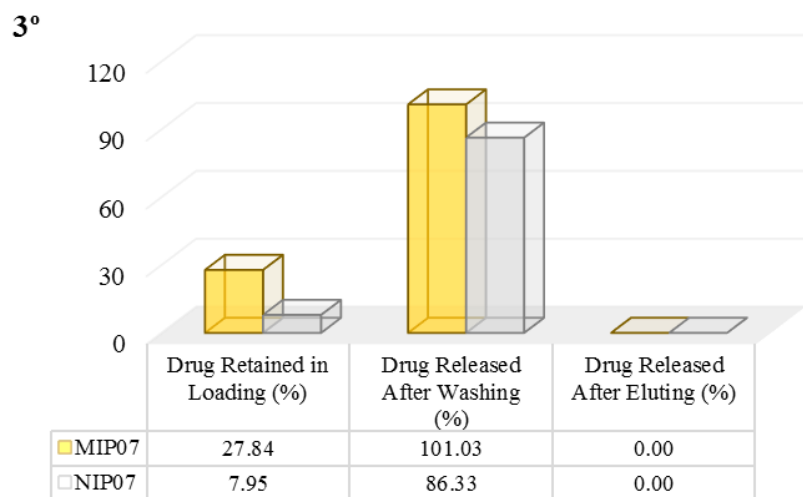
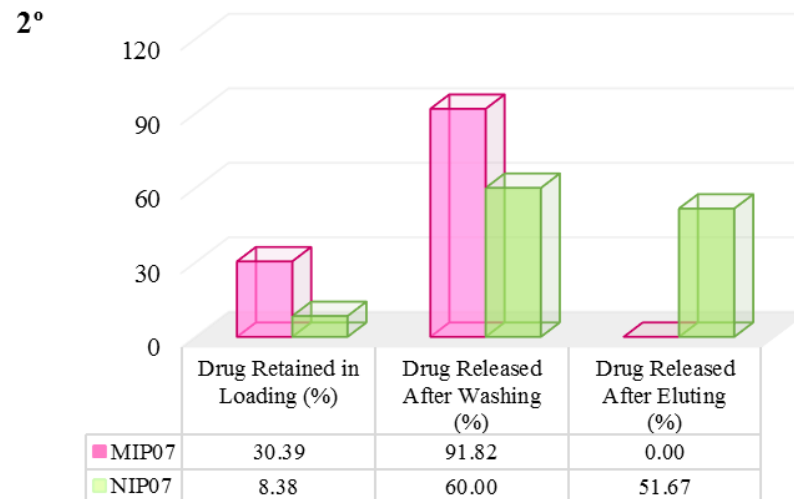
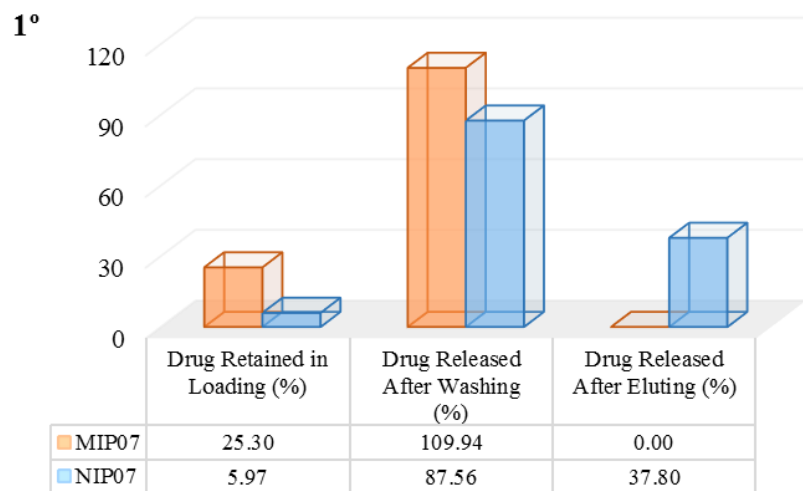
**Annex 7** - Study of adsorption and desorption of 5FU in the MIP<sub>06</sub>/NIP<sub>06</sub> (see Table 4.2). Characterization of the MIP by SPE (Loading, Washing and Eluting step).



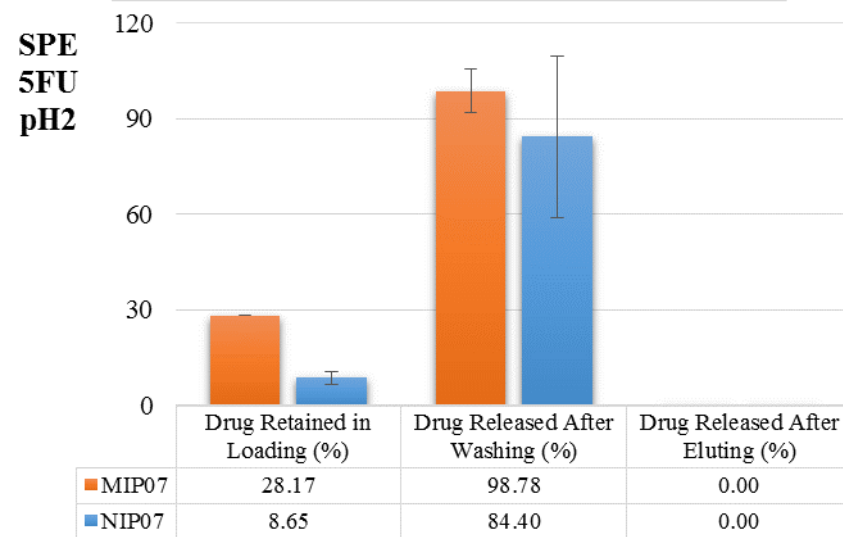
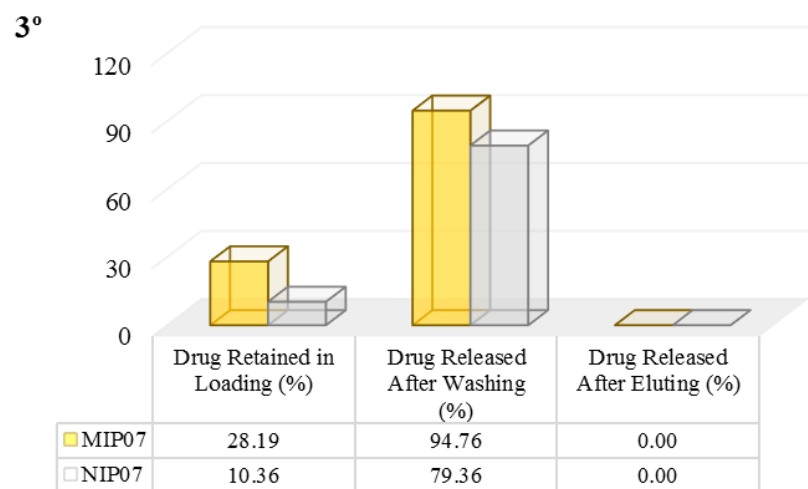
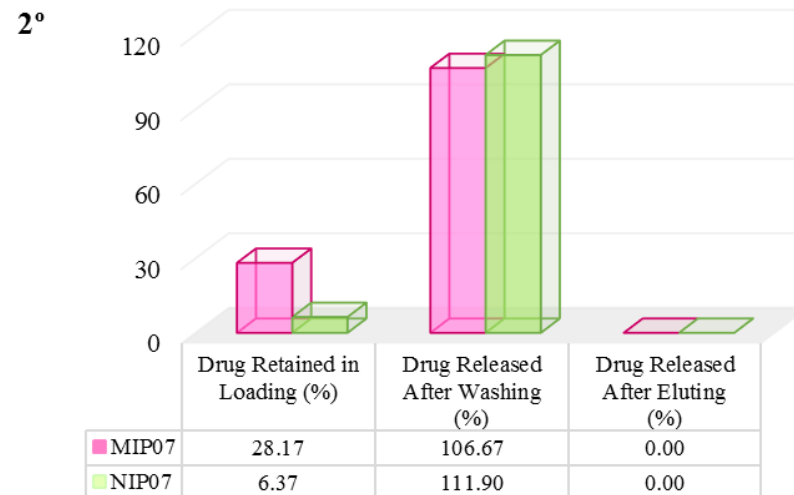
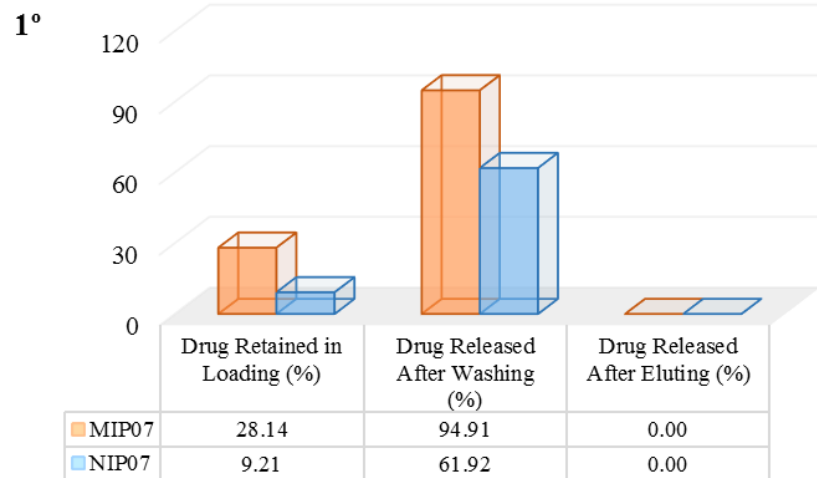
**Annex 8** - Study of adsorption and desorption of CAF in the MIP<sub>06</sub>/NIP<sub>06</sub> (see Table 4.2). Characterization of the MIP by SPE (Loading, Washing and Eluting step).



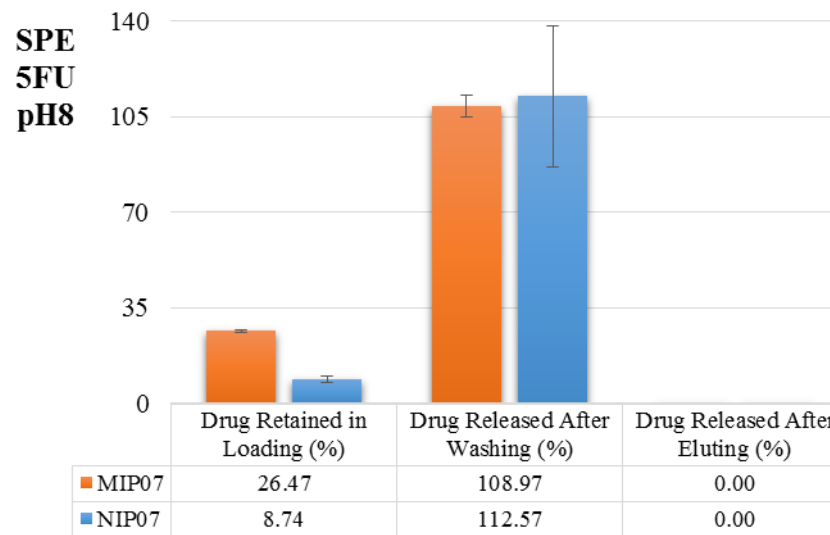
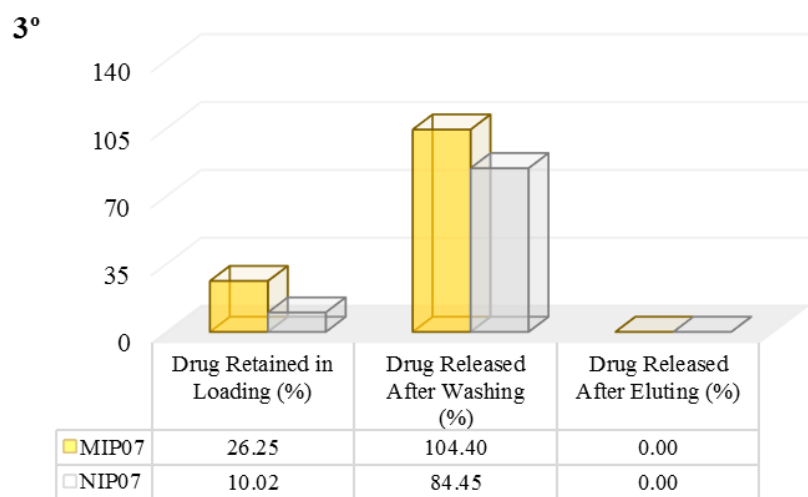
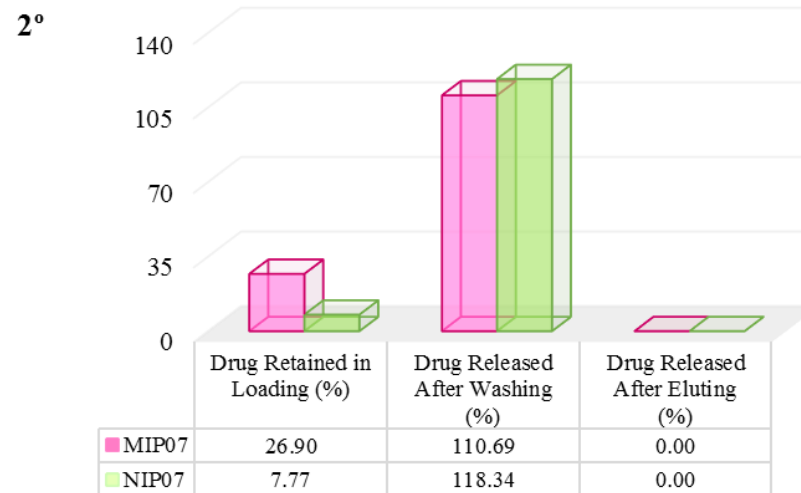
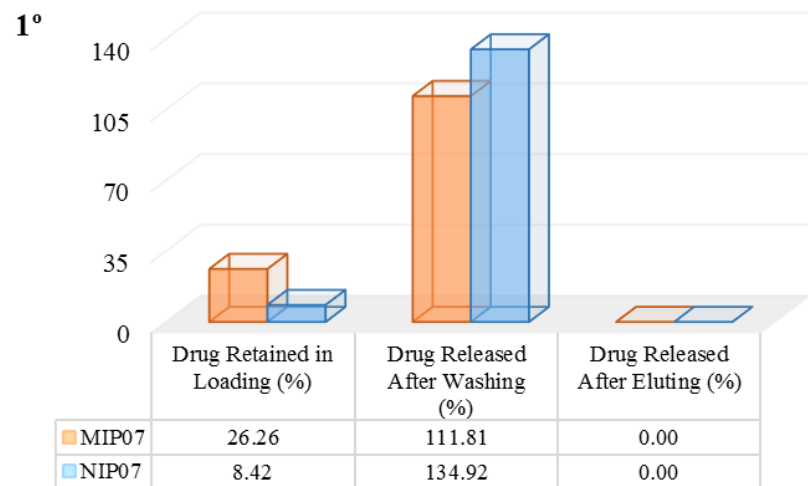
**Annex 9** - Study of adsorption and desorption of 5FU in the MIP<sub>07</sub>/NIP<sub>07</sub> (see Table 4.3). Characterization of the MIP by SPE (Loading, Washing and Eluting step).



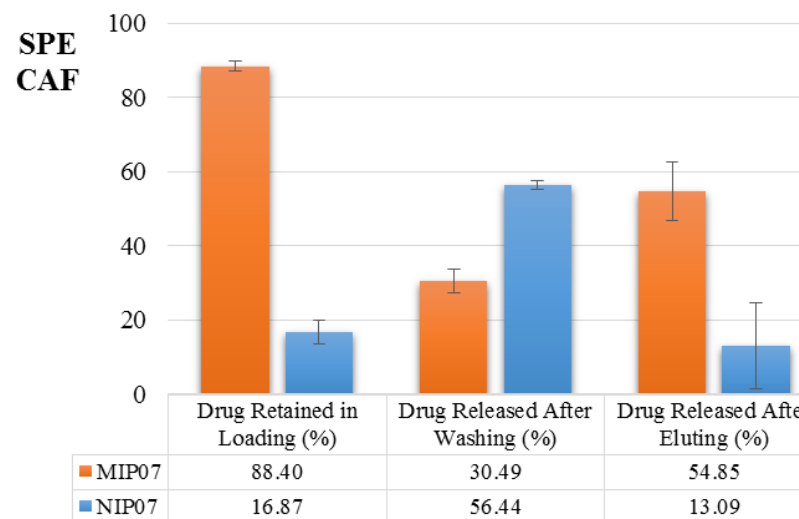
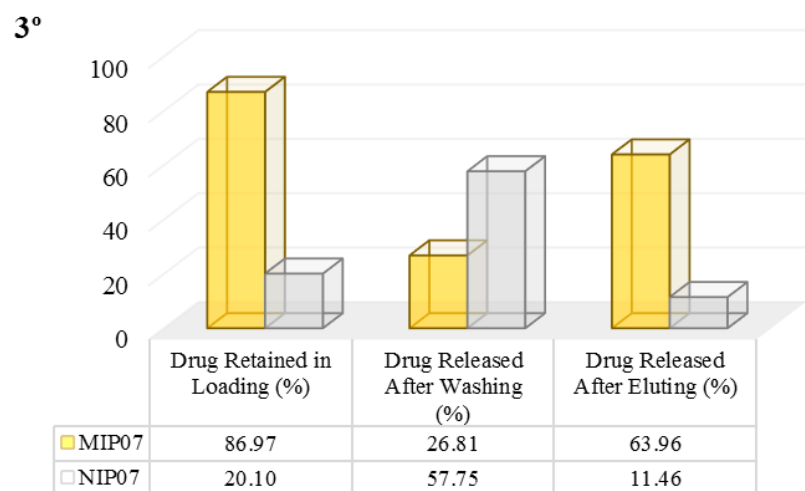
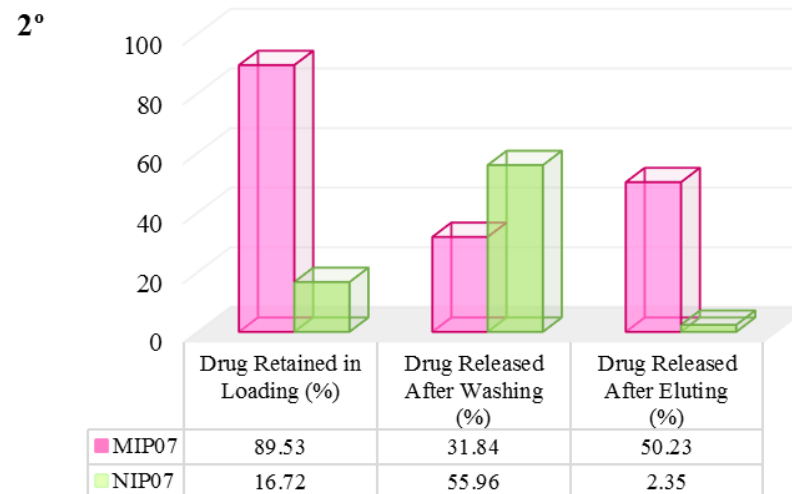
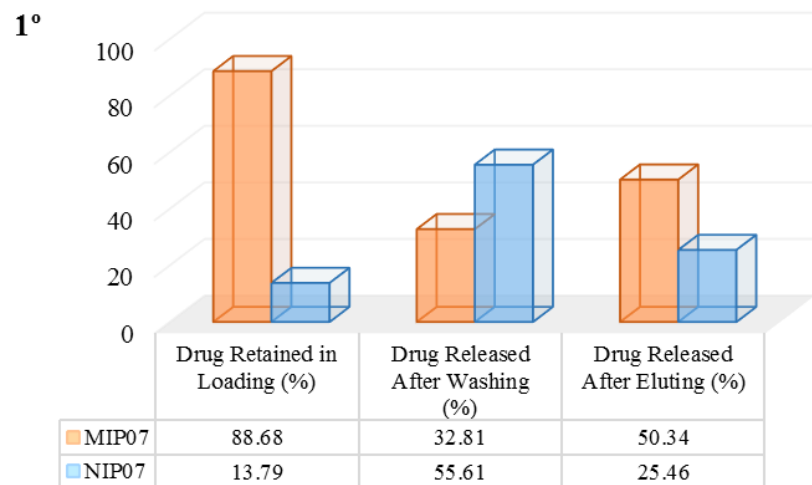
**Annex 10** - Study of adsorption and desorption of 5FU pH2 in the MIP<sub>07</sub>/NIP<sub>07</sub> (see Table 4.3). Characterization of the MIP by SPE (Loading, Washing and Eluting step).



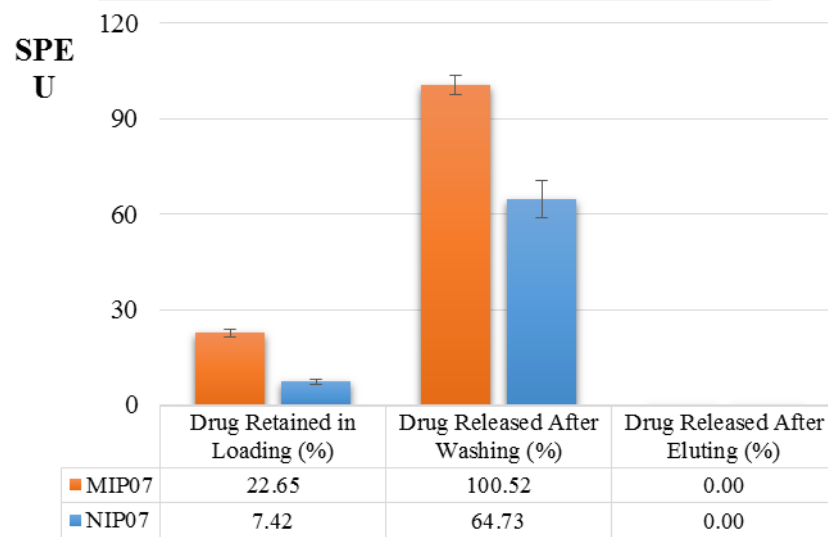
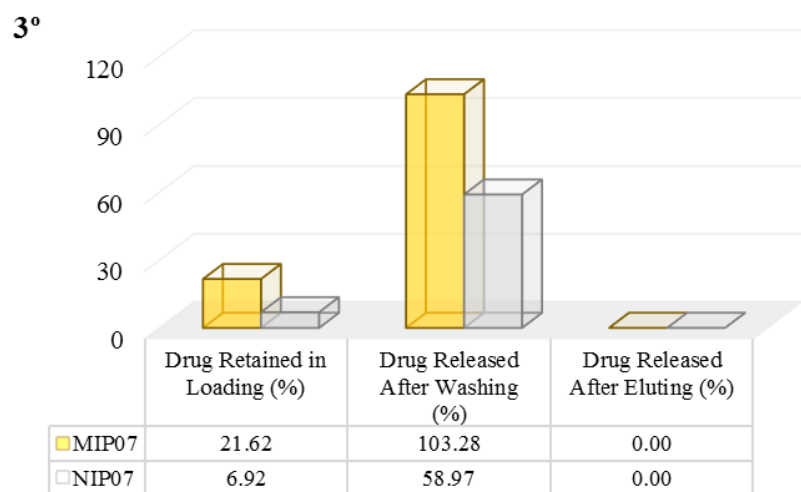
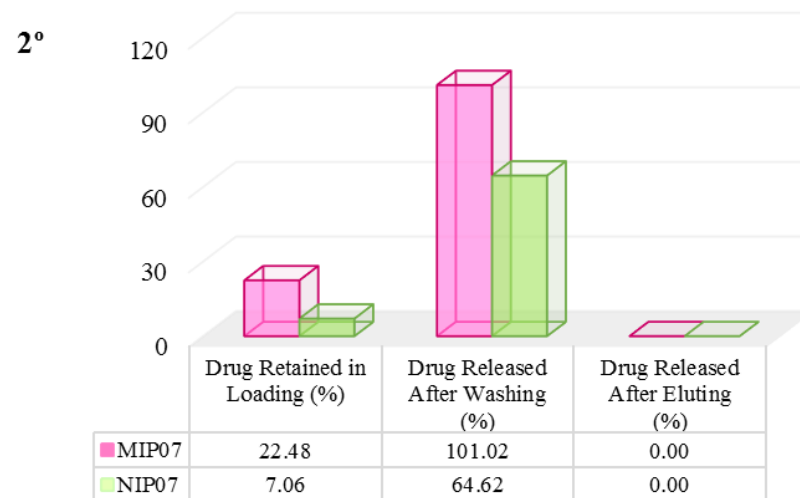
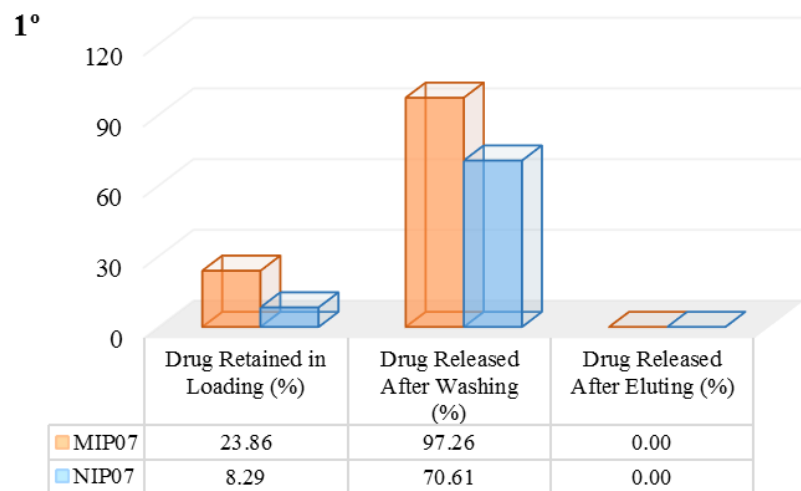
**Annex 11** - Study of adsorption and desorption of 5FU pH8 in the MIP<sub>07</sub>/NIP<sub>07</sub> (see Table 4.3). Characterization of the MIP by SPE (Loading, Washing and Eluting step).



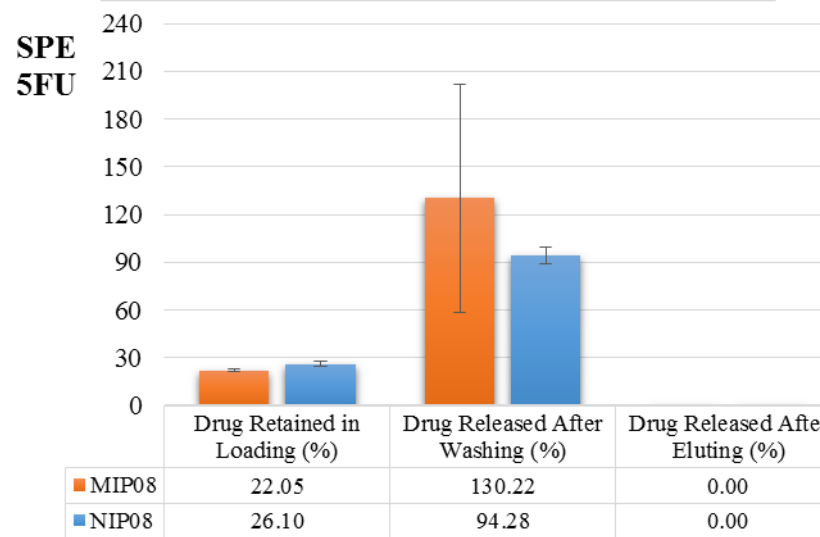
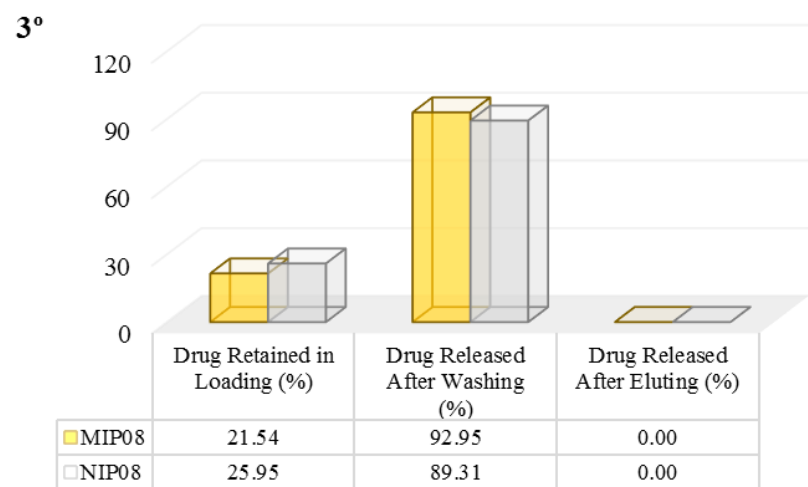
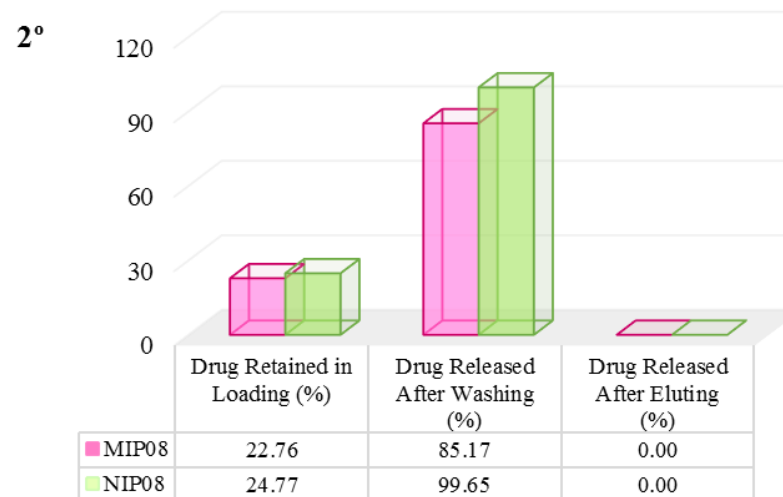
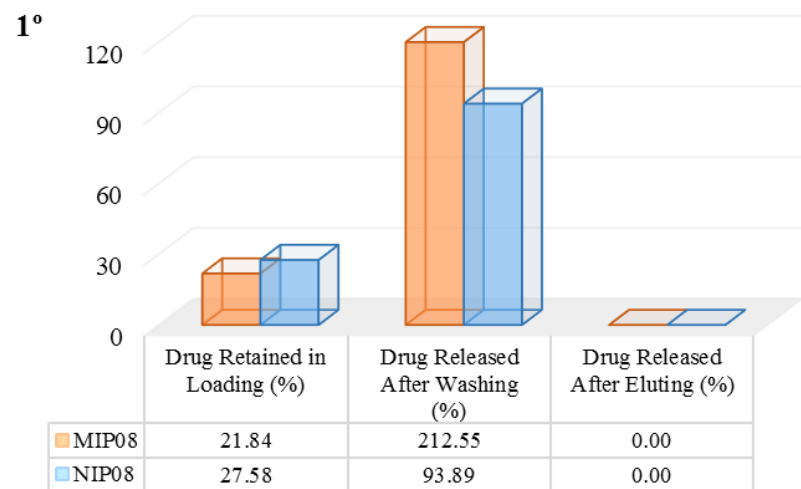
**Annex 12** - Study of adsorption and desorption of CAF in the MIP<sub>07</sub>/NIP<sub>07</sub> (see Table 4.3). Characterization of the MIP by SPE (Loading, Washing and Eluting step).



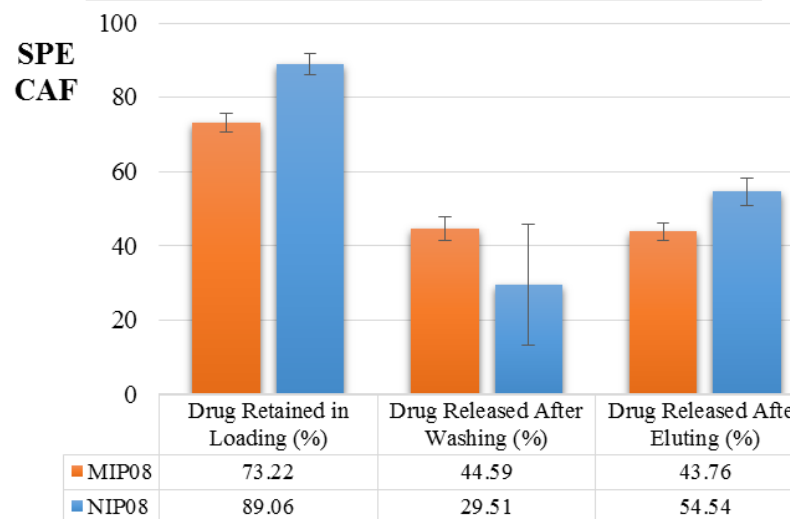
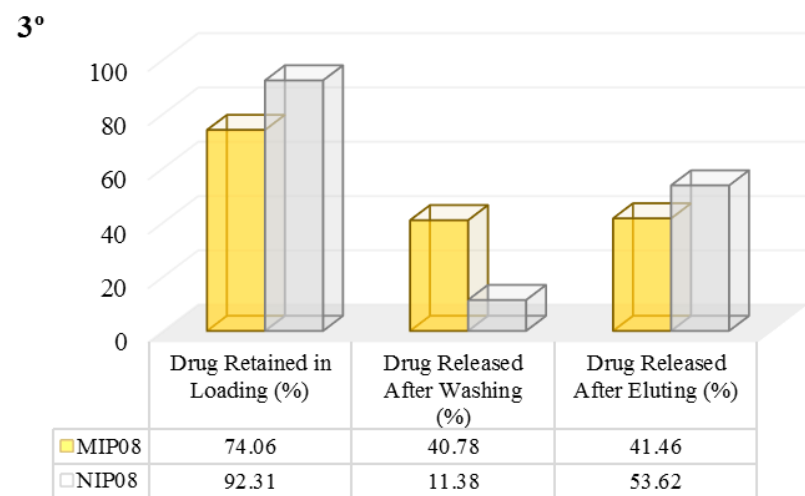
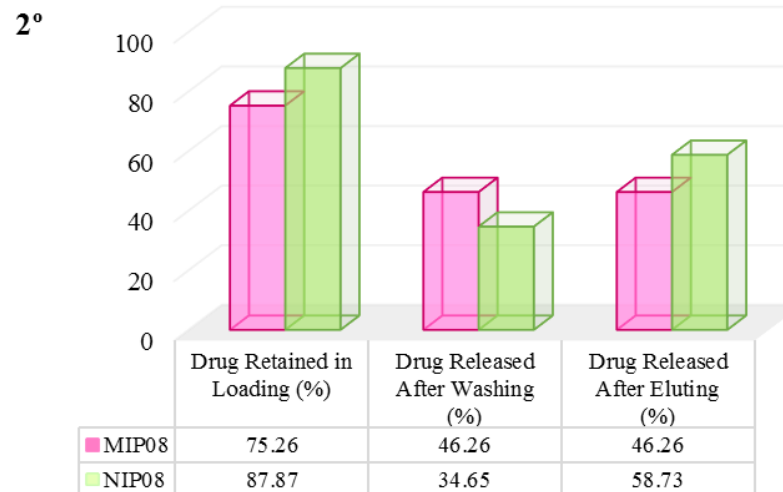
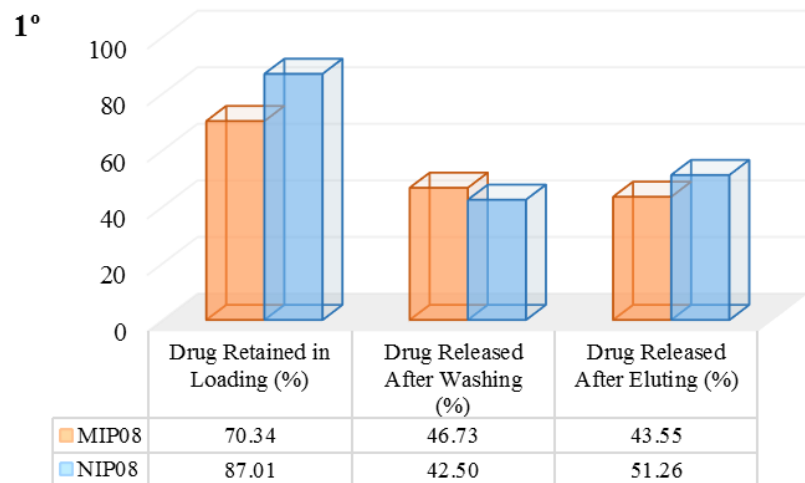
**Annex 13** - Study of adsorption and desorption of U in the MIP<sub>07</sub>/NIP<sub>07</sub> (see Table 4.3). Characterization of the MIP by SPE (Loading, Washing and Eluting step).



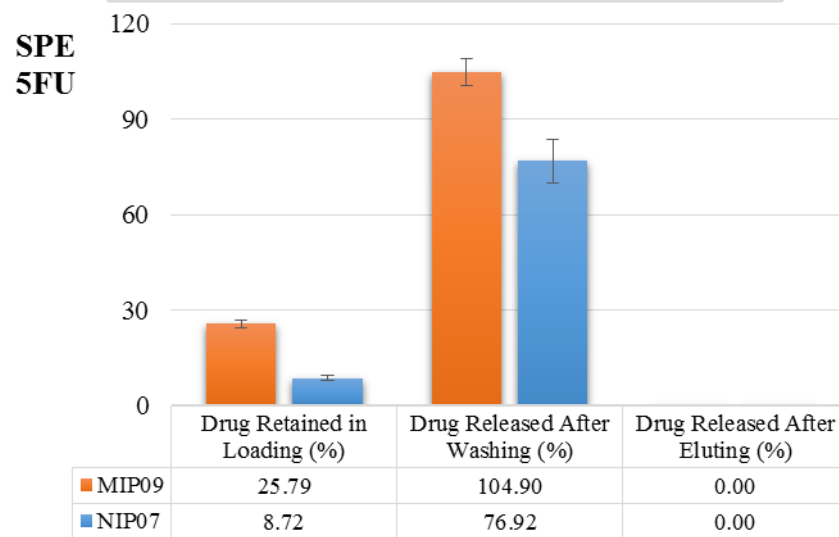
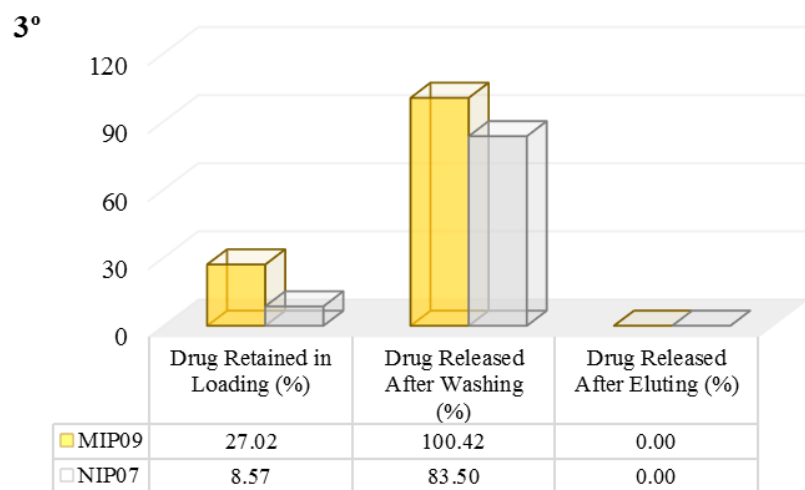
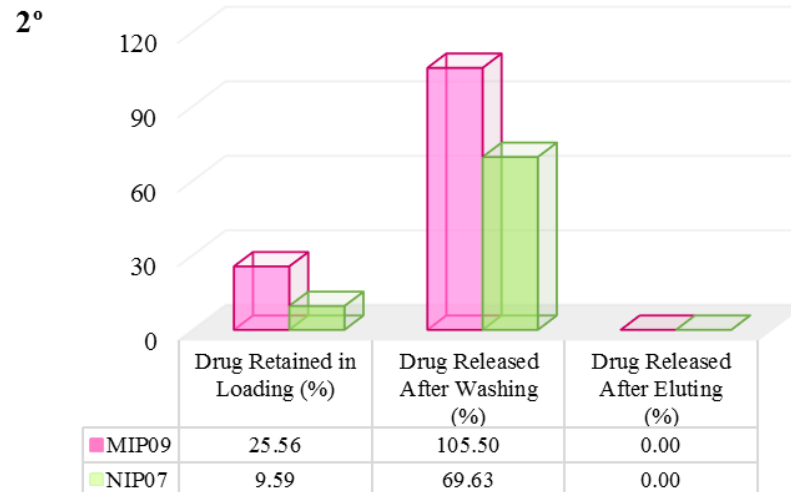
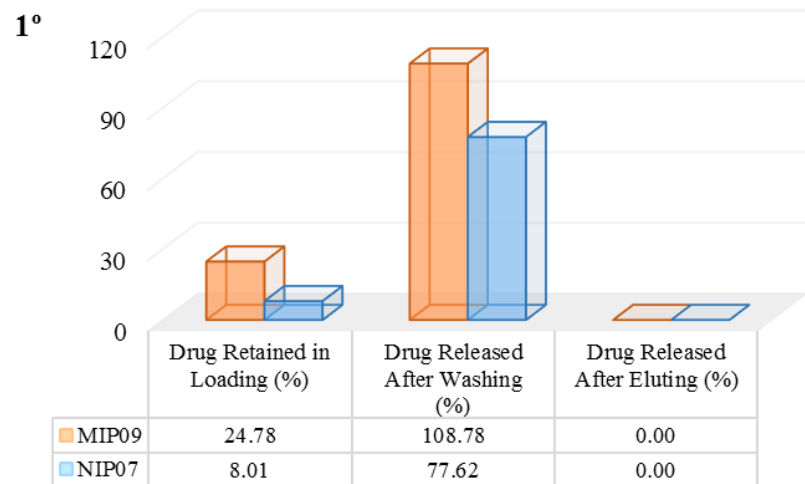
**Annex 14** - Study of adsorption and desorption of 5FU in the MIP<sub>08</sub>/NIP<sub>08</sub> (see Table 4.3). Characterization of the MIP by SPE (Loading, Washing and Eluting step).



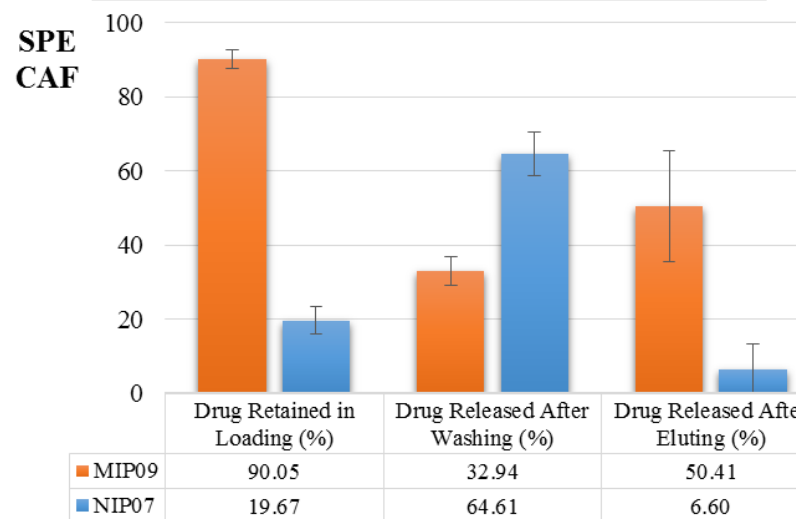
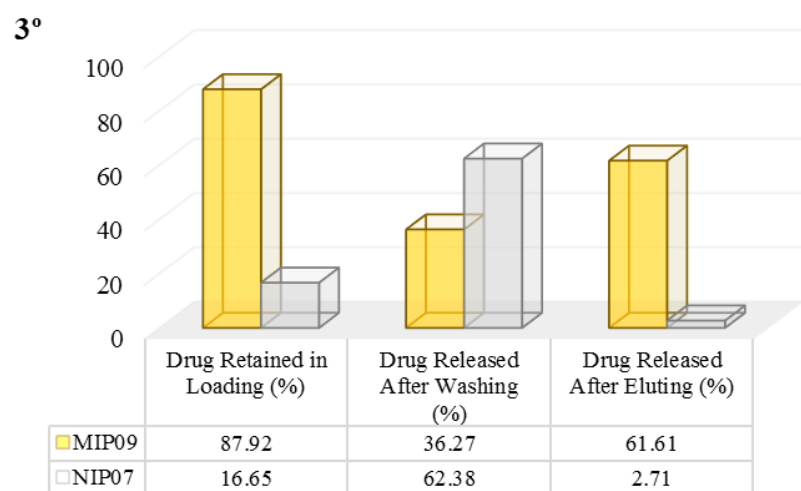
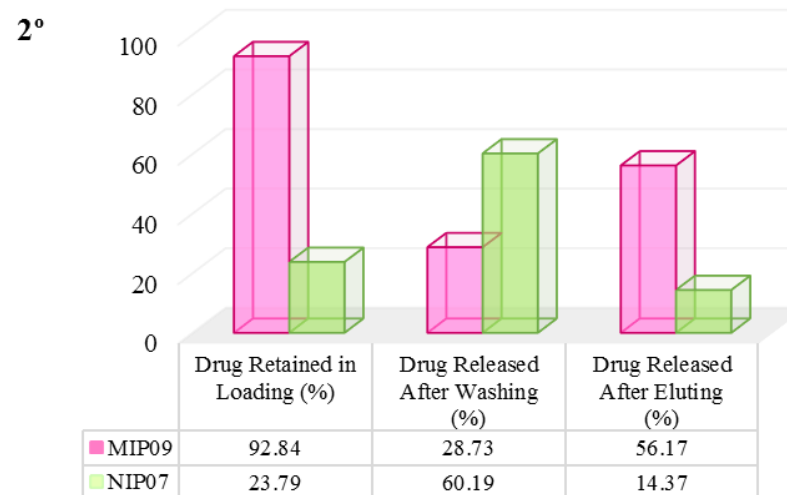
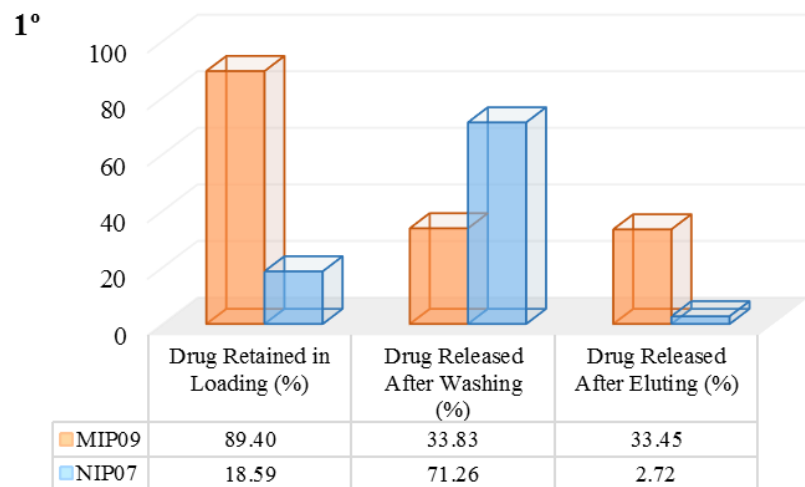
**Annex 15** - Study of adsorption and desorption of CAF in the MIP<sub>08</sub>/NIP<sub>08</sub> (see Table 4.3). Characterization of the MIP by SPE (Loading, Washing and Eluting step).



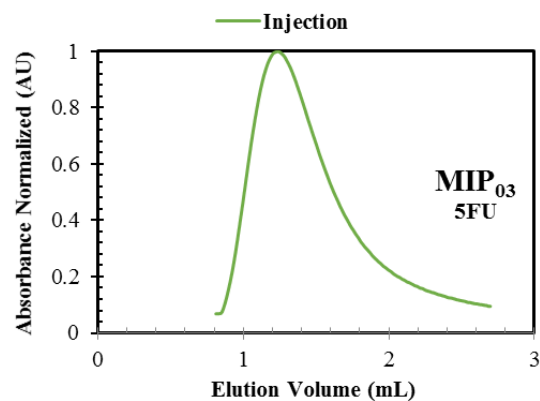
**Annex 16** - Study of adsorption and desorption of 5FU in the MIP09/NIP07 (see Table 4.3). Characterization of the MIP by SPE (Loading, Washing and Eluting step).



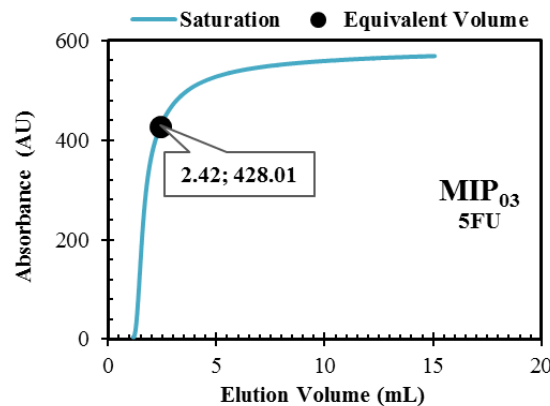
**Annex 17** - Study of adsorption and desorption of CAF in the MIP<sub>09</sub>/NIP<sub>07</sub> (see Table 4.3). Characterization of the MIP by SPE (Loading, Washing and Eluting step).



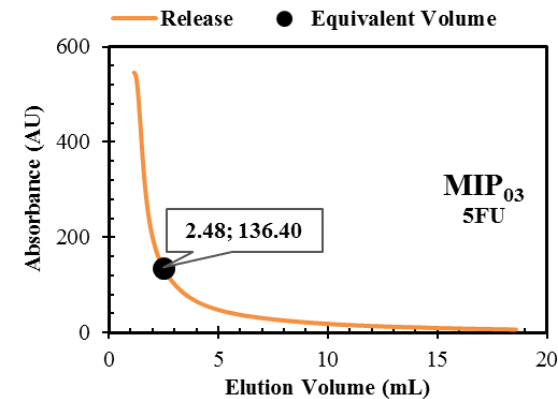
**Annex 18** - Study of injection, adsorption and desorption of 5FU in the MIP<sub>03</sub> (see Table 4.2). Characterization of the MIP frontal analysis by filling a column operating in continuous mode.



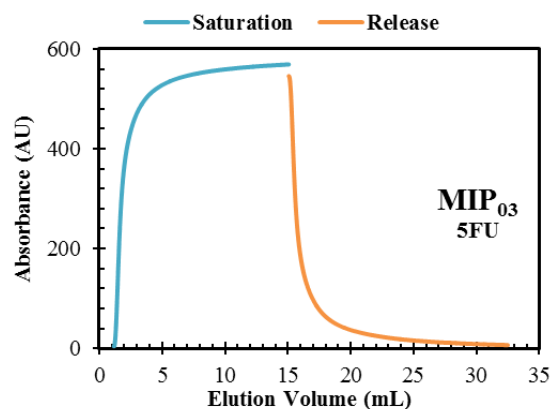
Profile observed for the injection of 5FU in a column packed with a MIP<sub>03</sub>.



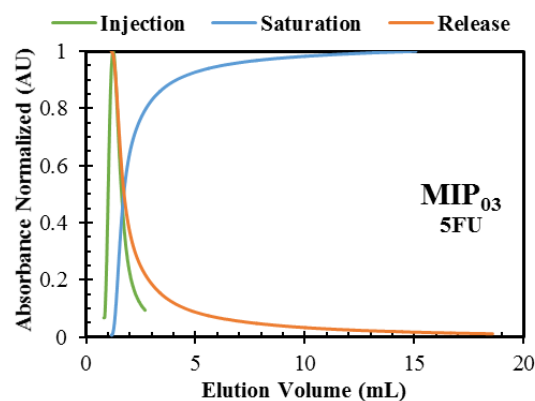
Profile observed for the saturation of 5FU in a column packed with a MIP<sub>03</sub>.



Profile observed for the release of 5FU in a column packed with a MIP<sub>03</sub>.



Profiles observed for the saturation and release of 5FU in a column packed with a MIP<sub>03</sub>.



Profiles observed for the injection, saturation and release of 5FU in a column packed with a MIP<sub>03</sub>.

---

**Operating conditions:**

Column: 4

$C_0 = 0.1 \text{ mM}$

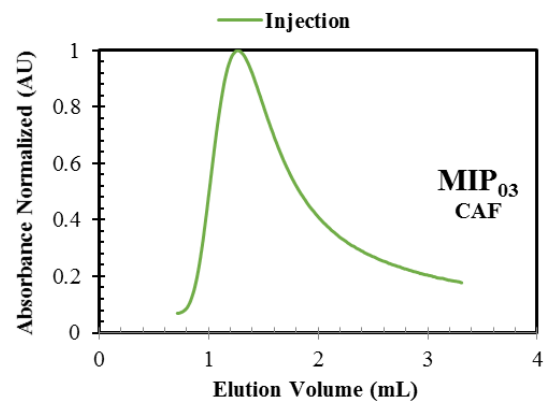
$Q = 1 \text{ mL/min}$

$T = 30 \text{ }^\circ\text{C}$

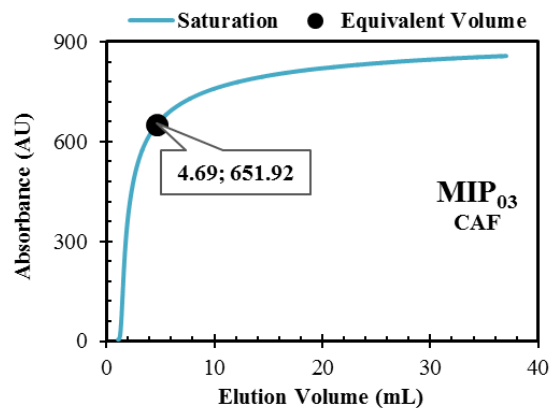
UV Detection: 265 nm

---

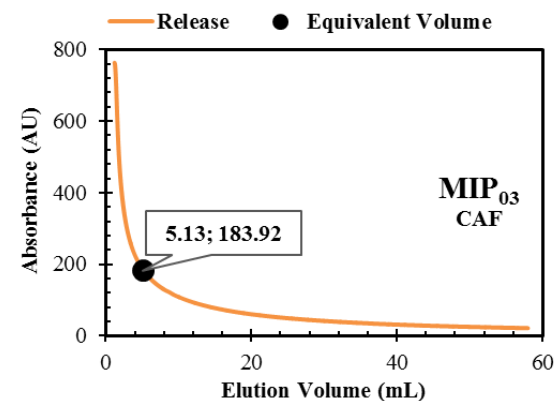
**Annex 19** - Study of injection, adsorption and desorption of CAF in the MIP<sub>03</sub> (see Table 4.1). Characterization of the MIP frontal analysis by filling a column operating in continuous mode.



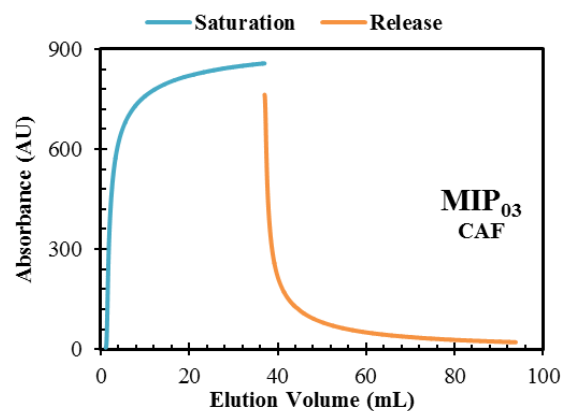
Profile observed for the injection of CAF in a column packed with a MIP<sub>03</sub>.



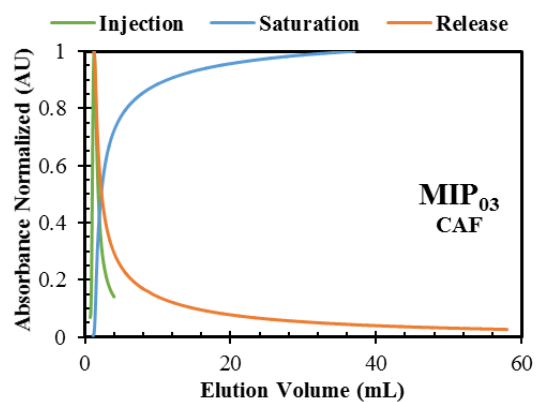
Profile observed for the saturation of CAF in a column packed with a MIP<sub>03</sub>.



Profile observed for the release of CAF in a column packed with a MIP<sub>03</sub>.



Profiles observed for the saturation and release of CAF in a column packed with a MIP<sub>03</sub>.



Profiles observed for the injection, saturation and release of CAF in a column packed with a MIP<sub>03</sub>.

**Operating conditions:**

Column: 4

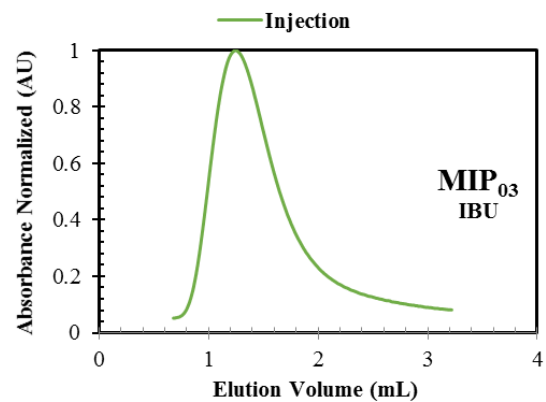
$C_0 = 0.1 \text{ mM}$

$Q = 1 \text{ mL/min}$

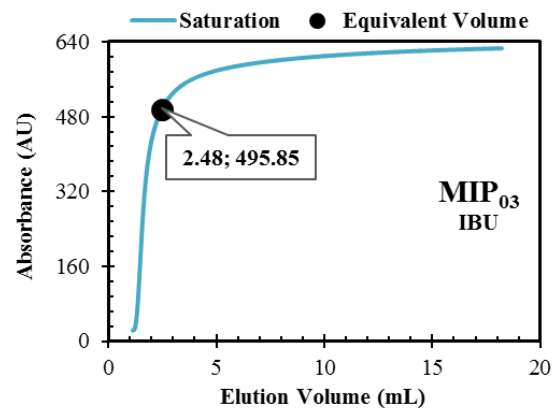
$T = 30 \text{ }^\circ\text{C}$

UV Detection: 273 nm

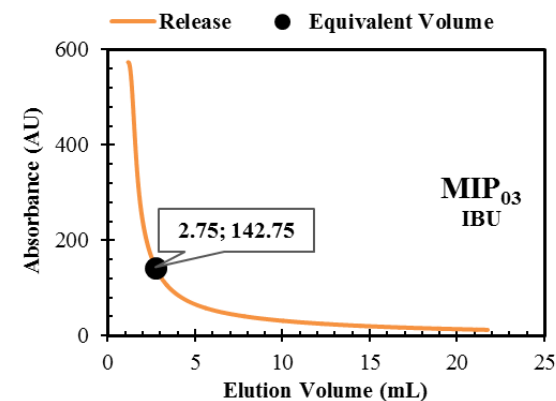
**Annex 20** - Study of injection, adsorption and desorption of IBU in the MIP<sub>03</sub> (see Table 4.2). Characterization of the MIP frontal analysis by filling a column operating in continuous mode.



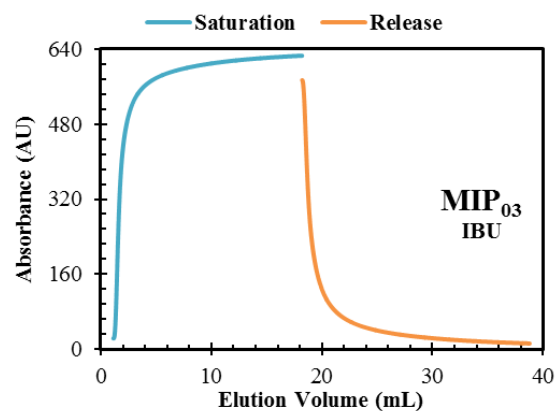
Profile observed for the injection of IBU in a column packed with a MIP<sub>03</sub>.



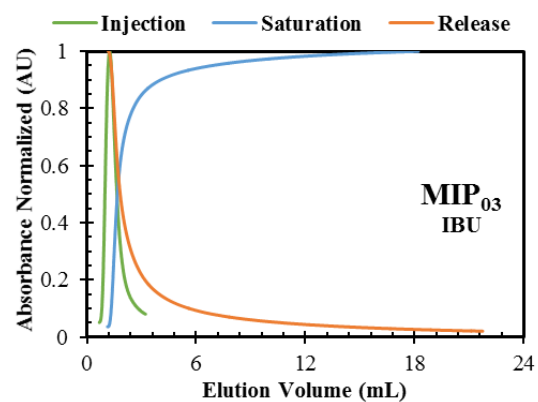
Profile observed for the saturation of IBU in a column packed with a MIP<sub>03</sub>.



Profile observed for the release of IBU in a column packed with a MIP<sub>03</sub>.



Profiles observed for the saturation and release of IBU in a column packed with a MIP<sub>03</sub>.



Profiles observed for the injection, saturation and release of IBU in a column packed with a MIP<sub>03</sub>.

---

**Operating conditions:**

Column: 4

$C_0 = 0.1 \text{ mM}$

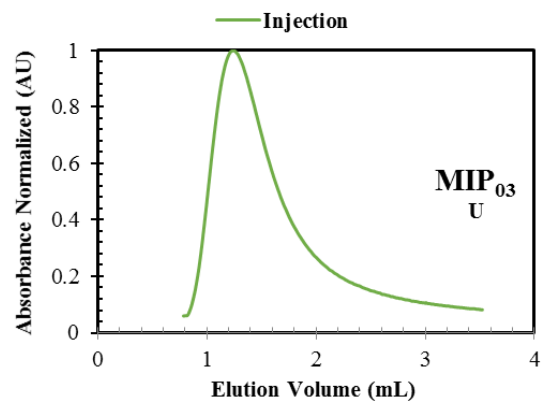
$Q = 1 \text{ mL/min}$

$T = 30 \text{ }^\circ\text{C}$

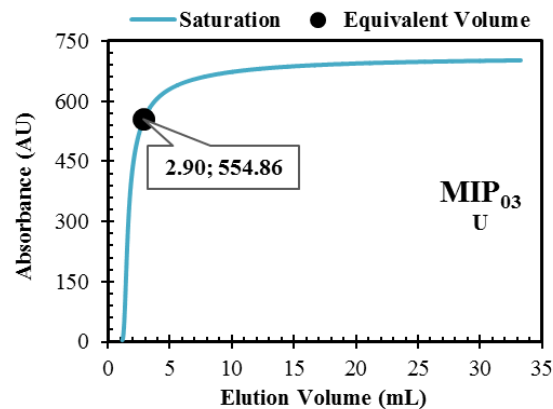
UV Detection: 223 nm

---

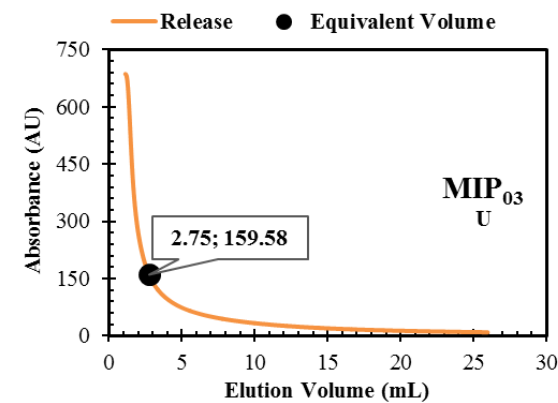
**Annex 21** - Study of injection, adsorption and desorption of U in the MIP<sub>03</sub> (see Table 4.2). Characterization of the MIP frontal analysis by filling a column operating in continuous mode.



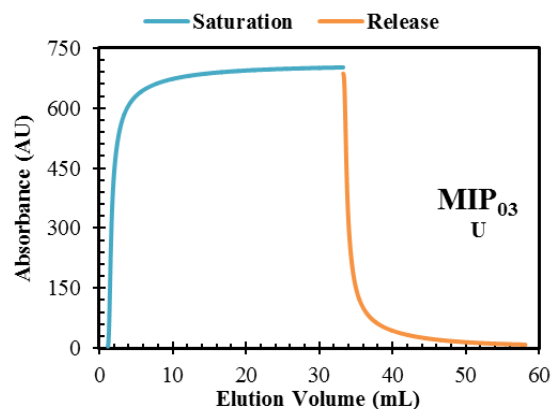
Profile observed for the injection of U in a column packed with a MIP<sub>03</sub>.



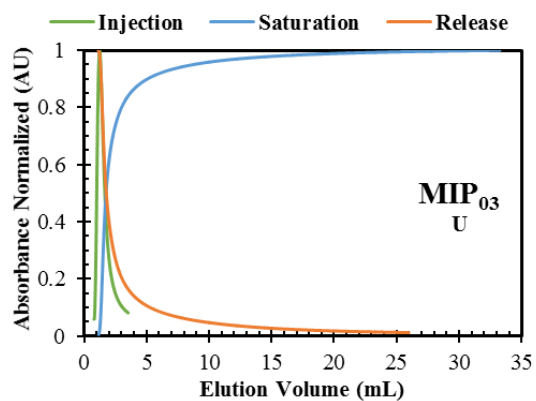
Profile observed for the saturation of U in a column packed with a MIP<sub>03</sub>.



Profile observed for the release of U in a column packed with a MIP<sub>03</sub>.



Profiles observed for the saturation and release of U in a column packed with a MIP<sub>03</sub>.



Profiles observed for the injection, saturation and release of U in a column packed with a MIP<sub>03</sub>.

**Operating conditions:**

Column: 4

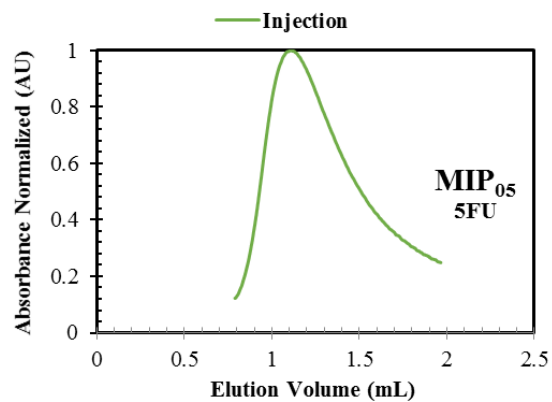
C<sub>0</sub> = 0.1 mM

Q = 1 mL/min

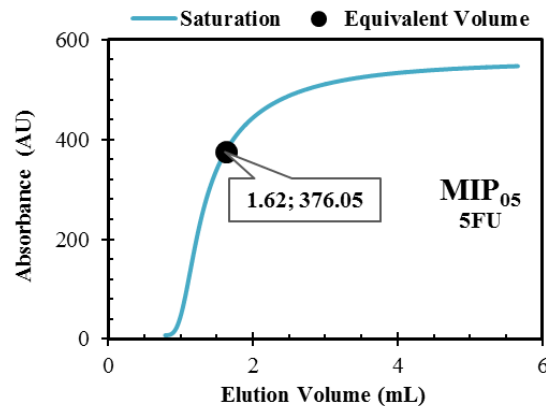
T = 30 °C

UV Detection: 258 nm

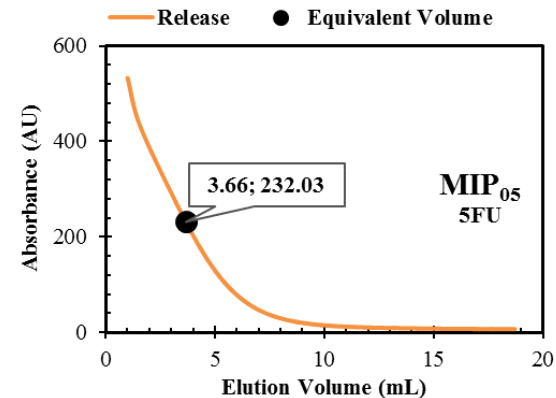
**Annex 22** - Study of injection, adsorption and desorption of 5FU in the MIP<sub>05</sub> (see Table 4.2). Characterization of the MIP frontal analysis by filling a column operating in continuous mode.



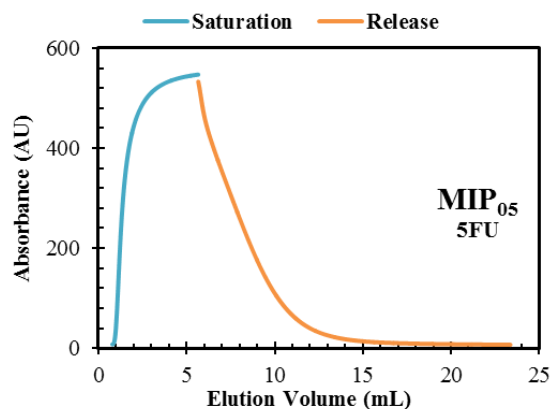
Profile observed for the injection of 5FU in a column packed with a MIP<sub>05</sub>.



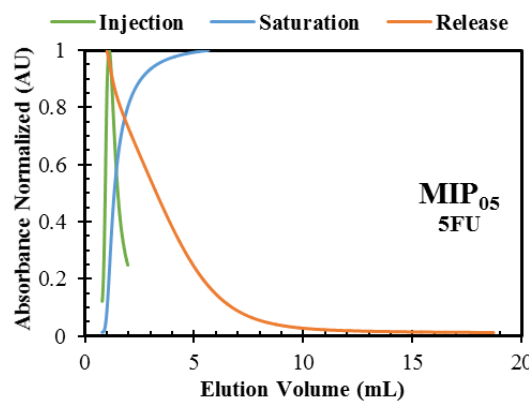
Profile observed for the saturation of 5FU in a column packed with a MIP<sub>05</sub>.



Profile observed for the release of 5FU in a column packed with a MIP<sub>05</sub>.



Profiles observed for the saturation and release of 5FU in a column packed with a MIP<sub>05</sub>.



Profiles observed for the injection, saturation and release of 5FU in a column packed with a MIP<sub>05</sub>.

---

**Operating conditions:**

Column: 2

$C_0 = 0.1 \text{ mM}$

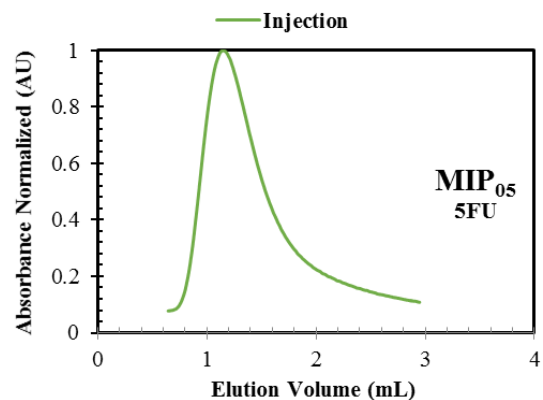
$Q = 0.5 \text{ mL/min}$

$T = 30 \text{ }^\circ\text{C}$

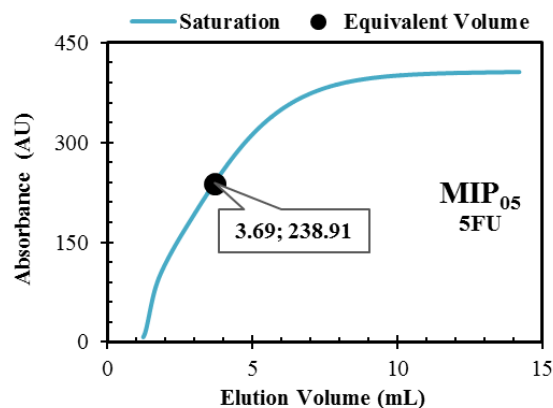
UV Detection: 265 nm

---

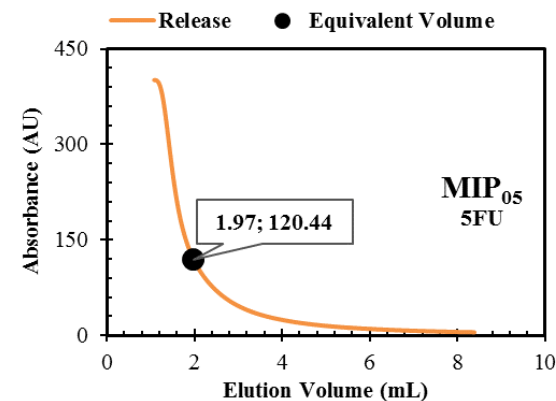
**Annex 23** - Study of injection, adsorption and desorption of 5FU in the MIP<sub>05</sub> (see Table 4.2). Characterization of the MIP frontal analysis by filling a column operating in continuous mode.



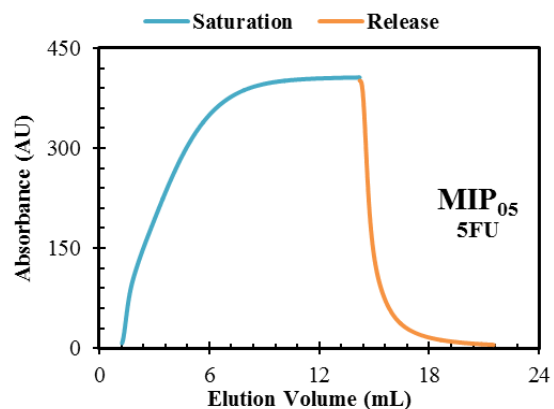
Profile observed for the injection of 5FU in a column packed with a MIP<sub>05</sub>.



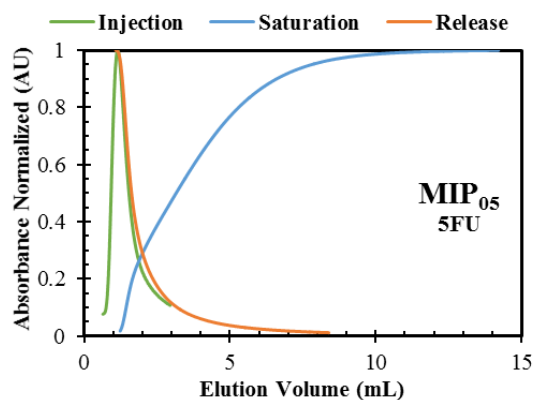
Profile observed for the saturation of 5FU in a column packed with a MIP<sub>05</sub>.



Profile observed for the release of 5FU in a column packed with a MIP<sub>05</sub>.



Profiles observed for the saturation and release of 5FU in a column packed with a MIP<sub>05</sub>.



Profiles observed for the injection, saturation and release of 5FU in a column packed with a MIP<sub>05</sub>.

**Operating conditions:**

Column: 2

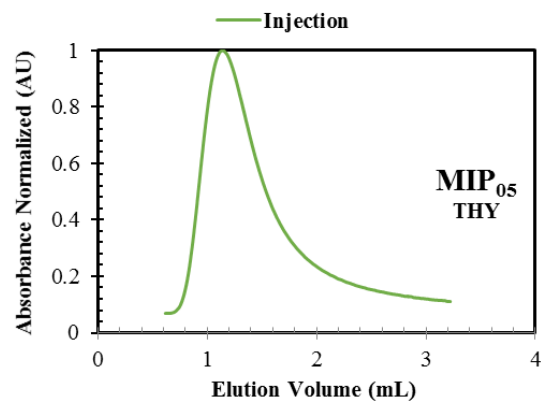
$C_0 = 0.1 \text{ mM}$

$Q = 1 \text{ mL/min}$

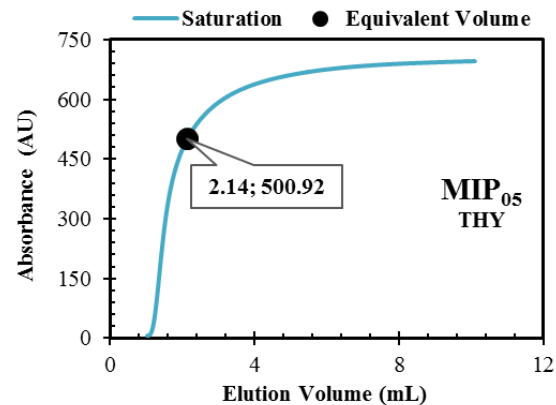
$T = 30 \text{ }^\circ\text{C}$

UV Detection: 265 nm

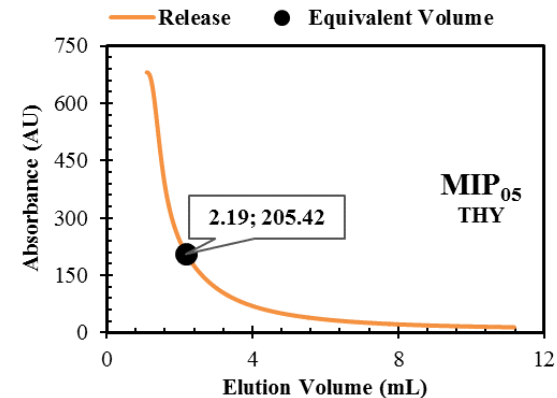
**Annex 24** - Study of injection, adsorption and desorption of THY in the MIP<sub>05</sub> (see Table 4.2). Characterization of the MIP frontal analysis by filling a column operating in continuous mode.



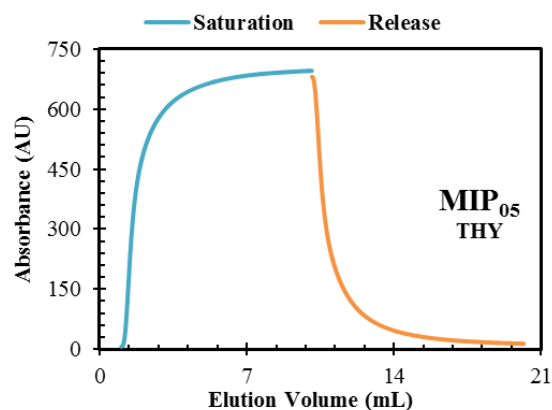
Profile observed for the injection of THY in a column packed with a MIP<sub>05</sub>.



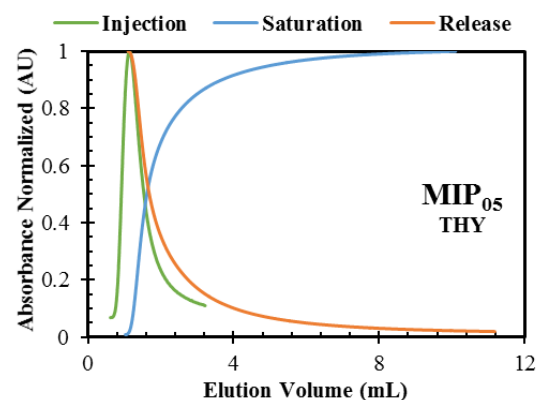
Profile observed for the saturation of THY in a column packed with a MIP<sub>05</sub>.



Profile observed for the release of THY in a column packed with a MIP<sub>05</sub>.



Profiles observed for the saturation and release of THY in a column packed with a MIP<sub>05</sub>.



Profiles observed for the injection, saturation and release of THY in a column packed with a MIP<sub>05</sub>.

---

**Operating conditions:**

Column: 2

$C_0 = 0.1$  mM

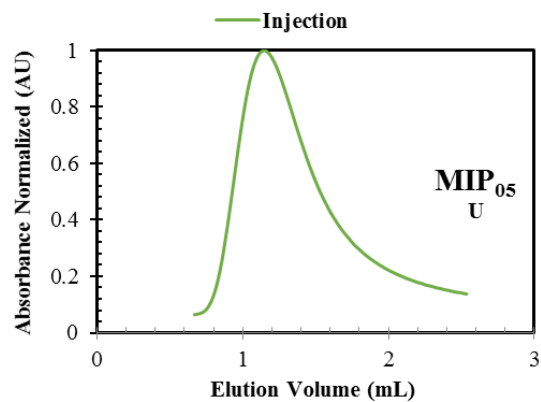
$Q = 1$  mL/min

$T = 30$  °C

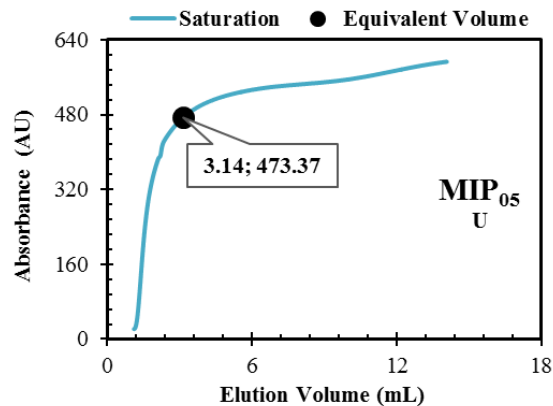
UV Detection: 263 nm

---

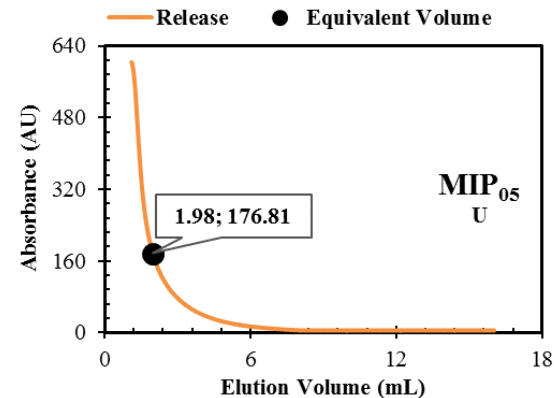
**Annex 25** - Study of injection, adsorption and desorption of U in the MIP<sub>05</sub> (see Table 4.2). Characterization of the MIP frontal analysis by filling a column operating in continuous mode.



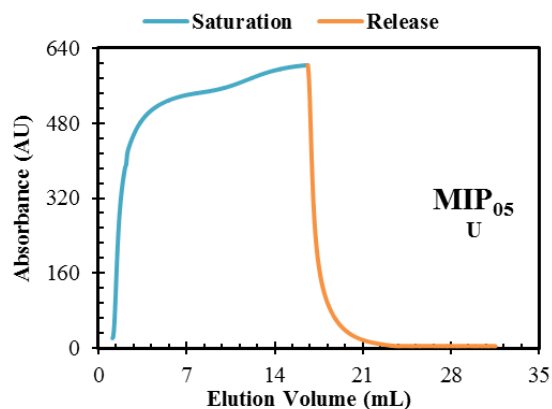
Profile observed for the injection of U in a column packed with a MIP<sub>05</sub>.



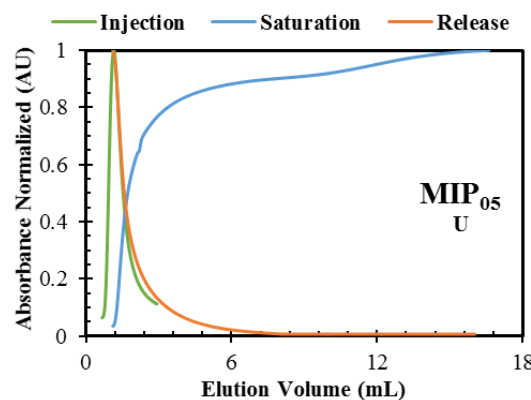
Profile observed for the saturation of U in a column packed with a MIP<sub>05</sub>.



Profile observed for the release of U in a column packed with a MIP<sub>05</sub>.



Profiles observed for the saturation and release of U in a column packed with a MIP<sub>05</sub>.



Profiles observed for the injection, saturation and release of U in a column packed with a MIP<sub>05</sub>.

**Operating conditions:**

Column: 2

C<sub>0</sub> = 0.1 mM

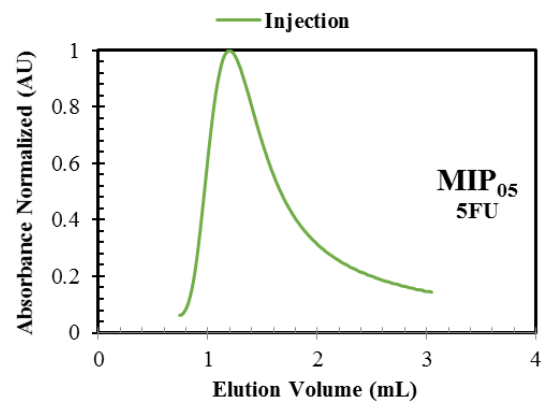
Q = 1 mL/min

T = 30 °C

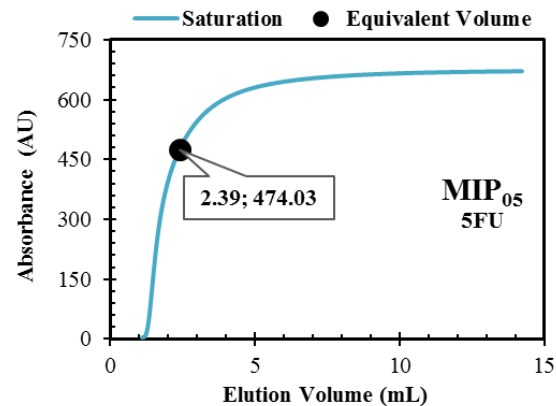
UV Detection: 258 nm

**\*Repeat**

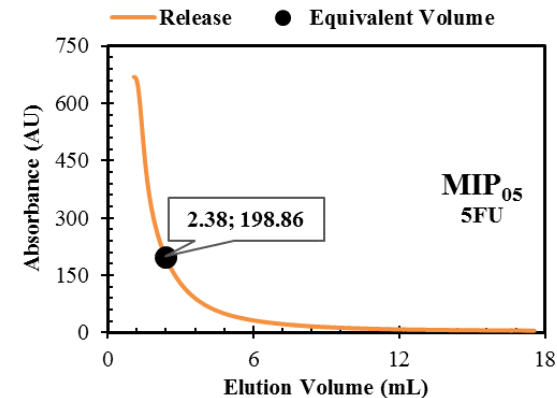
**Annex 26** - Study of injection, adsorption and desorption of 5FU in the MIP<sub>05</sub> (see Table 4.2). Characterization of the MIP frontal analysis by filling a column operating in continuous mode.



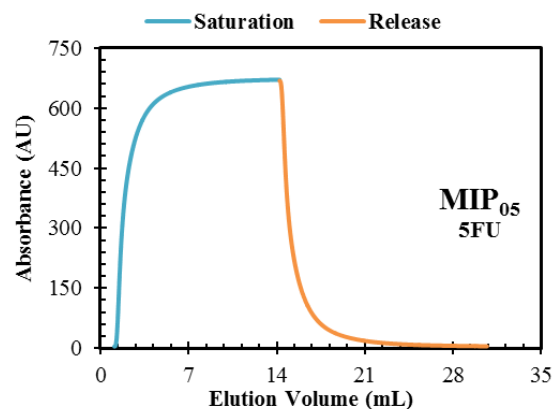
Profile observed for the injection of 5FU in a column packed with a MIP<sub>05</sub>.



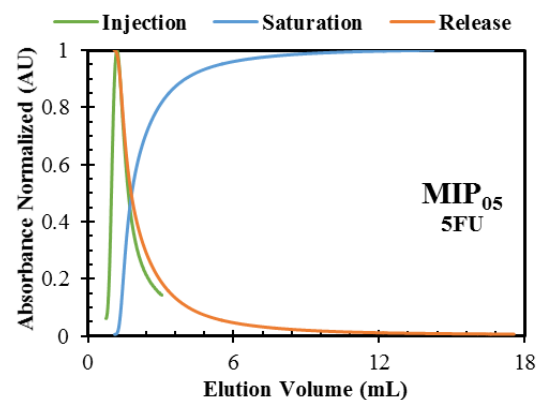
Profile observed for the saturation of 5FU in a column packed with a MIP<sub>05</sub>.



Profile observed for the release of 5FU in a column packed with a MIP<sub>05</sub>.



Profiles observed for the saturation and release of 5FU in a column packed with a MIP<sub>05</sub>.



Profiles observed for the injection, saturation and release of 5FU in a column packed with a MIP<sub>05</sub>.

---

**Operating conditions:**

Column: 3

$C_0 = 0.1 \text{ mM}$

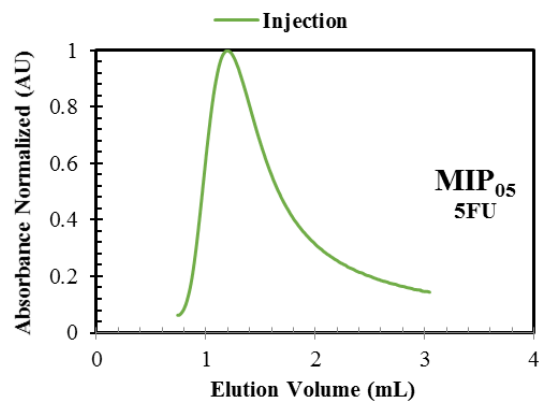
$Q = 1 \text{ mL/min}$

$T = 30 \text{ }^\circ\text{C}$

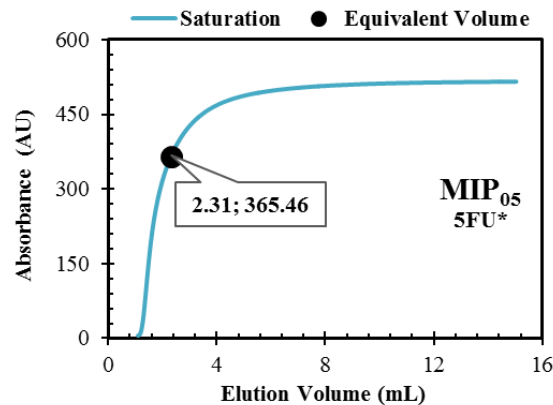
UV Detection: 265 nm

---

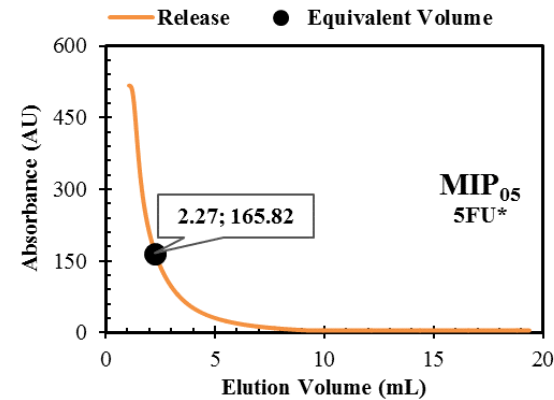
**Annex 27** - Study of injection, adsorption and desorption of 5FU in the MIP<sub>05</sub> (see Table 4.2). Characterization of the MIP frontal analysis by filling a column operating in continuous mode.



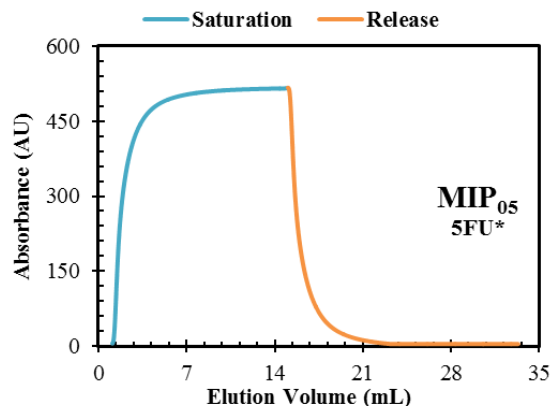
Profile observed for the injection of 5FU in a column packed with a MIP<sub>05</sub>.



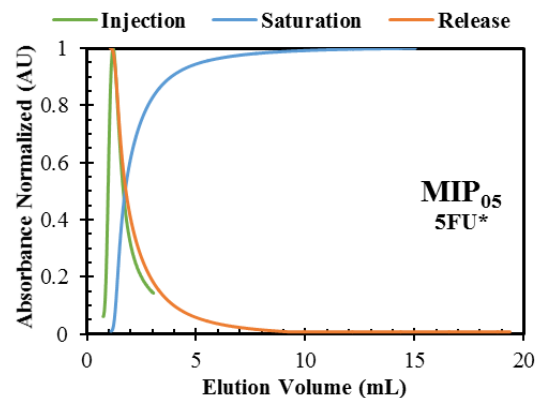
Profile observed for the saturation of 5FU in a column packed with a MIP<sub>05</sub>.



Profile observed for the release of 5FU in a column packed with a MIP<sub>05</sub>.



Profiles observed for the saturation and release of 5FU in a column packed with a MIP<sub>05</sub>.



Profiles observed for the injection, saturation and release of 5FU in a column packed with a MIP<sub>05</sub>.

**Operating conditions:**

Column: 3

$C_0 = 0.1 \text{ mM}$

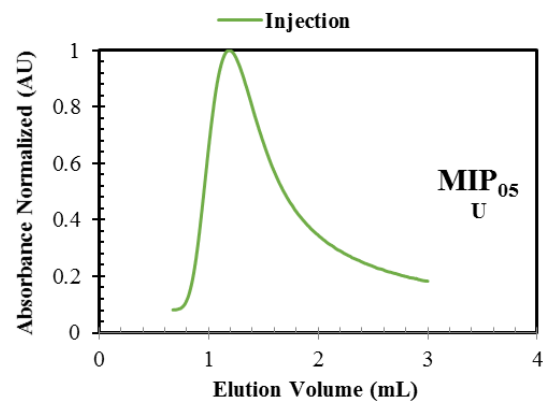
$Q = 1 \text{ mL/min}$

$T = 30 \text{ }^\circ\text{C}$

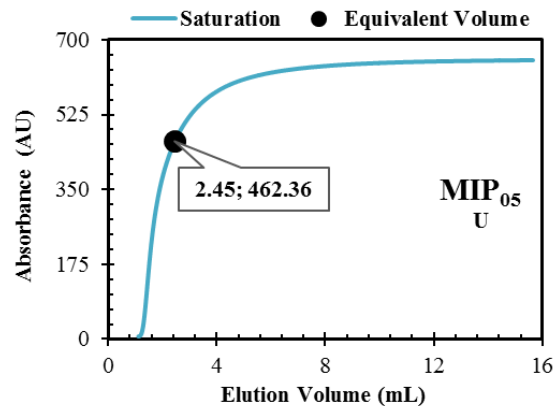
UV Detection: 265 nm

**\*Repeat**

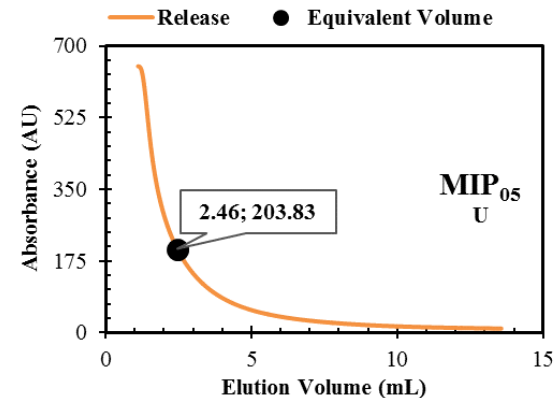
**Annex 28** - Study of injection, adsorption and desorption of U in the MIP<sub>05</sub> (see Table 4.2). Characterization of the MIP frontal analysis by filling a column operating in continuous mode.



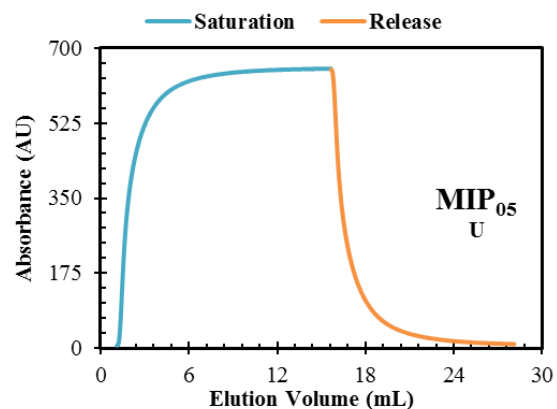
Profile observed for the injection of U in a column packed with a MIP<sub>05</sub>.



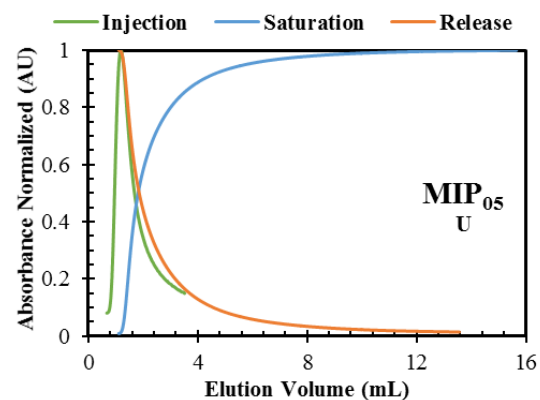
Profile observed for the saturation of U in a column packed with a MIP<sub>05</sub>.



Profile observed for the release of U in a column packed with a MIP<sub>05</sub>.



Profiles observed for the saturation and release of U in a column packed with a MIP<sub>05</sub>.



Profiles observed for the injection, saturation and release of U in a column packed with a MIP<sub>05</sub>.

---

**Operating conditions:**

Column: 3

$C_0 = 0.1 \text{ mM}$

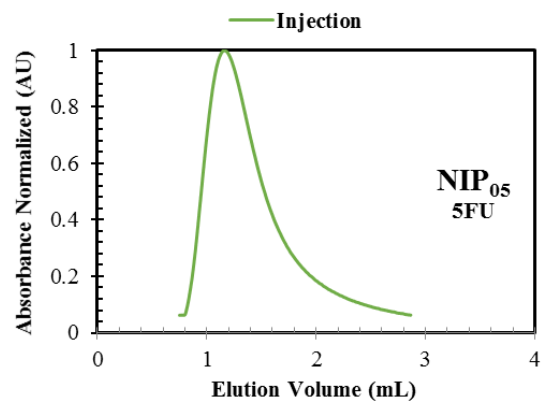
$Q = 1 \text{ mL/min}$

$T = 30 \text{ }^\circ\text{C}$

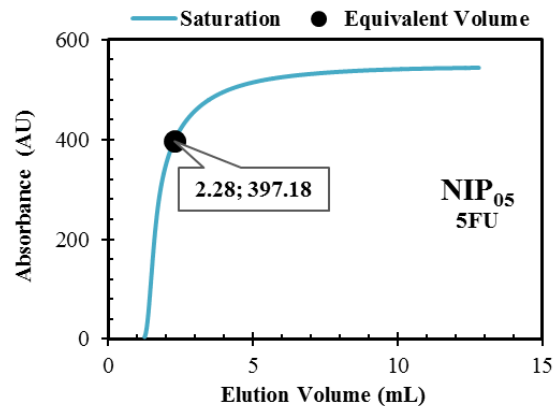
UV Detection: 258 nm

---

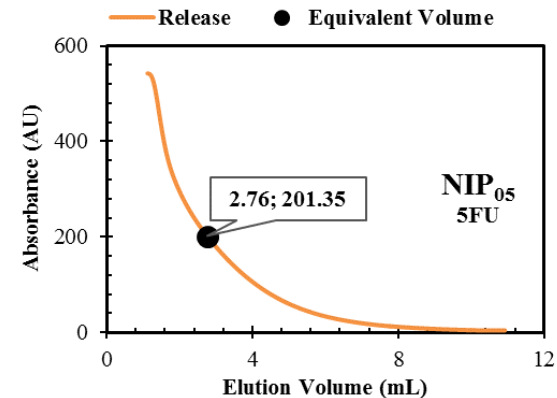
**Annex 29** - Study of injection, adsorption and desorption of 5FU in the NIP<sub>05</sub> (see Table 4.2). Characterization of the NIP frontal analysis by filling a column operating in continuous mode.



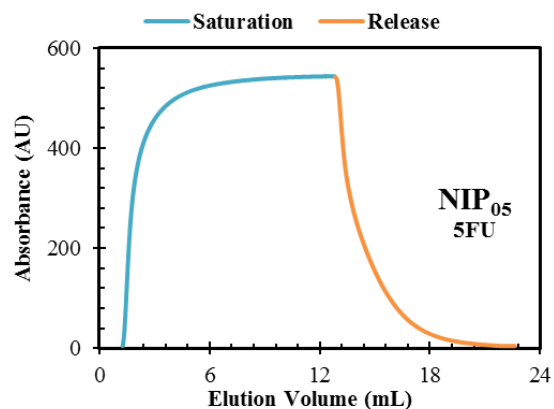
Profile observed for the injection of 5FU in a column packed with a NIP<sub>05</sub>.



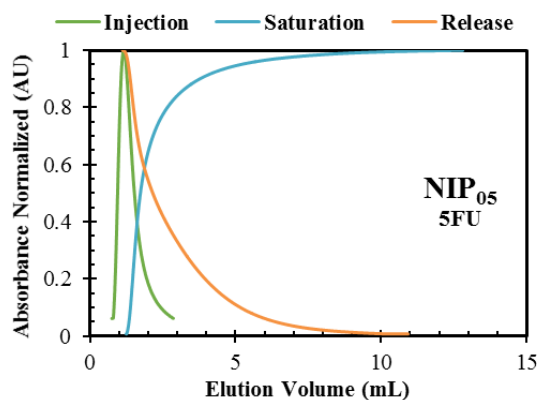
Profile observed for the saturation of 5FU in a column packed with a NIP<sub>05</sub>.



Profile observed for the release of 5FU in a column packed with a NIP<sub>05</sub>.



Profiles observed for the saturation and release of 5FU in a column packed with a NIP<sub>05</sub>.



Profiles observed for the injection, saturation and release of 5FU in a column packed with a NIP<sub>05</sub>.

**Operating conditions:**

Column: 2

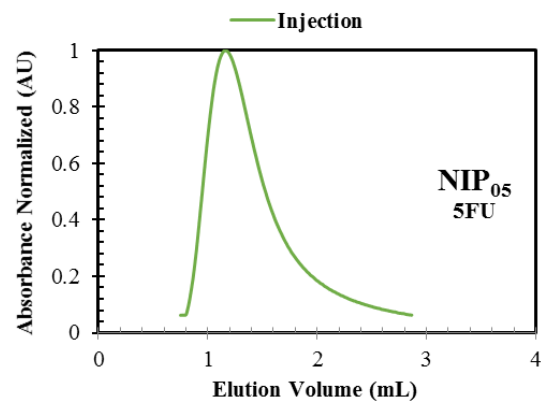
C<sub>0</sub> = 0.1 mM

Q = 1 mL/min

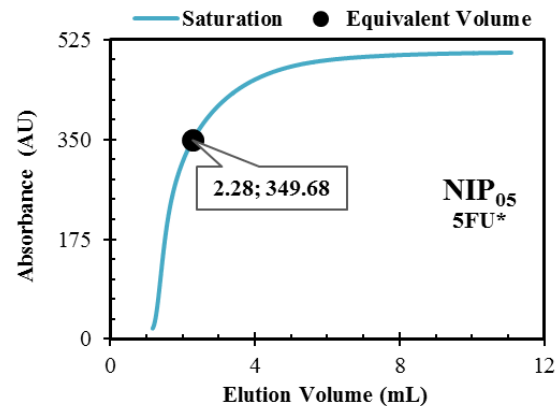
T = 30 °C

UV Detection: 265 nm

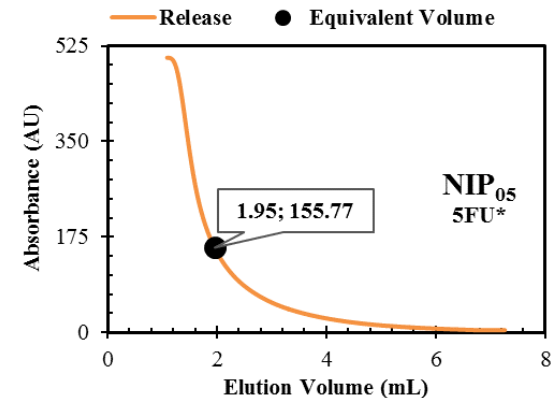
**Annex 30** - Study of injection, adsorption and desorption of 5FU in the NIP<sub>05</sub> (see Table 4.2). Characterization of the NIP frontal analysis by filling a column operating in continuous mode.



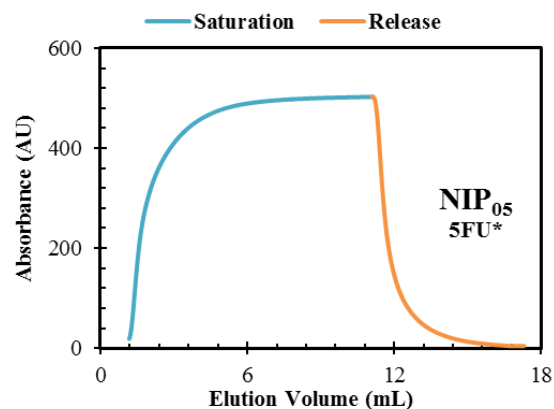
Profile observed for the injection of 5FU in a column packed with a NIP<sub>05</sub>.



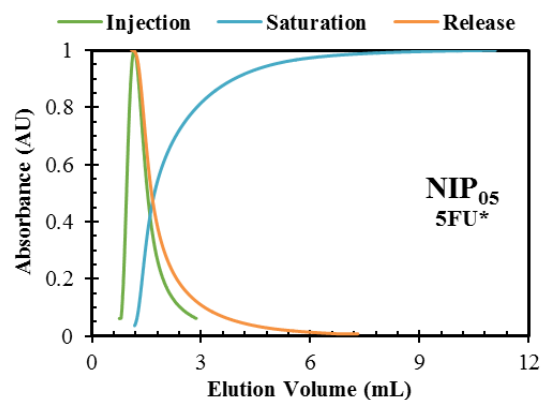
Profile observed for the saturation of 5FU in a column packed with a NIP<sub>05</sub>.



Profile observed for the release of 5FU in a column packed with a NIP<sub>05</sub>.



Profiles observed for the saturation and release of 5FU in a column packed with a NIP<sub>05</sub>.



Profiles observed for the injection, saturation and release of 5FU in a column packed with a NIP<sub>05</sub>.

---

**Operating conditions:**

Column: 2

$C_0 = 0.1 \text{ mM}$

$Q = 1 \text{ mL/min}$

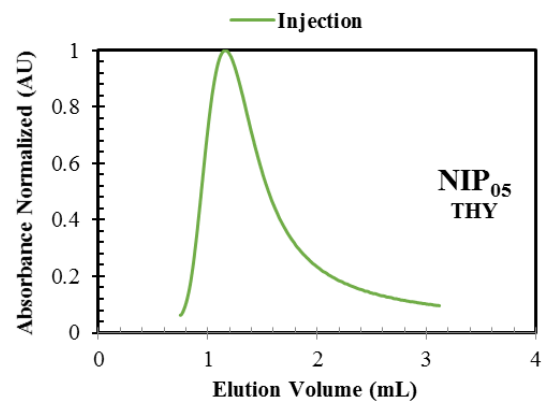
$T = 30 \text{ }^\circ\text{C}$

UV Detection: 265 nm

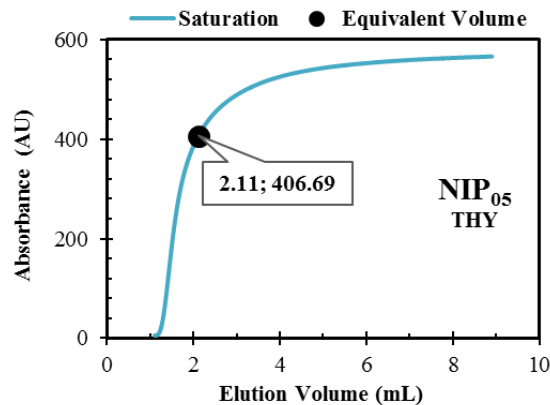
---

**\*Repeat**

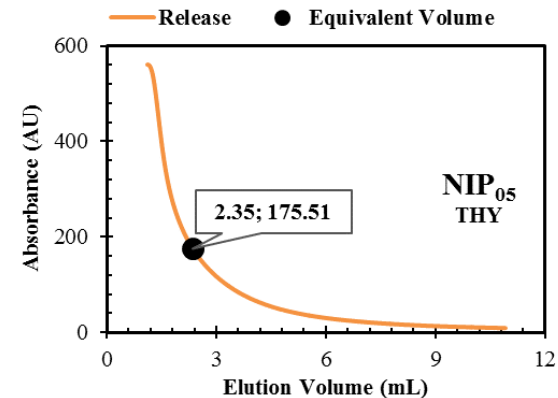
**Annex 31** - Study of injection, adsorption and desorption of THY in the NIP<sub>05</sub> (see Table 4.2). Characterization of the NIP frontal analysis by filling a column operating in continuous mode.



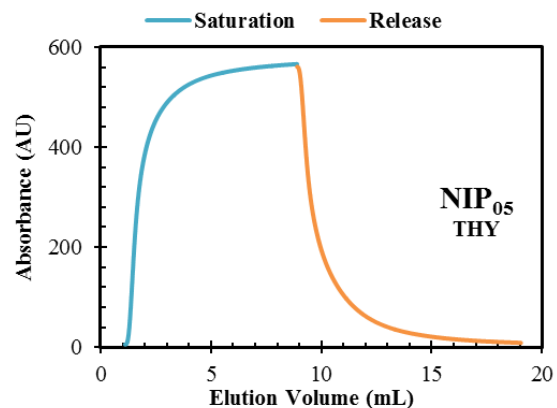
Profile observed for the injection of THY in a column packed with a NIP<sub>05</sub>.



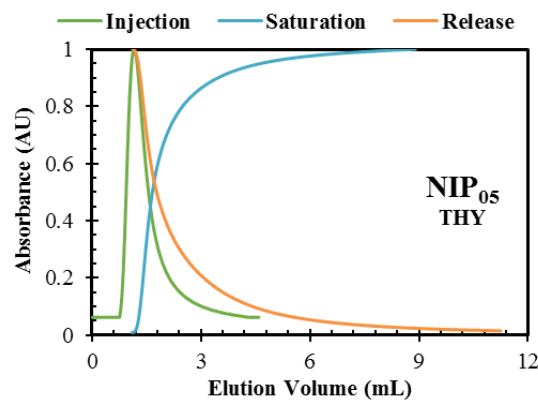
Profile observed for the saturation of THY in a column packed with a NIP<sub>05</sub>.



Profile observed for the release of THY in a column packed with a NIP<sub>05</sub>.



Profiles observed for the saturation and release of THY in a column packed with a NIP<sub>05</sub>.



Profiles observed for the injection, saturation and release of THY in a column packed with a NIP<sub>05</sub>.

**Operating conditions:**

Column: 2

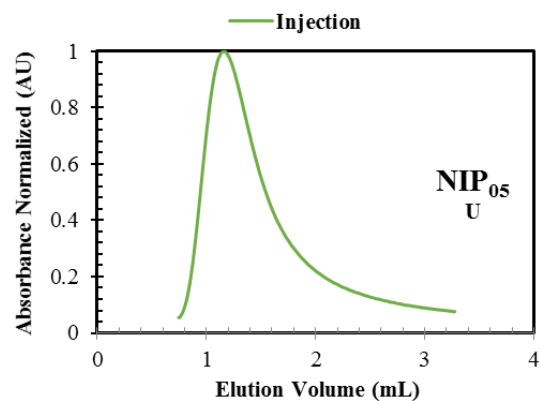
C<sub>0</sub> = 0.1 mM

Q = 1 mL/min

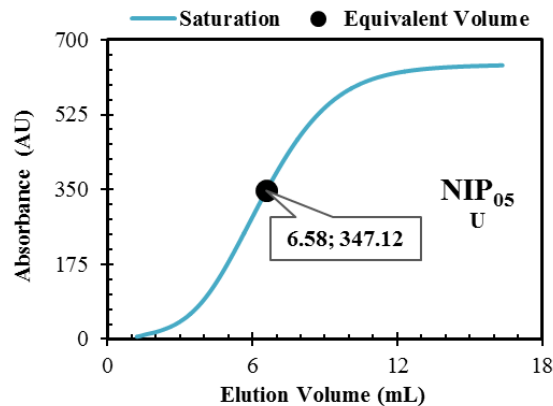
T = 30 °C

UV Detection: 263 nm

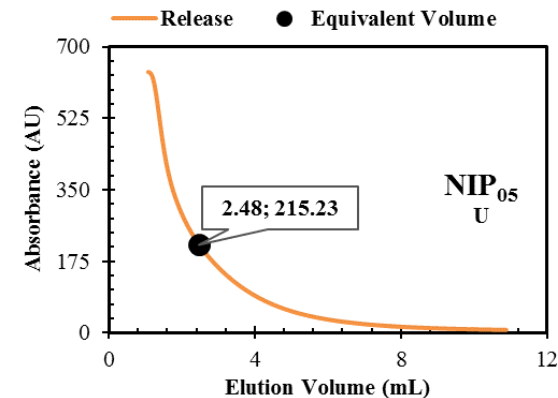
**Annex 32** - Study of injection, adsorption and desorption of U in the NIP<sub>05</sub> (see Table 4.2). Characterization of the NIP frontal analysis by filling a column operating in continuous mode.



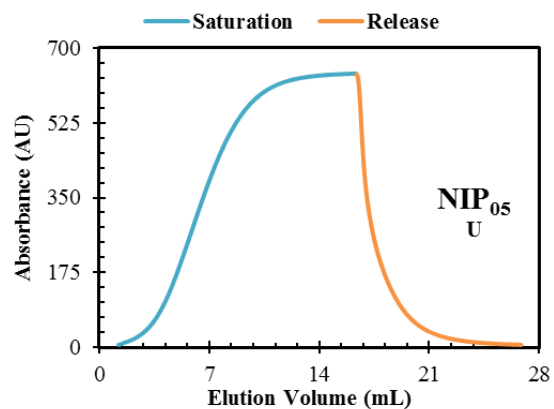
Profile observed for the injection of U in a column packed with a NIP<sub>05</sub>.



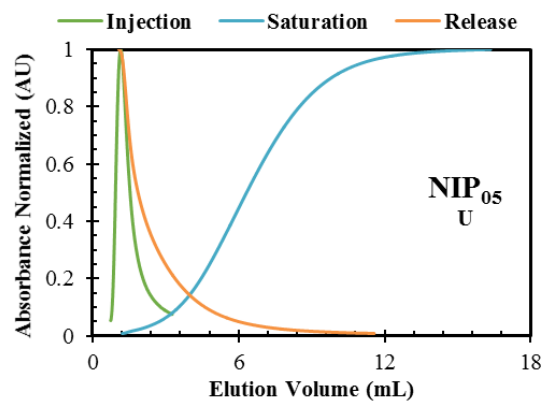
Profile observed for the saturation of U in a column packed with a NIP<sub>05</sub>.



Profile observed for the release of U in a column packed with a NIP<sub>05</sub>.



Profiles observed for the saturation and release of U in a column packed with a NIP<sub>05</sub>.



Profiles observed for the injection, saturation and release of U in a column packed with a NIP<sub>05</sub>.

**Operating conditions:**

Column: 2

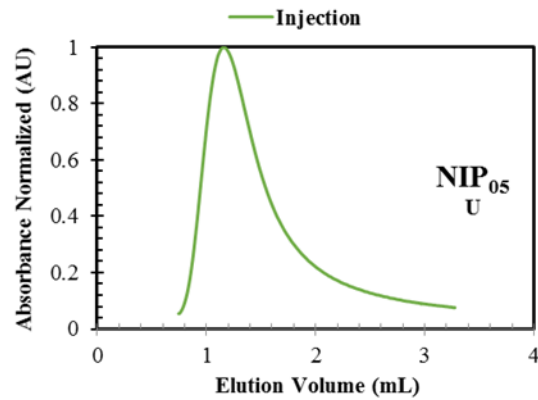
C<sub>0</sub> = 0.1 mM

Q = 1 mL/min

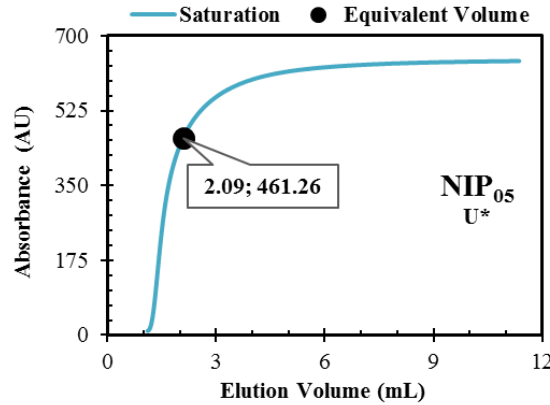
T = 30 °C

UV Detection: 258 nm

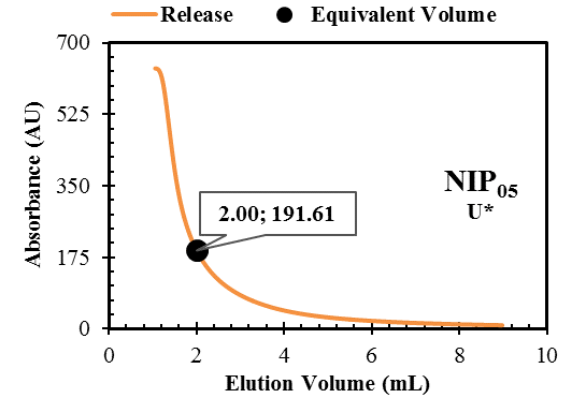
**Annex 33** - Study of injection, adsorption and desorption of U in the NIP<sub>05</sub> (see Table 4.2). Characterization of the NIP frontal analysis by filling a column operating in continuous mode.



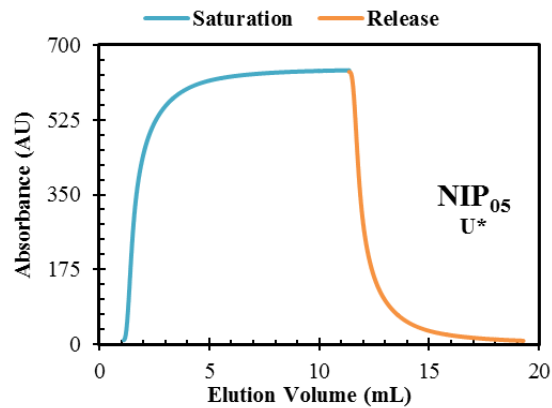
Profile observed for the injection of U in a column packed with a NIP<sub>05</sub>.



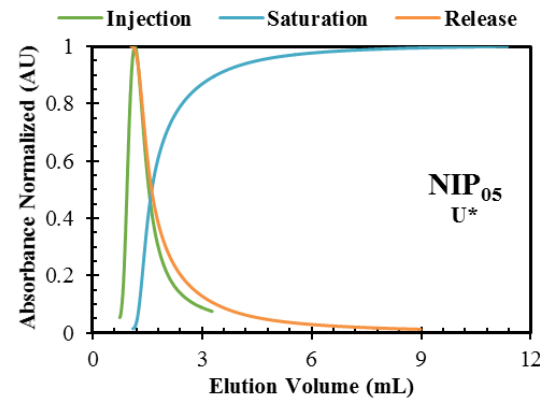
Profile observed for the saturation of U in a column packed with a NIP<sub>05</sub>.



Profile observed for the release of U in a column packed with a NIP<sub>05</sub>.



Profiles observed for the saturation and release of U in a column packed with a NIP<sub>05</sub>.



Profiles observed for the injection, saturation and release of U in a column packed with a NIP<sub>05</sub>.

**Operating conditions:**

Column: 2

C<sub>0</sub> = 0.1 mM

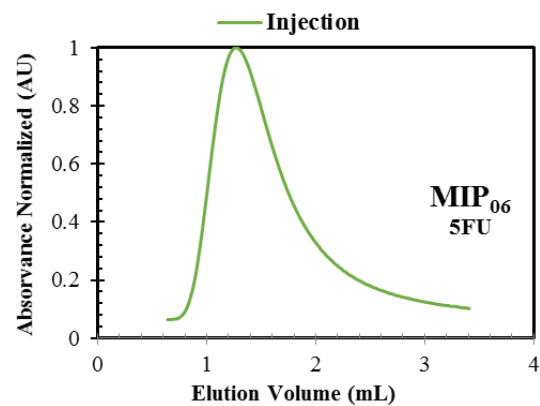
Q = 1 mL/min

T = 30 °C

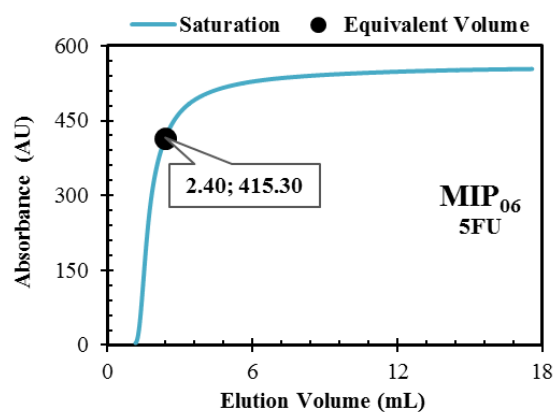
UV Detection: 258 nm

**\*Repeat**

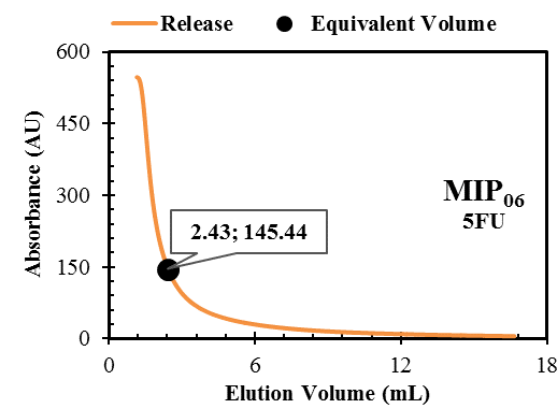
**Annex 34** - Study of injection, adsorption and desorption of 5FU in the MIP<sub>06</sub> (see Table 4.2). Characterization of the MIP frontal analysis by filling a column operating in continuous mode.



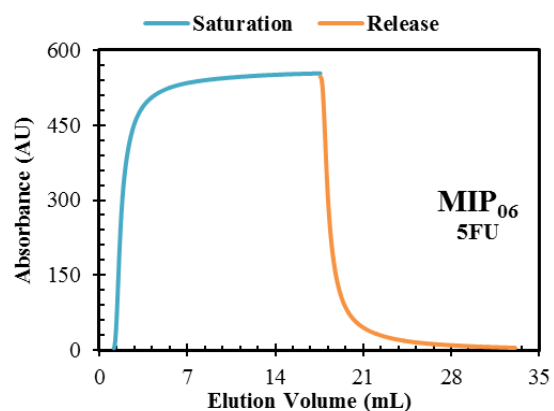
Profile observed for the injection of 5FU in a column packed with a MIP<sub>06</sub>.



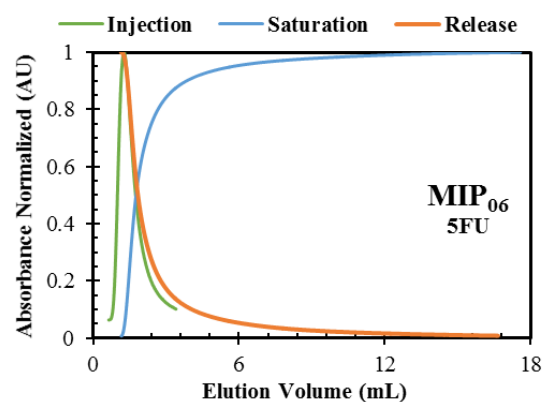
Profile observed for the saturation of 5FU in a column packed with a MIP<sub>06</sub>.



Profile observed for the release of 5FU in a column packed with a MIP<sub>06</sub>.



Profiles observed for the saturation and release of 5FU in a column packed with a MIP<sub>06</sub>.



Profiles observed for the injection, saturation and release of 5FU in a column packed with a MIP<sub>06</sub>.

---

**Operating conditions:**

Column: 2

$C_0 = 0.1 \text{ mM}$

$Q = 1 \text{ mL/min}$

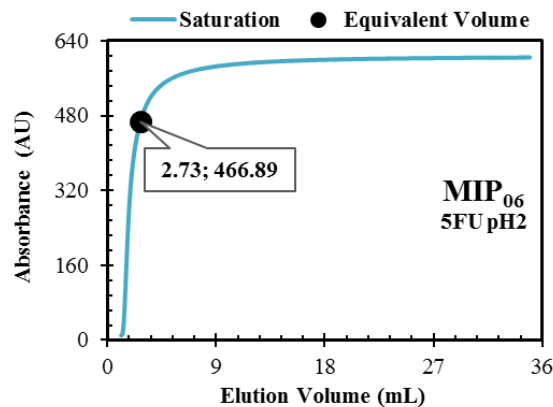
$T = 25 \text{ }^\circ\text{C}$

UV Detection: 265 nm

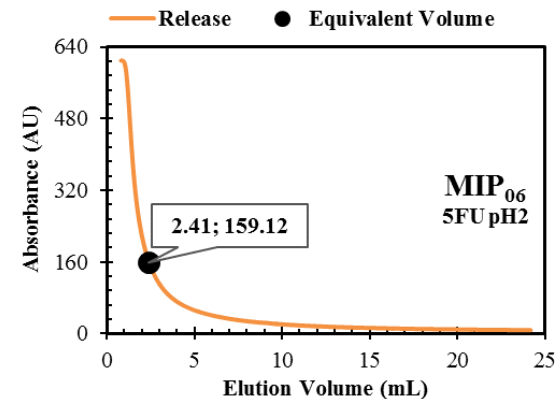
---

**Annex 35** - Study of injection, adsorption and desorption of 5FU pH2 in the MIP<sub>06</sub> (see Table 4.2). Characterization of the MIP frontal analysis by filling a column operating in continuous mode.

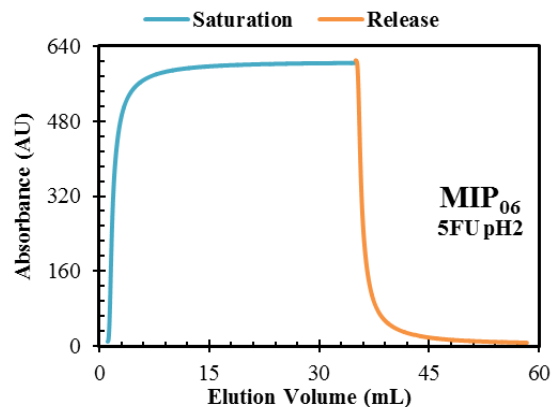
N/A



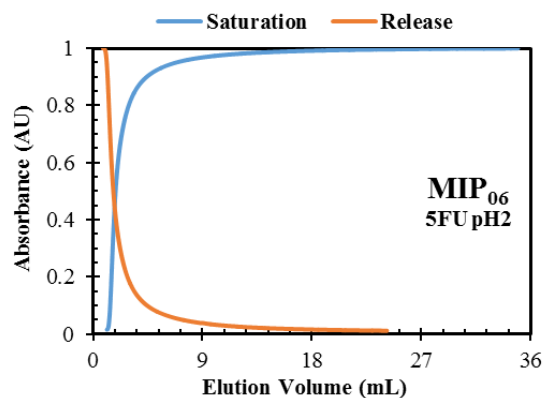
Profile observed for the saturation of 5FU pH2 in a column packed with a MIP<sub>06</sub>.



Profile observed for the release of 5FU pH2 in a column packed with a MIP<sub>06</sub>.



Profiles observed for the saturation and release of 5FU pH2 in a column packed with a MIP<sub>06</sub>.



Profiles observed for the injection, saturation and release of 5FU pH2 in a column packed with a MIP<sub>06</sub>.

**Operating conditions:**

Column: 2

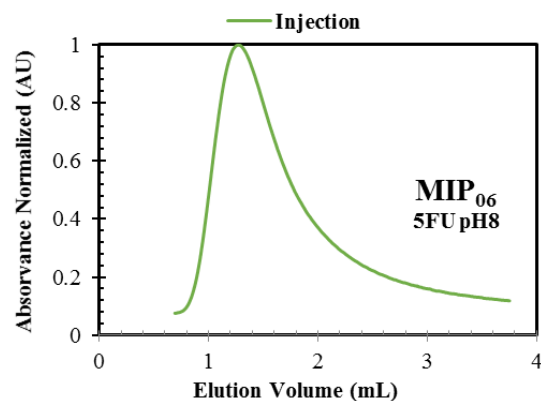
C<sub>0</sub> = 0.1 mM

Q = 1 mL/min

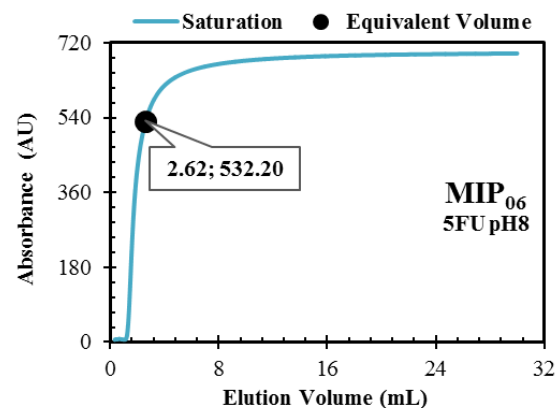
T = 25 °C

UV Detection: 265 nm

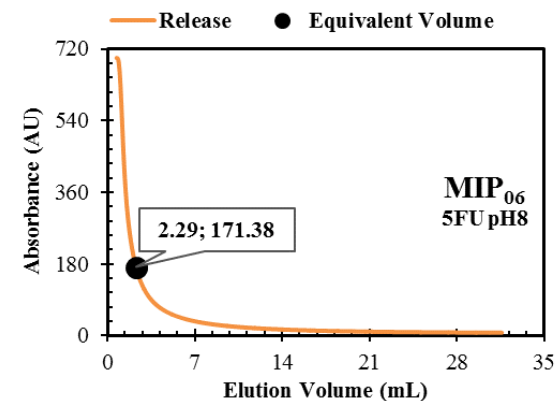
**Annex 36** - Study of injection, adsorption and desorption of 5FU pH8 in the MIP<sub>06</sub> (see Table 4.2). Characterization of the MIP frontal analysis by filling a column operating in continuous mode.



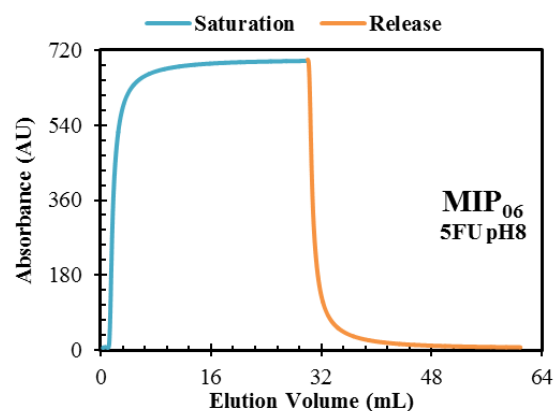
Profile observed for the injection of 5FU pH8 in a column packed with a MIP<sub>06</sub>.



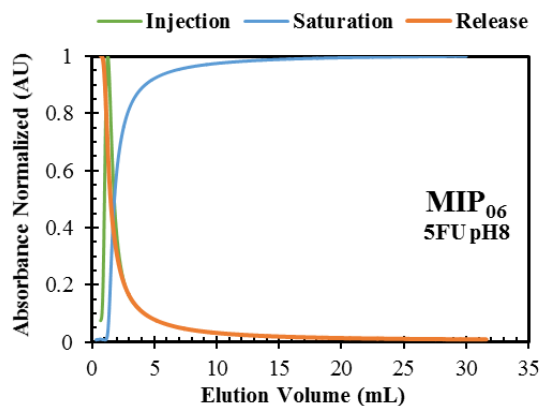
Profile observed for the saturation of 5FU pH8 in a column packed with a MIP<sub>06</sub>.



Profile observed for the release of 5FU pH8 in a column packed with a MIP<sub>06</sub>.



Profiles observed for the saturation and release of 5FU pH8 in a column packed with a MIP<sub>06</sub>.



Profiles observed for the injection, saturation and release of 5FU pH8 in a column packed with a MIP<sub>06</sub>.

---

**Operating conditions:**

Column: 2

$C_0 = 0.1 \text{ mM}$

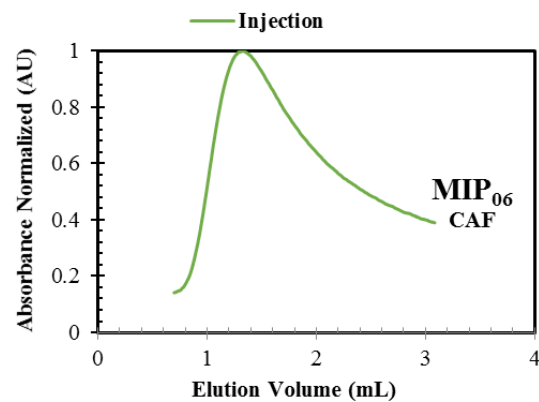
$Q = 1 \text{ mL/min}$

$T = 25 \text{ }^\circ\text{C}$

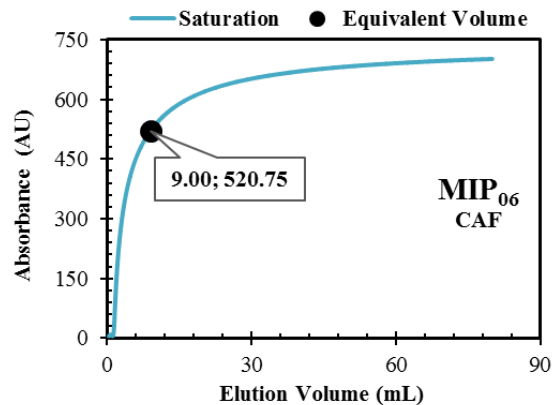
UV Detection: 265 nm

---

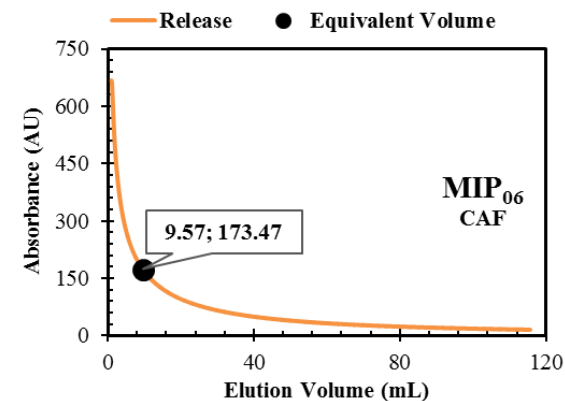
**Annex 37** - Study of injection, adsorption and desorption of CAF in the MIP<sub>06</sub> (see Table 4.2). Characterization of the MIP frontal analysis by filling a column operating in continuous mode.



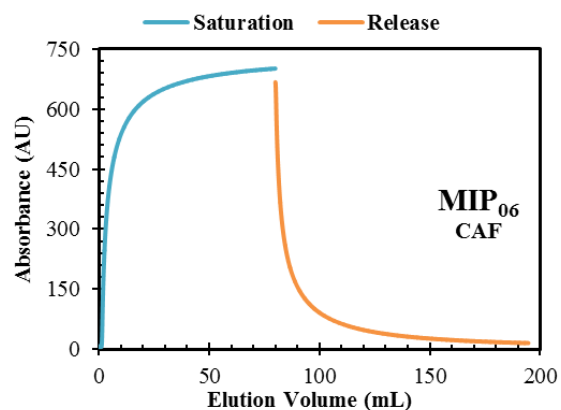
Profile observed for the injection of CAF in a column packed with a MIP<sub>06</sub>.



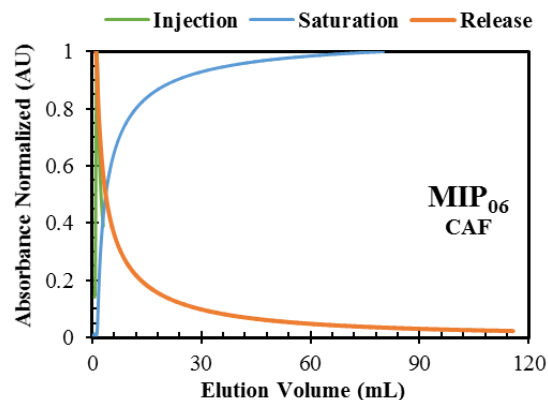
Profile observed for the saturation of CAF in a column packed with a MIP<sub>06</sub>.



Profile observed for the release of CAF in a column packed with a MIP<sub>06</sub>.



Profiles observed for the saturation and release of CAF in a column packed with a MIP<sub>06</sub>.



Profiles observed for the injection, saturation and release of CAF in a column packed with a MIP<sub>06</sub>.

**Operating conditions:**

Column: 2

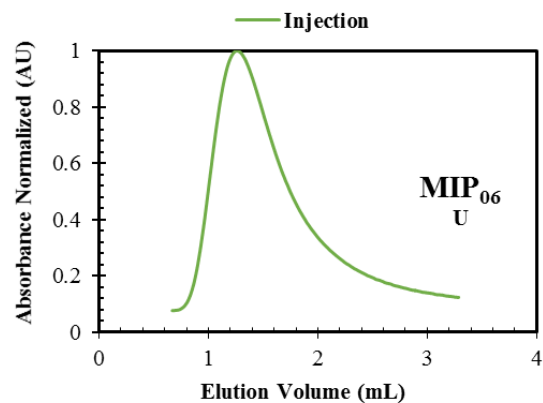
$C_0 = 0.1 \text{ mM}$

$Q = 1 \text{ mL/min}$

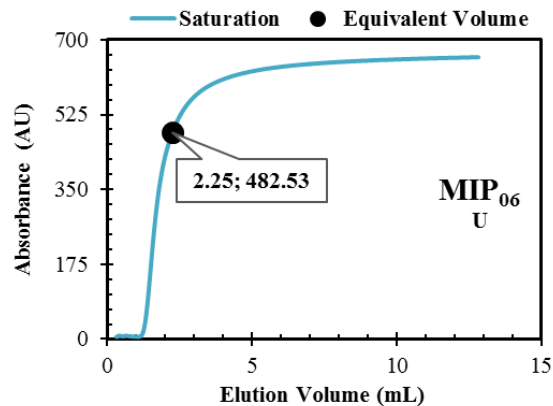
$T = 25 \text{ }^\circ\text{C}$

UV Detection: 273 nm

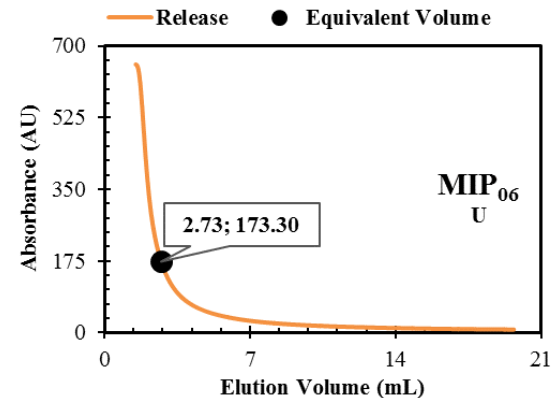
**Annex 38** - Study of injection, adsorption and desorption of U in the MIP<sub>06</sub> (see Table 4.2). Characterization of the MIP frontal analysis by filling a column operating in continuous mode.



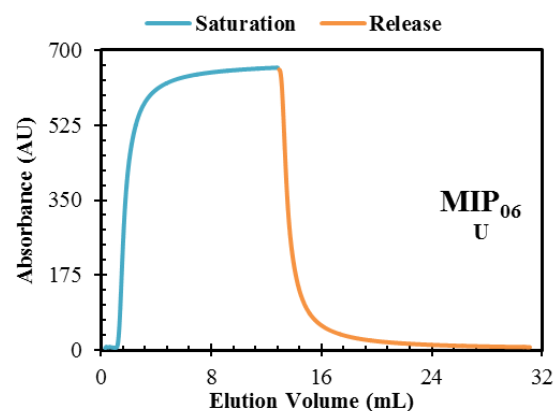
Profile observed for the injection of U in a column packed with a MIP<sub>06</sub>.



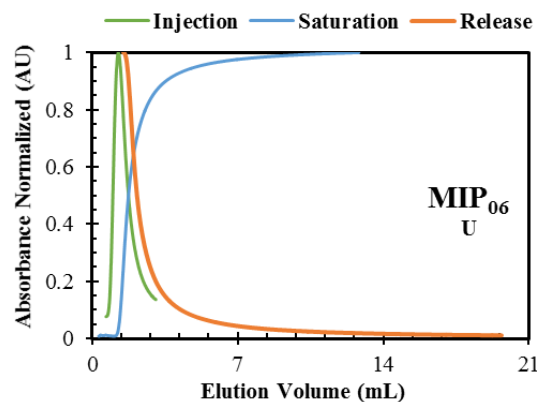
Profile observed for the saturation of U in a column packed with a MIP<sub>06</sub>.



Profile observed for the release of U in a column packed with a MIP<sub>06</sub>.



Profiles observed for the saturation and release of U in a column packed with a MIP<sub>06</sub>.



Profiles observed for the injection, saturation and release of U in a column packed with a MIP<sub>06</sub>.

**Operating conditions:**

Column: 2

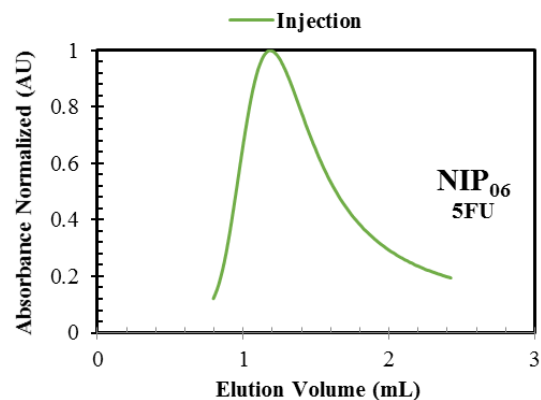
$C_0 = 0.1 \text{ mM}$

$Q = 1 \text{ mL/min}$

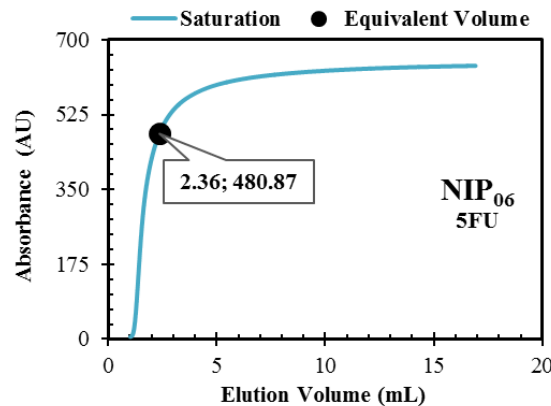
$T = 25 \text{ }^\circ\text{C}$

UV Detection: 258 nm

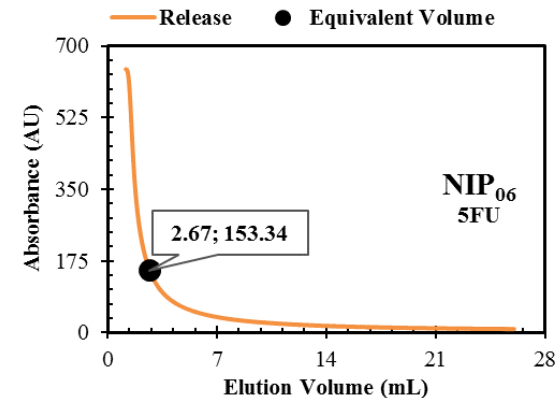
**Annex 39** - Study of injection, adsorption and desorption of 5FU in the NIP<sub>06</sub> (see Table 4.2). Characterization of the NIP frontal analysis by filling a column operating in continuous mode.



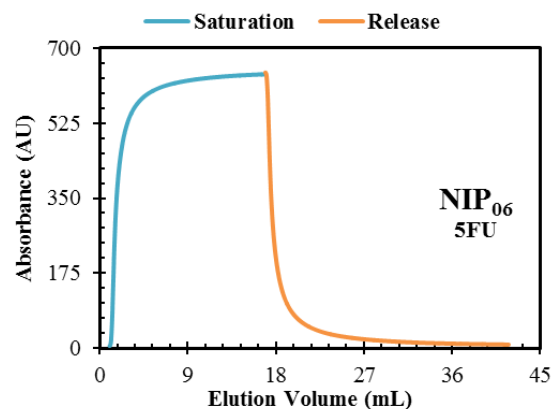
Profile observed for the injection of 5FU in a column packed with a NIP<sub>06</sub>.



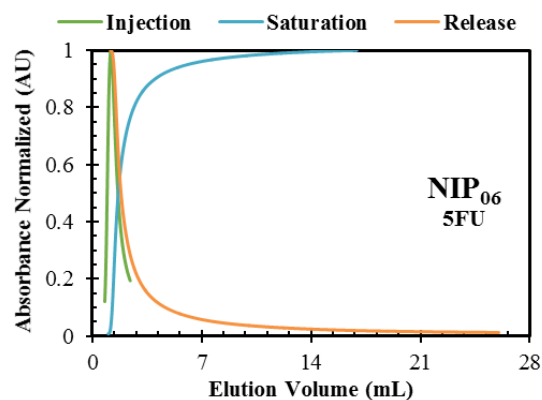
Profile observed for the saturation of 5FU in a column packed with a NIP<sub>06</sub>.



Profile observed for the release of 5FU in a column packed with a NIP<sub>06</sub>.



Profiles observed for the saturation and release of 5FU in a column packed with a NIP<sub>06</sub>.



Profiles observed for the injection, saturation and release of 5FU in a column packed with a NIP<sub>06</sub>.

**Operating conditions:**

Column: 2

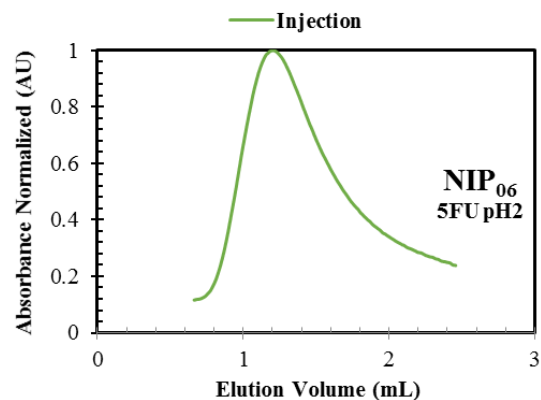
C<sub>0</sub> = 0.1 mM

Q = 1 mL/min

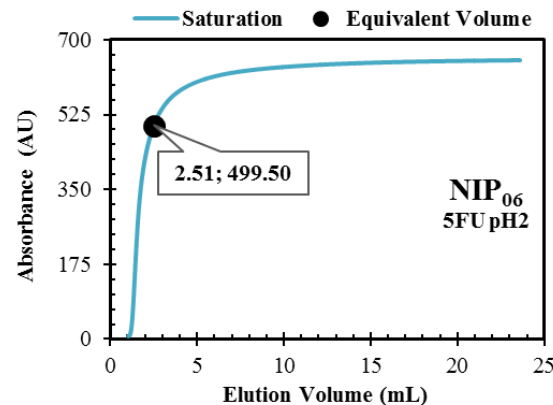
T = 25 °C

UV Detection: 265 nm

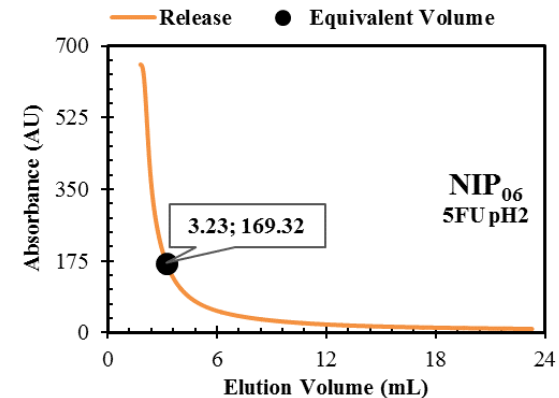
**Annex 40** - Study of injection, adsorption and desorption of 5FU pH2 in the NIP<sub>06</sub> (see Table 4.2). Characterization of the NIP frontal analysis by filling a column operating in continuous mode.



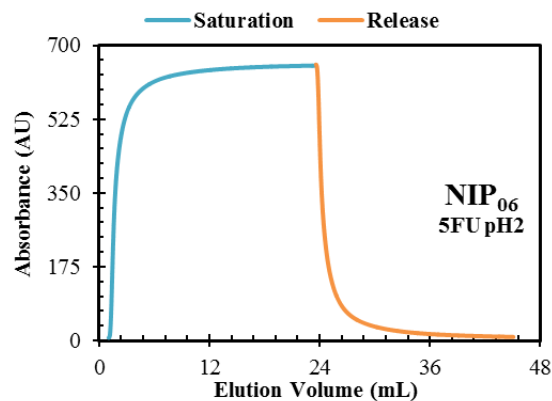
Profile observed for the injection of 5FU pH2 in a column packed with a NIP<sub>06</sub>.



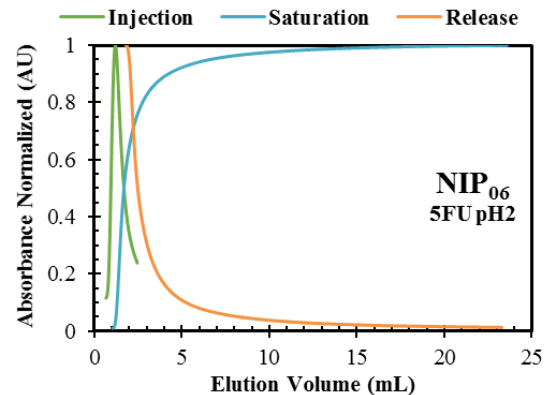
Profile observed for the saturation of 5FU pH2 in a column packed with a NIP<sub>06</sub>.



Profile observed for the release of 5FU pH2 in a column packed with a NIP<sub>06</sub>.



Profiles observed for the saturation and release of 5FU pH2 in a column packed with a NIP<sub>06</sub>.



Profiles observed for the injection, saturation and release of 5FU pH2 in a column packed with a NIP<sub>06</sub>.

**Operating conditions:**

Column: 2

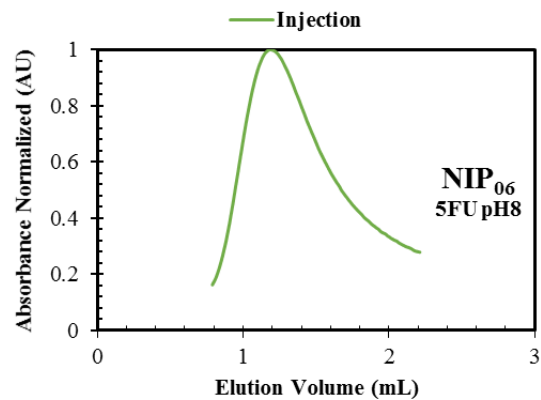
C<sub>0</sub> = 0.1 mM

Q = 1 mL/min

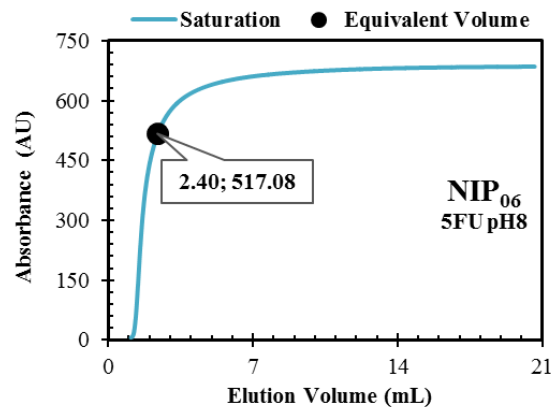
T = 25 °C

UV Detection: 265 nm

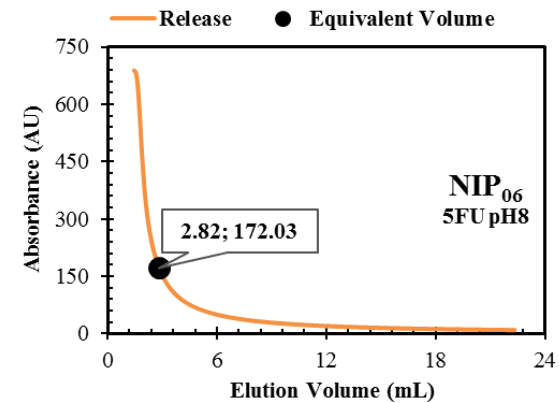
**Annex 41** - Study of injection, adsorption and desorption of 5FU pH8 in the NIP<sub>06</sub> (see Table 4.2). Characterization of the NIP frontal analysis by filling a column operating in continuous mode.



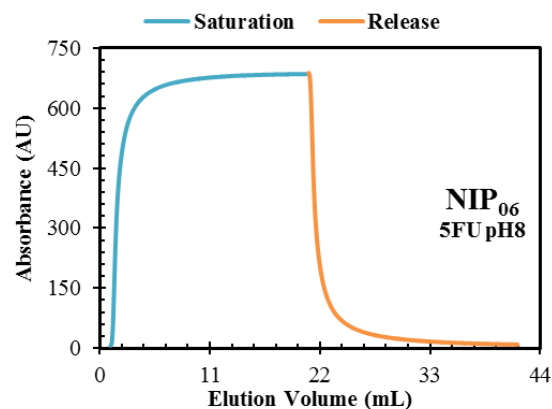
Profile observed for the injection of 5FU pH8 in a column packed with a NIP<sub>06</sub>.



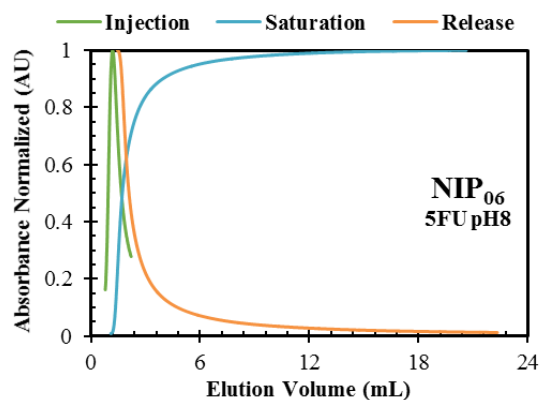
Profile observed for the saturation of 5FU pH8 in a column packed with a NIP<sub>06</sub>.



Profile observed for the release of 5FU pH8 in a column packed with a NIP<sub>06</sub>.



Profiles observed for the saturation and release of 5FU pH8 in a column packed with a NIP<sub>06</sub>.



Profiles observed for the injection, saturation and release of 5FU pH8 in a column packed with a NIP<sub>06</sub>.

**Operating conditions:**

Column: 2

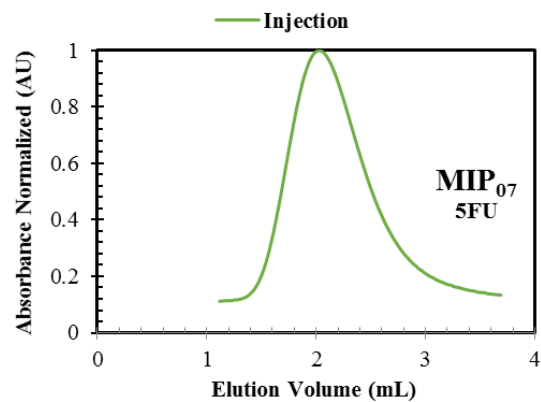
C<sub>0</sub> = 0.1 mM

Q = 1 mL/min

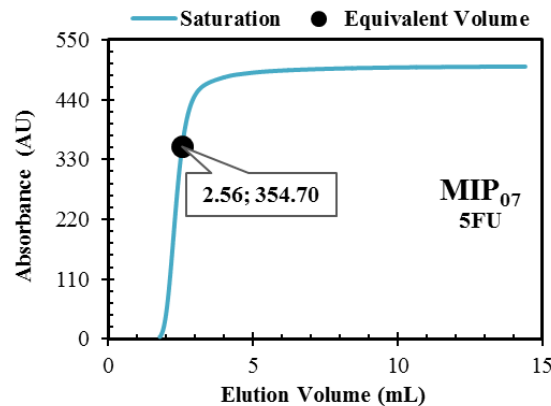
T = 25 °C

UV Detection: 265 nm

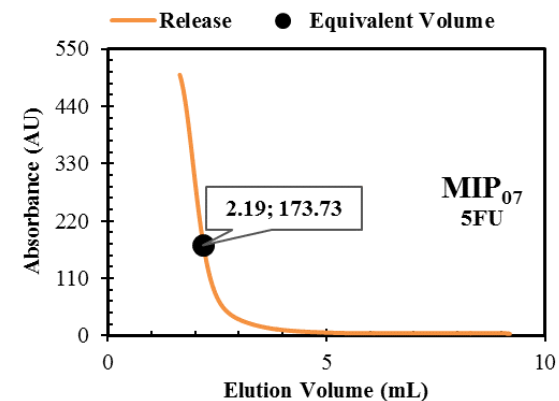
**Annex 42** - Study of injection, adsorption and desorption of 5FU in the MIP<sub>07</sub> (see Table 4.3). Characterization of the MIP frontal analysis by filling a column operating in continuous mode.



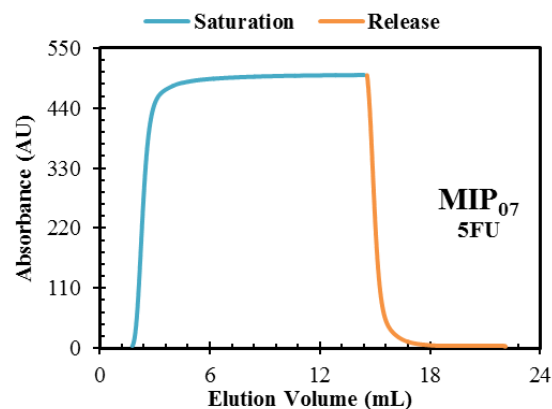
Profile observed for the injection of 5FU in a column packed with a MIP<sub>07</sub>.



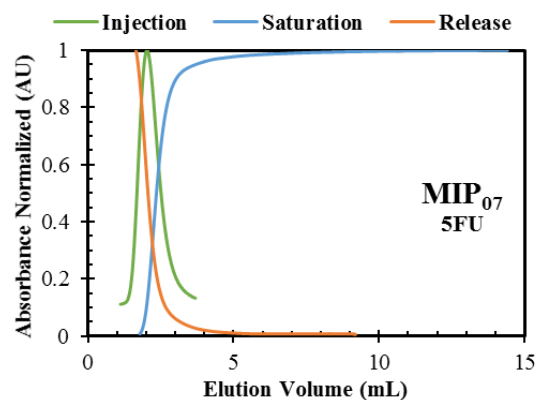
Profile observed for the saturation of 5FU in a column packed with a MIP<sub>07</sub>.



Profile observed for the release of 5FU in a column packed with a MIP<sub>07</sub>.



Profiles observed for the saturation and release of 5FU in a column packed with a MIP<sub>07</sub>.



Profiles observed for the injection, saturation and release of 5FU in a column packed with a MIP<sub>07</sub>.

---

**Operating conditions:**

Column: 2

$C_0 = 0.1 \text{ mM}$

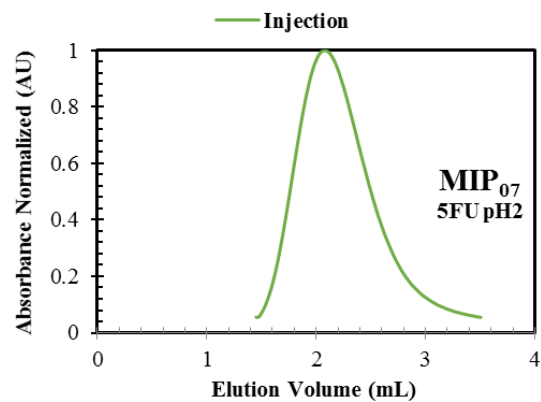
$Q = 1 \text{ mL/min}$

$T = 25 \text{ }^\circ\text{C}$

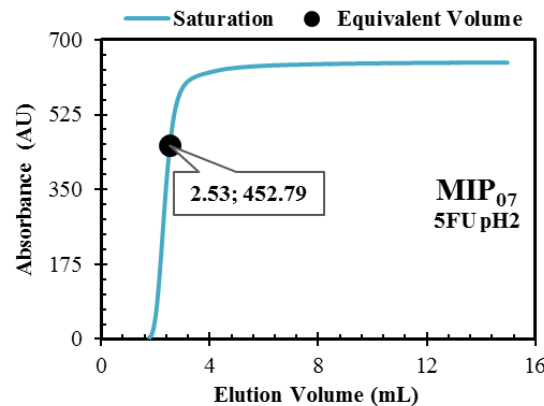
UV Detection: 265 nm

---

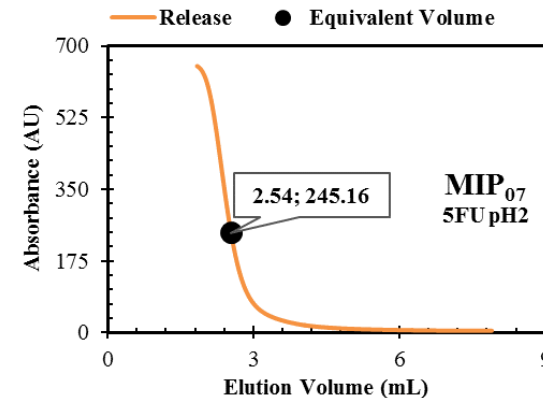
**Annex 43** - Study of injection, adsorption and desorption of 5FU pH2 in the MIP<sub>07</sub> (see Table 4.3). Characterization of the MIP frontal analysis by filling a column operating in continuous mode.



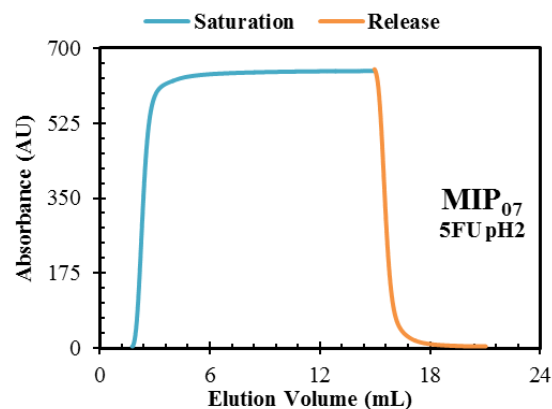
Profile observed for the injection of 5FU pH2 in a column packed with a MIP<sub>07</sub>.



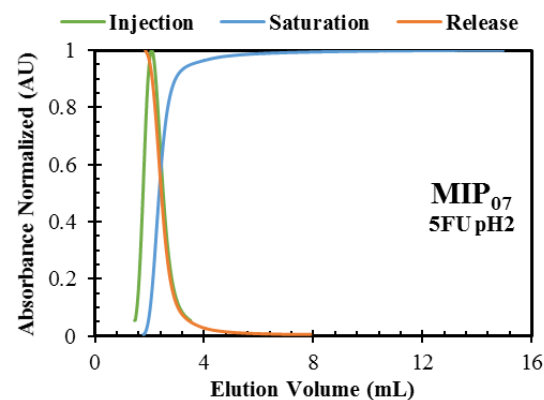
Profile observed for the injection of 5FU pH2 in a column packed with a MIP<sub>07</sub>.



Profile observed for the injection of 5FU pH2 in a column packed with a MIP<sub>07</sub>.



Profiles observed for the saturation and release of 5FU pH2 in a column packed with a MIP<sub>07</sub>.



Profiles observed for the injection, saturation and release of 5FU pH2 in a column packed with a MIP<sub>07</sub>.

**Operating conditions:**

Column: 2

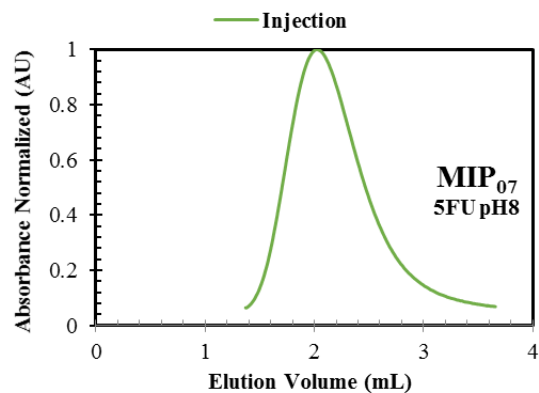
C<sub>0</sub> = 0.1 mM

Q = 1 mL/min

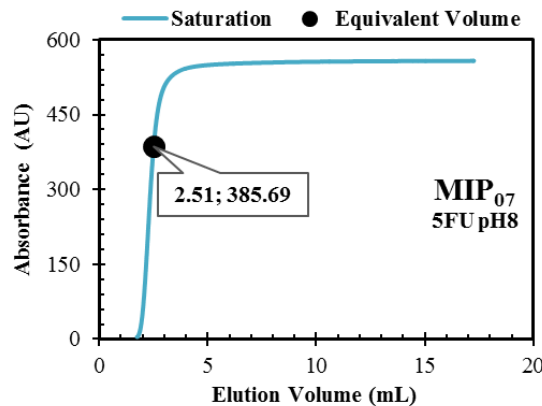
T = 25 °C

UV Detection: 265 nm

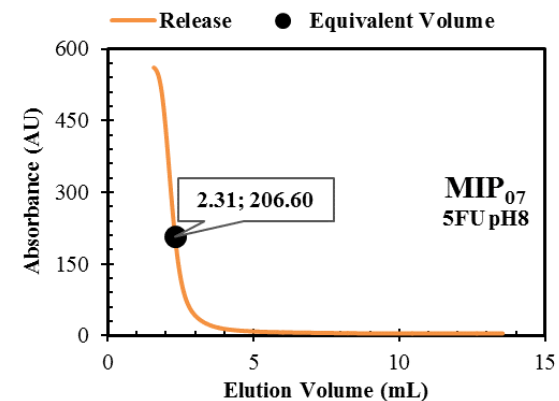
**Annex 44** - Study of injection, adsorption and desorption of 5FU pH8 in the MIP<sub>07</sub> (see Table 4.3). Characterization of the MIP frontal analysis by filling a column operating in continuous mode.



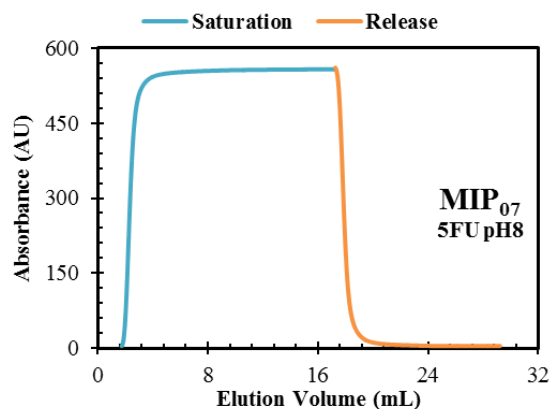
Profile observed for the injection of 5FU in a column packed with a MIP<sub>07</sub>.



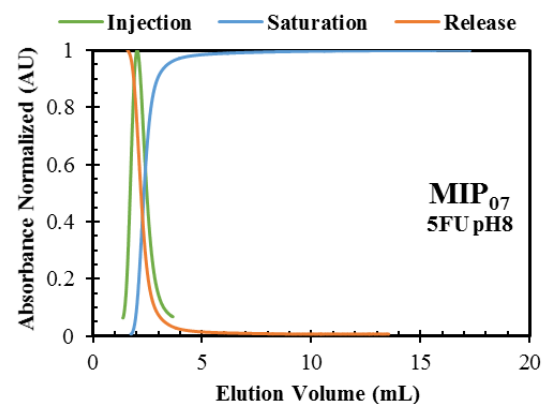
Profile observed for the saturation of 5FU in a column packed with a MIP<sub>07</sub>.



Profile observed for the release of 5FU in a column packed with a MIP<sub>07</sub>.



Profiles observed for the saturation and release of 5FU in a column packed with a MIP<sub>07</sub>.



Profiles observed for the injection, saturation and release of 5FU in a column packed with a MIP<sub>07</sub>.

---

**Operating conditions:**

Column: 2

$C_0 = 0.1 \text{ mM}$

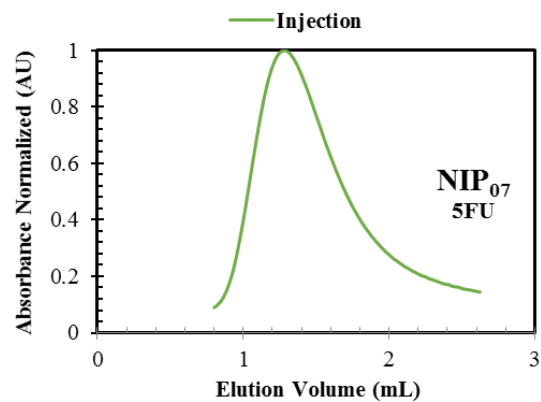
$Q = 1 \text{ mL/min}$

$T = 25 \text{ }^\circ\text{C}$

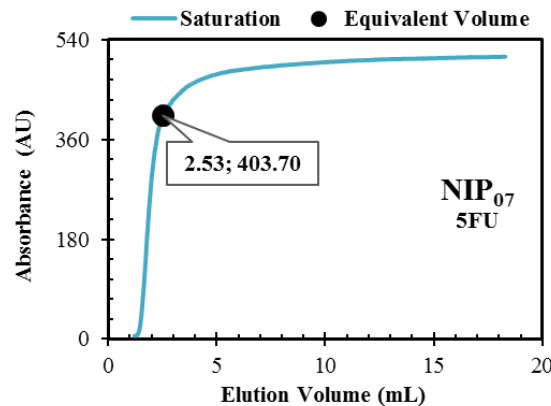
UV Detection: 265 nm

---

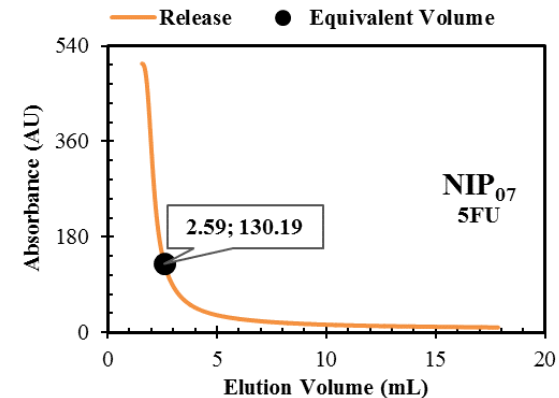
**Annex 45** - Study of injection, adsorption and desorption of 5FU in the NIP<sub>07</sub> (see Table 4.3). Characterization of the NIP frontal analysis by filling a column operating in continuous mode.



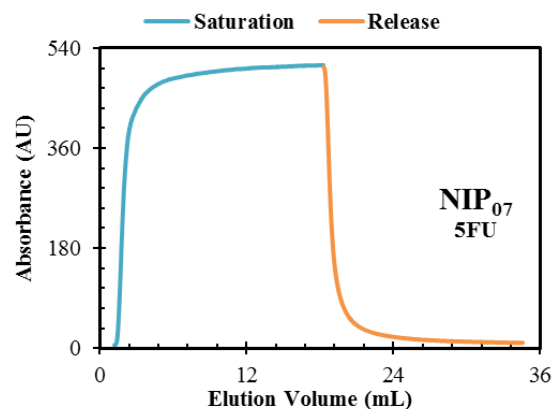
Profile observed for the injection of 5FU in a column packed with a NIP<sub>07</sub>.



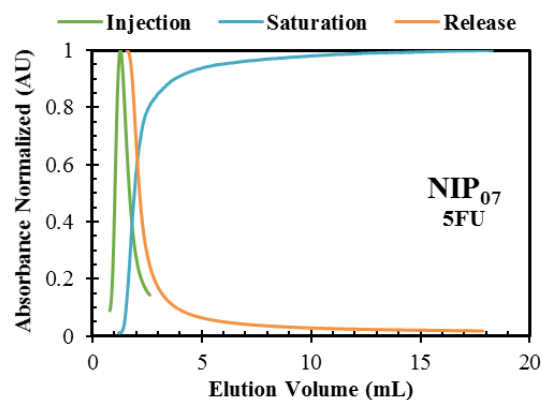
Profile observed for the saturation of 5FU in a column packed with a NIP<sub>07</sub>.



Profile observed for the release of 5FU in a column packed with a NIP<sub>07</sub>.



Profiles observed for the saturation and release of 5FU in a column packed with a NIP<sub>07</sub>.



Profiles observed for the injection, saturation and release of 5FU in a column packed with a NIP<sub>07</sub>.

**Operating conditions:**

Column: 2

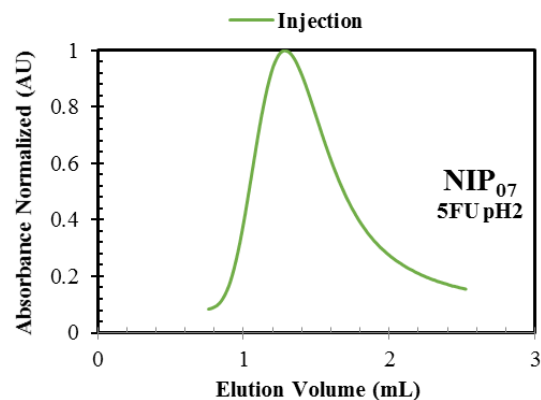
C<sub>0</sub> = 0.1 mM

Q = 1 mL/min

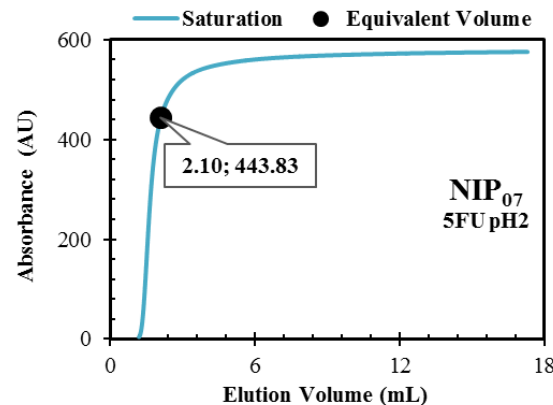
T = 25 °C

UV Detection: 265 nm

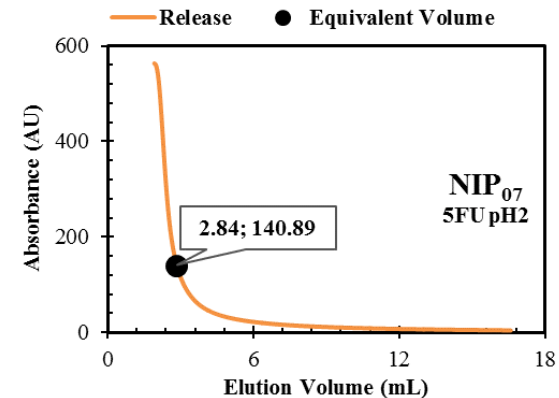
**Annex 46** - Study of injection, adsorption and desorption of 5FU pH2 in the NIP<sub>07</sub> (see Table 4.3). Characterization of the NIP frontal analysis by filling a column operating in continuous mode.



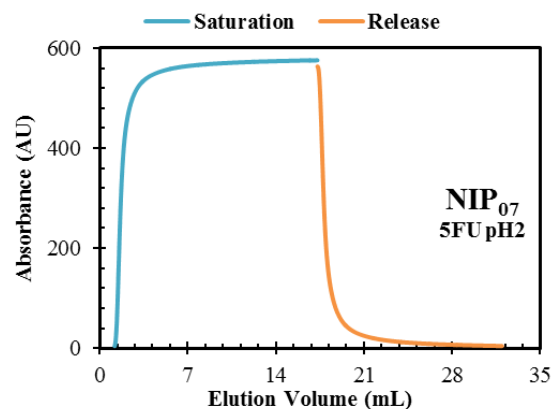
Profile observed for the injection of 5FU pH2 in a column packed with a NIP<sub>07</sub>.



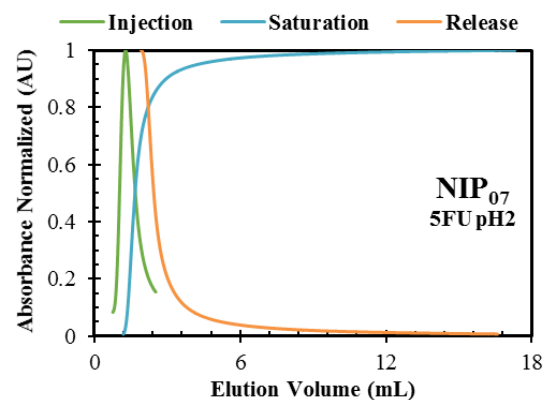
Profile observed for the saturation of 5FU pH2 in a column packed with a NIP<sub>07</sub>.



Profile observed for the release of 5FU pH2 in a column packed with a NIP<sub>07</sub>.



Profiles observed for the saturation and release of 5FU pH2 in a column packed with a NIP<sub>07</sub>.



Profiles observed for the injection, saturation and release of 5FU pH2 in a column packed with a NIP<sub>07</sub>.

**Operating conditions:**

Column: 2

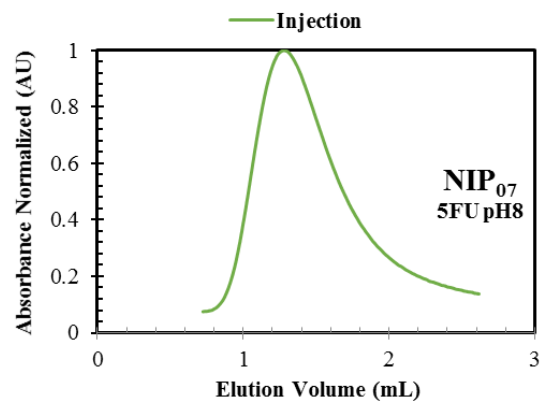
C<sub>0</sub> = 0.1 mM

Q = 1 mL/min

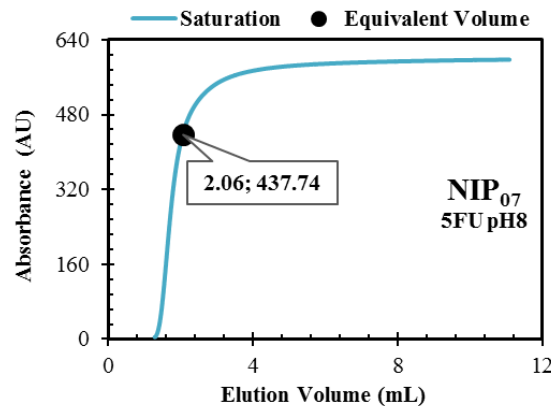
T = 25 °C

UV Detection: 265 nm

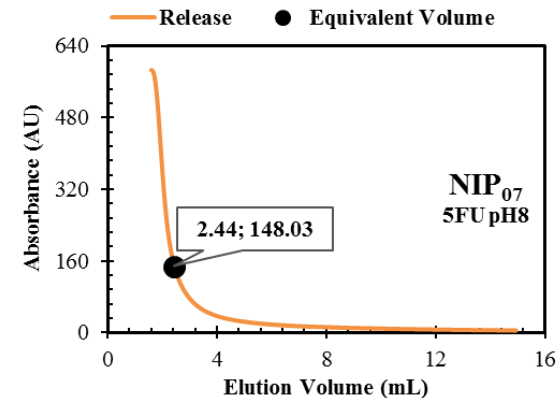
**Annex 47** - Study of injection, adsorption and desorption of 5FU pH8 in the NIP<sub>07</sub> (see Table 4.3). Characterization of the NIP frontal analysis by filling a column operating in continuous mode.



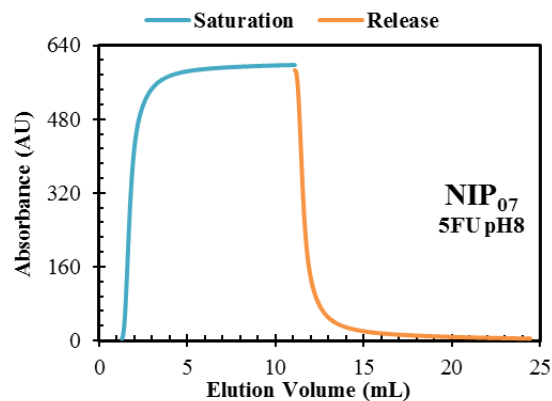
Profile observed for the injection of 5FU pH8 in a column packed with a NIP<sub>07</sub>.



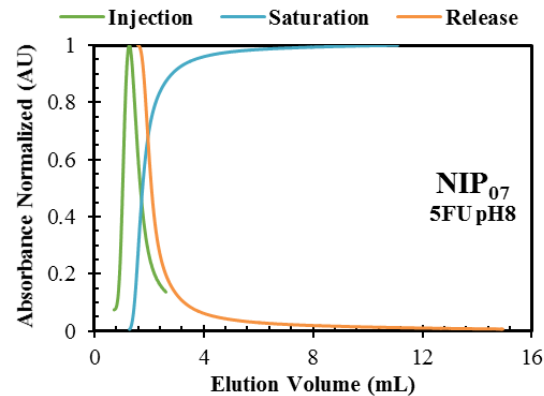
Profile observed for the saturation of 5FU pH8 in a column packed with a NIP<sub>07</sub>.



Profile observed for the release of 5FU pH8 in a column packed with a NIP<sub>07</sub>.



Profiles observed for the saturation and release of 5FU pH8 in a column packed with a NIP<sub>07</sub>.



Profiles observed for the injection, saturation and release of 5FU pH8 in a column packed with a NIP<sub>07</sub>.

**Operating conditions:**

Column: 2

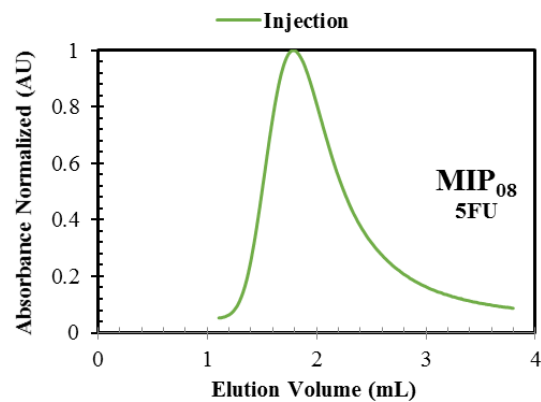
C<sub>0</sub> = 0.1 mM

Q = 1 mL/min

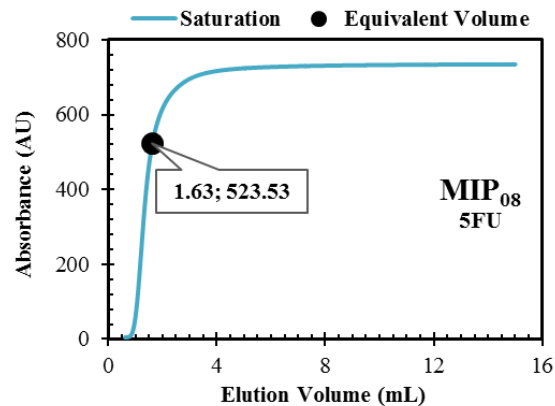
T = 25 °C

UV Detection: 265 nm

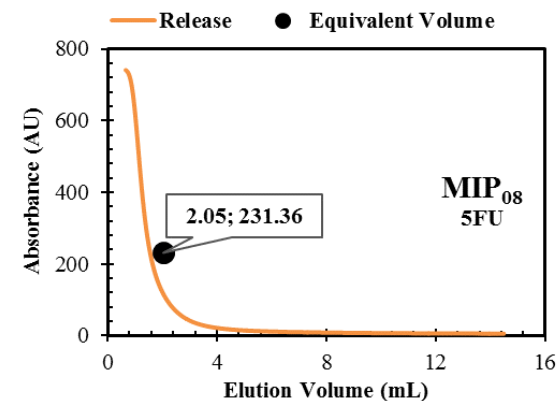
**Annex 48** - Study of injection, adsorption and desorption of 5FU in the MIP<sub>08</sub> (see Table 4.3). Characterization of the MIP frontal analysis by filling a column operating in continuous mode.



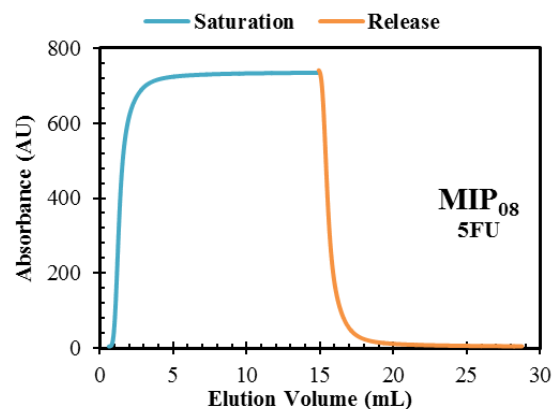
Profile observed for the injection of 5FU in a column packed with a MIP<sub>08</sub>.



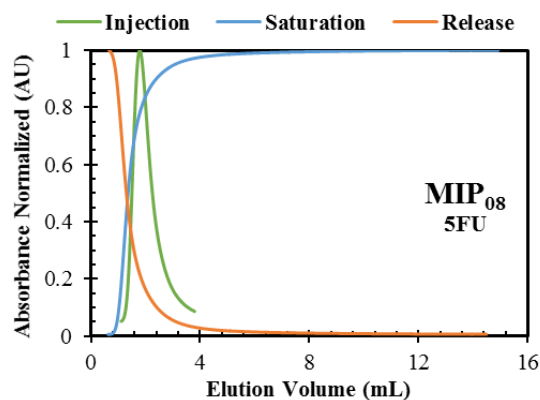
Profile observed for the saturation of 5FU in a column packed with a MIP<sub>08</sub>.



Profile observed for the release of 5FU in a column packed with a MIP<sub>08</sub>.



Profiles observed for the saturation and release of 5FU in a column packed with a MIP<sub>08</sub>.



Profiles observed for the injection, saturation and release of 5FU in a column packed with a MIP<sub>08</sub>.

---

**Operating conditions:**

Column: 2

$C_0 = 0.1 \text{ mM}$

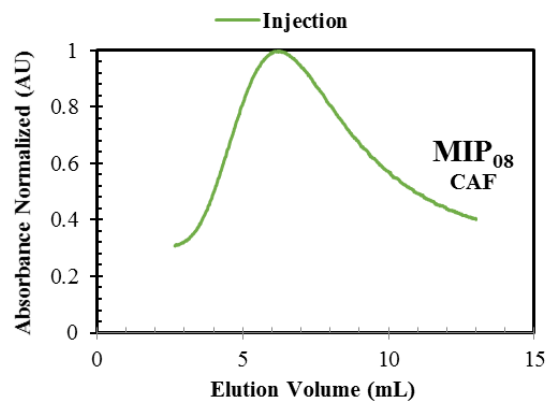
$Q = 1 \text{ mL/min}$

$T = 25 \text{ }^\circ\text{C}$

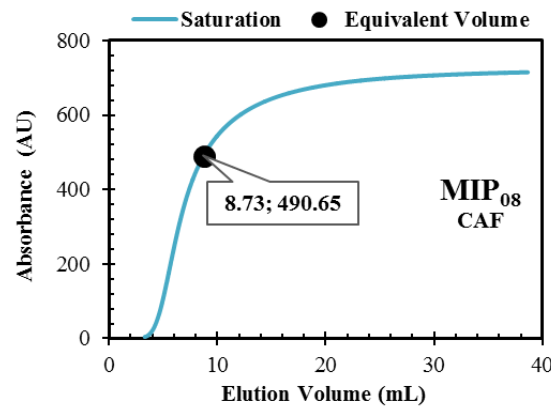
UV Detection: 265 nm

---

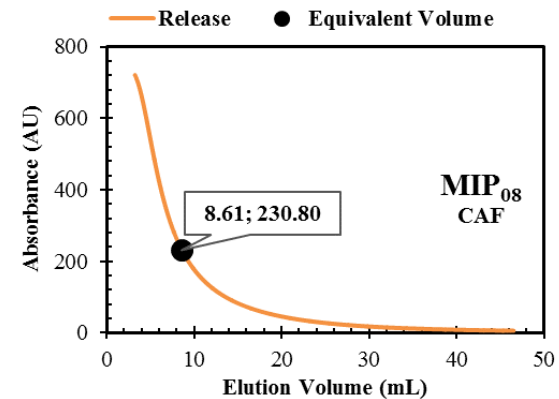
**Annex 49** - Study of injection, adsorption and desorption of CAF in the MIP<sub>08</sub> (see Table 4.3). Characterization of the MIP frontal analysis by filling a column operating in continuous mode.



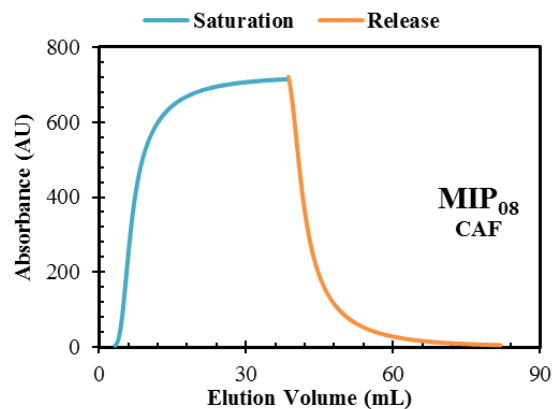
Profile observed for the injection of CAF in a column packed with a MIP<sub>08</sub>.



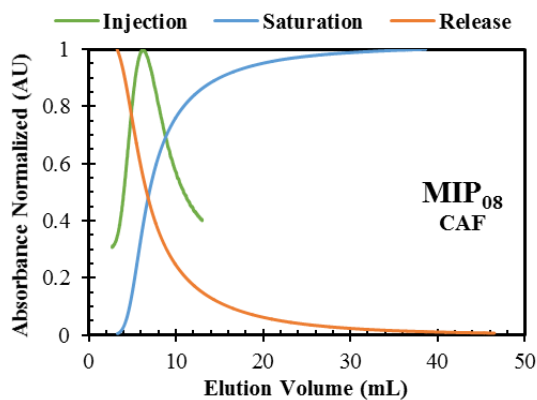
Profile observed for the saturation of CAF in a column packed with a MIP<sub>08</sub>.



Profile observed for the release of CAF in a column packed with a MIP<sub>08</sub>.



Profiles observed for the saturation and release of CAF in a column packed with a MIP<sub>08</sub>.



Profiles observed for the injection, saturation and release of CAF in a column packed with a MIP<sub>08</sub>.

**Operating conditions:**

Column: 2

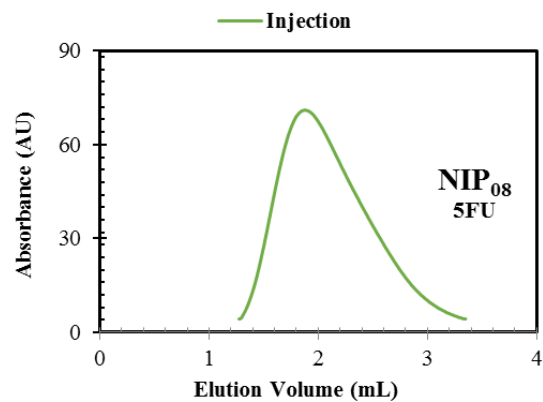
$C_0 = 0.1 \text{ mM}$

$Q = 1 \text{ mL/min}$

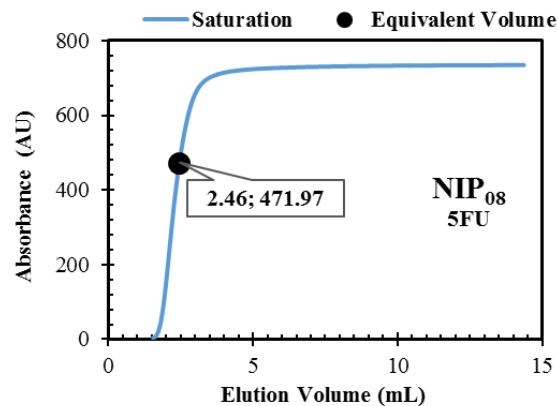
$T = 25 \text{ }^\circ\text{C}$

UV Detection: 273 nm

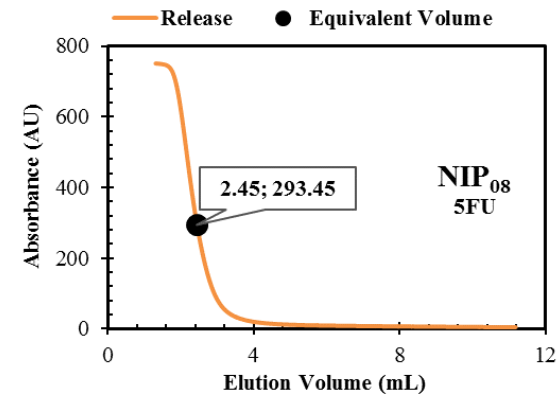
**Annex 50** - Study of injection, adsorption and desorption of 5FU in the NIP<sub>08</sub> (see Table 4.3). Characterization of the NIP frontal analysis by filling a column operating in continuous mode.



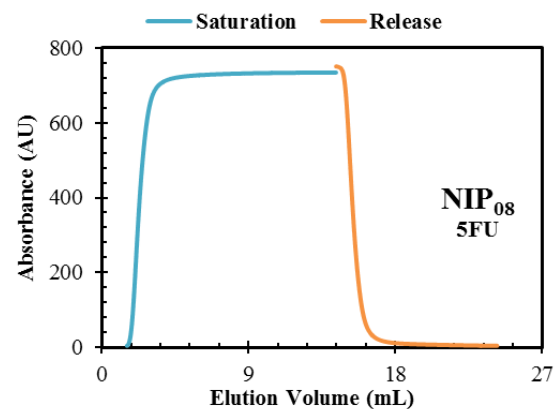
Profile observed for the injection of 5FU in a column packed with a NIP<sub>08</sub>.



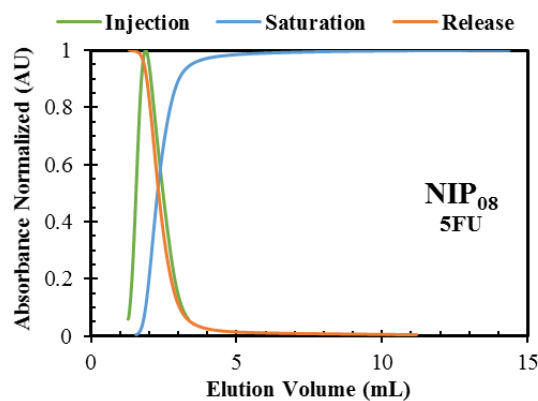
Profile observed for the saturation of 5FU in a column packed with a NIP<sub>08</sub>.



Profile observed for the release of 5FU in a column packed with a NIP<sub>08</sub>.



Profiles observed for the saturation and release of 5FU in a column packed with a NIP<sub>08</sub>.



Profiles observed for the injection, saturation and release of 5FU in a column packed with a NIP<sub>08</sub>.

---

**Operating conditions:**

Column: 2

$C_0 = 0.1$  mM

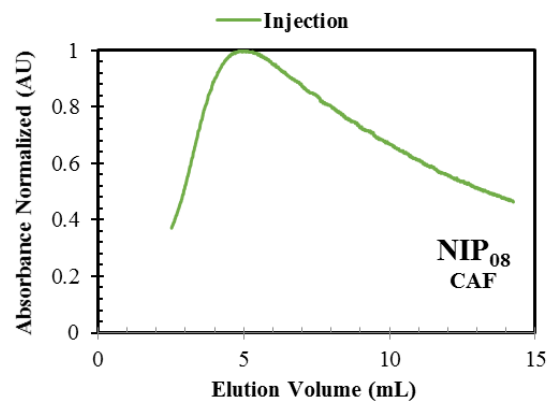
$Q = 1$  mL/min

$T = 25$  °C

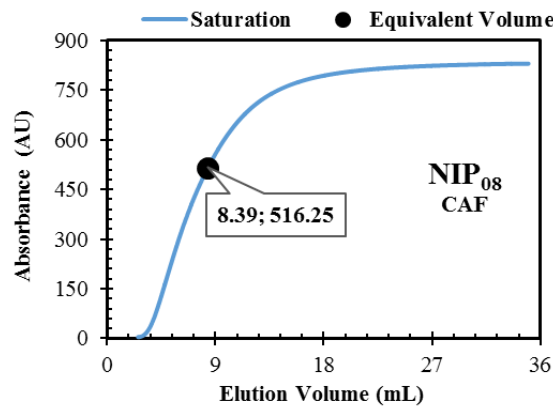
UV Detection: 265 nm

---

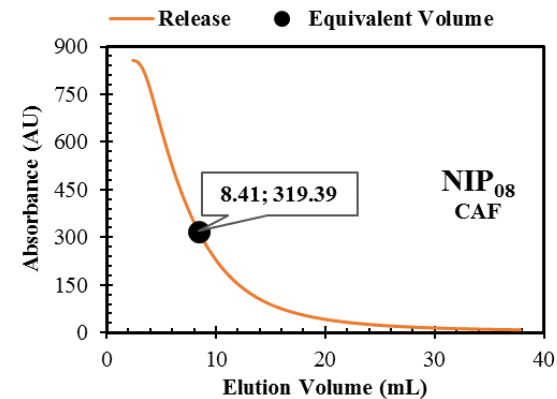
**Annex 51** - Study of injection, adsorption and desorption of CAF in the NIP<sub>08</sub> (see Table 4.3). Characterization of the NIP frontal analysis by filling a column operating in continuous mode.



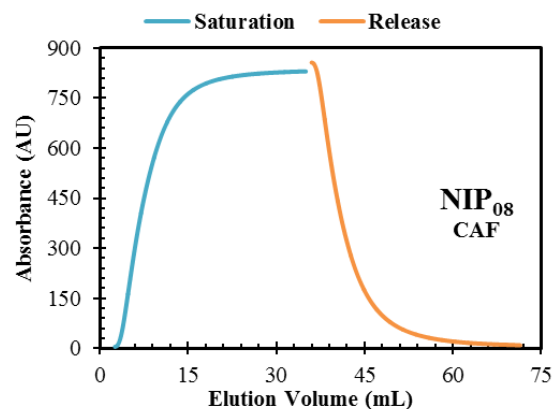
Profile observed for the injection of CAF in a column packed with a NIP<sub>08</sub>



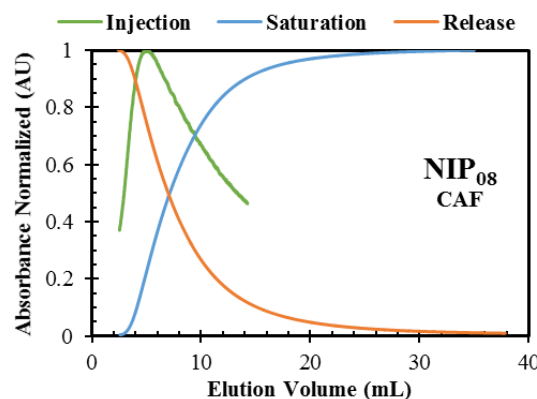
Profile observed for the saturation of CAF in a column packed with a NIP<sub>08</sub>.



Profile observed for the release of CAF in a column packed with a NIP<sub>08</sub>.



Profiles observed for the saturation and release of CAF in a column packed with a NIP<sub>08</sub>.



Profiles observed for the injection, saturation and release of CAF in a column packed with a NIP<sub>08</sub>.

---

**Operating conditions:**

Column: 2

$C_0 = 0.1 \text{ mM}$

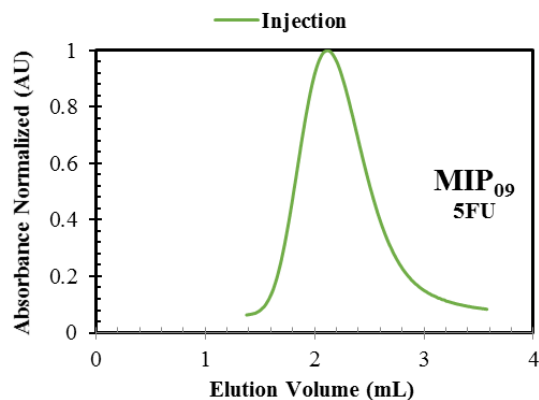
$Q = 1 \text{ mL/min}$

$T = 25 \text{ }^\circ\text{C}$

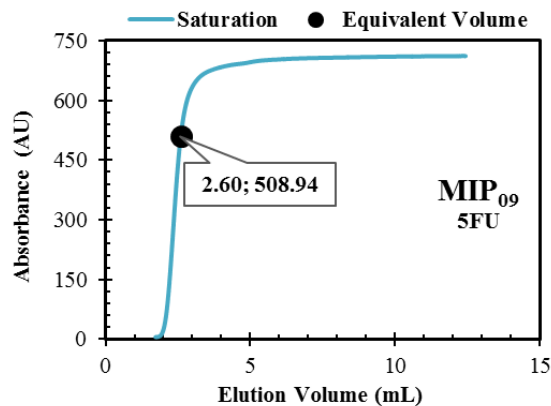
UV Detection: 273 nm

---

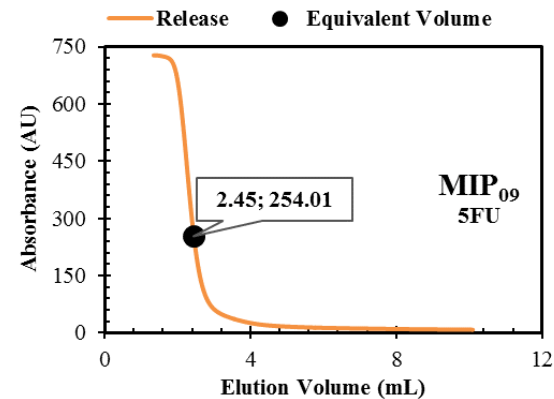
**Annex 52** - Study of injection, adsorption and desorption of 5FU in the MIP<sub>09</sub> (see Table 4.3). Characterization of the MIP frontal analysis by filling a column operating in continuous mode.



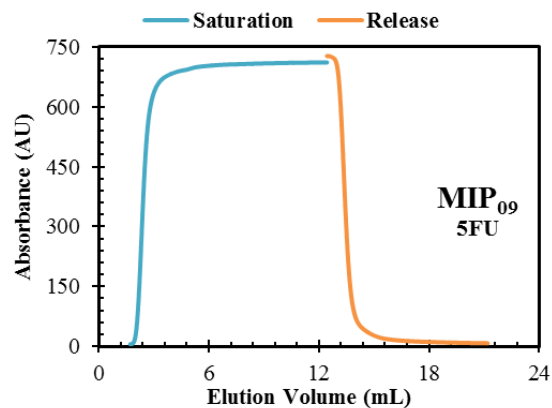
Profile observed for the injection of 5FU in a column packed with a MIP<sub>09</sub>.



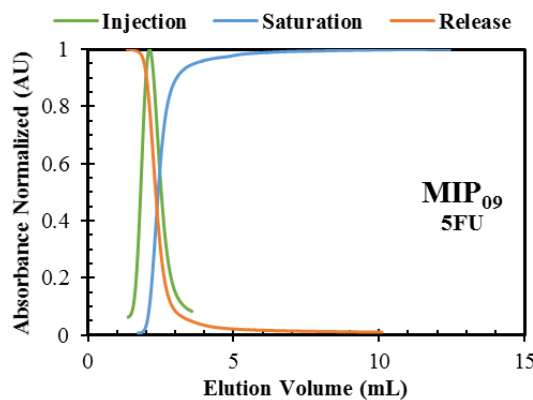
Profile observed for the injection of 5FU in a column packed with a MIP<sub>09</sub>.



Profile observed for the injection of 5FU in a column packed with a MIP<sub>09</sub>.



Profiles observed for the saturation and release of 5FU in a column packed with a MIP<sub>09</sub>.



Profiles observed for the injection, saturation and release of 5FU in a column packed with a MIP<sub>09</sub>.

---

**Operating conditions:**

Column: 2

$C_0 = 0.1 \text{ mM}$

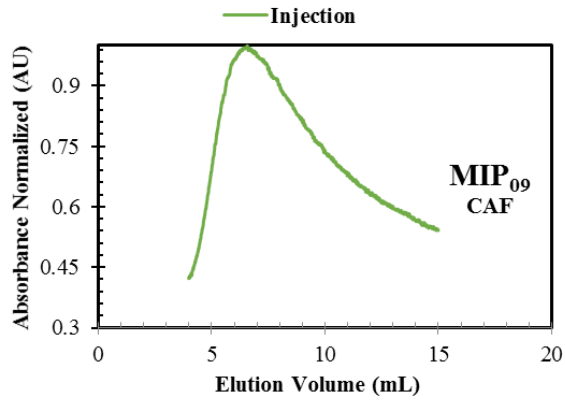
$Q = 1 \text{ mL/min}$

$T = 25 \text{ }^\circ\text{C}$

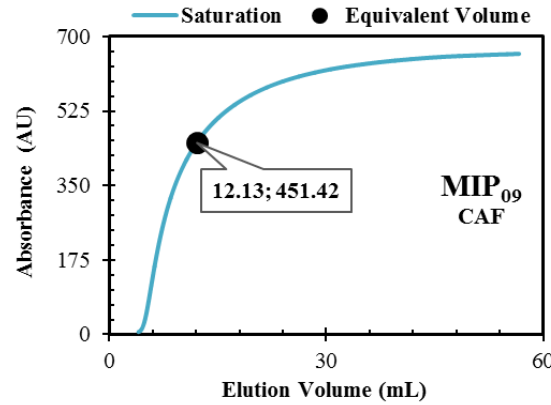
UV Detection: 265 nm

---

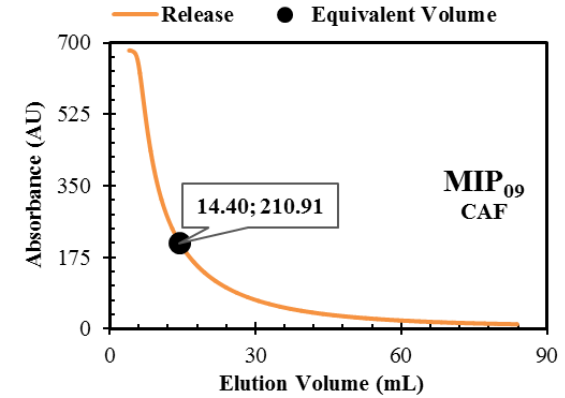
**Annex 53** - Study of injection, adsorption and desorption of CAF in the MIP<sub>09</sub> (see Table 4.3). Characterization of the MIP frontal analysis by filling a column operating in continuous mode.



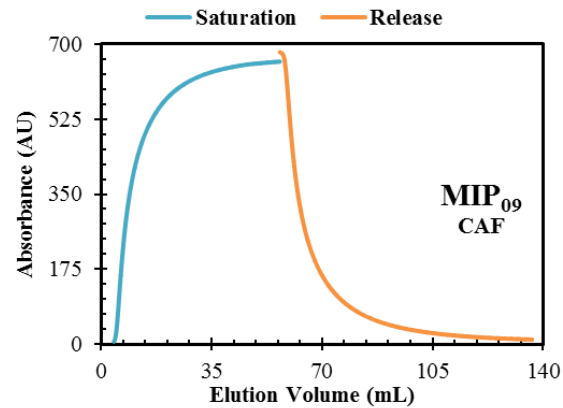
Profile observed for the injection of CAF in a column packed with a MIP<sub>09</sub>



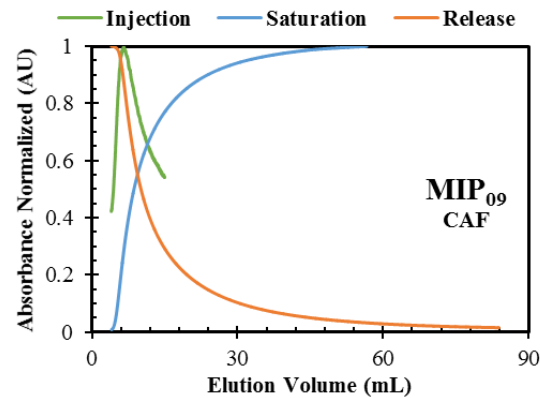
Profile observed for the saturation of CAF in a column packed with a MIP<sub>09</sub>.



Profile observed for the release of CAF in a column packed with a MIP<sub>09</sub>.



Profiles observed for the saturation and release of CAF in a column packed with a MIP<sub>09</sub>.



Profiles observed for the injection, saturation and release of CAF in a column packed with a MIP<sub>09</sub>.

**Operating conditions:**

Column: 2

$C_0 = 0.1$  mM

$Q = 1$  mL/min

$T = 25$  °C

UV Detection: 273 nm

